Development of Inducible Transgenic Mouse Models for Melanoma

Denggao Yao

A thesis submitted in fulfillment of the requirements of University of Glasgow for the degree of Doctor of Philosophy

Section of Dermatology

Division of Cancer Sciences and Molecular Pathology

Faculty of Medicine

University of Glasgow

July 2008

Dedication

This thesis is dedicated to my mother who gave me birth and cared for me over so many years but suffered from cancer and died soon after the viva, and my father who died during the writing of this thesis.

List of Contents

Page number

Page number

Page number

List of figures Page number

Page number

List of tables

Abbreviations

AA	— Alopecia Areata
4-ABP	— 4-Aminobiphenyl
AGA	— Androgenetic Alopecia
AUC	— Congenital Atrichia
α-MSH	— alpha- Melanocytes Stimulating Hormone
AKT/PKB	— Protein Kinase B
Apaf	— Apoptotic Protease Activating Factor
b–FGF	— basic Fibroblast Growth Factor
B[a]BP	— benzo[a]pyrene
BCC	— Basal Cell Carcinoma
BAD	— Bcl-2 Associated Death Promoter
BME	— β-Mercaptoethonal
BN	— Benign Melanocytic Nevus
CIAP	— Calf Intestinal Alkaline Phosphatase
CDK	— Cyclin-Dependent Kinase
CKi	— Conditional Knock In
CKo	— Conditional Knock Out
CMV	— Cytomegalovirus
Cre	— Cyclization Recombination gene of bacteriophage P1
CrePR1	— fusion of Cre with Progesterone Receptor ligand binding domain
dATP	— 2'-Deoxyadenosine 5'-triphosphate
dCTP	— 2'-Deoxycytidine 5'-triphosphate
dGTP	— 2'-Deoxyguanosine 5'-triphosphate

dTTP	— 2'-Deoxythymidine 5'-triphosphate
dNTPs	— Deoxynucleotide Triphosphates
DBACR	— Dibenz[c,h]acridine
DHPLC	— Denaturing High-Performance Liquid Chromatography
DMBA	— Dimethylbenzanthracene
DMEM	— Dulbecco’s Modified Eagle Medium
DMSO	— Dimethyl Sulfoxide
DTT	— Dithiothreitol
EAE	— Experimental Autoimmune Encephalomyelitis
ECM	— Extracellular Matrix
EDTA	— Ethylenediaminetetra-acetate
EGF	— Epidermal Growth Factor
EGFP	— Enhanced Green Fluorescent Protein
EMT	— Epithelial-Mesenchymal Transition
ER	— Endoplasmic Reticulum
Erk	— Extracellular Regulated Kinase
FADD	— Fas-associated protein with a Death Domain
FCS	— Fetal Calf Serum
FGF2	— Fibroblast Growth Factor 2
FRT	— Flp-recombinase Recognition Target
FSH	— Follicle-Stimulating Hormone
GAP	— GTPase Activating Protein
GDP	— Guanine Diphosphate
GEF	— Guanine-nucleotide Exchange Factors
GRB2	— Growth factor Receptor-bound protein 2
GSK3β	— Glycogen Synthase Kinase Beta

GTP	— Guanine Triphosphate
hCG	— Human Chorionic Gonadotropin
H&E	— Haemotoxylin and Eosin
HGF	— Hepatocytes Growth Factor
HSV TK	— Herpes Simplex Virus Thymidine Kinase promoter
IGF	— Insulin-like Growth Factor
LH	— Luteinizing Hormone
LOH	— Loss of Heterozygosity
MAPK	— Mitogen-Activated Protein Kinase
MAPKK(MEK)	— Mitogen-Activated Protein Kinase Kinase
MC1R	— Melanocortin 1 Receptor
MCS	— Multi Cloning Sites
MDM	— Murine Double Minute
MEM	— Minimal Essential Medium
MET	— Mesenchymal-Epithelial Transition
MHC	— Major Histocompatibility Complex
MITF	— Microphthalmia-Associated Transcription Factor
MMPs	— Matris Metalloproteinases
mTOR	— Mammalian Target of Rapamycin
NCC	— Neural Crest Cell
NF1	— Neurofibromin 1
NK-1R	— Neurokinin-1 Receptor
PBS	— Phosphate-buffered saline
PCNA	— Proliferating Cell Nuclear Antigen
PCR	— Polymerase Chain Reaction
PDM	— Primary Dermal Melanoma

PI3K — Phosphatidylinositol 3-Kinase

PIP3 — Phosphatidylinositol 3,4,5-triphosphate

PDK — Phosphoinositide Dependent Kinase

PLBD — Progesterone Ligand Binding Domain

PNM — Primary Nodular Melanoma

PMS — Pregnant Mare's Serum

PTPRD — Protein Tyrosine Phosphatase Receptor D

RASSF1A — Ras Association Family member 1A

Rb — Retinoblastoma

RGP-CMM — Radial Growth Phase of Cutaneous Malignant Melanoma

RPE — Retinal Pigment Epithelium

RSK — Ribosomal S6 Kinase

RT — Reverse Transcription

Ru486 — Mefipristone, an analogue of progesterone

SCC — Squamous Cell Carcinoma

SCF — Stem Cell Factor

SDS — Sodium Dodecyl Sulfate

SHC — Src Homology Containing protein

SHP2 — Src Homology Phosphatase 2

SK — Seborrheic Keratoses

SOS — Son of Sevenless protein

SP — Substance P

SSR — Site-Specific-Recombinases

STC — Short-term Cell

TEMED — N,N,N',N'-Tetramethyl-Ethylenediamine

TPA — 12-O-Tetradecanoylphorbol-13-Acetate

TRP2	— Tyrosinase Related Protein 2
TSG	— Tumour Suppressor Gene
UTR	— Untranslated Region
UVR	— Ultraviolet Radiation
VEGF	— Vascular Endothelial Growth Factor
VGP-CMM	— Vertical Growth Phase of Cutaneous Malignant Melanoma

Summary

Despite many studies on pathology and aetiology during the past decades, the molecular mechanism(s) of melanoma development remains largely unknown. Therefore the purpose of this project was to establish a transgenic mouse model able to investigate the molecular mechanism(s) of melanoma aetiology mediated by N-Ras and PTEN genes. To achieve this, an inducible gene switch approach was employed exploiting the Cre/*lox*P recombinase system. This approach has the advantage of avoiding embryonic lethality and helps to minimise disease(s) in other tissue(s) that may interfere with animal viability. It was envisaged that this inducible system would establish a model that accurately mimic the development of melanoma in humans. A disadvantage being that the tyrosinase-based promoter was only responsive to the inducer when melanocytes were proliferating.

Initially, regulator vectors were created by sub-cloning Cre under the control of a melanocyte-specific promoter either enhanced tyrosinase (EICre) or tyrosinase related protein 2 (Trp2Cre). A Cre responsive, target N-Ras^{lys61} transgene was also cloned, where expression was induced by Cre ablation of 'Stop' cassette (cmv.stop.N-Ras^{lys61}) together with a report target transgene (cmv.stop.EGFP) to aid in expression characterisation.

The functional activity and gene-switch specificity of these constructs were subsequently confirmed employing co-transfection of regulator and report target into B16 melanoma cells, but to confirm their activity in primary melanocytes, melanocyte culture conditions had to be defined for optimum growth and transfection as there is no optimized commercial medium available for murine melanocyte culture unlike for human melanocyte. In this study therefore, murine primary melanocyte culture method (50/50) has been defined, which exploited keratinocytes for initial melanocytes growth support as a feed layer. The other advantages of this 50/50 medium were that pigmented cells grew without spontaneous transformation and gave the higher transfection efficiency compared to media

exploited by other groups. Using primary melanocytes cultured in 50/50 medium, transgene construction and identification of regulator expression were performed by RT-PCR *in vitro* prior to *in vivo* analysis thereby avoiding unnecessary breeding.

When concerns had arisen regarding an unexpected lack of melanoma phenotype *in vivo* particularly in addition of PTEN loss, this culture protocol supplied a successful test of oncogenic potential of N-Ras^{lys61} and PTEN loss *in vitro*, where N-Ras^{lys61} expression transformed melanocytes and PTEN loss promoted N-Ras^{lys61} to give more aggressive cells. However a functional redundancy was identified, as transformed colonies were not immortalized and eventually senesced, possibly due to their opposing gene functions being on the same signalling pathway; i.e. PTEN fails to provide additional genetic aberrant pathway(s) for the cross-talk with Ras signalling necessary to form malignant tumours.

The *in vivo* experiments commenced by crossing transgenic expressers of EICre regulator with target cmv.stop.N-Ras^{lys61}, to generate bigenic EICre/N-Ras mice. Treatment with Ru486 initially apparently failed to exhibit an abnormal phenotype, despite confirmation of N-Ras^{lys61} expression following hair plucking to initiate the hair cycle and anagen melanocytes proliferation, therefore Δ5PTEN$^{flx/flx}$ mutation was introduced. Unexpectedly, a similar result was obtained following treatment of EICre/Δ5PTEN$^{flx/flx}$/N-Ras^{lys61} and EICre/Δ5PTEN$^{flx/flx}$ in the test of whether PTEN functional loss promoted N-Ras^{lys61} tumourigenesis. However with time, at 12-15 months (systemic) Ru486 treatment, phenotypes of enlarged eyes and harderian gland adenomas were obtained in N-Ras^{lys61} expressing mice, whilst PTEN loss did not produce additional melanocytic phenotype.

This confirmation of *in vivo* activity prompted a more careful analysis of treated mouse skin that discovered the appearance of white hair at treated sites which gave a subtle grey appearance to the coat colour compared to age matched untreated littermates or non-

transgenic controls. Subsequent analysis found that melanocyte apoptosis was induced by N-Ras^{lys61} mediated by caspsase-3, and this may explain the lack of melanomas. This new finding implied the existence of a cell defence system to protect mice from oncogenic expression, as a general feature or to overcome specific mutations that have the potential to induce melanoma. Furthermore, the same apoptotic pathway mediated by caspase-3 was mounted against PTEN functional loss. This implied a potential surveillance mechanism to compensate for PTEN function loss and also verified *in vivo,* the functional redundancy in melanocytes between these two genes observed *in vitro*, as it may be that until the appropriate anti-apoptotic pathway overcomes this sentinel mechanism, PTEN loss synergism with N-Ras^{lys61} is insufficient for melanoma tumourigenesis.

Due to the lack of melanoma, given the well characterized effects of the microenvironment in melanoma development, this study assessed the consequences of keratinocytes disruption. This was achieved employing a keratinocyte-specific K14Cre regulator transgenic line, expressed in proliferative basal cells, hair follicles and stem cells. In Ru486-treated tetragenic compound K14Cre/EICre/cmv.stop.N-Ras^{lys61}/Δ5PTEN$^{flx/flx}$ mice pigmented papillomas were produced. This identified a melanocyte survival loop generated by microenvironment disruption that enabled anagen melanocytes to escape apoptosis during papillomagenesis. Furthermore, the mechanism involved elevated Kit/SCF expression in papillomas. The co-localisation of Kit and TRP-2 positive melanocytes in papilloma basal layers revealed that a Kit/SCF paracrine survival loop resulted in melanocyte survival. These results clearly demonstrated melanocyte cooperation with its immediate microenvironment consistent with the requirement for proliferative keratinocyte support of primary murine melanocyte cultures. Furthermore, these pigmented papillomas, may represent a model relevant to development of human seborrheic keratoses, which are pigmented benign lesions similar to papilloma, and neither nevi nor melanoma (4-6). These murine data suggest that these lesions may arise where papilloma formation occurs

alongside anagen and the Kit/SCF paracrine survival loop creates an environment in papillomas sufficient to incorporate the survival and proliferation of anagen melanocytes, although the further studies are necessary to confirm this.

To date, most transgenic melanoma models employ H-Ras, with only recent development of a relevant N-Ras model where constitutive, but not inducible, N-Ras^{lys61} expression throughout embryogenesis eventually gave a hyperplastic melanocyte phenotype which is consistent with the report of N-Ras mutation common in congenital nevi but less in acquired nevi (9-13). As with H-Ras models, it appears that the CDKN2A locus deficiency is necessary for melanoma aetiology. In this study, unlike CDKN2A, PTEN loss failed to promote N-Ras melanoma tumourigenesis. This is possibly due to regulating the same signalling pathways, creating a functional redundancy, and the same susceptibility to apoptosis from newly identified potential compensatory surveillance systems. These results show the necessity of cross-talk between multiple genetic pathways to achieve malignant tumour formation and also the advantage of an inducible gene-switch approach to identify useful compensatory systems by allowing addition/deletion of many different interesting genes. Taking the insights from this study further, logically the introduction of p16/p19 deficient mice and/or other melanocyte/melanoma development related genes (specifically not on Ras signalling pathway, e.g. MC1R pathways) would provide an up-to-date, superior mouse model able to mimic molecular aetiology of human melanoma to investigate the functions and mechanisms of other genes such as MITF, B-Raf, MC1R etc involved in the development of human melanoma.

Acknowledgement

My first thanks are to my wife who looks after me and gives me all of her support, my daughters who can give me comfortable hugs when the situation was not good and all of my family members for their love and encouragement.

A big thank you to Dr David Greenhalgh for his efforts to make this possible, his supervision and guidance, and specifically to his hard work on my English.

Many thanks go to Dr Malcolm Hodgins and Dr Mike Edward for their kind and helpful support.

I would also like to thank Dr Jean Quinn for the transgenic mice production and her general help in the lab, Dr Eve Kandyba for her help on immunofluorescence staining and Mr Graham Chadwick for his IT support.

A special thank you to Mrs Pamela Sutherland for her little/big help during my last a few years in dermatology.

Thank you very much, Professor Hugh Willison, for your encouragement and it is impossible for me to resubmit this thesis without your sympathetic and kind encouragement.

Chapter 1: Introduction

1.1. Overview of melanoma and mouse models

Melanoma is a cancer that arises in pigment producing melanocytes that differentiate from neural crest progenitor cells during embryonic development and is most frequently found on skin, eyes and mucosal surfaces. As with all cancers, melanoma aetiology is a multistage process (14). Thus it has been suggested that melanoma develops as a series of lesions initially from a benign melanocytic nevus (BN), through melanocytic dysplastic nevus, to the radial growth phase of primary melanoma (RGP-CMM) followed by the vertical growth phase of primary melanoma (VGP-CMM) and finally to metastatic melanoma (15-17). Although, while it remains arguable whether melanoma does indeed develop directly from benign melanocytic nevus (18-20), it is clear that in human melanoma the most clinically critical stage is the progression from the relatively benign radial growth phase (RGP) to the vertical growth phase (VGP) which is more likely to bear deadly metastatic potential (21;22).

The frequency of malignant melanoma is increasing all over the world with over 132,000 malignant melanoma cases reported globally each year and whilst melanoma is the lesser of the common forms of skin cancer basal cell carcinoma (BCC) and squamous cell carcinoma (SCC), it is by far the deadliest, given that it is the most likely to metastasize and thus is responsible for 6 of every 7 deaths from skin cancer (23-25). Moreover, melanoma is one of the fastest growing cancers in the USA with a steady 3% annual increase in incidence since the 1970s (3) given increased sun exposure, and it is estimated that each hour, one person in the United States dies from melanoma (26) and alarmingly, there has been a 10 percent increase in new cases of melanoma from 2004 to 2005 (25). Similarly in the UK the incidence of melanoma is increasing, with approximately 10 cases per 100,000 populations *per annum* both in men and in women. (27-29;29).

Although the exact aetiology of melanoma remains unclear, melanoma is believed to be a

multifactorial disease in which many different environmental and genetic factors contribute to the development of disease. Overexposure to ultraviolet radiation (UVR) is widely accepted as the underlying cause for melanoma development by dysregulation of immune system (30-34). There is accumulating evidence to show an association of melanoma with UV radiation, specifically of the intensive episodic exposure during the childhood and an increased incidence of malignant melanoma development in their later life time (35-38). Results from mouse model studies confirmed that neonatal UV exposure is critical for malignant melanoma induction. A single UV exposure for short time (16 minutes) on 2–3 days old pups are able to induce *in situ* cutaneous malignant melanoma in pigmented transgenic mice initiated by H-Ras activation, with a penetrance of 57% by 12 months (39). Furthermore, a single dose of UV irradiation of hepatocyte growth factor/scatter factor (HGF/SF) mice at age 3.5 days resulted in melanoma development in adults (40). Therefore, experts suggested keeping children away from intensive UV exposure as an effective practical way to prevent melanoma development in later life. This effort may have had an effect on the decreased melanoma mortality rates, the onset of melanoma incidence levelling out and beginning to decrease in younger Australian cohorts as a result of increased photo protection (41). Recent studies show the trend of increasing melanoma incidence has halted, as in Swedish children (42), while the incidence of invasive melanoma among people younger than 35 stabilised since the Queensland Melanoma Project was launched in early 1960's. Although there maybe an element of a birth cohort effect as suggested for non-melanoma skin cancers by Giles (43), the primary prevention effort to decrease the overall melanoma incidence will take at least another 20 years (44) and a programme geared to early detection was believed to contribute to the increased melanoma incidence (45;46). Nonetheless, that the public campaign of UV protection contributed to the eventual decrease in melanoma rate was implied by the analysis of melanoma cases on the Victorian Cancer Registry, Melbourne, Australian in 1996 and 2000, which revealed a significant decrease in rates of tumours < 1 mm thick in 2000;

whereas little change (not significantly) in the age-standardized annual incidence per 100,000 people of in-situ or invasive melanoma was recorded (47).

To investigate the molecular mechanism(s) of disease development *in vivo*, conditional transgenic approaches, compared to the un-conditional transgenic technology, offers tractable models to aid in stage related disease developmental verification and functional analysis of disease susceptibility gene(s). However, as reported in this study, generation of a transgenic mouse model of inducible melanoma has proven more difficult than for other diseases, due to the murine melanocyte physiology, and in general the mouse has been a relatively poor model until recently with the advent of conditional approaches that prevent alternate disease(s) or lethality during oncogene expression or tumour suppressor gene (TSG) ablation.

1.2. Biology of the skin

1.2.1. General biology of skin

The external covering of an animal is skin which separates the organs from the surrounding environment to provide protection from harmful UVR and other harmful factors (including biological, physical and chemical insults). It perceives changes in the environment (e.g. temperature) and then communicates to the other organs of the body to activate the homeostatic systems that protect animals from environmental extremes.

1.2.2. Structure of skin

The skin consists of three layers: epidermis, dermis and subcutis. The external surface of the skin is the impermeable epidermis which has a multilayered, stratified structure. The epidermis is composed predominantly (95%) of keratinocytes that produce keratins which constitute 30% of the protein in the basal cells of the stratified epithelium and >85% in fully differentiated squamous. Epidermis expresses predominantly two pairs of keratin polypeptides. Basal cells express K5 and K14, whereas K1/K10 pair is only synthesized in differentiating epidermal cells following basal cell division and entry into the first suprabasal layer. The differentiation status of keratinocyte is controlled by extracellular calcium concentrations which are varies with epidermal location. Calcium concentration increases gradually from proliferative keratinocytes in the basal layer, through spinous and granular layers to the terminal differentiated, cornified layer of skin (48-50). Comprising approximately 5% of interfollicular human epidermal cells (but not mouse, see below) are the melanocytes, each surrounded by approximately 50–60 keratinocytes to form the so called ‘epidermal melanin unit’ that result from the close interaction between the epidermal melanocytes which synthesize melanosomes and the keratinocytes which acquired the melanosomes secondarily and served in their transport to localise above the nucleus (51;52). The epidermal melanin unit was proposed as the fundamental integrated multicellular system for melanin pigmentation.

The dermis, lies under the basement membrane and is conjugated to the epidermis through the dermal-epidermal junction to provide additional supportive structures to the skin. The dermis is composed mainly of a structural collagen matrix, elastin and ground substance although there are also epidermal appendages, nerve endings, resident cells and vessels embedded within the dermis. Below the densely packed dermal connective tissue is the subcutis layer, composed of fat lobules separated by fibrous trabeculae. This layer extends from the lower dermis to the fibrous surface of muscle, bone or cartilage and again its nature and composition varies between anatomical sites.

1.2.3. Hair follicles and the Hair Cycle

Most areas of a mammal's body are covered by a pilosebaceous structure with varying dense population dependant on the localization of body. This pilosebaceous structure is derived from the primitive epidermis and consists of a centrally positioned hair follicle. The hair follicle displays different histology during the hair cycle which runs from the proliferative anagen to the apoptotic catagen and the resting telogen phases. A typical mature hair follicle can be divided into three different parts (Fig 1): the lower portion (a transient component which exists only in the anagen and regresses in catagen phase of hair cycle) extends from the base to the insertion of the erector pili muscle; the part extending from the insertion of erector to the sebaceous duct is the middle portion where melanocyte stem cells reside in the bulge region (53); and the upper portion extends from the duct to the epidermal surface (54;55). In human skin, follicular melanocyte stem cells are thought to migrate to "niches" lacking melanocytes (53) and are potentially the source for both melanocytes of the hair follicle and of the epidermal melanin unit. However in murine skin, melanocytes are confined to the hair follicles (except a minor population in ears, tails and foot pad) as they mainly provide pigmentation for the hair (56;57) and are mostly absent from a resting follicle. Although the number of hair follicle in an adult mammal seems to

be fixed, following stimulation, telogen phase hair follicles re-enter hair cycle and new anagen follicle grows from the stem cells resting in the bulge region located within middle portion, to give a new population of proliferating melanocytes (56;57).

The ‘follicular-melanin unit’ resides in the proximal hair bulb of a typical hair follicle and consists of hair matrix melanocytes and keratinocytes, and partly regulated by the dermal papilla fibroblasts (58). Unlike the melanocytes in the epidermal melanin unit where every single cell is surrounded by approximately 50-60 keratinocytes, every melanocyte in the follicular-melanin unit is accompanied by about five keratinocytes in the hair bulb as a whole with the ratio of almost 1:1 in the basal epithelial layer next to the dermal papilla (59). In mice the follicular melanocytes are derived from pre-melanocyte melanoblasts/stem cells which migrate from the neural crest and arrive at the foetal epidermis and subsequently migrate to the developing follicle in neonates via SCF signalling during hair follicle morphogenesis to subsequently reside in the hair bulge/sub bulge region (53;60). Typically, these pigment cell sub-populations differ from epidermal melanocytes by being larger, more dendritic and by producing larger melanosomes after they have reached their respective distinct anatomic compartments of hair bulb (61)

Hair bulb melanocytes are activated cyclically, with melanogenesis being tightly coupled to the hair growth cycle (62) (Fig 1). Hair grows throughout a finite period of hair shaft formation (anagen), followed by a brief regression phase that results in the apoptosis-driven resorption of up to 70% of the hair follicle and when the majority of melanocytes die off following the hair bulb regression (catagen), and by a relatively quiescent period (telogen) when the transient portion of the hair follicle disappears (reviewed in (58)). Although the hair bulb melanocytes generate cyclically, the hair bulb melanocyte system has been perceived as self-perpetuating. Therefore, although fully differentiated melanocytes in the hair bulb undergo apoptosis during catagen and are removed from the regressing hair

follicles (63), some less-differentiated melanocytes appear to survive in catagen phase (64).

The ‘‘re-differentiating’’ melanocyte of early anagen is likely to be a newly recruited immature melanocyte derived from a melanocyte reservoir stem cell located in the bulge region (Fig 1). Using a TRP2-lacZ transgenic mouse model, Nishimura *et al* revealed that melanocyte stem cells are not only immature, but also slow cycling, self-maintaining and are fully competent to regenerate progeny at early anagen, following hair cycle initiation. These cells not only provide the source of re-differentiating melanocytes in the hair bulb, but also have the capacity to enter vacant niches, including via migration to, the epidermis (53). Interesting, by investigating the effects of hair cycle phase on BCC tumourigenesis induced by radiation in mice lacking one Patched allele (Ptc1neo67/+), Mancuso *et al*, revealed that early anagen of hair cycle irradiation was highly susceptible to tumour induction (65). Moreover, tumour histology demonstrated a qualitative difference in BCC tumourigenesis, depending on hair growth phase at the time of exposure. An association of tumour and follicular outer root sheath of anagen skin was also revealed by examination of anatomic and immunohistochemical relationships. These results confirmed the role of follicular bulge stem cells and their progenies with high self-renewal capacity in the formation of basal cell tumours (65).

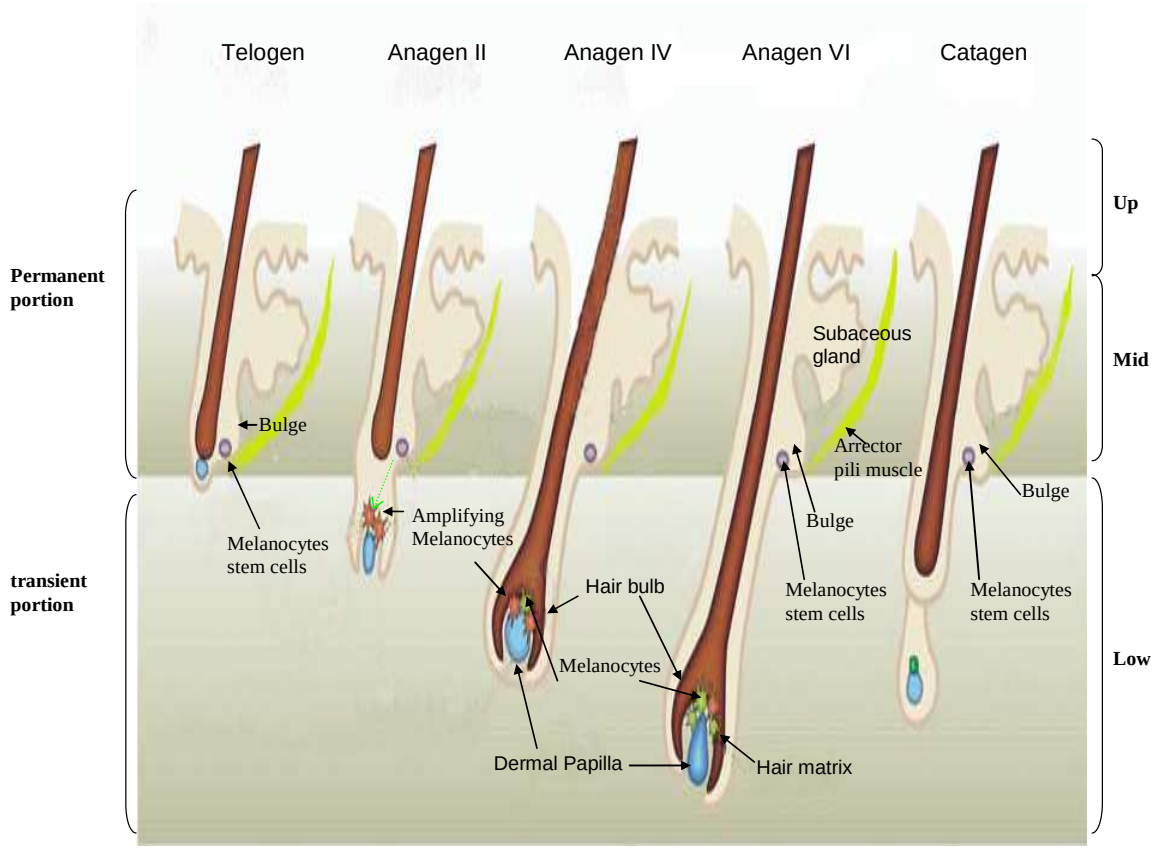

Figure 1: Typical structure of the hair follicle and the cycle of hair follicle development. The lower portion of a typical follicle (the base to the insertion of the erector pili muscle) is a transient portion in anagen that regresses in catagen; the middle portion where the follicular melanocyte stem cells reside, the part between the insertion of erector and the sebaceous duct; the upper portion extends from the duct to the epidermal surface (modified from Nishimura *et al*, Nature 416: 854, 2002). .

1.2.4. Melanocytes and pigmentation

The hair, skin and its pigmentation protect the body from harmful UVR, electro-magnetic radiation and other environmental insults such as physical, chemical and biological factors (25;66-69). In this highly complex regulation, a study by Bohm et al, demonstrated that one important molecule was α-MSH which regulates UVB induced apoptosis of human melanocyte. α-MSH not only induces photoprotective melanin synthesis but also reduces UVR induced DNA damage to protect skin from harmful UV radiation (66).

The pigmentation is produced by resident epidermal dendritic cells, the melanocytes, which are neural crest-derived cells and differentiate from melanoblasts which actively migrate during development to their final destinations including the eye (choroids), the mucosa lining, the upper aerodigestive tract, the anorectal region, the inner ear and the skin where they terminally differentiate (70-73). The only pigment cells not arising from neural crest precursors are those of the retinal pigment epithelium (RPE), iris and ciliary body which are derived from epithelial cells in the optic cup (1). As revealed from studies of mostly murine models, follicular pigmentation is under complex genetic control involving more than 150 alleles at over 90 loci (74;75).

1.2.5. Differences between melanocyte development in mouse and human skin

In general, the structure and histology of mouse and human skins are quite similar. Melanocyte developmental biology, however, is obviously different between these two species. Unlike human, mouse inter-follicular melanocytes decline from birth —fewer melanocytes were present at day four in the epidermis and non-follicular epidermal melanocytes could not be detected at day eighteen after birth —and epidermal melanocytes are localised to the follicles where they increase after the birth for about two weeks and decline as the hair growth ceases on progression from anagen to catagen (56;57). Thus, most proliferative murine melanocytes are located in the follicles and protected from UV radiation —hence studies revealed that UV treatment initiates and promotes various

tumours including SCC, BCC, papilloma and fibrosarcoma but little melanoma (76). Indeed, the adult mouse skin is almost devoid of melanocytes except during the anagen phase of the hair cycle, which can be induced following environmental/experimental stimulation (e.g. hair plucking) when melanocytes arise from the melanocyte stem cells. Because there are few interfollicular melanocytes when the skin is in the resting telogen phase, it is very difficult to induce melanoma by chemical carcinogenesis and UVR exposure in the mouse (57;57). Thus, in contrast to the other tumour models, the mouse had not been a good model for studying melanoma. This has now changed by employing transgenic and gene knock out/in technologies (1-3;23;77-82) that allow modelling various pathway defects and couple to UV exposure.

1.3. Introduction to melanoma

1.3.1. Incidence of melanoma

The number of melanoma cases worldwide is increasing faster than any other cancers (review in (83-85)). Between 2 and 3 million non-melanoma skin cancers and approximately 132,000 malignant melanomas occur globally each year. Alarmingly, it is estimated that there are 4500 melanoma cases attributed to the estimated 10% decrease in ozone levels world-wide (24). Although excellent prevention and early diagnosis education programmes have levelled out the melanoma incidence in the past years, Australia still has the highest melanoma incidence with a lifetime risk of currently at 1 in 29 (86). In the USA, the incidence has increased 2000% since the 1930s and stands at a lifetime risk of 1 in 62 in 2005 (24). In the UK melanoma incidence increased from 1.7 to 8.0 for men and 3.1 to 9.7 for women respectively per 100,000 population from 1971 to 1997; and in Scotland from 1979 to 1998, the age-standardized incidence rose three fold for male and two fold for females per 100,000 population (21;83).

1.3.2. Risk factors in general

The exact aetiology of melanoma currently remains unknown, however, it is commonly considered a multifactorial disease. Many different factors including genetics and behaviour are believed to predispose an individual to an increased lifetime risk of melanoma development. Major host factors include a family history of skin cancer, i.e. susceptibility genes; the number and type of nevi, and skin type/pigmentation have also been identified to give an individual and/or combined contribution. An association of melanoma and exposure to UVR has been extensively reported and UVR is now believed to be the most causal environmental factor contributing to increased melanoma risk (30;38;40;42;66;68;69;77-79;87-103). Those people, with fair skin, blue eyes, light coloured hair, many moles, freckles and who burn rather than tan, especially during childhood or who genetically have a family history of skin cancer, have a significantly

higher risk to develop melanoma in their life time than those people who have dark skin, brown eye, fewer moles, non-family history of skin cancer or are well protected from UVR exposure (24).

1.3.3. UVR contribution to melanoma

UVR can cause both non-melanoma skin cancer and fatal cancer of malignant melanoma. The extensive studies of an association of UVR and melanoma revealed that UVR causes melanoma through DNA damage, escape from cell growth arrest leading to failed DNA repair, resistance to apoptosis and re-entry into the cell cycle resulting in deregulated proliferation (23;106-109). Since VJ McGovern suggested an association between UVR and melanoma back in 1952 ((104) reviewed in (23)), the relationship of UVR and melanoma has been extensively studied and therefore, UVR is now believed to be the most important environmental factor to the increased risk of melanoma although some cases (i.e. vulva melanoma) are apparently not linked to the UVR (105).

There are accumulating evidences to show an association of UVR, specifically intensive episodic exposure during childhood and an increased incidence of malignant melanoma (35-38). Such an association has also been proven by a transgenic model employing metallothionein-gene promoter to force HGF/SF over expression in skin melanocytes and keratinocytes. UV irradiation of mice at age 3.5 days, 6 weeks or both, showed that melanoma development following UVR at both day 3.5 and 6 weeks was indistinguishable from that seen in single dose irradiation at day 3.5, whereas single dose irradiation at 6 weeks resulted in no melanoma development (40). Also recently, a single low dose of UV exposure on mouse pups aged 2-3 days produced malignant melanoma with a penetrance of 57% within 12 month. Hacker *et al*, confirmed that neonatal UV exposure is critical for malignant melanoma induction, whilst H-Ras alone transgenic mice failed to produce any melanoma (39).

The neonatal melanocyte is more susceptible to UVR induced transformation than adult melanocyte, however the exact mechanism is unclear, but may derive from population of immature and not fully differentiated melanoblasts/stem cells with proliferative potential, still located in newborn skin epidermis (as in human skin) unlike in adult the fully differentiated melanocytes which are invariably located in the papillary dermis in adult dorsal skin where the cells are better protected. Therefore, UVB exposure at the neonatal stage (children in human), accelerated the development and increased the risk of melanoma. Thus, WHO suggested that protecting children from sun burn is a good sensible and practical way to prevent melanoma development in their later life, especially those who have a family history of melanoma and thus may carry melanoma susceptibility gene(s) e.g. CDKN2A ablation.

1.3.4. Individual risk factors

1.3.4.1. Family history

An association of family history and melanoma is a general concept (88). There is no significant histological difference between familial and sporadic melanomas. Possibly due to the increased awareness of melanoma development among those family members, however, familial melanomas have some common factors which include development of disease at an earlier age, with a relatively smaller tumour size and lower Clark's level compared to sporadic melanomas (110). Familial melanoma patients also have bigger, more numerous nevi on the body and are more likely to develop multiple primary melanomas, but they display a decreased risk of other non-melanoma skin cancer development (110;111).

Based on a study of approximately 3000 patients versus 4000 control cohorts from many countries, geographically located in wide range of latitudes, thus ignoring the association of

melanoma risk and UVR, Ford *et al*. revealed that first-degree relatives of individual melanoma patients had a 2-fold increased risk compared to people without a family-history. Such an increased risk was also independent of age, number of nevi, hair and eye colour as well freckles (112). Several other studies also support the idea that a family history of melanoma stood as an independent high risk factor to the development of melanoma (113-115). For instance, Begg *et al* examined melanoma incidence in the relatives of 2508 patients in relation to population incidence rates, and the authors concluded that the relatives of melanoma patients were at a higher risk to develop melanoma, especially where relatives had been diagnosed at a young age (116).

1.3.4.2. Number and type of nevi

The total number of melanocytic nevi on the body, either congenital or acquired, has been demonstrated to have a strong association with cutaneous melanoma development whether self counted (117) or by examiners. Moreover, this association is not affected by the type of nevi (118-126). The evidence to support the relationship of nevi and melanoma is still accumulating. After a comprehensive literature search, Watt *et al* conducted a systematic analysis of existing data and analyzed results from eight studies containing a total of 432 large congenital melanocytic nevi patients, the results confirmed that large congenital melanocytic nevi and total nevi numbers were associated with increased risk of melanoma development (127). Data obtained from 295 families unselected by family history and 53 melanoma-prone families revealed that number of nevi influenced melanoma incidence in both families (128). More recent studies involving various numbers of patients and control cohorts are supportive for considering the number of nevi on the body as an independent melanoma developmental risk regardless of the type of nevi being either benign or atypical (113;129-132). In addition to Caucasian populations, in the Japanese, the number of nevi was also identified as a high risk factor for non-acral melanoma development but not for acral melanoma (133). In a study, a multivariate model, carried out by Nijsten *et al*

revealed that people with three or more atypical nevi were at a more than 10-fold increased risk of developing malignant melanoma compared to those without atypical nevi (134). Richtig *et al*, found 35.3% of ocular melanoma patients had more than 5 dysplastic nevi compared to only 1.2% in the control cohorts which suggested that more dysplastic nevi could be among the high risk factors for ocular melanoma development as well as cutaneous melanoma (135). Thus the total number of nevi (regardless of type) and number of dysplastic nevi can both be considered as independent melanoma high risk factors.

1.3.4.3. Other host factors

In addition to a family history of skin cancer and the number/shape of nevi, other host factors including fair skin, the colour of eye and hair, freckles, age and sex have also been studied as individual risk factors for melanoma development. In general, white populations exhibited over a wide range average higher risk for melanoma development and females commonly have a higher incidence than males while non-white populations displayed a much lower incidence of melanoma development (94;136). Red hair conferred a two fold increased risk, which was not affected by adjustment for freckling, the number of nevi or skin colour. Light skin colour, light eyes and extensive freckling also showed an association with increased risk of melanoma development (130;137). Cho *et al* revealed that older age or light hair colour was each associated with significantly elevated risk of melanoma (113) and studies from Nijsten and Strouse *et al* confirmed age is also among those high risk factors of melanoma development (134;138).

1.3.5. Summary of incidence factors

The actual aetiology of melanoma development varies among different cases and individual studies initiated by different consortia that took into account many risk factors, revealed that a conglomerate of individual factors were associated with melanoma risk. Among all factors, UVR is the most intensively studied and is now believed to be the most important environmental aetiologic factor. The strongest evidence for this conclusion comes from the broken increasing trend of melanoma incidence in children in Sweden and the stabilized incidence of invasive melanoma among those people younger than 35 years, who were born when the Queensland Melanoma Project was launched in early 1960's. Each host factor, including susceptibility genes, family history of melanoma, total number of nevi and/or dysplastic nevi, type of skin, eye and hair complexion, age and sex, could be identified as an independent contributor to the high incidence of melanoma development, if it was isolated from the other ones for statistic analysis. As an independent melanoma high risk factor, however, any of such host factors could 'co-operate' with environmental UVR due to the common behaviour within the same family and therefore, the study of defining the exact mechanism underlying aetiology of melanoma will be a really complex project.

1.4. Genes and Melanoma

1.4.1. Melanoma genes in general

Whatever factors cause tumour development, the hallmark is the acquisition of multiple genetic defects involving the inactivation of tumour suppressor genes and/or activation of proto-oncogenes. In cutaneous melanoma, non-random deletions and rearrangement are seen in several regions of chromosomes including 1p, 6q, 7q, 9p, 10q, 11q, 12q, 17q, 18q and 20q (14;139-144). As mutation or loss of chromosome regions 1p36, 9p21 and 12q14 occurred at high frequency in cancer prone families, some tumour suppressor genes which were located within these deleted regions became associated with melanoma have been subsequently identified as familial melanoma susceptibility genes (139;145-147). The most intensively studied TSGs involved in melanoma include p53, PTEN, CDKN2A (including $p16^{INK4a}$ and $p19^{ARF}$), Kit/SCF, the oncogenes B-Raf, Ras, MITF, as well E-cadherin which acts as an anti-invasion gene and switches to N-cadherin expression to facilitate invasion through the dermal matrix. In addition to familiar melanoma TSGs, melanoma susceptibility genes such as MC1R, GST and many others, have been reported to modify and influence melanoma development. However the molecular mechanism of melanoma development is still poorly understood, although it is being intensively studied employing many different models.

1.4.2. Ras genes

1.4.2.1. Ras Family

It was more than four decades ago that the first Ras member was discovered from the observations of viruses causing tumour formation in mice (148). The viral genes responsible were called ras for rat sarcoma, and subsequently turned out to be mutated versions of mammalian genes that encode enzymes with intrinsic GTPase activity involved in trans-membrane signalling as molecular turnstiles. Following the discovery of H-Ras, later K-Ras (149) and N-Ras were discovered by transfection of human tumour DNA into

NIH 3T3 cells (150). These thus form the classic Ras family group of the small GTPase superfamily and express closely related p21 Ras proteins with similar transmembrane signalling functions.

Ras is a small GTPase, a name to distinguish from the large heterotrimeric GTPases, which functions as a molecular switch determined by the binding status of GDP-Ras (guanine diphosphate, inactive form) or GTP-Ras (guanine triphosphate, active form). GDP-bound Ras proteins are activated by GEFs, a large structurally diverse class of proteins family termed for Guanine-nucleotide Exchange Factors, which catalyze the release of GDP and then the displaced GDP is rapidly replaced by more abundant GTP to form the active GTP-Ras form (151). Various GTPase activating proteins (GAPs) also bind to Ras proteins in their GTP-bound state. GAPs act as negative regulators by greatly enhancing the low intrinsic GTPase activity of the Ras proteins through hydrolysis of GTP to GDP to cause an allosteric change of the Ras to the inactive state.

By cycling between GTP- and GDP-bound states, Ras proteins switch their binding to effectors on and off. Well-recognized downstream effectors of Ras proteins are the mitogen-activated protein kinase (MAPK) signalling system including Raf kinase and phosphatidylinositol 3-kinase (PI3K), which is a negative regulatory target of the PTEN TSG (152). Ras-dependent Raf activation promotes cellular proliferation while the activation of PI3K sustains cell survival. The functions of these GTPases are not limited to their roles in cell growth, proliferation and cell survival, Ras expression is also involved in cell migration and adhesion by causing marked changes in integrin profiles (153). A surprising recent development of Ras gene study has been the discovery that germline mutations can occur in genes encoding Ras proteins and other components (e.g. B-Raf and MEK) in these signalling pathways, resulting in developmental defects such as Costello syndrome, Noonan syndrome (Fig 2) (154;155) although it is not expected that continual

expression of fully activated Ras is not sufficient for complete carcinogenesis, underlining the fact that many other molecular steps are needed for progression to tumour formation (152).

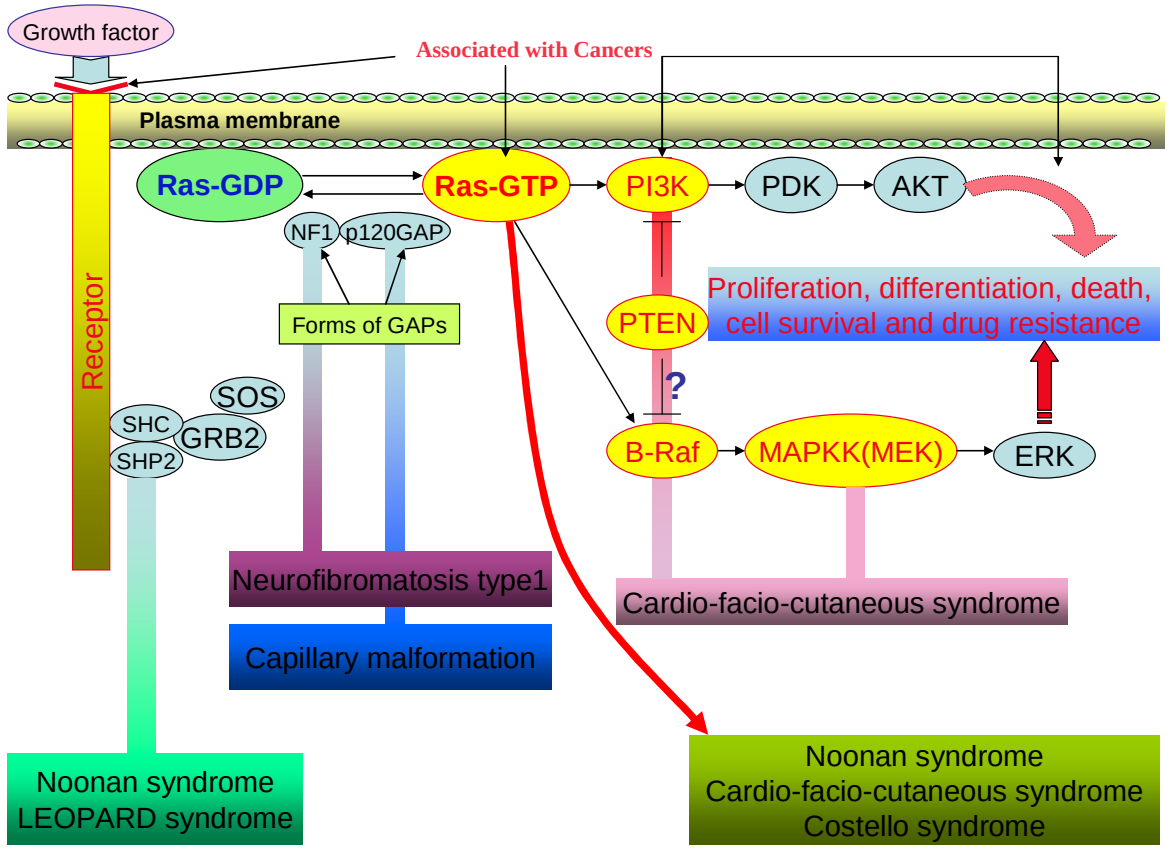

Figure 2: Mutations of Ras Signalling pathway are associated with human diseases other than tumourigenesis (modified from Downward J, Science 314 (5798): 433-434, 2006). Germline mutations can be occurred in genes encoding Ras proteins and other components (e.g. B-Raf, PTEN as well GEFs and GAPs) in these signalling pathways, resulting in developmental defects such as Costello syndrome, Noonan syndrome, Capillary malformation rather than tumour although it is not expected that cells are tolerant of continual expression of fully activated Ras.

1.4.2.2 N-Ras

Human N-Ras was the third discovered member of the Ras family being initially recognized in 1982 by DNA transfection of NIH 3T3 cells (150) and almost simultaneously isolated from a human fibrosarcoma cell line HT1080 (156), a neuroblastoma line SK-N-SH (157) hence N-Ras, and the promyelocytic leukaemia line HL60 (158). Cross-hybridization to the other cloned Ras genes (H- and K-) implied it to be a member of the Ras gene family and studies with somatic cell hybrids located it to chromosome 1p32 (156;159). A complete biological functional transforming or activated N-Ras together with its normal N-Ras proto-oncogene were isolated from human fibrosarcoma cell line HT1080 and normal human fetal liver tissue respectively (160).

Sequencing analysis concluded that N-Ras encodes a 189 amino acid sequence with a predicted size of 21-KDa protein and homology to functional human H- and K-Ras genes. Comparing the coding sequence of the three genes, it is revealed that N-Ras differs by only 15% of amino acids and 27% of nucleotides (within the coding sequence) from H-Ras, (16% and 24% for K-Ras respectively), but these differences are not evenly distributed throughout the whole coding sequence. The first two exons have an almost identical amino acid sequence, differing by only 4 amino acids out of 97 whilst the third exon shows a little more divergence of 9/53 between N- and H-Ras. The most striking divergence between N-Ras and the other two Ras proteins are within the 4^{th} exon (49 amino acids) with a 15 amino acids difference from H-Ras, whereas 22 positions are different from K-Ras. This major variable region is located near the C terminus just upstream from a conserved cysteine residue that is required for post-translational processing, membrane localization and transforming activity of the proteins. C terminus of the p21 Ras protein within exon 4 is necessary and sufficient to anchor the protein on the plasma membrane and the binding of lipid through Cys-186 is required for the migration of the protein from its synthesis in the cytosol to the plasma membrane (161). It is likely, therefore, that the fourth exon-

encoded domain of the p21 protein product of Ras genes may play a vital role in determining the different functions of three Ras gene products (162).

As indicated above, the location of the introns within the coding sequence is identical for all three Ras genes. The sequence and length of each intron, however, are significantly different, hence the size of the whole genes are dissimilar. Thus, the K-Ras gene spans more than 35-kb, whereas N- and H-Ras genes span approximately only 7- and 3-kb respectively. Furthermore, the structural difference of the Ras mRNAs is also considerable, in contrast to the 1.2-kb H-Ras transcript (163), K-Ras produces a much larger 5.5-kb transcript which produces two subtypes of K-Ras 4A and 4B by alternative coding of fourth exons (164;165), whereas N-Ras produces two transcripts of 2.2- and 5.2-kb in length (156;158;160). There is no publication yet to show whether these two different transcripts of N-Ras produce different functional subtype proteins as K-Ras does by alternative reading frame.

1.4.2.3. Ras mutation in human cancer

Activating Ras gene mutations are estimated to occur in 25-30% of human tumours. N-Ras mutations are common in leukaemia (166) and melanoma, whereas K-Ras mutations are almost ubiquitous in pancreatic tumour and also quite common in lung and colorectal cancers, whilst H-Ras mutations are found mainly in bladder and kidney cancers (166-168). In many tumours where Ras gene mutations are absent, the Ras proteins are often overexpressed (169;170). Dysregulation of the Ras activation state also contributes to human cancers, for instance many growth factor receptors and Ras GEFs possess transforming properties, whereas both neurofibromin NF1-a Ras GAP or Ras association family member 1A (RASSF1A), a putative Ras inhibitor, act as tumour suppressor genes (171;172). Often as a counter to oncogenic Ras expression in both primary rodent and human cells, a permanent G1 arrest is accompanied by accumulation of p53, $p16^{INK4a}$ and $p21^{CIP1}$ (173). Activating Ras mutations are commonly found at codon 12, 13 or 61, which

render the encoded GTPase protein constitutively active and thus subsequently growth stimulatory (167). The Ras family of small GTPase proteins functions as a relay switch downstream of cell surface tyrosine kinase receptors and upstream in the Ras-Raf-MAPK-Erk signalling pathway respectively, which transduces various growth signals from the cell surface to the nucleus (168) (Fig 2).

The K-Ras mutation studies found that the majority of mutations were at codons 12, 13 and 61(174-176). These mutations are somatic rather than germ-line and consist of single base-pair substitution which leads to the single amino acid change. While the wild-type K-Ras gene encodes for glycine at codon 12, the most common amino acid substitution was found to be aspartic acid most for glycine (46%), followed by valine (32%), arginine (13%), cysteine (5%), serine (1-2%) and alanine (<1%). Such mutations result in constitutive activation with Ras state in the GTP-bound and cell proliferation (174;175).

In human, primarily observed Ras mutations are H-Ras gene rather than K-Ras or N-Ras in the cancers of urinary tract and bladder (166). The loss of abnormal H-Ras allele and amplification of mutant H-Ras were also found in aggressive breast cancer (180). One tenth of GTPase activating proteinase activity of the wild type H-Ras revealed the role of cell proliferative promotion by H-Ras mutation (179).

H-Ras can be activated by truncation of a 5' uncoding exon (exon-1) in absence of mutation (181) leading to over expression of the normal allele, thus the specific point mutations of H-Ras codons may not be necessary for transformation. However, in various chemicals (dimethylbenzanthracene-DMBA, dibenz[c,h]acridine-DB[c,h]ACR or benzo[a]pyrene - B[a]BP) induced mouse skin cancer models either by complete or initiation-promotion protocols as well in hepatoma model (4-aminobiphenyl - 4-ABP) induced tumours have a specific A----T transversion at the second nucleotide of codon 61, the hottest mutation code

for the other two Ras alleles (K-, and N-) in human cancers, of the H-Ras gene(182-185). The G12V and Q61L versions of H-Ras were initially discovered as the consequences of oncogenic mutations in H-Ras genes and later shown to result in a constitutively active form of H-Ras (165;177). G12E mutation of H-Ras was revealed by analysis of nine mammary carcinomas induced by a single injection of nitroso-methylurea into 50-day-old Buf/N female rats, contained a transforming H-Ras-1 gene (178). And in human, analysis of primary SCC and BCC occurring on sun-exposed body sites for mutations in codons 12, 13, and 61 of H-Ras revealed that there were 46% SCC and 31% BCC harbouring a specific mutation at the second position of H-Ras codon 12 (GGC----GTC), predicting a glycine-to-valine amino acid substitution (186). Such an unusual high incidence for H-Ras, possibly reflected the Caucasian population employed in this Texas-based study, is in conflict with the previous study (187) and a latter study carried out by Campbell et al in which the authors are capable to detect 4-8% of the total alleles of Ras mutation, while there is no mutation at all in all screened BCC and SCC samples (188).

N-Ras mutations are primarily detected in Leukaemia (166), but also detected in many other diseases including melanoma (see below), non-melanoma skin cancer, brain cancer, stomach cancer, myelodysplastic syndrome, thyroid cancer, embryonic lung cancer and rhabdomyosarcomas (187;189-195). In malignant melanoma, various reports cite a high mutation rate of N-Ras which remained the hottest mutated and most studied gene (9;196-201) until the discovery of the B-Raf V600E mutation (200). In melanomas, as with N-Ras activation in the human fibrosarcoma cell line HT1080 (160), sequence comparison with normal alleles showed only one base pair difference at codon 61(202). Both functional and genetic evidence indicate that B-Raf and N-Ras act linearly in the signalling pathway, which is confirmed by almost mutual exclusiveness of mutations in these genes and consequent Erk activation (200;202-204).

1.4.2.4. N-Ras mutation in melanoma

In melanoma it is the N- allele of Ras family activated typically via mutation at codon 61. Initial reports of association of N-Ras and melanoma suggested a mutation frequency of approximately 5-10% (205;206) but later studies have shown that the frequency was higher than previously thought. Ball *et al* showed up to 69% N-Ras mutations at codon 61 in malignant melanoma (207), whereas the other detectable mutation rates are various from 13 to 46% employing different type and number of analysed samples (9;196-201;208). Comparing sequences of both the active and inactive alleles at the very first time of N-Ras gene isolation, the only difference detected between two alleles was a C to A transversion at codon 61 which results in an amino acid alteration of glutamine (CAA) in the normal gene to lysine (AAA) in the transforming allele (160). This result indicated that N-Ras mutations of codon 61 could be the major target to constitutively activate N-Ras protein in tumours. The subsequent studies confirmed that codon 61 CAA(Gln, Q)→ AAA(Lys, K) and CGA(Arg, R) mutations have such a high frequency, detected in many N-Ras mutated melanomas, it suggests a hypermutability phenotype resulting in a potential hereditary predisposition to melanoma development in certain patients (9;197;201;209-211).

In general, point mutations in N-Ras at codon 61 are detected in 20-30% of all melanoma cases with slightly higher incidence in metastatic than in primary melanomas. However, up to 95% familial melanoma cases which harbour an INK4a mutation have detectable N-Ras codon 61 mutation (212-214), indicating that N–Ras mutation (codon 61) in melanoma coupled well with INK4a mutation and thus, tumour suppressor gene CDNK2A ($p16^{INK4a}$ and $p19^{ARF}$, see below) deficient background mouse was employed to create the recent first successful N-Ras transgenic melanoma mouse model (215). Previous models (below) had been limited to activating H-Ras expressing transgenic mouse models, which although rare in humans, such mutations could induce melanoma following chemical initiation or neonatal exposure of UV (39;216) or on a CDKN2A deficient background (217-219). Analysis of N-Ras mutation at codons 12, 13 and 61 from both dysplastic nevi and

congenital nevi, found no mutation detected in 18 dysplastic nevi, but 28% congenital nevi (12/43) contained N-Ras mutation (9). A similar (19%) (11) and a very high N-Ras mutation rate (82%) (220) were detected in congenital nevi by more recent studies, but again a low incidence (5.9%) (12) was revealed in common benign nevi. N-Ras mutations are thought to occur early in primary melanomas rather than in the metastatic stage and that once the mutations have occurred, they persist throughout tumour progression (202), which unlike another highly mutated gene B-Raf that mutation frequency is significantly less in primary melanoma cases than reported in both nevi and metastatic melanoma (213).

1.4.2.5. Transgenic mouse models of Ras and melanoma

Although the majority of Ras mutations in either melanoma cell lines or melanoma specimens are N-Ras, the first melanoma transgenic model of Ras-mediated melanoma utilized a H-Ras not N-Ras transgene (216). In this model, the 1.3-Kb tyrosinase promoter was employed to target the mutated human T24 H-Ras (V12G) oncogene expression in pigment-producing cells of transgenic mice. There were only two survived transgene carrying founders which had altered coat colour, deeply pigmented skin with multiple nevi but no melanoma. Histopathological analysis of the tissues revealed hyperpigmentation and/or melanocytic hyperplasia in the skin, eyes and inner ear. Although the activated H-Ras transgenic mouse itself failed to produce melanoma, cutaneous melanoma could be induced following treatment of UV exposure or DMBA, whilst TPA treatment induced a small number of papillomas but no nevi or melanomas. Cell lines generated from those induced melanomas showed chromosomal abnormalities of homozygous or partial allelic deletions in the region of chromosome 4 where the CDKN2A gene resides to express $p16^{INK4a}$ and $p19^{ARF}$ (221;222). Subsequently, a transgenic mouse model of spontaneous cutaneous melanomas was successfully generated by expressing activated H-Ras (V12G) on an INK4a-deficient background (217). Further by using Tet on/off switch system, the first conditional mouse melanoma model was successfully generated and the results

revealed that the melanoma genesis and maintenance were strictly dependent upon expression of H-Ras V12G, but again this model was also required to be produced on INK4a deficient background (223), hence the attempts in this study to investigate if a similar but separate requirement for another TSG, PTEN, loss existed. To investigate the molecular targets of UV's mutagenic actions, a melanoma model driven by active H-Ras and loss of $p19^{ARF}$ function was generated. In this model, UV accelerates melanoma formation and moreover, all UV exposure induced melanoma harbouring p16 loss and CDK6 amplification which identify components of the Rb pathway as critical biological targets of UV-induced mutagenesis in the development of murine melanoma *in vivo* (224).

All mouse melanoma models described above involved activated H-Ras. In human cutaneous melanoma, however, a predominantly activated Ras gene is not the H- but N-allele (specifically Q61K), and only very recently has an N-Ras mouse model more closely mimicking the human disease been successfully produced. This transgenic mouse model was generated by targeting expression of activated human N-Ras (Q61K) to the melanocyte lineage through embryonic development by a similar tyrosinase regulatory sequence employed in Chin' model and again, to engender the appropriate phenotypes (see section 4), this was performed in a CDKN2A deficient background. Additional investigations revealed that fibroblast growth factor 2 (FGF2) was not essential for melanoma progression and metastasis in such a CDKN2A deficient N-Ras induced mouse model (215;225). Hence, given that PTEN is the second most frequently mutated TSG in melanoma after p16/p19 (see below), with intimate links to p53, prior to these Ras models, this project had commenced to analyse the effects of inducible PTEN loss for similar responses to that of p16/p19 knockout. But as outlined below, this study found an apparent redundancy of PTEN functional loss with N-Ras expression and the induction of an apoptotic mechanism which is sensitive to a pathway of early N-Ras activation as well as to PTEN functional loss that compensates to its normal PTEN function.

1.4.3. PTEN

1.4.3.1. Biology of gene

The second most commonly deleted TSG in melanoma (226), PTEN (Phosphatase and Tensin homolog deleted on chromosome Ten) was named based on function, sequence and location on chromosome. Mapping of homozygous deletions on chromosome 10q23 led to the virtually simultaneously isolation and identification of PTEN gene in 1997 from two groups giving the additional name of MMAC1 for mutation in multiple advanced cancers (227;228), while a third group identified the same gene a few months later in a search for new dual-specificity and epithelial cell-enriched phosphatase and named it TEP-1 for TGF-beta-regulated and epithelial cell-enriched phosphatase (229).

The PTEN gene is approximately 50-kb in size containing 8 introns and 9 exons to encode a 403 amino acid protein. PTEN was initially identified as a TSG because PTEN loss in the vast majority (>90%) of human glioblastoma. These initial studies also indicated that 10q23.3 abnormalities were commonly mutated in multiple advanced cancers, hence the appellation MMAC1 (above). There is seen 99.75% homology of the amino acid between human and mouse suggesting it represents a highly conserved gene whose regulation and activities play important roles in cellular processes (227-229).

Structure analysis of PTEN gene has identified two major domains: N-terminal phosphatase domain from the first amino acid to 185aa and C-terminal domain from amino acid 186 to 403 (230-232). The N-terminal phosphatase domain, where PTEN mutations mainly occur, is composed of β-sheets surrounded by α-helices giving a structure that resembles previously characterized protein tyrosine phosphatases and an enlarged active site that can account for its ability to bind phosphatidylinositol 3,4,5-triphosphate (PIP3) —a major substrate of PTEN.

The C-terminal domain was further divided into three sub-domains including a lipid-binding C2 domain, PEST domain and a PDZ domain. The C2 domain including amino acids 186 to 351 appears to bind PTEN to the plasma membrane, and it might orient the catalytic domain appropriately for interactions with PIP3 and other potential substrates. The PEST domain includes amino acids 350 to 375 and 379 to 396, which are critical for PTEN stability. Mutagenesis studies demonstrate that phosphorylation of certain serine and threonine residues S380, T382 and T383 within this domain can modulate both the enzymatic activity and the stability of PTEN. Protein kinase CK2 is known to be a key enzyme that regulates the phosphorylation of this C-terminal cluster of serine and threonine residues, which modulates PTEN stability and proteasome-mediated degradation. At the end of the C-terminus is a PDZ domain which is important in protein-protein interactions thought to play roles in altering the balance of PTEN effects on potential downstream signalling targets (e.g. Akt/PKB –Protein Kinase B), versus some other system, such as Rac signalling. The C-terminal domain is composed of antiparallel β-sheets which are linked together by short α-helices.

1.4.3.2. PTEN gene functions

PTEN is now known to play major roles not only in suppressing cancers including melanoma (below), but also in embryonic development, cell migration and apoptosis. PTEN is a dual-specificity phosphatase which dephosphorylates protein substrates as well as lipid substrates. Thus one primary function of PTEN is to act as a lipid phosphatase in the regulation of crucial signal transduction pathways (233). Myers *et al* revealed that enzymatic activity of PTEN is necessary for its ability to function as a tumour suppressor because mutations in PTEN resulted in the ablation of phosphatase activity (234). However, biological primarily relevant targets of PTEN were not phosphoproteins but rather inositol phospholipids (233), which was confirmed using several independent patient-derived PTEN mutants which retained protein phosphatase activity but lost the

ability to dephosphorylate PtdIns (235;236). The finding that PTEN dephosphorylate PtdIns phosphates leads to a model for how PTEN acts as a tumour suppressor that links PTEN to PI3K control (237) and regulation of AKT activity (238) ─a critical pathway which controls the balance between survival and apoptosis through many different downstream genes during tumourigenesis (Fig 3). Accumulating evidence has proved that PTEN, as a tumour suppressor, regulates cell survival signalling through the PI3-kinase/Akt pathway. PTEN opposes the action of PI3-kinase by dephosphorylating the signal lipid PIP3, a second messenger essential for the translocation of Akt to the plasma membrane where it is phosphorylated and activated by phosphoinositide dependent kinase (PDK) 1 and PDK2. PI3K activated Ras stimulates several downstream targets including the serine/threonine protein kinase Akt, an important protein involved in many different pathways to affect a variety of important cell functions (233;236;239-243).

Recently, using transfected MCF-7 Tet-Off breast cancer cell lines, two different nuclear localization sequence mutant PTEN genes were compared with those cells transfected with wild-type PTEN. Chung *et al* concluded that cytoplasmic and nuclear PTENs play different roles, that nuclear PTEN is required for cell cycle arrest consistent with binding to p53 (244) whereas cytoplasmic PTEN is required for apoptosis and moreover, they down- or up-regulate different proteins respectively. Their observations suggested that nuclear-cytoplasmic portioning regulates the cell cycle and apoptosis differentially, and nuclear import of PTEN play an essential role during the carcinogenesis (245). Indeed, the recently published carcinogenesis study demonstrated that PTEN loss promotes H-Ras mediated papillomagenesis via dual up-regulation of AKT activity and cell cycle deregulation, but malignant conversion proceeds through PTEN-associated pathways requiring TPA promotion (246). This later result being consistent with our findings in this study where N-Ras cooperation with PTEN resulted in only papillomas (section 3.9).

Germ-line mutations of PTEN causes Cowden syndrome –an increased risk for development of tumours in a variety of tissues, and Bannayan-Riley-Ruvalcaba syndrome (227;228;231;234;247). Unlike relative high gene ablation often detected in melanoma cell lines (248), tissue samples underline that mutations of PTEN are not an essential event in the onset of malignant melanoma of the skin, but could have an impact on tumour progression (249). Although point mutation of PTEN can be less common in some short-term cell lines (STC, 7%) and melanoma specimens (1-11%), over 30% (up to 58%) samples revealed loss of PTEN heterozygosity (LOH) (87;101;147;248-258). Altered PTEN expression is common in primary melanoma and is associated with aggressive melanoma behaviour (259). Indeed, PTEN inhibited the tumourigenicity of B16F10 melanoma cells in soft agar assay and its anti-metastatic function was also revealed by experimental pulmonary metastatic animal model. Employing this model, the authors revealed that PTEN tumour suppressor protein inhibits tumourigenicity and metastasis through regulation of MMP, IGFs and VEGF expression (260). Also, PTEN deficiency was necessary for TGF-beta type I receptor induced invasive behaviour of SV40 large T immortalised melanocytes (261). PTEN is the second most abnormal TSG in melanoma after CDKN2A (250;252) but yet its involvement in melanoma has not been relatively well studied in the few models to date nor its functional role(s) well detailed. PTEN co-operates with p16 and H-Ras in melanoma both *in vivo* and *in vitro* experiments implicated that PTEN involved in mouse melanoma development (262). Thus in addition to existing transgenic mouse melanoma models (e.g. p16, Ras and others), the creation of a PTEN-melanoma mouse model is useful for complementary/interactive studies. Furthermore, it may imply new insights on disease progression and melanocyte development, for instance in an attempt to generate a PTEN null mouse model, mice die at the embryonic stage demonstrated that PTEN is also essential for embryonic development (243), and PTEN deficiency from E12.5 revealed that neurological defects cause premature lethality in these mice and PTEN deficiency increases susceptibility to carcinogen-induced melanoma (263).

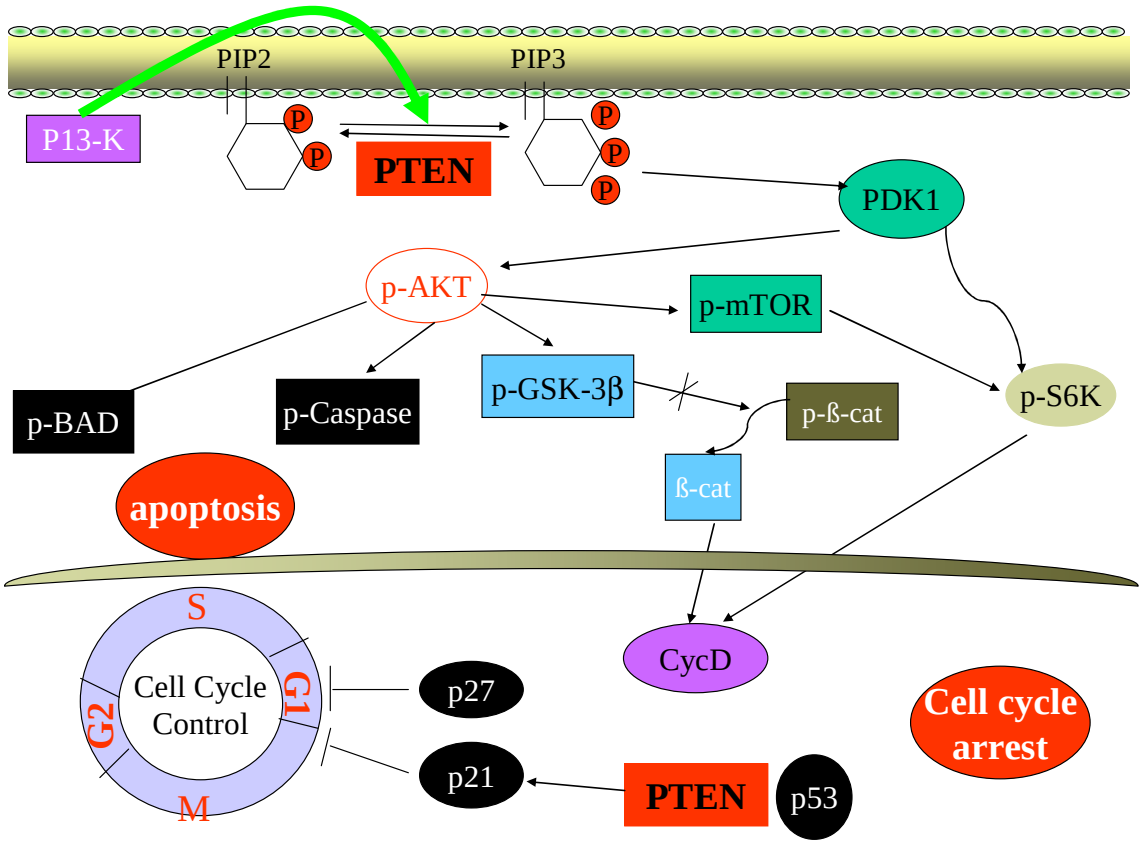

Figure 3: PTEN roles in cell signalling pathways (Modified from B. Stiles *et al.* Developmental Biology 273: 175–184, 2004). As a lipid phosphatase, PTEN dephosphorylates PIP3 to inhibit the growth factor signals transduced through PI3K, normal cellular physiology. PTEN deficiency thus leads to accumulation of PIP3 that trans-activates several signalling molecules including PDKs, S6 kinase, mTOR and AKT. This is a well characterised molecular mechanism that helps to control the balance between apoptosis and cell survival through downstream pro-apoptotic factors such as BAD, caspase 3/9 etc. PTEN also inhibits PI3K signalling to trans-activate p53 and to result in cell growth suppression which is mediated by its ability to block cell cycle progression in the G1 phase through down-regulation of cyclins and up-regulation of the CDK inhibitors p21 and p27 expression.

1.4.3.3. PTEN and melanoma

In the initial analysis, commonly mutated in glioblastomas, PTEN mutations were not detectable in the few melanoma samples (only 4) analysed (227;228) which may reflect that PTEN mutation is less common in primary melanoma than in cell lines (264). However, other studies in melanoma cell lines and primary or metastatic melanomas soon demonstrated that disruption of PTEN by allelic loss or mutation contributed to the pathogenesis of malignant melanoma (147;248;257;258;265). Furthermore, as found for B-Raf genes (266-269), to date no PTEN abnormality has been observed in uveal melanoma unlike in cutaneous melanoma(270).

Considering that gross genetic lesions of chromosome 10 occur in 30-50% of sporadic human melanomas, Robertson *et al* developed an *in vitro* loss of heterozygosity approach in which a wild-type chromosome 10 was transferred into melanoma cells and selected for breakage as well for regional deletion. The overlap of these events at band 10q23, the site of PTEN location, provided direct evidence that PTEN is a potential target in malignant melanoma and furthermore, vectors containing full-length PTEN or mutant PTEN were transfected into both PTEN expressing normal and abnormal melanoma cell lines revealed that transfected normal PTEN expression caused dramatic reduction of cell growth in PTEN expressing abnormal parental cells but neither in PTEN expressing normal parental cells nor in those mutant PTEN transfected cells (256). Further studies supported a role for PTEN loss in the pathogenesis of melanoma finding that while PTEN expression was observed in benign melanocytic lesions, it was lost in a large proportion of primary cutaneous melanomas (255).

The synergism of PTEN loss with other genes during melanoma development was also investigated. PTEN functions as a lipid and protein phosphatase that down-regulates Akt and MAPK signalling, potentially suggesting that Ras and PTEN have antagonistic

functions in both protein and lipid kinase signalling pathways (reviewed in (271)). A useful model for elucidating the role of omega-6/omega-3 fatty acid ratio in tumourigenesis, a fat-1 mice line was recently engineered which can convert n-6 to n-3 fatty acids and have a balanced ratio of n-6 to n-3 fatty acids in their tissues and organs independent of diet. Implanting mouse melanoma B16 cells into fat-1 transgenic, PTEN gene was significantly up-regulated in the fat-1 mice to inhibit tumour growth and formation (272). 60% and 56% mutation of B-Raf in cell lines and metastatic melanoma respectively together with 80% and 100% PTEN alteration demonstrated a possible cooperation between B-Raf activation and PTEN loss in melanoma development (254). P53 and PTEN mutations were always accompanied with B-Raf alterations, while PTEN loss was found in association with CDKN2A or P53 mutations in the absence of B-Raf activation (87). In examining the biological consequences of Pten and/or Ink4a/Arf deficiency in cells and mice, You *et al* found that relative to single mutant controls, Ink4a/Arf-/-PTEN+/- mouse embryonic fibroblast cultures exhibited faster rates of growth in reduced serum, grew to higher saturation densities, produced more colonies upon low density seeding, and showed increased susceptibility to transformation by oncogenic H-Ras. Ink4a/Arf deficiency reduced tumour-free survival and shortened the latency of neoplasia associated with PTEN heterozygosity. Compound mutant mice also exhibited an expanded spectrum of tumour types including melanoma and squamous cell carcinoma. Therefore, the authors concluded that the co-operation of PTEN with p16 and H-Ras in melanoma both *in vivo* and *in vitro* experiments implicated the involvement of PTEN in mouse melanoma development (262).

1.4.4. Kit/SCF

Kit and its ligand SCF (stem cell factor, also called as Kitl for ligand of Kit, SL or SLF for steel factor and MGF for mast cell growth factor) were identified as gene products of the W mutant mouse and Sl mutant mouse loci. Both of them are known to play important roles in melanoblast/melanocyte survival, migration and differentiation during embryogenesis, and may also help to define the melanocyte stem cell niche (53). Loss or significant reduction of expression/function of Kit in malignant melanoma indicated that this signalling system plays an essential role during melanoma development, possibly at the critical late stage transition from RGP to VGP melanoma ((273) and reviewed in (274)).

1.4.4.1. Gene discovery and specificity

Kit was initially isolated from a feline fibrosarcoma and identified in 1986 as the transforming gene of the Hardy-Zuckerman 4 feline sarcoma virus termed v-kit (275), and soon after its 145-Kd cellular homolog c-kit (thereafter termed as Kit) was cloned and sequenced (276). It was virtual simultaneously found that Kit is allelic with the dominant white spotting (W) of mice in 1988 (277;278). Whilst the mutations within Steel (Sl) locus in mutant mice give rise to a phenotype very similar to mutations in Kit, resulting in the discovery of SCF. It was demonstrated that the product of the Steel locus was identical to SCF, the ligand for Kit (279;280), hence the name of Kitl.

Four isoforms of Kit have been identified in human while two isoforms occur in mice as a result of alternative splicing (281;282), due to alternate use of 5ϕ splice donor sites (283). Similarly, alternative splicing of the human SCF pre-mRNA transcript results in secreted and membrane-bound forms of the protein and their different/synergism active functions during melanocyte development were also revealed. Soluble SCF is required for melanoblast dispersal and initial survival during migration, while membrane-bound form of SCF promotes melanocyte precursor survival in the dermis (284).

1.4.4.2. The role of Kit/SCF in melanocyte development

SCF in mammalian skin is generally thought to be an important regulator of melanocyte and mast cell survival, migration and proliferation. By analysis of both molecules in wild type and white spotting mutant mice, Kit and SCF were shown to play multiple roles in the development of melanocyte in murine ontogeny. Functional blockade of Kit by specific monoclonal antibody illustrated distinct Kit dependent and independent stages during melanocyte development. During mouse skin development, Kit positive cells are present in the SCF-producing areas at the time when melanoblasts proliferate and differentiate (285). Comparing results of injections of recombinant human SCF and a Kit inhibitory antibody K44.2, SCF injection increased, whereas Kit inhibition decreased the number, size and dendricity of melanocytes. Expression of melanocyte differentiation antigens was also markedly increased by treatment with SCF but decreased by Kit inhibitor treatment. Increased Ki67-positive (cellular marker for proliferation) melanocytes in the SCF-treated tissue and loss of melanocytes with a Kit inhibitor, suggest a direct proliferative effect of SCF signalling. These findings demonstrate that the Kit/SCF pathway has a role of controlling cutaneous melanocyte homeostasis (286). The data from in situ hybridization analysis, comparing the expression profiles of Kit and SCF transcripts during mouse embryogenesis, confirmed that Kit and its ligand SCF complex (Kit/SCF) provides a homing mechanism during melanoblast stem cell migration in early development, as well as in the late stage development for cell proliferation, differentiation and survival (287).

Employing TRP2 (tyrosinase related protein 2, also referred to as Dct) expression, as a melanocyte-specific marker probe to investigate the mechanism of SCF mutation in melanocyte development, the results revealed that the membrane-bound SCF was necessary for the melanoblast survival but not the early migration and initial differentiation (284;288). However, in later studies targeting SCF expression to epidermal keratinocytes, the results not only suggested that SCF was involved in melanocyte survival but also that it

stimulated the migration and promoted proliferation and differentiation *in vivo* (60). As SCF regulates integrin expression at the protein level and that SCF has pleiotropic effects on attachment and migration to extracellular matrix (ECM) ligand, it suggests therefore that SCF could alter melanocyte adhesion and migration involving ECM ligand, to control melanocyte migration during the development of skin (289). The mutations of the Kit receptor tyrosine kinase encoded at the W locus do not alter early migration or differentiation of melanoblasts, but rather severely affect survival, crucially up until E11 and Kit plays an important role for melanoblast proliferation in later development (290;291). Using lacZ report transgene controlled by the SCF promoter, detected report expression in the dermal papillae of the hair follicle also revealed SCF roles to support melanocyte growth and development in the hair follicle (292), which is consistent with the findings in this study that melanocytes survived through the SCF/Kit loop during the papillomagenesis induced by disruption of melanocytes microenvironment (section 4.4).

1.4.4.3. Kit/SCF and melanoma

A Kit expression-pattern comparison study of normal human and murine skin melanocytes versus melanoma cells implied that loss or a marked reduction in Kit gene expression either promoted or was a consequence of transformation in melanocyte. While Kit protein was readily observed in normal human skin and murine melanocytes, malignant melanoma and cell lines established from melanoma samples, or transformed murine melanocytes, did not express detectable levels of Kit mRNA or protein (293;294).

Unlike cutaneous melanoma, however, Kit expression was demonstrated in most choroidal melanoma tumours (75%) by immunohistochemistry and western blotting analysis (295). Whilst in acral lentiginous melanomas, Kit was strongly expressed in all cases where melanoma cells grew in the basal layers of the epidermis, but was lost in melanomas which grew in the upper layers of the epidermis or vertically into the dermis (294). This is

consistent with the findings in this study, that Kit expressing melanocytes were primarily located in the basal epidermal layers of the pigmented papillomas, induced to assess effects of the microenvironment (see section 3.10). Apart from SCF, however, there is evidence to show that additional mast cell growth factors are secreted by fibroblasts and keratinocytes, indicating a complex orchestration of several growth factors in the regulation of cutaneous growth and differentiation in which SCF plays only one part of this regulation (296).

Kit loss or significant reduction in cutaneous malignant melanoma and melanoma cell lines, suggested a key role of Kit/SCF during melanoma development. Introduction or re-activation of Kit and SCF activity in melanoma cells produced several biological responses. SCF inhibited rather than stimulated the growth of metastatic melanoma cells as opposed to those observed in normal melanocytes and similarly, and enforced Kit expression in melanoma cells significantly inhibited their growth and metastatic potential in nude mice (297). These opposite effects in melanoma cells compared to normal melanocytes may be the results of abnormal signal transduction by Kit in response to SCF, given that the loss of function of Kit, as well as the enhanced expression of MACM, an adhesion molecule, is regulated by transcription factor AP-2, which does not express in metastatic melanoma (297;298). Furthermore, melanoma cell lines, particularly those known to metastasize *in vivo*, lose the ability to express membrane-bound SCF-2 isoform but not the soluble SCF-1 isoform, which indicates that the different expression patterns of SCF isoforms could serve as a prognostic markers for malignant melanoma (299). The majority of invasive and metastatic malignant melanomas fail to express Kit suggesting Kit has a TSG role which is lost during melanoma development and indeed only 2 cases of metastatic malignant melanoma (2%) possessed Kit expression (due to a Kit-activating mutation) (300). The Kit mutation incidence in melanoma may differ between anatomical sites as well since UVR exposure studies found Kit mutation and/or amplification in 39% of mucosal, 36% of acral and 28% of melanomas on chronically sun-damaged skin, but there is no mutation detected

in melanomas of skin without chronic sun damage (301) similar to previous report (300).

1.4.4.4. Kit/SCF and apoptosis

The loss of Kit expression in malignant melanoma may allow melanoma cells to escape SCF/Kit-mediated apoptosis pathway and therefore contribute to tumour metastasis. Enforcing Kit expression in Kit-negative, highly metastatic human melanoma cells and subsequent analysis of tumourigenic and metastatic potential, concluded that Kit-positive cells produced significantly slower growing tumours and fewer lung metastases than did in control cells (273). On the other hand, exposure of Kit-positive melanoma cells *in vitro* and *in vivo* to SCF triggered apoptosis of these cells but not of Kit-negative melanoma cells or normal melanocytes. Similar results were obtained from the analysis of Ewing's sarcoma and peripheral neuro-ectodermal tumours (302;303). In contrast to the data obtained from metastatic melanoma cells, as expected, SCF removal increased apoptosis significantly in cultured neural crest cells (NCC) and further increases were achieved by addition of Kit functional blocking antibody to obstruct SCF/Kit pathway during a SCF-dependant period (304).

Disruption of MITF in melanocytes or melanoma triggered profound apoptosis can be rescued by Bcl-2 over expression and, Bcl-2 down-regulation in Kit functional blocking induced NCC apoptosis demonstrated that Bcl-2 played an essential role in such a SCF/Kit mediated apoptosis (305;306). Data obtained from the melanocyte apoptosis analysis of Kit (w-v) and p53 double mutant mice demonstrated that defective Kit signalling *in vivo* results in apoptosis through a p53-independent pathway in melanocyte and mast cell lineages although by a p53-dependent pathway in male sperm cell apoptosis (306;307)

Fas, a member of tumour necrosis factor superfamily of receptors and an upstream cell death inducer in human cancers, functions through recruiting adaptor factor FADD (Fas-

associated protein with a Death Domain) which then serves as a docking surface and facilitates auto-processing and activation of other molecules to trigger a caspase cascade (8, 10) to transduce apoptotic signal (308). It plays an important role in SCF/Kit mediated melanocyte/melanoblast apoptosis.

Fas up-regulation was observed in chemotherapy (cyclophosphamide) induced apoptosis of hair follicular melanocytes, which confirmed by significant decreasing apoptosis in Fas knock-out mice (309). Employing neural crest cell line (NCCmelb4), Kimura *et al* revealed that up-regulation of Fas together with Caspase-8 play an important role in regulating the SCF/Kit mediated NCC apoptosis during embryogenesis while other molecules of Bcl-2, Erk and RSK (ribosomal S6 kinase) downregulated (306). Taking together, SCF/Kit mediated apoptosis related to many factors including molecules on Fas-apoptosis pathway (310) as well as anti-proliferation molecules but not in a p53 dependant fashion. However, which caspase molecule downstream of Fas induced apoptotic pathway transduces Kit/SCF mediated apoptotic signal is not well investigated although caspase-8, a molecule upstream of caspase-3 in Fas signalling pathway, activation was revealed.

1.4.5. CDKN2A

1.4.5.1. General biology of the gene

The CDKN2A (Cyclin-Dependent Kinase Inhibitor 2A) locus located on chromosome 9p21 was identified as a cancer hot spot because of its high frequency of homozygous deletion in many cancer cell lines derived from different tumour types (311-313). Two different CDKN2A mRNAs have been identified in several different tissues and two transcripts arise from different promoters (314;315). The α form is identical to the cDNA reported to encode the $p16^{INK4a}$ protein, which inhibits cell-cycle progression by repressing the activity of CDK4/6 cyclin complexes via preventing the phosphorylation of pRb (316). Its coding sequence is divided into three exons: the first exon comprises 150 base pairs to encode amino acid 1 to 50, exon 2 of 309 base pairs which encode amino acids 51-152, and a very small exon 3 of only 12 base pairs which encode the last 4 amino acids of 153 to 156. The β form is identical to α form in exons 2 and 3 but contains a different exon 1 (exon 1β) which is transcribed from its own promoter. The altered resulting RNA of exon 1β incorporates exons 2 and 3 and specifies a distinct protein $p14^{ARF}$ ($p19^{ARF}$ in mouse) because exon 2 is translated in a different reading frame to that used for $p16^{INK4a}$, hence the name of ARF (alternative reading frame). The β form transcript encodes $p14^{ARF}$ protein, which is entirely different in its amino acid sequence from $p16^{INK4a}$ (317).

Numerous studies have been performed in attempts to understand the cancer suppression activities of $p16^{INK4a}$, and the results obtained have shown accumulation of $p16^{INK4a}$ in response to diverse cancer relevant stimuli, including passage in culture, growth at high density, DNA damage, oncogene activation and advancing age (reviewed in (318)). $p16^{INK4a}$ deficient mice develop phenotypically normal but are prone to tumours and sensitive to carcinogens, which suggest a little or no role of $p16^{INK4a}$ in normal mice development but instead serves to limit inappropriate or aberrant cellular proliferation. Polymorphism data of $p16^{INK4a}$ protein and its susceptibility to UV-induced melanoma in

fish suggest that its role in abrogating neoplasia is conserved over a large phylogenetic distance while tumour-permissive hypomorphic mutations have also been found in mice and humans (319-321).

Mice with exon 1β disruption ($p16^{INK4a}$ normal) developed tumours indicated that $p19^{ARF}$ functions as a tumour suppressor gene in its own right (322) in human. Furthermore, the genetic data collected from human cancers clearly supports and complements the results obtained from the mouse (reviewed in (318)). Analysis of cloned cDNA of $p19^{ARF}$ revealed that cell-cycle arrest induced by $p19^{ARF}$ expression could not be abrogated by D-type cyclin expression (317) and displayed different functions from $p16^{INK4a}$ protein on cell cycle control (323). $p19^{ARF}$ was overexpressed in p53-null cells and the tumours obtained in $p19^{ARF}$ deficient but p53 normal mice that suggested a common genetic pathway of $p19^{ARF}$ and p53 (223;322). $p19^{ARF}$ protein induces cell-cycle arrest or apoptosis, in part either via stabilization of the p53 tumour suppressor protein by sequestering murine double minute (MDM) 2 oncogene in the nucleolus, thereby inhibiting its E3 ubiquitin ligase activity (324) or without p53 stabilization and MDM2 relocalization (325). Additionally $p19^{ARF}$ can induce cell-cycle arrest in mouse embryo fibroblasts lacking $p21^{CIP1}$ or p53 indicating that the protein has p53-independent functions (326).

1.4.5.2. Gene ablation in melanoma

CDKN2A, as a candidate tumour suppressor gene, was pinpointed to chromosome 9p21 in 1994 because of deletions in melanoma cell lines and was later identified as a candidate for the chromosome 9p melanoma susceptibility locus (93;311;313). Since then, genetic analysis in ethnically diverse populations have reported a variety of germline mutations in melanoma-prone families, in melanoma cases diagnosed at a young age, or in multiple primary tumours (reviewed in (327) and (208)). In sporadic cutaneous melanoma, INK4a/ARF mutations are a less frequent event than reported in those familial melanoma

and additionally, its functional loss can also occur through epigenetic mechanisms such as promoter hypermethylation (328-330). The importance of $p16^{INK4a}$ has been further reinforced by finding of alterations that target its biochemical partners, that is, CDK4 point mutations inhibit binding to $p16^{INK4a}$ or overexpression of CDK6 (331). In early onset melanoma cases or a strong familial association with melanoma, the CDKN2A locus was found to be ablated in 25–40% of melanoma families (332-337). Analysis of melanoma families in Scotland revealed that 22% possessed CDKN2A mutations, with one new mutation of H83N reported (338). Through analysis of 2137 patients from 466 melanoma families, CDKN2A mutations were identified in 41% of families, of which most were $p16^{INK4a}$ (95%). A strong association between CDKN2A mutations and pancreatic cancer, but not neural system tumours, was also revealed (339). Studies of multiple-case families have indicated that the lifetime risk of melanoma in CDKN2A mutation carriers is very high, ranging from 58% in Europe to 91% in Australia by age of 80 years (340). The risk of melanoma in CDKN2A mutation carriers was approximately 14% by age 50 years, 24% by age 70 years and 28% by age 80 years in USA (341). In addition, 75% of melanoma samples were found to have CDKN2A methylation to result in CDKN2A function loss at the transcriptional level (342).

Cell lines generated from UVB/H-Ras induced mouse melanomas showed chromosomal abnormalities of homozygous or partial allelic deletions in the region of chromosome 4 where the CDKN2A gene resides (221;222) which confirmed that the familial melanoma gene CDKN2A encodes potent tumour suppressor activity, whose loss is necessary for melanoma formation. In human melanoma cells, inactivation of CDKN2A locus can lead to abrogation of both Rb and p53 functionality through loss of $p16^{INK4a}$ and $p19^{ARF}$ respectively (343). The transfection of UV-damaged DNA into normal mouse fibroblast cells revealed that loss of function of either $p16^{INK4a}$ or $p19^{ARF}$ reduced the cells ability to repair DNA damaged by UV exposure and furthermore, loss of DNA repair ability was

independent of the cell-cycle (108).

1.4.5.3. Transgenic melanoma mouse model and CDKN2A

Interestingly, although INK4a/ARF null mice did not exhibit melanoma susceptibility (316), $p16^{INK4a}$ specific gene targeting can facilitate melanomagenesis, particularly after exposure to DMBA, but the majority of tumours were SCC (343-345). Mice expressing CDK4 mutation R24C that renders the CDK4 protein insensitive to inhibition by $p16^{INK4a}$, are highly susceptible to melanoma development following DMBA initiation, which mutates Ras and significantly increases penetrance of melanoma in a H-Ras expressing model following UV induction (346-348). On a genetic background devoid of CDKN2A (INK4a/ARF), a role for CDKN2A in UV-induced melanomagenesis was directly assessed by expressing HGF/SF transgene, demonstrating that CDKN2A plays a critical role in UV-induced melanomagenesis and confirming that sunburn is a highly significant risk factor, particularly in families harbouring abnormal CDKN2A gene (349), although loss of heterozygosity of 9p is not confined to melanoma but also detected in other melanocytic lesions and other genetic changes (e.g., loss of 10q, 6q, and 18q) may play an important role in development of malignant melanoma (14). Employing a $p16^{INK4a}$ deficient mouse model, components of the Rb pathway were identified as being critical biological targets of UV-induced mutagenesis in the development of melanoma (224), whilst loss of vascular integrity upon inactivation of Ras was revealed as an active process rather than a consequence of loss of cell viability in CDKN2A deficient mouse melanomas (350).

By expressing activated H-Ras (V12G) on a $p16^{INK4a}$ deficient background a high incidence of melanoma was produced within a relatively short latency (217), although in an earlier model, activated H-Ras alone failed to produce melanoma resulting in hyperpigmentation and/or melanocytic hyperplasia in the skin, eyes and inner ear (216). Significantly, based on previous studies and the data presented in this thesis, all activated Ras (H- and N-

alleles) induced mouse melanoma models (see above 1.4.2.5. Transgenic mouse models of Ras and melanoma) to date appear to require an INK4a/ARF deficient background and specifically, all Ras induced melanomas were shown to be $p16^{INK4a}$ null/heterozygous or possessed of $p19^{ARF}$ deficient background (217;224), indicating that a strong synergism exists between dysregulations of MAP kinase signallings which includes B-Raf, PTEN/PI3K/AKT and p16/p19 mediated.

1.4.6. Other genes in melanoma

Apart from those genes described above, there are many other genes involved in melanoma development, such as p53, B-Raf, MC1R, MITF.

The tumour suppressor protein p53 plays a critical role in the orchestration of the cellular responses to a variety of genotoxic and cytotoxic stresses. The abrogation of the function of p53 is the most prevalent molecular alteration in solid human tumours. However its causal involvement in melanoma is still controversial to date. p53 mutation frequency is very high in human non-melanoma skin cancers (NMSC) (reviewed in (351)) but relative very low in melanoma (352-354). Although the low p53 mutation rate in uncultured specimens may indicate that inactivation of p53 is not a critical event in the progression of melanoma (reviewed in (355)), UVB induces p53 elevation, although not at mRNA level, in human skin (69) presumably in its attempt at a protective role. Results from one study, showed UVA and UVB-induced apoptosis in a dose dependent manner, where wild type p53 melanoma cell lines were much more vulnerable than the mutant cell lines and this result suggested that p53 plays a role in UV-induced apoptosis in melanoma cell lines. On the other hand, there was little difference in p53 expression patterns between the primary and matched metastatic melanomas, indicated that expression of p53 *in vivo* maybe insufficient to induce apoptosis in melanoma as it does in cell lines, or the p53 pathway is compromised by alternate event *in vivo* (356). Therefore, one or more genes involved in p53 regulation might be the preferred targets ((322;357) and reviewed in (223;355)) and in this respect, much attention has been paid to the tumour suppressor gene ARF. The tumour-suppressor activity of ARF regulates p53 in response to oncogenic signalling or aberrant growth by binding and inactivating MDM2 (324;325;358;359). While the ARF-p53 axis is inactivated in the vast majority of melanoma cell lines by mutation of p53 or deletion of ARF, alterations in these genes are not always mutually exclusive (87;359). Although the concept of whether ARF and p53 act in the same pathway during the melanoma

development remains open to argument, there is sufficient evidence to suggest that ARF plays its own role as an important melanoma suppressor (see 1.4.5 above; reviewed in (355)) via inducing p53-independent senescence (357).

Of the Raf family of protein kinases, B-Raf is the only member to be frequently activated by mutation in cancer. A single amino acid substitution (V600E) accounts for the vast majority of mutation and results in constitutive activation of B-Raf kinase function. The first evidence of a direct association between Raf gene mutations and human cancers was provided in 2002 by Davies H. et al (200). Following this report, more intensive studies were performed to detect the B-Raf mutation spectrum in both malignant melanomas and relevant pre-malignant lesions. Brose and co-workers identified activating B-Raf mutations in 66% of sporadic melanomas of which 90% mutations were V599E (360) (thereafter V599E was identified as V600E, reviewed in (361)). Additional research suggested that the V600E missense mutation by a single substitution (T→A) may play an important role for malignant melanoma development (208;362-367). However as there is no such mutation detectable in 42 familial melanoma patient samples, it suggested that this V600E mutation is a somatic mutation associated with melanoma development and/or progression, occurring in only a proportion of affected individuals (368) an idea confirmed by other studies (369;370). A lack of V600E B-Raf mutation in uveal melanoma was first reported by Edwards and co-workers in 2003 (371) and later confirmed by other groups employing various number of uveal melanoma cases (266-269). Despite a similar high frequency (62-72%) of B-Raf mutations identified in melanocytic nevi, VGP melanomas, metastatic melanomas and melanoma cell lines (200;360;372), there is only a 10% mutation frequency appeared in the earliest stage of RGP melanomas. This striking contrast result to the high frequency in other samples suggested that B-Raf oncogenic mutation correlated with progression of the transition from RGP to VGP and/or metastatic melanoma rather than with initiation of human melanoma (373). Alternatively, when B-Raf mutation is an early

event in the pathogenesis of some melanomas it is preserved throughout tumour progression once mutated (212;374), and some studies suggested that B-Raf mutation in melanoma is most likely to occur prior to the development of metastatic disease (363). In many cancer cell lines, B-Raf expression is necessary to ensure tumour growth and proliferation. B-Raf also leads to benign tumour growth and these can progress to malignancy only with additional genetic mutations (review in (375)). Given the established involvement of UV exposure in melanoma development, an association between UVR and B-Raf mutation was identified by mutation analysis of primary cutaneous melanomas arising from UV exposure sites versus unexposed sites, and revealed a high frequency mutation rate (33% and 62% respectively) following UV exposure (73;371). Conversely, a later study suggested that UV light is not necessary required for the acquisition of the B-Raf(V600E) mutation (10). Although high frequency B-Raf mutation detected in melanoma is linked to UV exposure, it is still unclear why B-Raf mutations are preferentially selected in melanoma and the mechanism of acquisition of the B-Raf V600E mutation remains to be clarified (reviewed in (375)).

MITF regulates melanocyte development, function and survival by modulating various differentiation and cell-cycle progression genes. MITF mediates differentiation effect of α-MSH (376;377) by regulating expression of TYR, TYRP1 and DCT (378-380) (the enzymes that are essential for melanin production), and by controlling genes involved in melanosome genesis or structure such as MART1, Silver and GPR143 (OA1) (reviewed in (381)). Rab27A has also recently been identified as a new direct transcriptional target of MITF, linking MITF to melanosome transport (382) ─another key parameter of melanocyte differentiation and skin pigmentation, while microRNA-137 (miR-137) has been revealed to act as a regulator of MITF expression and to down regulate MITF expression in melanoma cell lines (383). MITF is important for the initial survival of melanocyte progenitor cells in the proliferation and migration from the neural tube (384).

Its relevance in melanocyte stem cells has also been revealed by Nishimura (53), where it has been demonstrated that MITF amplification acts as an oncogene in a sub-set of human melanomas. Although MITF has been described as a highly sensitive immunohistochemical marker for melanoma diagnosis (385;386) since 1999, the evidence of MITF as an oncogene came from a study in which B-Raf mutation as well as p16 inactivation accompanied MITF amplification in melanoma cell lines and ectopic MITF expression in conjunction with the B-Raf mutant (V600E) transformed primary human melanocytes (387). MITF amplification was found in 12% of analysed melanoma cell lines in keeping with 10% in primary melanomas and 15-20% in metastatic melanomas (208;387). MITF amplification in metastatic melanoma is also associated with a decrease of five years in survival (387). MITF expression in melanoma biopsy is highly variable. In some cases, MITF levels are high (i.e. amplification), but in others MITF levels are low or decreased (388;389). Thus, why are MITF expression lost/reduced during progression of some melanomas but amplified in others? A reasonable explanation is that the fundamental differences existed among classes of melanoma and such differences might account for such an opposite effects of MITF expression during melanoma progression. Although MITF has been directly implicated in melanoma oncogenesis, its oncogenic activities are still poorly understood and the studies of MITF roles in melanoma development have just begun (reviewed in (381)).

Different colour of skin and hair are genetically determined by variation in the amount, type and packaging of melanin polymers produced by melanocytes and secreted into keratinocytes. Pigmentary phenotype is genetically complex but up to date, there is only one gene, the melanocortin 1 receptor (MC1R), has been identified to explain the variation of skin and hair in a normal population (reviewed in (390)). MC1R is an unique bifunctionally controlled receptor, activated by α-MSH and antagonized by agouti, both contributing to the variability of mammalian coat colour (review in (391)). The human

MC1R was cloned and located at 16q24.3 (392-394), with most red hair people harbouring homozygous diminished-function alleles at the MC1R (33), and not necessarily the null phenotype of MC1R (395). α-MSH protects UV radiation-induced DNA damage and apoptosis (66) and has immunosuppressive effects in human acting via MC1R on monocytes and B lymphocytes but not the antigen-induced lymphocyte proliferation (31). A recent mapping study in dogs identified another locus, termed K, encodes a member of the β-defensin family of antimicrobial peptides (396) and surprisingly, the product of the K locus promotes eumelanin production by binding directly to MC1R and acting as a competitive inhibitor of Agouti (397).

The MC1R gene is remarkably polymorphic in white populations (398-400) and an association of MC1R variants and cutaneous melanoma was revealed in 2000 by Palmer et al (401). A relationship between CDKN2A and MC1R in melanoma was established in 2001 (402;403) due to MC1R variants in addition to a CDKN2A mutation that significantly increased the melanoma penetrance. By analysis of extensive clinical and epidemiologic data, Goldstein et al., also evaluated the relationship between MC1R and melanoma risk in CDKN2A melanoma-prone families, finding that multiple MC1R variants are associated with the development of multiple melanoma tumours in patients with CDKN2A mutations (404), consistent with previous studies (405-407). An association between MC1R and sporadic melanomas was also revealed (406-408), but the study failed to establish the relationship of MC1R and ocular melanoma (409). A recent study failed to show an association between MC1R variant and melanoma in Italy (410) but it conflicts with the previous studies (406;408) which indicated that the differences in melanoma risk across geographic regions justify the need for individual studies. The effect of MC1R is not solely accounted through hair or skin colour (400) and therefore, additional molecular events downstream of MC1R activation, and their effects on melanoma risk need to be further studied to understand the causal pathways (e.g.MC1R) of melanoma.

There are many genes involved in melanoma tumourigenesis and the genes described above represent some of the extensively studied. Others including E-cadherin, MDM2, VEGF, NF-kappaβ etc have also been well studied and many other genes (e.g. XPF, GSH, BCL-2, PTPRD, Apaf1, Rb etc) have also been identified in melanoma cell lines and primary melanomas. To describe all genes and their pathways involved in melanoma development is an impossible task, beyond the scope of this thesis. Also, as melanoma research progresses, more genes and their functions involved in melanoma development will be discovered and elucidated.

1.5. Transgenic mouse models for melanoma

During the past decades, significant progress has been achieved on the investigation of the causes of many human diseases, which benefited from the development of new biotechnologies —one of them being the transgenic animal approach that permits scientists to identify and test the causality of specific gene(s) that are involved in certain human disease. Identification of an important role for the suspected specific gene in a particular disease creates a new dimension of bio-research to understand the molecular mechanism that underlies the cause of that disorder. The development of an animal model specific for a disease and mimicking the *in vivo* situation is often a crucial step in this process and recent transgenic technology advances have made such an animal model generation easier, more rapid and more accurate. Technologies that allow for the addition, alteration or elimination of individual genes from the genome to create a transgenic animal are now widely employed in bio-research. Moreover, the advanced inducible gene-switch system allows induction of highly localized disease by controlling of the target gene expression under a specific promoter (e.g. tyrosinase in melanocyte). Employing such an inducible gene-switch system, animals remained disease free until treatment that increases viability and minimizes unnecessary suffering as well as to minimize the number usage of animals involved in the experiment (3Rs).

Melanoma, one of the most morbid human cancers, is rising steadily and faster than any other neoplasmas, but compared to other cancers there are still relatively few useful models available that are able to directly assess relevant genetic causality and the underlying molecular mechanisms *in vivo*. To understand the molecular mechanisms of melanoma initiation and development, a transgenic mouse model designed to accurately mimic human melanoma aetiology is highly desirable and the ultimate goal of these studies. Moreover, by generating an *in vivo* model to mimic human melanoma aetiology it may potentially establish a test system to evaluate novel treatment modalities. To study the

genes suspected to be causal in melanoma development, such as CDKN2A, Ras, B-Raf, PTEN, MITF, MC1R and p53, a TSG much less mutated in melanoma than in non-melanoma skin cancers (reviewed in (411;412)), transgenic mice may generate useful models to elucidate their mechanisms of melanoma development. By introducing one (215;221) or more (40;215;223;413) insults via breeding these models can assess melanoma development as a multistage process and take into account melanocyte physiology as well. Further, the latest conditional gene switch approaches, which leaves animals disease free until inducer treatment activates regulatory transgenes to subsequently switch target genes on (detailed below) or inactivate TSGs, will allow investigators to explore the temporal causal role(s) in each stage of melanoma development.

1.5.1. General introduction of melanoma transgenic model

Many studies on the pathology, epidemiology and genetics of melanoma have been performed and thus, we now know that genetic factors are the most important of the known risk factors. The most important epigenetic factor, overexposure to UVR in sunlight, is believed to be a contributing factor to at least many cases, even if not all, of melanoma. Indeed, even short periods of intensive exposure specifically episodic exposure during the childhood, such as sunbathing is associated with a two-fold increase in melanoma risk (25). In mouse melanoma models, either HGF/SF over-expressing or active form H-Ras expressing new born pups (2-3 days old) exposed to a single low dosage of UV radiation developed melanoma in later life (12 months) (39;40). However, the molecular mechanisms of melanoma progression remain relatively unknown despite the fact that the worldwide incidence of melanoma is increasing more than any other neoplastic disease (1;83-85;414).

1.5.2. Advantages of transgenic models

The development of techniques for the production of genetically engineered mammals was initiated by the pioneering microinjection efforts of Lin back in 1966 (415). Since the first transgenic animal produced more than two decades ago, many transgenic animal models such as pig, sheep, goat and cattle have been generated to understand molecular mechanism(s) of major diseases that afflict humanity and to investigate their potential application on agriculture and pharmaceutical industries beside the factor of basic biomedical research. Such 'new' technologies that allow the investigators to introduce specific-disease related gene(s) of interest primarily into the mouse genome exploiting microinjection of DNA into pro-nuclear stage embryos (416;417), or delete gene(s), for example TSGs from the genome by homologous recombination in pluripotent embryonic stem cells (418), have facilitated the generation of a host of experimental models of human disease (review in (419)). The transgenic mouse technology has already had a reverberating effect on studies of the aetiology of cancer, skin disease, motor neuron disease, diabetes, cardiovasculogy and hepatology etc. Often, transgenic animal models have not only clarified existing hypotheses, but have also implied new insights on disease progression and provided an invaluable starting point in the search for effective therapies and pharmaceutical production (review in (420)).

To investigate the molecular mechanism of human disease before the advent of transgenic mice, previous rodent models were only produced fortuitously as a result of a spontaneous genetic mutation. Indeed, phenotypic observation in non-transgenic models sometimes does approximate pathological conditions associated with human diseases. However, a major caveat has to be mentioned is that the phenotypes obtained from the non-transgenic animal models do not often share the same underlying molecular/genetic mechanisms of diseases because such phenotypes are spontaneously derived or disease has been generated in immunodeficient mice where mutated gene did not really mimic the genetic basis. The

huge benefit of ability of transgenic technology to add or delete defined human disease related genes in animals, has the potential to produce models that accurately reflect genetic mechanism of human diseases by defining its genetic basis. In addition, the generation of such models enable studies to mimic the *in vivo* condition of the human diseases more accurately than previous non-transgenic models.

The advantages of a transgenic model are many. A main point is that this model can dissect downstream processes of the initial genetic event —e.g. the addition or deletion of specific defined gene(s) and which ultimately leads to the disease state. Therefore, the model can provide strong evidence that a particular gene is responsible for certain disease development. Thus, once identified, events downstream of the specific gene(s) provide a wider range of targets for therapeutic intervention.

The applicability of a transgenic system to molecular pathology is not limited to recapitulating a genetically well characterized malady but often raises new concepts relating to gene expression and gene function in disease, which may open up a new research direction of a defined gene associated human disease. Although the versatile aspect of a transgenic model is most employed to serve as a proving ground for testing hypotheses regarding the genetic mechanism of disease currently (review in (420)).

Moreover, in the most advanced inducible conditional gene switch systems, where an inducible tissue/cell specific promoter drives the gene(s) of interest (target), normal conditions are maintained until trigged by an active regulator and therefore, the tissue/cell specific target gene expression can be controlled on/off by application/removal of inducer at specific times, dependant on the goals of experimental design. Thus, the genetically modified animal remains disease free due to the inducible expression of the causative target gene which increases their viability and provides an ability to study multiple insults *in vivo*.

To study the molecular mechanism of multistep-development melanoma (14;19;421;422), the conditional gene switch approach provides investigators with a powerful tool to search the disease related genetic ablation spectrum in every stage during melanoma development.

1.5.3. Inducible conditional gene switch systems

Annotating the specific functions and the cooperation of individual genes during cancer development *in vivo* has become the primary task of cancer studies in the postgenome era, geared to search for potential novel therapeutic methods and to improve the life quality of the cancer patients. In addition to conventional approaches of transgenic and gene targeting technologies, the recent development of conditional gene modification technologies has provided a real opportunity for elucidating specific gene function and their cooperation at the level of genome. To understand the cancer aetiology at the molecular level, tissue/cell specific gene modifications in the mouse have been made possible by using site-specific DNA recombinases, conditional alleles and tissue/cell specific promoters to tightly control the timing and location of individual gene or gene co-expression. The studies have revealed novel basic insights for exploitation by the pharmaceutical industry.

The creation of a conditional gene switch system is based on the SSRs (Site-Specific-Recombinases) technologies. The most used this kind recombinases are Cre (causes recombination of the bacteriophage P1 genome) and Flp (named for its ability to invert or "flip" a DNA segment in S. cerevisiae) which are able to recombine defined DNA sequences with high fidelity without the need of cofactors (reviewed in (423))(424). These two recombinases have been used widely and effectively to generate gene deletions, insertions, inversions and exchanges in exogenous systems such as flies (425;426), mammalian cell culture (427;428) and mice (429;430). Both Cre and Flp can recombine DNA at defined target sites, termed *lox*P (locus of crossover (x) in P1) (431) and FRT (Flp recombinase recognition target) (432) respectively, at a very high efficiency (99.98% and 100% respectively) (427;433) (note: with 34bp in both recognized sequences, there is only

$1/4^{34}$ chance to find a same sequences which is far lower than 1/number of genetic base pairs of a mouse genome) in both actively dividing and postmitotic cells in most tissue types.

A more recently established Streptomyces phage-derived ϕC31 SSR is also been employing for the use to generate genomic recombined mouse model. Unlike Cre and Flp, ϕC31 SSR mediates recombination only between the heterotypic sites attB (34bp length: CGCGCCCGGGGAGCCCAAGGGCACGCCCTGGCAC) and attP (39 bp length: CCCCCAACTGAGAGAACTCAAAGGTTACCCCAGTTGGGG), named for the attachment sites for the phage integrase on the bacterial and phage genomes respectively, each containing an imperfect inverted repeats that are likely bound by ϕC31 homodimers. The ϕC31-mediated recombination occurs in a core triplets CAA sequence (underline indicated in the sequences) within each sites (434).

1.5.4. Mechanism of Cre-and Flp- based gene switches

Cre and Flp, members of the λ integrase superfamily of SSRs, share a common mechanism of DNA recombination that involves strand cleavage, exchange and ligation (435). Both Cre and Flp catalyze DNA recombination at the specific target sites, *lox*P and FRT respectively, which are distinguishable at the nucleotide level (below)

*lox*P: ATAACTTCGTATAATGTATGCTATACGAAGTTAT

FRT: GAAGTTCCTA T**T**CTCTAGAAAG**T**ATAGGAACTTC

However, both *lox*P and FRT share an overall structure which includes two 13-bp unique inverted repeats sequences (one base pair exception not inverted in FRT, **bold red** indicated), separated by a 8-bp asymmetric core sequence (or called spacer). Cre and Flp recombinases defined DNA with the same catalytic mechanism in a gene-switch model. In

the presence of two target sites, recombinase monomers bound to the inverted repeats to promote DNA synaptic complex formation and recombination between two sites (436), whereas strand cleavage, exchange and ligation occur within the spacers (437). Because of spacer asymmetry, strand exchange is possible only when target sites are connected by synapsis in one orientation (438). Consequently, the relative orientation of target sites with respect to one another determines the outcome of recombination: Cre/Flp either excises a circular molecule from between two directly repeated target sites and accompanied to integrate a circular molecule into a linear molecule each possessing a target site; or inverts the DNA between two inverted sites (Fig 4).

Unlike gene inversion, because of the loss of a circular reaction product, the excision reaction (Fig4, left) effectively results in gene activation or silence and therefore, this technique has been employed in mouse models in which either TSG (Conditional Knock Out –Cko, e.g. (439) and PTEN function loss in this study) inactivation or activation of oncogene preceded by *lox*P-stop-*lox*P flank (Conditional Knock In –Cki, e.g. (347) and N-Ras^{lys61} expression in this study) to generate tumourigenesis/developmental models of defined single/multiple gene(s) expression/silence for basic molecular and pharmaceutical studies.

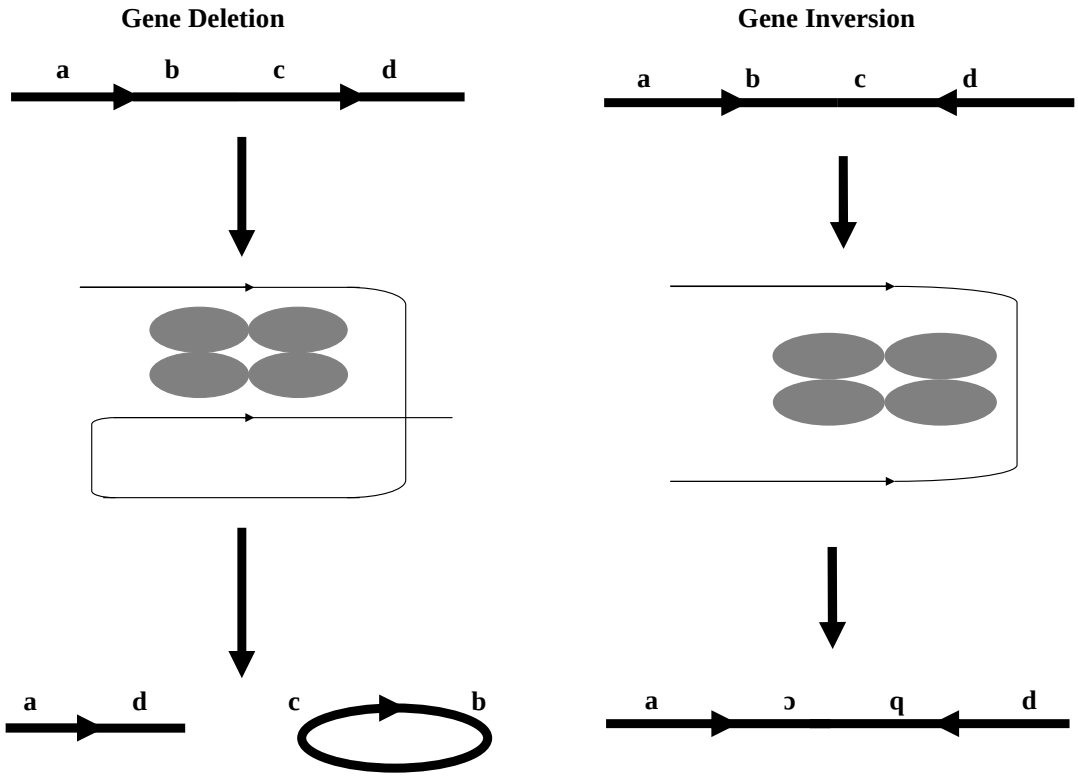

Figure 4: Diagram of Cre recombinase to recombine flank DNA. Recombinase reaction catalysed by Cre/Flp. Black triangles indicate recombinase recognition sites; black lines present chromosomal DNA, with orientation indicated by the letters a, b, c and d. Grey ovals are recombinase monomers. In the presence of two target sites, recombinase (Cre/Flp) monomers bound to target sequences to promote DNA synaptic complex formation and recombination between two sites whereas strand cleavage, exchange and ligation occur to result in DNA excision (left panel) or inversion (right panel). Cre/Flp excises a circular molecule from between two directly repeated target sites and accompanied to integrate a circular molecule into a linear molecule each possessing a *lox*P or FRT site to (in)activate the target gene between two target sites for the gene-targeting purpose (left panel, gene deletion); or only inverts the DNA between two inverted sites to fail to target gene expressing (right panel, gene inversion).

1.5.5. CrePR gene switch

In this study, a gene switch has been employed based on the Ru486 inducible progesterone receptor couple to the Cre/*lox*P system described above. By fusing the Cre recombinase gene with a truncated progesterone receptor ligand-binding domain, Kellendonk *et al*, created a valuable system for inducible gene targeting. Here the CrePR fusion protein recombinase recognises and binds Ru486 (mefipristone), an analogue of progesterone, (440). The CrePR fusion protein, previously sequestered in the cytoplasm then translocates to the nucleus where the recombinase functions to either excise critical flank (*lox*P floxed) exon/promoter or whole gene sequences to ablate function, or to excise inhibitor sequences (e.g. 'Stop' cassette) to induce target transgene expression. By using tissue/cell specific promoter to drive the regulator Cre half of the gene switch, the floxed target gene could be switched on/off only in specific tissue/cell and at a specific time(s) controlled by Ru486 (inducer) application. Therefore, animals remained disease(s) free before inducer application and this ability to induce defined temporal and highly localised of target gene expression presents a significant advantage over straightforward transgenic models, in terms of viability and the ability to study multiple targets in tumourigenesis and of developmental biology.

Thus in this study, with the goal of generation of an inducible Cre-based conditional gene-switch mouse model for melanoma, two lines of transgenic mouse, regulator and target lines each containing half of the gene-switch components, are produced and mated to create the complete gene-switch system. The regulator CreP half was coupled to a melanocyte-specific expression promoter (i.e. Tyrosinase or TRP2 for melanocyte expression) for the purpose of controlling the target gene expression in bigenic compound lines, with the target half constructed to be relatively generic, harbouring genes (i.e. our N-Ras and EGFP) driven by generic promoter such as the CMV promoter and thus be activated by any cell specific Cre transgene.

1.5.6. Gene (in)activation by Cre/*lox*P switch

To conditionally activate a target gene *in vivo*, a DNA 'Stop' cassette sequence containing poly(A) signal is placed between two '*lox*P' sites (floxed) and cloned upstream of the target gene to stop downstream target gene expression until Cre is activated. Ideally, the 'Stop' cassette and target gene should be designed under the control of a general promoter to allow the gene to be active in all of the cell types once the 'Stop' cassette has been removed by active Cre recombinase. Because of the cloning of upstream 'Stop' cassette, target genes remained inactive until the regulator Cre activity switches on its expression by excision of the 'Stop' silencer following application of the inducer, unless the promoter is leaky (e.g. Trp2Cre). In contrast, inactivation of a target gene *in vivo* is achieved by floxing functional exon(s), the gene promoter/transcription elements or the whole gene, so that the gene remained functional until target gene excision by Cre recombinase following inducer application.

1.5.7. Requirement for transgenic melanoma models

In mice unlike humans, inter-follicular melanocytes decline at birth and epidermal melanocytes are localised to the follicle where they increase after birth for about 2 weeks and decline as the hair growth ceased on progression from anagen to catagen. Thus, as most proliferative murine melanocytes are located in the follicles, coupled to the fact that the adult mouse skin is almost devoid of melanocytes in the resting phase of the hair cycle until the occasional follicles enter anagen when melanocytes arise from their stem cells, it is very difficult to induce melanoma by chemical carcinogenesis or UV exposure in the mouse (57;76). Therefore, the mouse has not been a good model for studying melanoma in the past (2). But despite these limitations, transgenic approaches have been employed to generate melanoma mouse models by genetic modification of mouse genome in mouse embryo/stem cells to express customer-designed oncogene(s) or to ablate the certain chromosomes locus(es) which is(are) susceptible to melanoma development.

The advantages of transgenic and conditional knock-out/in technologies have attracted many researchers to put their effort to assess the *in vivo* mechanisms of the oncogenes/TSGs during the tumour development. Thus, the first transgenic melanoma mouse model was generated by expressing simian virus 40 early-region transforming sequences driven by a tyrosinase, melanocyte-specific promoter in 1991 (441;442) with the idea of disrupting the then most famous TSGs p53 and Rb. The SV40 transforming gene, however, is not a human melanoma development related gene and therefore, melanoma related oncogene transgenic mouse model was developed by expression of activated H-Ras following UV exposure, although H-Ras alone failed to produce melanoma (221;222). Taking the advantage of inducible conditional gene-switch system, Chin *et al* developed another H-Ras induced melanoma model by controlling H-Ras expression in a INK4a deficient background (223), in which an essential role of Ras expression in melanoma development was identified. To recapitulate the aetiology of UV causality on melanoma, mouse models either over-expressing HGF/SF or activated H-Ras were generated and results confirmed that neonatal UV exposure is critical on melanoma development (39;40). Surprisingly, only recently was a mouse model with melanotic and metastatic melanoma produced that recapitulated genetic lesions frequently found in human melanoma by crossing activated N-Ras(Q61K), a hot spot N-Ras mutation in human melanoma, to a CDKN2A deficient mouse (215). In this model 90% mice developed melanomas within 6 months compared to the 25% and 2 months in the previous H-Ras models respectively. Searching the literature, there remains few melanoma mouse models available to study the molecular mechanism and the causative factors of disease development. Melanoma is one of the deadliest diseases with an over-all 5-year survival rate less than 20% in the US and a higher survival rate reported in Europe (443-445), where the survival rate is related to the histology of tumour, given PDM (primary dermal melanoma) has remarkably prolonged survival compared with patients with malignant melanoma or PNM (primary nodular

melanoma) of similar thickness (446;447). Thus, to more accurately mimic the aetiology of human melanoma, additional transgenic models (specifically inducible conditional gene switch models for multi-stage investigation) production is necessary for the investigation of molecular mechanism and/or identification of any new biological mediators (new genes, new pathways) for drug development.

1.6. Aims of the study

To create a model that avoids rapid melanoma development, mimic the early phases of nevi and to model epidermal/dermal junctional pathology of the RGP-VGP transition to mimic this vital development step in human melanoma, the inducible gene switch system provides a tool for these stage-related investigations whilst allowing the animal to develop normally. Therefore, the overall aim of this study was to create inducible transgenic melanoma mouse models to investigate the role of genes related to human melanoma development.

1. Oncogenic N-Ras^{lys61} was chosen to generate melanoma mouse model because it is the allele often mutated in human melanoma rather than H-allele which is less mutated in human melanoma but often used to generate mouse melanoma models by other groups.

2. PTEN TSG was introduced into this model to test if this TSG was able to promote N-Ras triggered tumourigenesis, based on its role in melanoma progression and in pathological development revealed by the other studies. PTEN is the second most abnormal TSG after CDKN2A in melanoma, yet its involvement in melanoma has not been relatively well studied in the few models to date nor its functional role(s) well detailed.

3. The role(s) of inducible N-Ras^{lys61} expression and/or PTEN function loss specifically in melanocyte during the melanoma development will be investigated.

4. Technically it became necessary to optimize the primary mouse melanocyte culture method for the identification of transgenic expressers and ideally the method should allow melanocytes to grow for extended periods without spontaneous transformation, which was necessary for the development of an *in vitro* transformation analysis.

5. Finally, the regulation of keratinocyte disruption on melanoma development will be studied in this inducible gene-switch model to assess whether and how does the microenvironment (keratinocytes) of melanocyte effects melanoma development.

Chapter 2: Materials and Methods

2.1. Materials

2.1.1. Cloning reagents

2.1.1.1. Plasmids

1. Phagemid vector pBK-CMV to supply the CMV promoter and multiple cloning sites (MCS) was obtained from Stratagene Europe, Amsterdam, Netherlands.
2. pBS302 plasmid supplied '*lox*P-Stop-*lox*P' cassette was obtained from Life Technologies, Inc.
3. Enhanced Green Fluorescent Protein (EGFP) DNA was cut from pEGFP-1 plasmid purchased from Clontech (Takara Bio), USA.
4. Plasmids containing, CrePR1 or generic intron individually were generously supplied by Dennis Roop, Bayler College of Medicine, Houston, USA.
5. pSL1180 plasmid to provide extra MCS was purchased from Pharmacia (now G.E. Healthcare);
6. Tyrosinase, Trp2 and the tyrosinase enhancer, N-Ras^{lys61} were generous gifts from Paul Overbeek, Baylor College and Frederich Beermann, Switzerland respectively.

2.1.1.2. Restriction Endonuclease

1. Enzymes from New England Biolabs: Afl II, ApaL 1, Asc I, Eag I, Nde I, Nsi I
2. Enzymes from Promega, UK: Apa I, Ava I, BamH I, Bcl I, Cla I, Hpa II, Nhe I, Not I, Sal I, Sma I, Ssp I, Xba I
3. Enzymes from Invitrogen, Paisley, UK: Bgl II, EcoR I, EcoR V, Hind III, Kpn I, Pst I, Pvu II, Sca I, Spe I, Sph I, Sst I and Xho I

2.1.1.3. Other Cloning Enzymes

DNA polymerase I large (Klenow) Fragment and Calf Intestinal Alkaline Phosphate (CIAP) were from Promega, UK; T4 DNA Ligase and T4 DNA Polymerase were from

Invitrogen, UK.

2.1.1.4. Other cloning materials

Ampicillin, Kanamycin, Select peptone, Yeast Extract, Select Agar and Agarose were purchased from Sigma, UK; 1Kb+ DNA marker; Stabl II and DH5α competent cells were from Invitrogen, UK.

Gel electrophoresis tanks, tray, comb and power supplies were purchased from Bio-Rad, UK.

2.1.2. Cell culture materials

2.1.2.1. Reagents

Fugene-6 transfection reagent obtained from Roche (cat #11815091001); L-Glutamine, Penicillin/Streptomycin, Phosphate buffered saline (PBS) without Ca^{2+} and 2.5% trypsin were from Invitrogen; basic fibroblast growth factor (b–FGF, F9786), alpha- Melanocyte Stimulating Hormone (α-MSH, M7909), Chelex 100 sodium form (C7901), Mefipristone (Ru486, M8046), G418 (A1720), Sodium orthovanadate (Na_3VO_4, S-6508), N^6,2'-O-dibutyryladenosine 3,5-cyclic monophosphate (dbcAMP, D0627), 12-O-tetradecanoyl phorbol-13-acetate (TPA, P8139), ethanol, dimethyl sulfoxide (DMSO) were obtained from Sigma. All other chemicals were purchased from Fisher Scientific.

2.1.2.2. Tissue Culture Media

1. DMEM (Dulbecco's Modified Eagle Medium) and Ham's F12, foetal calf serum (FCS) and normal horse serum were purchased from Invitrogen.
2. KBM without Ca^{2+} plus component additives including: 0.5ml Insulin (cc-4021E), 0.5ml rhEGF (cc-4015E), 0.5ml GA-1000 (cc-4081E), 0.5ml Hydrocortisone (cc-4031E) and 2.0ml BPE (cc-4002E) per 500ml KGM were purchased from Cambrex,

UK

3. The in house designed 50/50 medium for primary mouse melanocyte culture comprised: 50% of DMEM supplemented with 10% chelexed FCS (prepared by treating FCS with Chelex 100 sodium form following manufacture's instruction to remove calcium) and 50% KGM with additions of calcium to 0.05mM Ca^{2+}, 10ng/ml TPA and 1ng/ml b-FGF.
4. Halaban's medium for melanocytes culture comprised: Ham's F12, 7% horse serum plus 2% FCS, 50ng/ml TPA, 5.0x 10^{-5}M dbcAMP and 1.0μM Na_3VO_4.

2.1.2.3. Cell lines

The B16F1 melanoma cell line was obtained from Ian Hart, London and originally established by Isaiah J. Fidler, MD Anderson Cancer Centre, Houston TX.

2.1.3. Other molecular materials

2.1.3.1. PCR and RT-PCR reagents

Taq DNA polymerase —Cancer Research UK;

dNTPs —Roche diagnostics;

10x PCR buffer (500mM KCl, 100mM Tris pH 9.0, 1% Triton X-100, 15mM $MgCl_2$) and 6x DNA loading buffer (30% glycerol, 0.25% bromophenol blue, 0.25% xylene cyanol FF) were prepared in house.

2.1.3.2. Molecular Biology Kits

From Qiagen Ltd: DNeasy tissue kit (#69504), RNeasy mini kit (#74104), Qiaquick PCR purification kit (#28104), Qiaquick Gel extraction kit (#28704), QIAREP Spin miniprep kit (#27104), QIAFILTER Plasmid max kit (#12262) and Endofree plasmid mega kit (#12362).

Stratagene: Absolute RNA mini (#400800)

Amersham Biosciences: First Strand cDNA synthesis kit (#27-9261-01),

2.1.4. Immunohistochemistry and histology reagents

2.1.4.1. Antibodies

Santa Cruz Biotechnology: goat anti-Trp2, goat anti-Kit and goat anti-SCF.

RDI Research Diagnostics Inc: rabbit anti-K1 and guinea pig anti-K14.

Vector Laboratories: Biotinylated anti-goat IgG, biotinylated anti-rabbit IgG, biotinylated anti-guinea pig IgG, Texas red avidin, Fluorescein avidin D, Texas red anti-goat IgG, Texas red anti-rabbit IgG, Texas red anti-guinea pig IgG, Fluorescein anti-goat IgG, Fluorescein anti-rabbit IgG and Fluorescein anti-guinea pig IgG.

Cell signal technology: anti-caspase-3 and anti-caspase-9.

2.4.1.2. Other reagents

Normal horse/goat sera are from Invitrogen, Paisley, UK;

PBS, Xylene, Ethanol, Haematoxylin, Eosin are from Fisher Sciences.

PermaFlor, slides and cover slips are from BDH.

2.2. Methods

2.2.1. Primary Cell Culture

2.2.1.1 Primary melanocyte culture

Mouse melanocytes were isolated from neonates no later than 48 hours old when melanoblasts are still proliferative prior to their migration to the hair follicle papillae because later the newly developing follicles make the dermis and epidermis difficult to separate leading to fibroblast contaminations. Newborn mice were killed by injection of urethane under PPL 60/2929, Schedule 1. The dead mice were soaked in 70% ethanol to sterilize and the skin was carefully separated from the mouse body using scissors and tweezers. Following classical protocol, entire skin was stretched on the cover of a 60-mm dish to dry for a few minutes to prevent curling when floating on trypsin which inhibits separation of epidermis and dermis resulting in increased numbers of contaminating fibroblasts (448). The skin was taken off the dish lid and floated dermal side down on 5ml of 0.25% sterile trypsin, overnight at 4^0C. The following day the epidermis was then stripped off the dermis and epidermal cells (keratinocytes and melanocytes) isolated from the cornified layer by gently rocking for approximately 15 minutes in 15ml Falcon tubes, containing 13ml DMEM medium with normal 10% FCS. To separate cornified layer debris from epidermal cells, the cell suspension was filtered through sterile gauze. Cells were then centrifuged for 3 minutes at 1000 rpm and cell pellets were gently resuspended in 5ml 50/50 medium at 5 x 10^6 cells/60mm dish. Medium was changed 24 hours later to remove dead/differentiated cells and primary cells were kept in culture for 3-4 weeks by which time keratinocytes had differentiated, leaving melanocytes for either transfection or required analysis, with medium changes every 3-4 days.

2.2.1.2. Primary melanocyte culture in Halaban medium

Epidermal cell pellets isolated from new born mice as described above were also

resuspended in Halaban medium (449) comprised of Ham's F12, 7% horse serum plus 2% FCS, 50ng/ml TPA, 5.0 x 10^{-5}M dbcAMP and 1.0μM Na_3VO_4, and plated at 5 x 10^6 cell per dish as did for cells in 50/50 medium. Cells were washed with PBS at 24 hours post plating to remove any dead cells/debris and then replace medium twice weekly as above.

2.2.1.3. Primary keratinocyte culture

To isolate primary transgenic keratinocytes, newborn K14Cre/N-Ras^{lys61} skin was prepared as described above and following successful genotyping, which had been performed within 24 hours by PCR (see below), appropriate transgenic epidermis were pooled and primary keratinocytes plated at 5 x 10^6 cells per 60mm dish in low Ca^{2+} medium (DMEM, 10% chelexed FCS, 0.05mM Ca^{2+}). The following day, cells were washed with PBS to remove dead and differentiating cells prior to adding fresh medium with or without 10^{-9}M Ru486. Cells were harvested 4 days later for analysis of K14Cre mediated N-Ras^{lys61} transgene expression by RT-PCR.

2.2.2 Cloning of the transgenes

2.2.2.1. Restriction endonuclease digestion

For general DNA purification purposes, 5µg DNA was digested in a 50µl total volume including: 1-2µl of enzyme and 1x buffer (diluted from 10x stock) specified by the manufacture for each enzyme for 2 hours at 37^0C (except: Sfi 1 at 50^0C, Sma1 at 25^0C and Sml 1 at 55^0C according to the manufacture's protocol), followed by agarose gel electrophoresis and Qiaquick gel purification to isolate the required DNA fragments. Where a second digestion was necessary, the salt concentration of reaction buffer was adjusted by adding more sodium (or potassium) chloride to create the working conditions for the second endonuclease enzyme or the DNA sample was purified using Qiaquick PCR purification kit following the manufacture's instructions followed by the second restriction endonuclease digestion.

For general diagnostic cloning purposes, 1µl of Qiaquick miniprep kit isolated DNA solution, together with 2µl of 10x specific enzyme buffer and 0.5µl enzyme was diluted with dH_2O to 20µl total volume and incubated at 37^0C (occasionally at other temperatures) for one hour followed by running a 0.8% agarose gel and the DNA migration pattern analysed to identify correct colonies.

2.2.2.2. Blunt end DNA digestion

3' overhanging DNA was blunt ended by T4 DNA polymerase following the manufacture's protocol. Briefly, 2µg restriction endonuclease digested DNA, 5µl buffer, 1.0µl T4 DNA polymerase, 0.2µl of 25mM dNTPs (to make 100µM final concentration) was diluted with dH_2O to 50µl and incubated at 37^0C for 5 minutes to blunt the ends, the reaction stopped by adding 2µl of 0.5M EDTA and then DNA purified using Qiaquick PCR purification kit (as above). The eluted blunt end DNA fragment was then ready for further digestion or ligation as required.

To generate blunt ends from a 5' overhanging DNA, DNA polymerase I large (Klenow) fragment was employed following the manufacture's instructions. Briefly, 1-4µg restriction endonuclease digested 5' overhanging DNA, 5µl reaction buffer and 1 unit Klenow fragment per microgram of DNA were incubated in a total volume of 50µl for 10 minutes at room temperature, followed by heating at 75^0C for 10 minutes to stop the reaction and DNA fragments purified as described above for the subsequent experiments.

2.2.2.3. Dephosphorylation of DNA fragment

To significantly reduce the ligation background by stopping the self-ligation of the vector, DNA dephosphorylation was occasionally necessary. Following manufacture's instructions, up to 10pmol of DNA (1µg of 10-Kb DNA = 0.152pmol), 5µl of 10x CIAP reaction buffer, 0.05 unit CIAP and dH_2O added to 50µl, was incubated for 15 min at 37^0C and then 56^0C for another 15 min. A second aliquot of CIAP was added into the reaction mixture and incubation repeated at both temperatures. To stop the reaction, 300µl CIAP stop buffer (10mM Tris-Cl, pH 7.5; 1mM EDTA, pH 7.5; 200mM NaCl and 0.5% SDS) was added and followed by DNA purification as described above. DNA is ready for ligation or further digestion as required.

2.2.2.4. Ligation and transformation

Following successful isolation and preparation of both insert and vector, the two fragments were ligated using T4 DNA ligase following manufacture's instructions. A total of 100 femtomol (fmol) of DNA at 3:1 (molar) ratio of insert: vector, 2µl of 5x ligation buffer, 0.2 µl T4 DNA ligase (1 unit) and dH_2O was added to 10µl, mixed and incubated overnight at 16^0C to obtain maximum ligation efficiency.

Plasmid DNA was prepared and screened for correct recombination, via transformation of the ligated DNA into competent bacterial cells. 2µl overnight ligation mixture was

transferred into 50-100µl of Stabl II cells for enhanced tyrosinase (Stabl II was developed to stabilize DNA sequences containing many single repeats, which exist in the tyrosinase enhancer) or more generally into DH5α comptent cells. The mixture incubated on ice for 30 minutes followed by a 42^0C shock for 45 second and immediate transfer to ice to incubate for a further 2 minutes. Following addition of 0.9ml SOC medium, the transformed cells were incubated at 37^0C for 1 hour in a shaking bath and 0.1ml culture medium was spread onto LB-agar plates containing 100µg/ml Ampicillin or Kanamycin depending on the antibiotic selection gene in the plasmid construct. Plates were incubated overnight at 37^0C for production of colonies.

2.2.2.5. Colony screening

Single colonies obtained above were picked and transferred into 5ml LB medium containing either 100µg/ml Ampicillin or Kanamycin and grown overnight for DNA preparation using a Qiaquick Miniprep kit. Briefly, cells were harvested by centrifugation at 1000 rpm for 10 minutes, and resuspended in buffer P1 followed by alkaline lysis in buffer P2 and neutralized by adding buffer P3 which precipitated protein. Precipitated protein was removed by centrifugation for 10 minutes at 13000 rpm, and the suspension containing plasmid DNA was loaded onto columns and centrifuged for 1 minute at maximum speed to combine DNA with silica membrane. Filtrate was discarded and washing buffer was loaded into the column to remove salts and endonucleases by centrifugation at maximum speed. Plasmid DNA was finally eluted from column membrane by adding 50µl dH_2O and centrifugation at maximum speed for 1 minute.

Eluted purified DNA was digested by a series of diagnostic endonuclease restriction enzymes. Following agarose gel electrophoresis, correct recombinants were identified by comparing patterns of DNA gel migration with the theoretical map of vector DNA fragments with correct insertion. The colonies were confirmed by sequencing to prove that

no mutations had occurred during the cloning process.

2.2.2.6. Melanocyte-specific regulator transgene construction

The regulator is based on the backbone of plasmid pCrePR1 which was generous supplied by Professor Dennis Roop (Bayler College of Medicine, Houston, USA) in which fusion protein CrePR1 expression is driven by the HSV TK promoter (440). To express the CrePR1 fusion protein exclusively in melanocytes, an enhanced tyrosinase promoter (Etyr) replaced the generic HSV TK promoter. This Etyr promoter had been previously constructed in the creation of Etyr.p65, a non–Cre based regulator transgene (Forrow, S *et al*; unpublished) by cloning a 200 bp SSP1 fragment of an upstream enhancer located at 12kb upstream of the mouse tyrosinase gene (450) into a plasmid vector containing a 1.3kb fragment of 5' mouse tyrosinase promoter sequence (451). The Etyr was released from Etyr.p65 and subcloned into pCrePR1 at the Pst1 and Bgl II sites via shuttling through a pSL1180 plasmid to create the EtyrCrePR1 regulator transgene (See results section 3.1.1).

To further increase gene expression in transgenic mice, a final version of this tyrosinase vector was designed to include a generic intron, which was not in the EtyrCrePR1 (ECre) and increases message stability and efficient processing (452;453). To amplify this generic intron from pCrePR1 for multiple cloning purposes, two primers were designed:

Fwd: 5'-CTCCTCTAACTAGTAGCTTTAAATTTGC-3'
Spe I

Rev: 5'-TTAACAACTGGTACCTCTTGAACTATAG-3'
Kpn I

to produce 5' Spe I and 3'Kpn I sites to facilitate cloning into ECre, as the 5' Spe I site of generic intron was compatible to the Nhe I site of the ECre transgene; whilst a Kpn I digested generic intron was blunt ended at 3' by T4 DNA polymerase and ligated to Bgl II digested and polymerase I fragment blunt ended ECre plasmid DNA. This final version

was named EICre and released for microinjection by Not I digestion of plasmid DNA followed by recovery of a 5.6-kb DNA fragment.

Tyrosinase related protein 2 (TRP2), a promoter which is cited to be stronger than tyrosinase and possibly expressed in melanoblast stem cells (53), was also cloned by replacing the Etyr promoter of EICre vector to produce another melanocyte specific regulator TRP2Cre. It was envisaged that CrePRI driven by the TRP2 promoter would give a stronger and wider window of CrePRI expression in transgenic mouse melanocyte. The TRP2Cre regulator was cloned by cutting plasmid TRP2-p(A) (Paul Overbeek, Baylor College of Medicine, Houston, USA) (454) with EcoR V and Not I to discard the vector p(A). The discarded vector p(A) in TRP2-p(A) was then replaced by the Intron-CrePR1-p(A) fragment excised from EICre (described above) following digestion of Kpn1/blunt ending and Not I (they are compatible to the EcoR V and Not I sites of TRP2 fragment obtained from TRP2-p(A) respectively). As described above for EICre, successful colonies were identified by diagnostic restriction enzyme analysis and the transgene DNA sequenced to assure no additional mutations had arisen.

2.2.2.7. Construction of transgenic target vectors

To test the flox-Cre based conditional gene-switch system in cultured melanocytes prior to transgenic production, a Cre responsive target vector containing EGFP report sequence was created by excising the '*lox*P-Stop-*lox*P' cassette from plasmid pBS302 (Gibco, NCBI data base U51223/GI: 1277147), which contained serial stop codes flanked by two '*lox*P' sites (428;429), via digestion of Spe I and EcoR I. This 'Flx-Stop' fragment was then cloned into plasmid pEGFP-N1 (Clontech, US: Gene Bank access number U55762/GI: 1377911), which expresses EGFP downstream of the CMV promoter by ligating with double digestion of Nhe I and EcoR I to make ends compatible with the 'Flx-Stop' fragment (Nhe I to Spe I at 5' and EcoR I at 3' respectively).

The resulting vector was further modified by insertion of the generic intron between 'Flx-Stop' cassette and EGFP protein via digestion of Spe I(5') and Kpn I(3') to create cmv.stop.EGFP. This target gene remains silent until Ru486 activation of a Cre regulator to evict the floxed ‘Stop’ cassette between CMV promoter and EGFP gene. The successful cloning was screened and identified as described above via diagnostic digestion and sequencing.

To construct the oncogenic target transgene cmv.stop.N-Ras^{lys61}, the mutant form of N-Ras was released from a tk-N-Ras^{lys61} plasmid (originally constructed by replacing the CAT report sequence from tk.CAT (455) with human N-Ras^{lys61} cDNA cloned from the HT1080 fibrosarcoma cell line (160)), via sequential digestions by Spe I, blunt ending using DNA polymerase I large fragment (Klenow) and Apa I. In parallel, report target vector cmv.stop.EGFP was sequentially cut with Not I, blunt ended by Klenow fragment and digestion of Apa I to remove the EGFP sequence. The two fragments, N-Ras^{lys61} (blunt Spe I/Apa I) and cmv-stop-intron (blunt Not I/Apa I) were ligated overnight at 16^0C followed by transformation, cell amplification and colony mini preparation. To identify successful construction, cmv.stop.N-Ras^{lys61} vector DNA was analysed by diagnostic restriction enzyme digestions and sequencing as above.

2.2.3. Transgenic line production

2.2.3.1. Transgene DNA preparation

Following successful construction of the regulator and target vector, endotoxin free DNA was prepared to minimize the potential toxicity of DNA and maximise surviving embryos following pro-nucleus microinjection, employing the Qiagen Endofree plasmid kit following manufacture's instructions.

To obtain the EICre transgene regulator sequence, a 5.6-kb band was recovered from agarose gel following Not I digestion of the EICre regulator vector and purified using QiaQuick gel purification kit following manufacture's instructions. Similarly, following Nsi I and partial Afl II digestions, a 3.5kb oncogenic target cmv.stop.N-Ras^{lys61} transgene was cut from the agarose gel and purified. Transgene DNA was eluted into embryo transfer water (Sigma, #W1503).

Transgene DNA concentrations were determined by running various volumes of gel purified transgene DNA through a 0.8% agarose gel against a series amount of certain DNA marker rather than quantification by UV spectrophotometer given the low concentrations of DNA employed. Transgene DNA was then diluted to the optimal concentration of 1-2ng/µl in microinjection buffer (5mM Tris, pH7.4 and 0.1mM EDTA) and was further purified to remove any possible particles which may interfere with pro-nucleus microinjection by spinning centrifugation at 13000 rpm through a Ultra free-MC 0.1µM filter (Millipore, USA). Following this additional purification step, a second agarose gel was run to confirm the concentration and quality, i.e. no DNA degradation of transgene for pro-nucleus microinjection.

2.2.3.2 Transgenic mouse production

The transgenic lines were produced following the typical transgenic mice production procedures (456) and all procedures were performed in central research facility (CRF) in the Glasgow University under Project licence 60/2929 and personnel licence 60/8633.

Briefly, following the preparation of regulator EICre and target stop.N-Ras^{lys61} transgene DNAs as described above, 1-2µl transgene DNA solution was microinjected into one pronuclei cell harvested from mice 22-23 hours after superovulation. To induce superovulation, 5 IU PMS (pregnant mare's serum to mimic follicle-stimulating hormone (FSH)), was intraperitoneally injected into a B6/D2/F1 mouse followed by injection of 5 IU hCG (human chorionic gonadotropin to mimic luteinizing hormone (LH)), with an interval of 46-47 hours. The female was placed in cage with a stud mouse after the injection of hCG and was checked for a copulation plug the next morning before harvesting. Microinjected embryos were implanted into pseudopregnant mice generated by mating of an ICR females and a sterile male (vasectomized), which was set while a mating was setting for superovulating as described above.

Following the birth of transgenic pups, tail tips were removed from 5-6 weeks old mice to isolate DNA for PCR genotyping (described below), and positive founders were bred with normal C57BL mouse to identify germline transmitters and transgenic expressers.

Following identification of germline transmitters, transgenic neonates were produced by crossing transgenic founders with normal C57BL to obtain primary cultured melanocytes to be used for identification of transgenic expressers. To identify regulator expressers, primary cultured pure transgenic melanocytes were harvested directly and assessed for regulator activity, cmv.stop.EGFP DNA was transfected and cells were treated with 10^{-9}M Ru486 and RNA isolated using an absolutely RNA kit (cat #400800, Stratagene UK)

followed by RT-PCR analysis or assessment for positive green cells, as described below. The target line (cmv.stop.N-Ras^{lys61}) expresser identification was assessed in bigenic K14Cre/N-Ras^{lys61} keratinocyte via RNA isolation and RT-PCR employing well characterized K14Cre regulator to avoid difficulties of primary melanocyte culture and transfection.

2.2.3.3. Tail cutting and genomic DNA isolation

5-6 week-old weaned mice were briefly anaesthetized to remove approximately 3-4mm of tail tip and the wound was cauterised. Tissue was digested in 400µl of DNA extraction buffer (50mM Tris/HCl pH 8.0, 100mM EDTA pH 8.0, 100mM NaCl, 1% SDS and 200µg/ml fresh proteinase K) in an eppendorf tube at 55^0C overnight. To isolate tail genomic DNA, tail lysates were centrifuged for 10 minutes at maximum speed to remove tissue debris and degraded protein and the supernatant was transferred into a new eppendorf tube containing an equal volume of absolute ethanol to precipitate genomic DNA. Cluster DNA was picked by gently stirring a pipette tip and DNA was left dry in air for 1-2 minutes to evaporate any residual ethanol which may interfere in the following reaction. Tail DNA was then transferred into a new eppendorf tube containing 400µl dH_2O to dissolve. To ensure DNA was dissolved properly, DNA solution was left at room temperature or at 55^0C overnight.

2.2.4. Genotyping and identification of excised "floxed" sequences in target transgenes

Generally, 1µl of tail DNA solution was used as a template in a 25µl reaction volume containing 0.5µM reverse and forward primers specific for each transgene (Table 1), 2mM Mg^{2+}, 0.25mM dNTPs and 1 unit Taq polymerase in a 200µl PCR tube. PCR programmes for each transgene were pre-optimized by gradient PCR using plasmid DNA (equal to 1 copy of transgene in 100ng mouse genomic DNA) to determine suitable annealing temperature for each individual primer pairs. The programmes for each transgene are:

initial DNA denature for 2 minutes at 95^0C, 30 cycles of 30 second at 95^0C denature, 30 second annealing at 60^0C (K14Cre, EICre), or 45 second at 63^0C (cmv.stop.N-Ras^{lys61}), or 60 second at 64^0C (PTEN) and extension for 45 second (K14Cre, EICre and cmv.stop.NRas^{lys61}) or 90 second (PTEN) at 72^0C, with a final extension cycle at 72^0C for 10 minutes. This gave the following transgene specific bands: 410-bp K14Cre, 500-bp EICre, 850-bp N-Ras^{lys61} and PTEN products were 1.1-kb (floxed), 0.9-kb (wild type) or 1.1-kb plus 0.9-kb (heterozygote) respectively.

To PCR DNA from tissues to identify excision of floxed sequence following application of Ru486 and resultant activation of CrePRI fusion protein, DNA was isolated using Qiagen DNeasy tissue kit following the manufacture's instructions and a hot start PCR programme was employed given the difficulty of the product detection. PCR programme was run at 59^0C for 60 seconds annealing, 72^0C for 60 seconds extension.

Table 1: Oligos used in PCR analysis

Name	Genotyping for	Sequences
K14Cre.fwd	K14CrePR1	TCATTTGGAACGCCCACT
K14Cre.rev	K14CrePR1	GATCCGAATAACTACCTGTTTTG
PTEN.fwd	PTEN knockout	ACTCAAGGCAGGGATGAGC
PTEN.rev	PTEN knockout	GTCATCTTCACTTAGCCATTGG
Rosa.fwd	Rosa26	AAAGTCGCTCTGAGTTGTTAT
Rosa.rev	Rosa26	CGAAGAGTTTGTCCTCAAC
P1 and P76	N-Ras^{lys61} forward	CTAGAATTCCATCAAGCTTAGGA
P2	N-Ras^{lys61} forward	CTAGAATTCGCTGTCTGCG
P3 and P 28	N-Ras^{lys61}reverse	TCGCCTGTCCTCATGTATTG
ECre.fwd	ECre (p29)	ATTGGTGCAGATTTTGTATG
ECre.rev	ECre(p72)	CATCTTCAGGTTCTGCGG
P42	cmv.stop.N-Ras	ACACCACAGAAGTAAGGTTCCT
P61	cmv.stop.N-Ras	CAGAAAACAAGTGGTTATAGATGG
P62	cmv.stop.N-Ras	TCCCACTAGCACCATAGGTAC
P66	cmv.stop.N-Ras	TAAATCTGTCCAAAGCAGAGG
P67	cmv.stop.N-Ras	AAATGTGGTATGGCTGATTATG
P75	cmv.stop.N-Ras	GTTTAGTGAACCGTCAGATCC

2.2.5. RNA isolation and RT-PCR to confirm transgene expression

RNA was isolated from cells and tissue using an absolute RNA mini kit following the manufacturer's instructions. Transfected cells were harvested by trypsinisation and centrifugation for 5 minutes at 1000 rpm to obtain cell pellet and tissues were homogenised using motor-pestle. Briefly, harvested cell pellet or homogenised tissues were resuspended in 350µl lysis buffer containing fresh 7µl/ml β-mercaptoethanol. Lysate was spun down through a pre-filter column to remove debris, filtrate was recovered to precipitate RNA by adding an equal volume of absolute ethanol and the solution was gently mixed by inverting the tube. The mixture was loaded onto an RNA-binding column followed by pre-washing, DNase digestion and final-washing steps. RNA was finally eluted in a various volumes of RNase-free water depending on the number of cells (normally 20-50µl for $2x10^5$-$1x10^6$ cells) to obtain about 1mg/ml concentration of RNA.

Reverse Transcription (RT) was carried out immediately after RNA isolation to avoid any degradation using a First-strand cDNA synthesis kit following manufacture's instructions (#27-9261-01, Amersham-Pharmacia Biotech, UK). Briefly, 8µl eluted RNA was denatured at 65^0C for 10 minutes, chilled in ice for 2 minutes. 1µl of 0.2µg/ml of oligo-d(T)n, 1µl DTT and 5µl Bulk buffer (reverse transcriptase, dNTPs and reaction buffer mixture) were added followed by one hour incubation at 37^0C creating the cDNA for the following PCR amplification.

In a 200µl PCR tube, 1µl of RT product from above was used. Each PCR reaction mixture contained 2mM Mg^{2+}, 0.5µM reverse and forward primers, 0.25mM dNTPs and 1 unit Taq DNA polymerase and total volume was adjusted to 25µl using dH_2O. PCR was run 35 cycles at annealing temperature of 62^0C, 57^0C and 51^0C for N-Ras^{lys61}, EGFP and regulator EICre expression analysis respectively.

2.2.6. Transfection

The B16 melanoma cell line and regulator primary transgenic melanocytes were employed to confirm biological activity of regulators and target vectors following successful cloning and to identify transgenic expressing founders in transfection experiments. Regulators and/or target constructs were (co-)transfected into B16 cells to identify functional gene switch prior to transgenic production. To confirm regulator transgene expression *in vitro* prior to the breeding to produce oncogenic phenomenon, regulator primary melanocytes from transgenic mice were transfected with the report DNA employing Fugene-6 transfection reagent. This carrier was identified as the best transfection reagent for both melanocyte cell line and primary cells in experiments that compared other DNA delivery vehicles (Lipofectin, Lipofectamine, Transit, calcium phosphate) which gave either higher toxicity and/or lower transfection efficiency.

2.2.6.1 Transfection of B16 cells

Routinely, B16 melanoma cells were cultured in minimal essential medium (MEM)/10% FCS and medium changed every 3-4 days. These cells were split weekly and plated at 1:50 approximately $2x10^5$ cells/60mm dish in normal culture to avoid confluence as, once confluent, B16 cells die quickly.

Employing cmv-EGFP plasmid DNA as a transfection efficiency positive control and co-transfection of pCrePRI DNA (CrePRI expression under control of the generic HSV tk promoter to allow CrePRI to express in all cells) together with cmv.stop.EGFP plasmid as gene switch positive controls, 24 hours prior to transfection, B16 cells were trypsinized and seeded at 1 x 10^5/per 60mm dish. Fugene-6 transfection reagent was employed following the manufacturer's instructions, finding the ratio of 3:1 or 3:2 (for co-transfection) of Fugene-6 reagent to DNA (6µl Fugene-6:2 µg/or 2µg + 2µg DNA of cotransfection) as optimum.

The transfection was carried out as follows: 100µl of serum free MEM medium was aliquoted into a Nunc cryovial subsequently followed by adding 6µl of Fugene-6 reagent, tapping the tube briefly to mix the solutions and adding up to 4µg endotoxin free plasmid DNA (e.g. 2µg of each for EICre and cmv.stop.EGFP for co-transfection). The mixture was incubated at room temperature for 30 minutes to form reagent-DNA complex and added dropwise onto dish and the dish swirled slowly to allow an even mix of the reagent-DNA complex on the cells. Following overnight incubation, cells were washed and fed with medium containing 10^{-9}M Ru486 to activate the CrePRI fusion recombinase to subsequently excise the 'Stop' cassette of the target vector to express target genes or the medium without Ru486 in control dishes. For report assays, transfected cells were assessed for fluorescent green cells 48-72 hours after transfection of cmv.stop.EGFP or 96-120 hours after co-transfection of regulator and target transgenes DNA under a fluorescence microscope, counted and photographed.

2.2.6.2. Primary melanocytes transfection

Primary melanocytes cultured in 50/50 or Halaban medium were washed twice with PBS to remove dead cells and fed with fresh medium 24 hours prior to transfection. Employing cmv-EGFP as a positive transfection control and pCrePR1 as a regulator positive control, regulator (EICre or TRP2Cre) or target (cmv.stop.EGFP or cmv.stop.N-Ras^{lys61}) DNAs were (co)transfected with Fugene-6 as described above for B16 cells. The fluorescent green cells (EGFP transfection) were viewed under a fluorescence microscope 3 days (cmv-EGFP) or 4-5 days (regulator/target cotransfection and cmv.stop.EGFP transfected regulator primary melanocytes) post transfection respectively and then harvested for confirmation of EGFP expression by RT-PCR. Parallel transfected target (cmv.stop.N-Ras^{lys61}, PTEN) cells were left in culture for EGFP cell proliferation or G418 selection in colony formation analysis.

2.2.7 Transformation of primary melanocytes and colony formation analysis

Co-transfection of TRP2Cre with cmv.stop.EGFP or G418 resistant vector CMV-neo into target (Δ5PTEN$^{flx/flx}$ and/or cmv.stop.NRas^{lys61}) transgenic primary melanocytes cultured in 50/50 medium were carried out as described above. In these co-transfections, DNA ratio of 3 (TRP2Cre) to 1 (cmv.stop.EGFP or CMV-neo) was used to ensure all green cells (EGFP expression following 'Stop' excision by active TRP2Cre) or G418 resistant N-Ras^{lys61} expressing cells (neomycin expression) transfectants containing TRP2Cre regulator.

In the "green" colony formation assay, transfected melanocytes were left for continuous culture until the colony formed and cells were checked daily 4 days post-transfection under a fluorescence microscope for EGFP expression. In G418 resistant experiment, initially various concentrations of G418 (20-600μg/ml) were tested to optimize the G418 concentration for primary melanocyte colony selection prior to transfection and 200 μg/ml of G418 was optimized to select colonies due to the minimum toxicity for cell growth and selective pressure for colony formation. G418 was added 24 hours after transfection and then routinely employed until the end of experiment.

2.2.8. Importation of K14CrePR1 and Δ5PTEN$^{flx/flx}$ mice

K14CrePR1 positive control mice (developed by Dennis Roop, Bayler College of Medicine, Houston, TX) and mice expressing PTEN exon 5 flanked by '*lox*P' sites (floxed) (Hong Wu, UCLA School of Medicine, CA) were imported from USA under licence and strict Home Office regulations. Following rabies quarantine and re-derivation by embryo transfer in class II hoods, and screening of sentinel mice to prevent import of diseases, quarantined transgenic mouse tails were cut in class II hoods following regulate procedures and genotyped via PCR. Using PCR positive mice, a typical mating was set to establish the colonies. Generally, the male was removed from the breeding cage once pregnancy was confirmed and pregnant females were separated, and neonates checked for

phenotype (if any). Mice were weaned at 4-5 weeks, ear tagged and the tails were cut for genotyping 1-2 weeks after weaning depending on the size. Negative mice were recorded and culled under PPL schedule 1 and positive progenies were kept for breeding or source of melanocytes or keratinocytes.

2.2.9. Immunofluorescence staining

2.2.9.1. Preparation of Samples

(i) Induction of adult melanocyte growth *in vivo*: Mice were briefly anaesthetized and back hair was plucked with tweezers to start the anagen phase of the hair cycle and begin melanocyte proliferation. At this time (day 0) gene induction procedure was commenced by topical application of 10^{-9}M Ru486 in ethanol. Skin biopsies (5 x 3mm) were taken at each required time point from the mice on procedure and small wound sealed by wound clips which were taken off within 1-2 weeks. Biopsy samples were immediately fixed in 10% buffered formalin for 24 hours at 4^0C, embedded in paraffin and 4μm thickness sections were cut for immunofluorescence analysis.

(ii) Phenotypic samples: Phenotypic mice were killed by Schedule 1 methods and immediately post-mortem, phenotypic site(s) were biopsied, a portion was frozen in liquid nitrogen and the other was placed into formalin fix solution immediately for 24 hours at 4^0C, embedded in paraffin and 4-6μm thickness sections were cut for immunofluorescence analysis.

2.2.9.2. Immunofluorescence analysis

Paraffin sections were incubated for 30 min at 60^0C and subsequently followed by immersion in xylene to remove paraffin wax, immersion in a series of decreasing ethanol concentrations for 3 min to rehydrate. Antigen retrieval was performed as follows: pre-warm 1 litre citrate buffer (18ml of solution A: 9.6g citric acid in 500ml dH_2O and 82 ml of

solution B: 14.7g Tris-sodium citrate in 500ml dH_2O and made up to one litre with dH_2O) for 4 minutes at full power of 800W microwave. The sections were immersed in this solution and transferred to a pressure cooker and once pressurised, the sections were boiled for further 7 minutes.

After 20 minutes cooling, slides were removed and immersed in PBS. Sections were blocked in 20% normal horse serum for 15 minutes followed by incubation overnight at 4^0C with primary antibodies which were diluted to the manufacture recommended concentration in 10% normal horse serum. To highlight the epidermis and follicles when staining for melanocytes via endogenous TRP2 expression, a K14 primary antibody was normally added. The following day, sections were incubated for 45 minutes with biotinylated horse anti-species of the primary antibody (1: 100 diluted in 10% normal horse serum) and then by incubating in FITC or Texas red conjugated avidin at room temperature for a further 1 hour followed by 3x washes in PBS. For double immunofluorescence staining, biotinylated anti-species first antibody was employed for additional amplification followed by Texas Red-conjugated avidin and followed by incubation of FITC conjugated the anti-second primary antibody before being mounted with PermaFlor mountant.

2.2.10. Induction of melanocyte specific transgene expression *in vivo*

Prior to Ru486 treatment procedure, bigenic mice were checked for the lack of spontaneous phenotypes due to transgene insertion. To induce target transgene expression, anagen was initiated by hair plucking using tweezers followed by topical painting and intraperitoneally injection at day 0. Typically, mice were painted twice a week with 10^{-9}M Ru486 in ethanol and injected with 0.4mg/kg Ru486 in sesame seed oil due to its insolubility in water. The mice on procedure were treated continuously until biopsy samples were taken or the mice were culled because of the phenotypes affecting eyes and harderian glands. Treated mice were monitored weekly for checking of health conditions and phenotype development.

Chapter 3: Results

3.1. Cloning of the constructs

The creation of a conditional gene switch mouse model requires generation of two transgenic lines containing the regulator and target halves, which are produced by micro-injection of transgene DNA into pronucleus of one cell embryos. Typically the regulator transgene is expressed from cell/tissue specific promoters giving the specificity necessary for gene expression *in vivo*, while the target transgene is expressed from a generic promoter. A regulator can express any one of specific recombinases (see introduction) and this approach employs the Cre recombinase, which remains inactive in the cytoplasm until application of inducer. The Cre recombinase was translocated to the nucleus to switch on the target transgene or eliminate a *lox*P flanked sequence following inducer application.

In this project, Cre recombinase (regulator) was fused with progesterone ligand binding domain to create fusion protein CrePR1 which is responsible to application of Ru486 (an analogue of natural progesterone) but not to endogenous progesterone. By cloning of a melanocyte-specific promoter (enhanced tyrosinase or Trp2) in front of CrePR1 fusion recombinase, the regulator should specifically express in melanocytes but Cre remains inactive until application of inducer Ru486. The target half was constructed by cloning report gene (EGFP) or oncogene (N-Ras^{lys61}) under the control of generic promoter CMV which lies downstream was followed by a floxed 'Stop' cassette, a Cre responsive element, to silence target gene (EGFP, N-Ras^{lys61}) under normal, untreated conditions. In the imported Δ5PTEN$^{flx/flx}$ mouse, floxed exon 5 of PTEN gene was responsive to CrePR1 to be ablated as 'Stop' cassette in our constructed target genes in bigenic mouse (crossing of regulator and target lines) by application of inducer Ru486 (Fig 5).

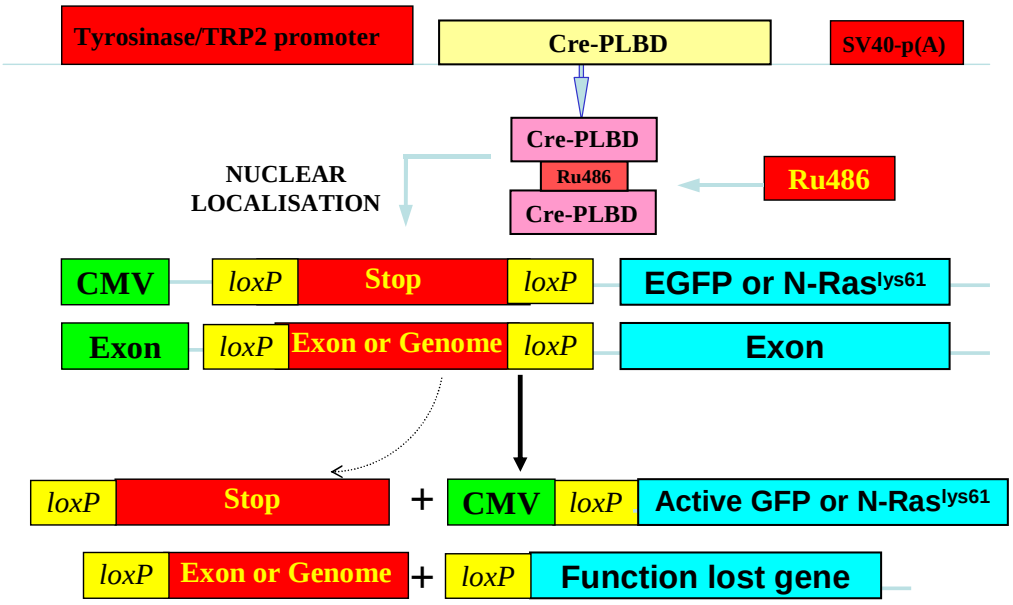

Figure 5: Scheme of the melanocyte-specific, progesterone receptor-based Cre/loxP gene switch. To achieve inducible melanocyte-specific transgene expression following application of inducer Ru486, the PLBD (progesterone ligand binding domain) of the progesterone receptor was fused to Cre recombinase (Cre-PLBD) and this regulator construct was expressed from an enhanced melanocyte-specific Tyrosinase promoter (EICre) or TRP2 (TRP2Cre). Thus following application of inducer Ru486, the Cre-PLBD fusion protein binds Ru486, dimerizes and translocates to the nucleus where Cre recombinase is activated and subsequently acts to evict sequences flanked by *lox*P sites (floxed). Thus regulator and target lines are bred to create complete gene switch. In the resulting bigenic (trigenic/compound) mice, cellular specificity is provided by the regulator promoter and the cell/tissue specific active Cre recombinase either evicts a 'Stop' sequence (stop- EGFP or stop-N-Ras) to activate target transgene expression or inactivate target gene activity via loss of functional exons (e.g. PTEN) in designed cell/tissue depending on the 'floxed' sequences within the target vector. Please also see Fig 4.

3.1.1. Regulators

As outlined in the methods, plasmid pEtyr-P65 containing Etyr promoter, an enhanced tyrosinase promoter, was cut with Asc I and Kpn I to obtain Etyr promoter for cloning into pSL1180, a vector harbouring multiple cloning sites, which was linearized by digestion with the same enzymes AscI and KpnI to produce vector pSL1180-Etyr (Fig 6) following typical precedures for gene cloning as described in material and methods. The pSL1180-Etyr construct therefore contains the cloning sites for the next step construction to result in the regulator ECre (Fig 7).

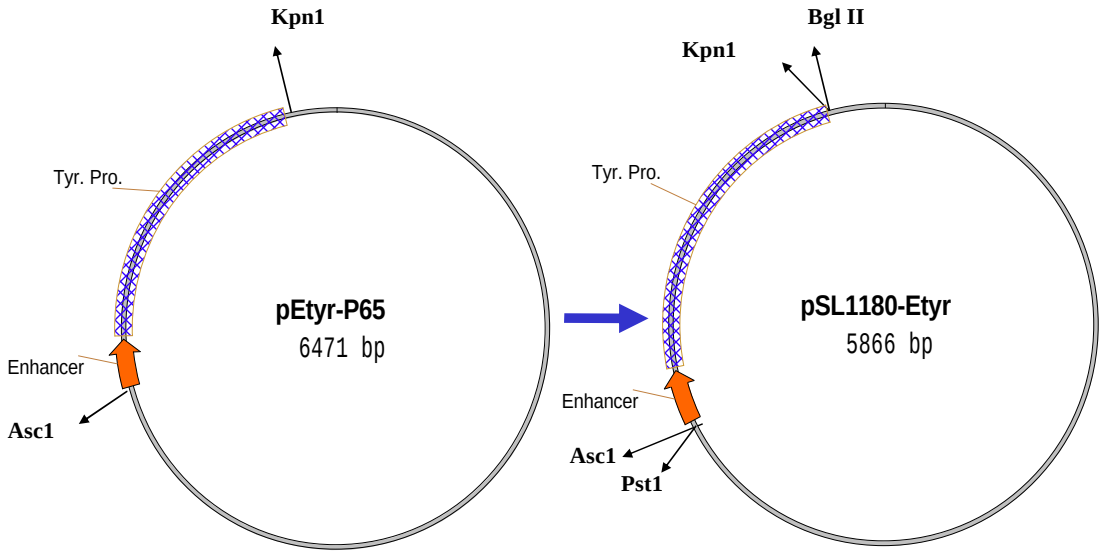

Figure 6: Construction of intermediate plasmid pSL1180-Etyr. Intermediate vector pSL1180-Etyr was constructed to give convenience MCS (specific Pst 1 at 5' and Bgl II at 3' for this purpose) for further cloning of Etyr promoter into pCrePR1.

Shuttle cloning of pSL1180-Etyr provided the Bgl II site essential for insertion of the Etyr promoter into pCrePR1 vector. To create the melanocyte-specific regulator construct where CrePR1 fusion protein was under the control of Etyr promoter, a fragment was cut from pSL1180-Etyr by Pst I and Bgl II enzymes which were also employed to recover the CrePR1 fusion gene from pCrePR1 and thus discard the HSV-tk general promoter. Through ligation of Etyr and CrePR1 fragments and screening of positive colonies, the regulator plasmid ECre was generated in which CrePR1 fusion gene was controlled by melanocytes specific expression promoter Etyr (Fig 7) to limit target gene expression exclusively in melanocytes.

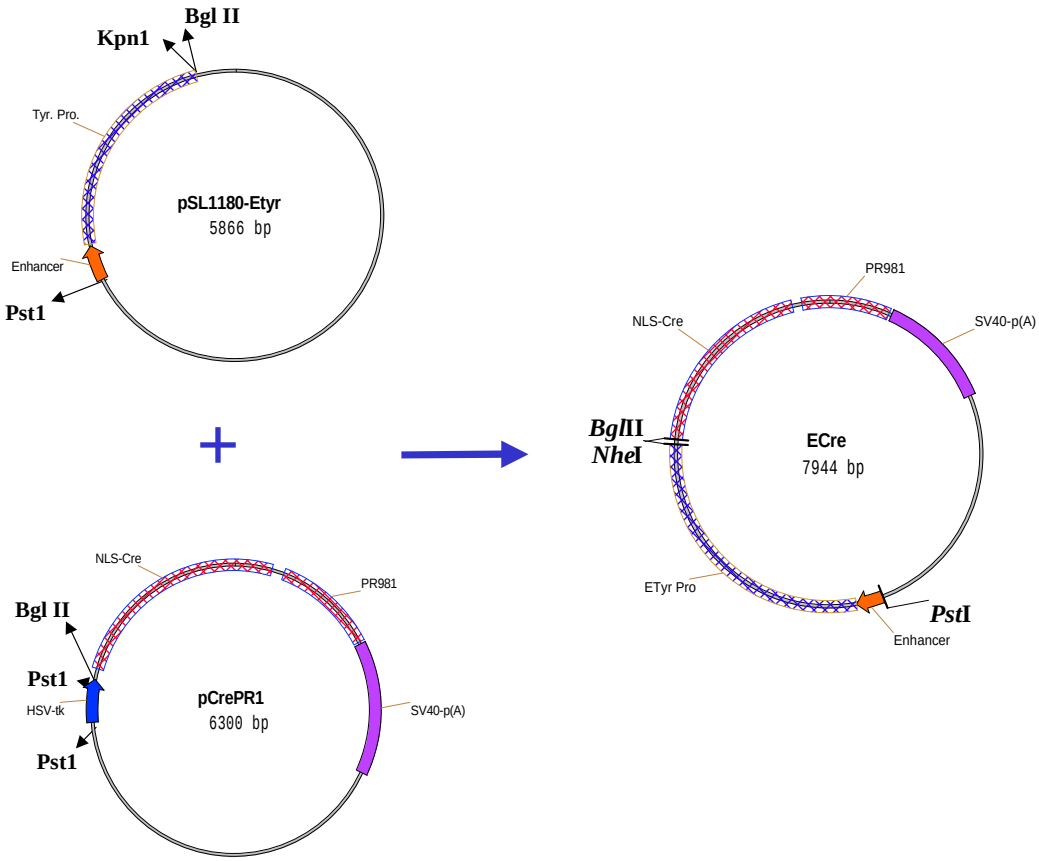

Figure 7: ECre plasmid creation. ECre regulator without generic intron was cloned via intermediate vector pSL1180-Etyr and pCrePR1. The CrePR1 fusion gene was under control of Etyr in the resulting vector ECre.

To further increase gene expression, a final version of the enhanced tyrosinase vector was designed to include a generic intron, which increases message stability and efficient processing thereby accumulating cytoplasmic RNA to elevate gene expression in transgenic mice (452;453). Thus, a generic intron cut from K14CrePR1 vector was inserted into ECre between Etyr promoter and CrePR1 gene via ligation of Nhe1/Spe1 at 5' and Kpn1 (blunt)/Bgl II (blunt) at 3' from ECre/generic intron respectively. The final version of this regulator construct was named EICre. A 5.6-kb transgene fragment can be obtained following digestion of Not I (Fig 8).

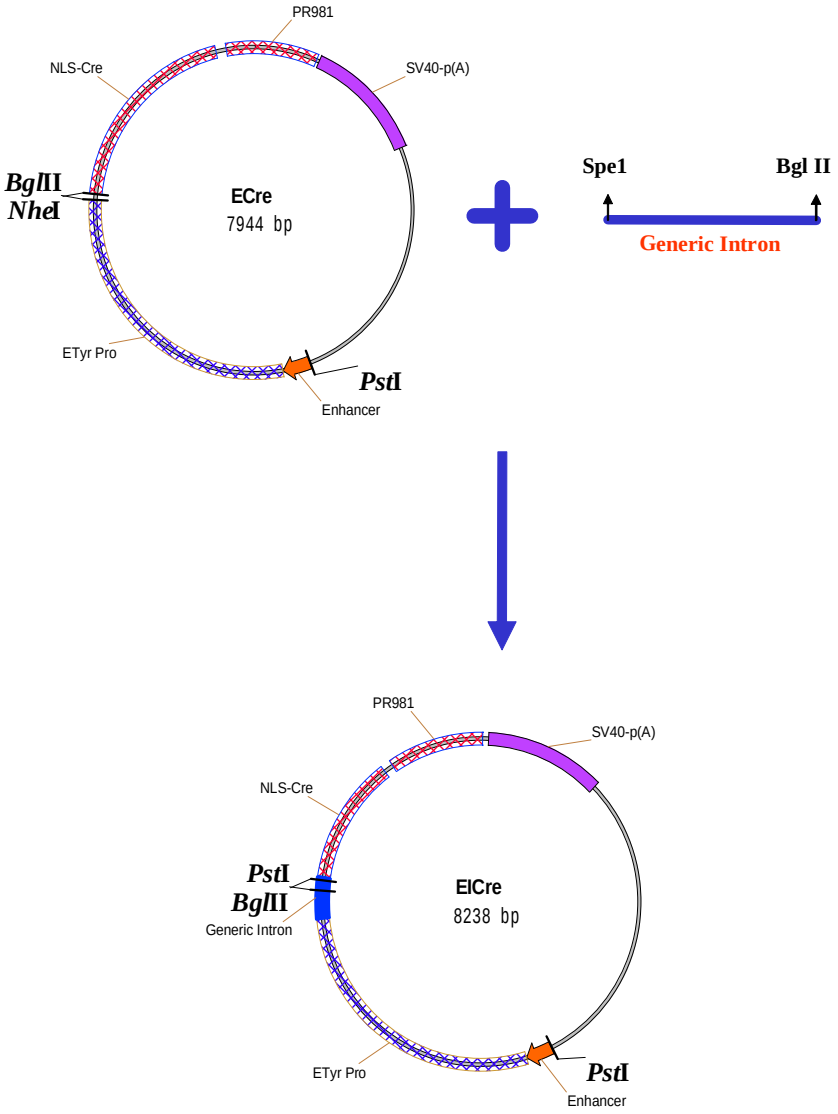

Figure 8: Construction of regulator EICre. Final version of regulator EICre was cloned by insertion of generic intron into ECre.

Another regulator was also constructed based on the tyrosinase related protein 2 (TRP2) promoter, which is cited to be a stronger promoter and possibly expressed in melanoblast stem cells (288;454). The TRP2Cre regulator was cloned by cutting plasmid TRP2-p(A) with EcoRV and Not I to discard the vector's p(A) which to be replaced by Intron-CrePR1-p(A) fragment excised from EICre by Kpn1/blunt and Not I. Following ligation, transformation and screening of colonies as described in material and methods, successful clones were sequenced to confirm the absence of mutation within the junction of TRP2 promoter and Intron–CrePR1. A 4.62-kb fragment of transgene was released following Afl II partial cut and Not I digestion for microinjection into pro-nucleus (Fig 9)

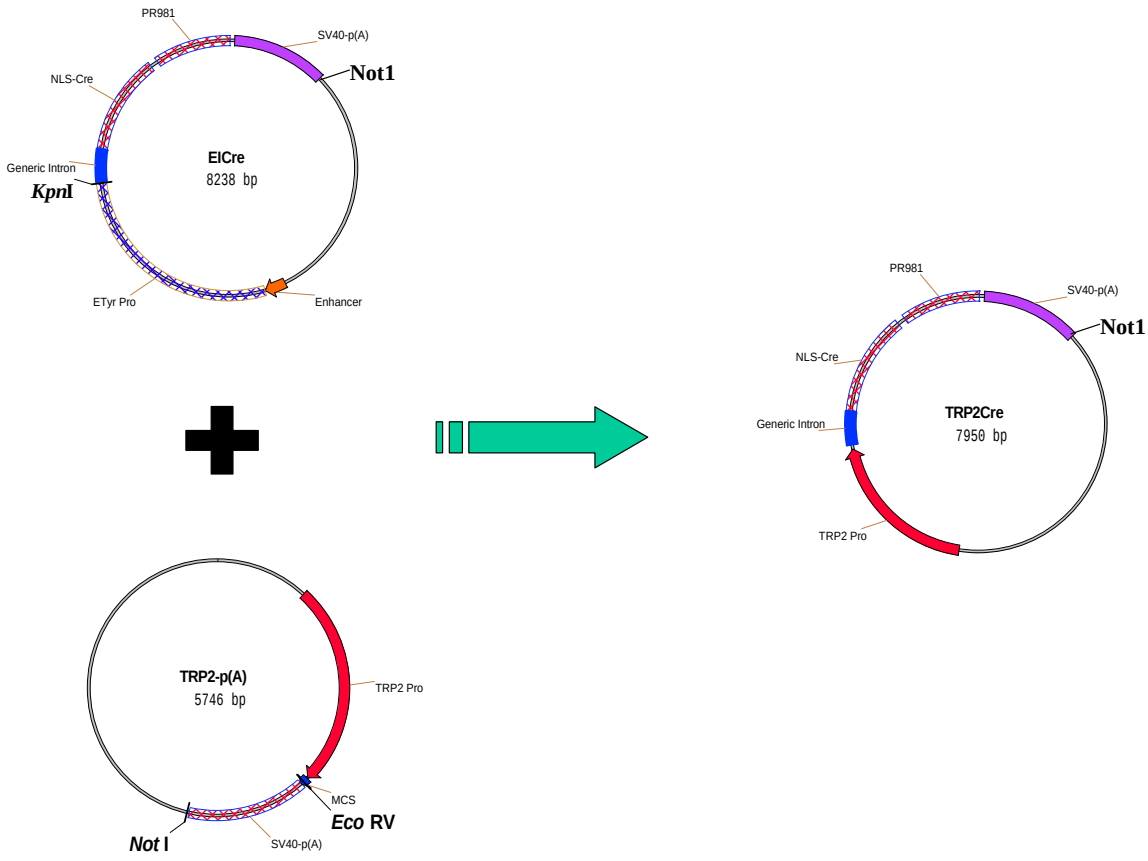

Figure 9: TRP2Cre construction. TRP2Cre regulator was constructed via replacement of the Etyr in regulator EICre with TRP2 promoter which was isolated from CrePR-p(A).

3.1.2. Target construction

3.1.2.1. Report target

To produce an easy analysis method to confirm functional regulator and successful target switch *in vitro,* a report target was constructed in which report gene EGFP allowed successful target gene switch activity to be easily visualized by immunofluorescence microscopy.

In this construct, the 'Stop' cassette flanked by two '*lox*P' sites at 5' and 3' ends respectively was employed and excised from pBS302 (NCBI data base: U51223, gene bank identification number: 1277147) by Spe 1/blunt and EcoR 1 digestion. In parallel, CMV driven EGFP in plasmid vector pEGFP-N1 (NCBI data base: U55762, gene bank identify number: 1377911) was linearized between CMV promoter and EGFP gene employing Nhe1 digestion, followed by blunt-end with DNA polymerase I large fragment (Klenow) and further EcoR 1 digestion. These two fragments, 'Stop' cassette and linearized 'VMC-PFGE' fragments were ligated to produce the CMV-Stop-EGFP report construct in which EGFP expression was silenced by 'Stop' insertion between promoter (CMV) and target gene (EGFP) under normal conditions until the excision of '*lox*P-Stop-*lox*P' sequences by active CrePR1 recombinase. To further increase gene expression (452;453), a final version of target vector was designed to include a generic intron as for regulator. Thus, the generic intron was cut from K14CrePRI vector and inserted between 'Stop' cassette and EGFP gene to generate final version of construct cmv.stop.EGFP (Fig 10). This report vector was employed as a positive control in tests of the gene switch and also to visualize 'transformed' melanocytes in *in vitro* analysis.

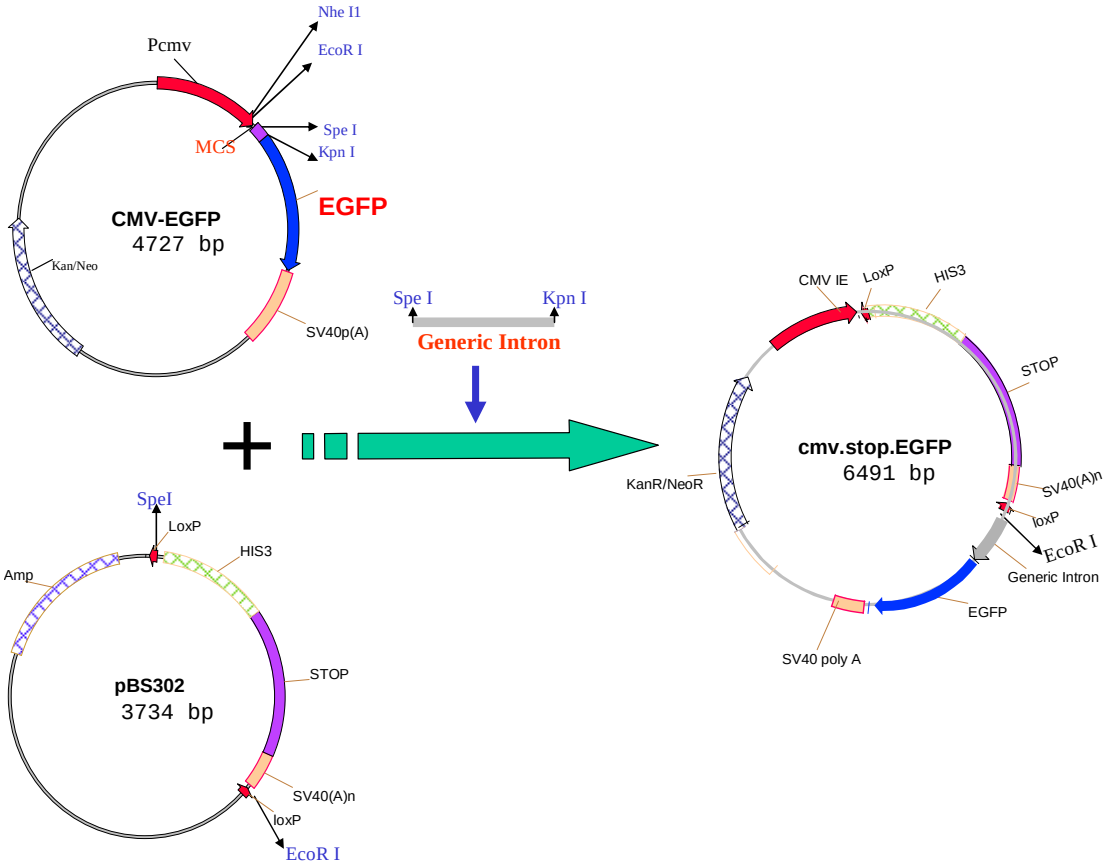

Figure 10: Construction of report target vector cmv.stop.EGFP. Report target vector cmv.stop.EGFP was cloned by insertion of a 'generic intron', obtained from K14CrePR1, and '*lox*P-Stop-*lox*P' which was released from plasmid pBS302 into plasmid CMV-EGFP between CMV promoter and EGFP report gene.

3.1.2.2. Construction of N-Ras^{lys61} target transgene

Following the construction of the report target vector cmv.stop.EGFP, a target gene containing a codon 61 mutant N-Ras oncogene (GAA (Gln, Q) → AAA (lys, K)) was obtained by excising N-Ras^{lys61} from tk-N-Ras^{lys61} via digestion of Spe1, blunt-ended with DNA polymerase I large fragment (Klenow) and the following Apa1 digestion. The resulting 600-bp N-Ras^{lys61} fragment was ligated with linearized CMV-Stop-Intron, a fragment obtained from cmv.stop.EGFP by discarding EGFP gene following blunt-ended Not1 and Apa1 digestion, to create cmv.stop.N-Ras^{lys61}. The final construct was diagnosed by a panel of restriction endonucleases digestion followed by sequencing of the junction area to confirm the accurate sequence (Fig 11).

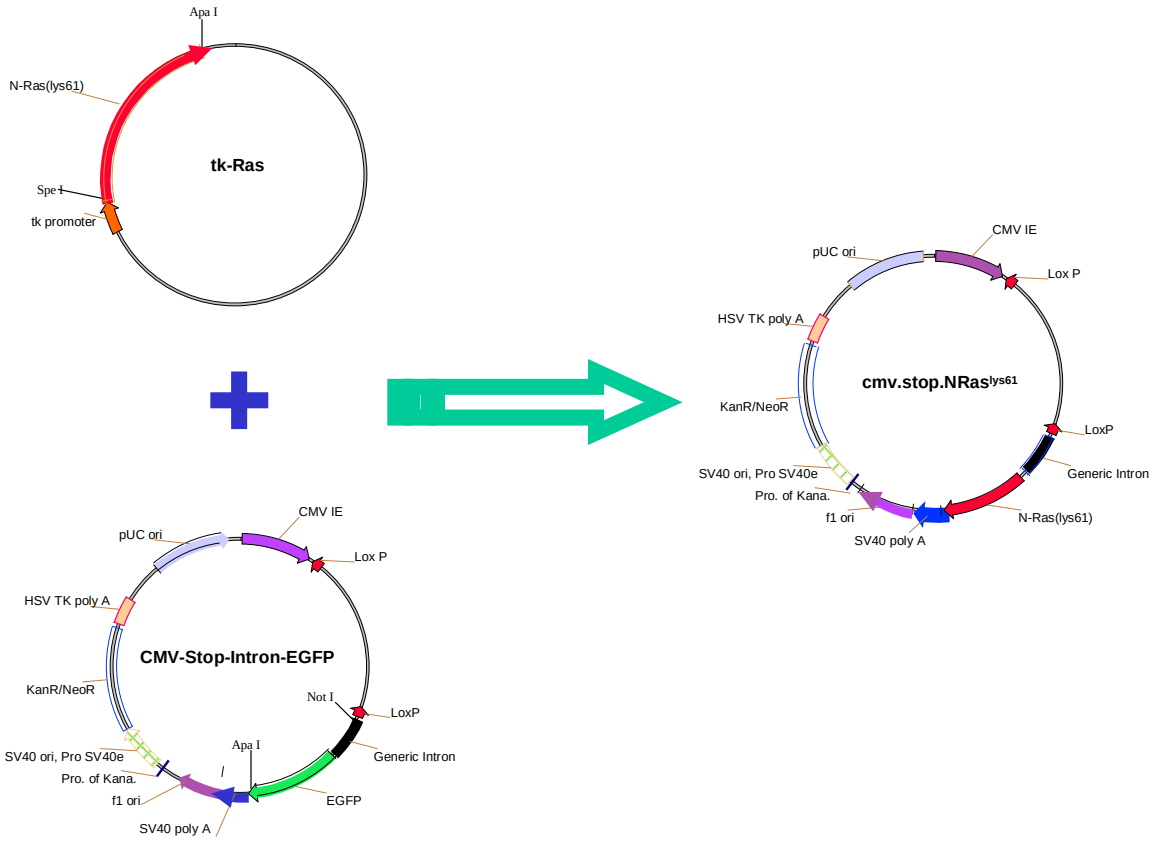

Figure 11: Construction of oncogenic target cmv.stop.N-Ras^{lys61}. cmv.stop.N-Ras^{lys61} was constructed by replacing EGFP gene in report target vector cmv.stop.EGFP with oncogene N-Ras^{lys61} which was released from plasmid tk-Ras

3.2. Establishment of optimum primary mouse melanocyte culture

3.2.1 Design and test of mouse melanocytes culture medium

In order to be able to rapidly screen transgenic expressers prior to expensive breeding typically, following successful genotyping, cells were isolated from new-born skin. Separated epidermis was plated in an appropriate medium and cells were grown for expression analysis or in this case to perform transfections to ensure biological and cell specific (data not shown) activities of the gene switch. This occurs ideally in primary melanocyte culture from F1 germline transmitters without contaminating cells, however, unlike human primary melanocyte, it turned out that such culture of primary murine melanocyte was difficult (457;458). Also optimum culture conditions had to be defined that avoid the use of feeders which would complicate the *in vitro* expression analysis experiments and avoid conditions where melanocytes quickly transformed and lost pigmentation. Thus it was necessary to test several experimental regimes where after typically plating at 5×10^6, epidermal cells comprised mainly of keratinocytes (57;76), primary murine melanocytes could be grown in various media to define optimum conditions.

Initially, a method expounded by Prof D Bennett's group was tried (459;460). Cells were grown in MEM with additive cholera toxin, 200mM TPA to promote melanocytes proliferation. In being a high-calcium medium, murine keratinocytes differentiated very quickly and failed to support melanocyte growth despite the presence of TPA. Typically, the cells grew poorly and quickly senesced (Fig 12).

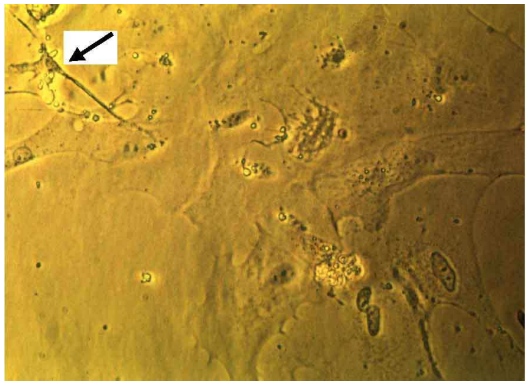

Figure 12: Primary melanocyte growth in Bennett's medium. Poor melanocytes obtained from the culture that murine epidermal cells were grown in Bennett's recipe comprised of MEM, cholera toxin and TPA. Picture shows only very low density and poor melanocytes grow in the medium tried first. Photo was taken at 100x.

Due to the poor melanocyte growth in the medium developed by Bennett *et al*, mouse melanocytes were grown in a commercial melanocyte growth medium designed primarily for optimum growth of human melanocytes (cc-4435, Cambrex, UK). In this medium, basal growth medium KBM (cc-3112, Cambrex, UK) was supplemented with 1ng/ml b–FGF, TPA, insulin, hydrocortisone and 2% serum for melanocyte growth. Again, keratinocytes differentiated due to the higher calcium condition (0.09mM) than mouse keratinocytes needed (0.05mM). Indeed, melanocytes did grow and could be passaged over 4 –5 weeks but senesced at passages 3 or 4 because this medium was primarily for human melanocyte but sub-optimum for mouse melanocyte growth and was very expensive.

Other groups (57;460) have reported success with employing feeder layers. Murine primary keratinocytes have also been employed as an initial feeder layer grown in DMEM supplemented with 10% chelex FCS and 0.05mM Ca^{2+} which then differentiate over a period of 2-3 weeks (461;462). On addition of TPA (10ng/ml) and b–FGF, melanocytes grow well enough to supply sufficient number of cells for expression analysis and provide cells for transfection. Melanocytes/melanoblasts become dendritic at subculture but cells can be kept for till passage 4 (6 weeks).

In a final modification, using the most optimum medium, it was discovered that the keratinocytes feeder layer grew better and was maintained for longer in a medium which consists of 50% low calcium (0.05mM Ca^{2+}) DMEM and 50% commercial serum free KGM medium, containing epidermal growth factor (EGF), hydrocortisone and transferrin. Addition of TPA and b-FGF to this final version of optimum primary murine melanocyte growth medium defined as 50/50 medium induced the greatest melanocyte growth.

Keratinocytes cultured in 50/50 medium grew quickly for first a few days as a confluent feeder layer and gradually terminal differentiated to die out after 2-3 weeks while the melanocytes continued to grow and to proliferate, presumably due to the matrix provided by the keratinocytes. In this optimum 50/50 medium, the first presence of pigmented melanocytes can be observed at as early as day 3 after plating. At day 6, melanocytes are obviously prominent following keratinocytes differentiation. The reversed trends of increasing number of melanocytes and decreasing number of keratinocytes will last for approximately two weeks, although most of keratinocytes disappeared following in culture for 9-10 days (Fig 13). This increased melanocytes growth was more than sufficient for protein analysis, RNA isolation and transfection experiments to identify transgenic expressers and supplied sufficient cells up to passage 5 without spontaneous transformation or loss of melanin production by active tyrosinase. By passage 6 melanocytes ceased proliferation but if plated in sufficient numbers, could be maintained for several weeks longer (>10) without spontaneous transformation. On occasion e.g. to help assess for cellular immortality, the keratinoyte papilloma cell line, SP-1 (463), was used as a feeder layer (457) (data not shown).

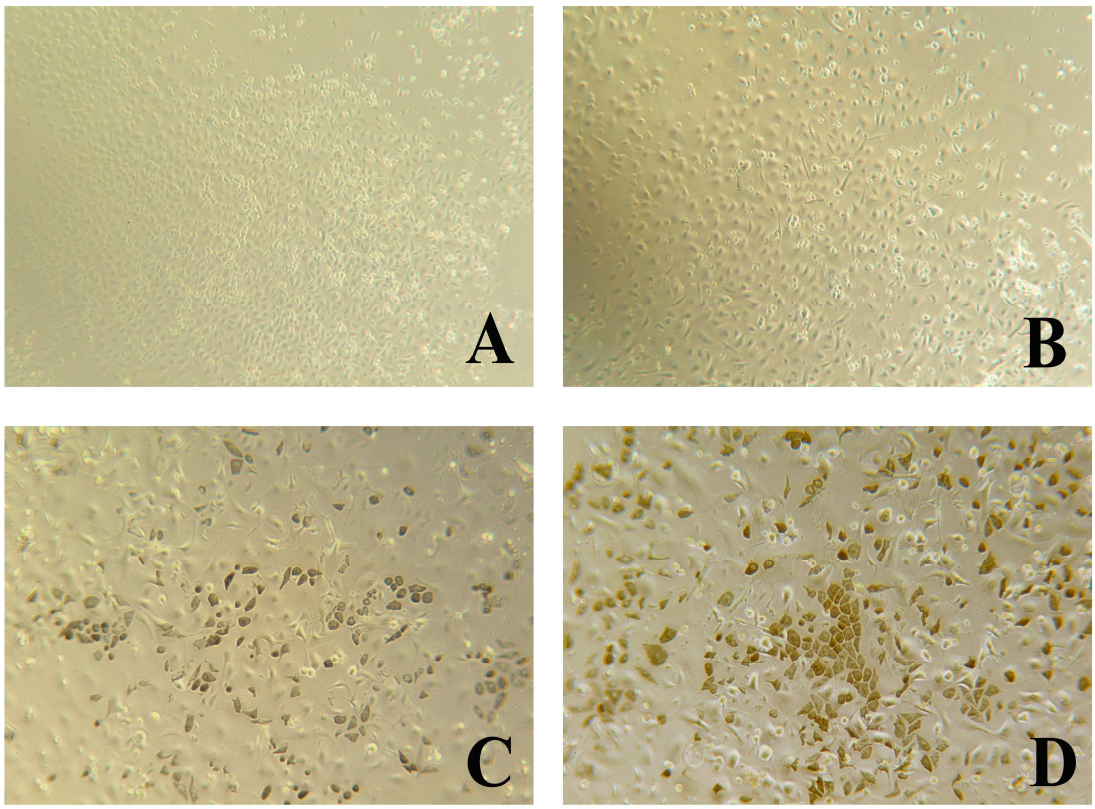

Figure 13: Growth of murine melanocytes in low calcium 50/50 medium. Primary murine melanocytes grew in 50/50 medium which contained 0.05mM Ca^{2+}, 1ng/ml b-FGF and 10ng/ml TPA. (A) Primary new born murine keratinocytes/melanocytes were plated where keratinocytes grow as a feeder layer for melanocyte growth at 24hrs, cells attach in colonies then differentiated to disappear gradually whilst melanocytes grow and proliferate. (B), Although pigmented melanoblasts/melanocytes are distinguishable from keratinocytes as early at day 2, (C) obvious melanoblasts/melanocytes presented at day 6 or 7 and (D) dominate the dish at day 9 or 10. A-D: photographs were taken at 1, 2, 7 and 10 days respectively after plating. A, B were taken at 50x and C, D were taken at 100x

3.2.2. Comparison of mouse melanocytes growth media

To verify our murine primary melanocyte growth medium (50/50), primary cells isolated from new born skin were cultured in this house-made medium and in medium exploited by Dr Halaban (a quite popular recipe used in many laboratories, thereafter termed as Halaban medium) (449) respectively. Melanocyte growth behaviour and the changes of cell morphology following long term continuous culture were recorded for comparison.

Fig 14 shows that melanocytes grow well in both media but with different growth characteristics. Although the presence of sodium orthovanadate (Na_3VO_4) which inhibits tyrosine phosphatases to prolong the activity of endogenous tyrosine kinases in Halaban medium, possible due to the higher TPA concentration to result earlier melanocytes appearance and high calcium caused quick differentiation of keratinocytes which involved in regulation of pigmentation (464) therefore, melanocytes grow as colourless and thus, melanocytes are visible mainly because of the light reflection on their 3-D dimension but hardly visible once the cells became flat after the transfection (see below 3.3.2) (449). Melanoblasts/melanocytes in 50/50 medium present as brown colour and various shapes including round (majority), triangle and spindle, in contrast to the cells in Halaban medium are mostly colourless and single spindle shape in the first a few days, although there do have a few pigmented melanocytes. Furthermore, melanocytes in Halaban medium are not distinguishable from keratinocytes as easy as in 50/50 medium because of the non-pigmentation of most melanocytes appeared.

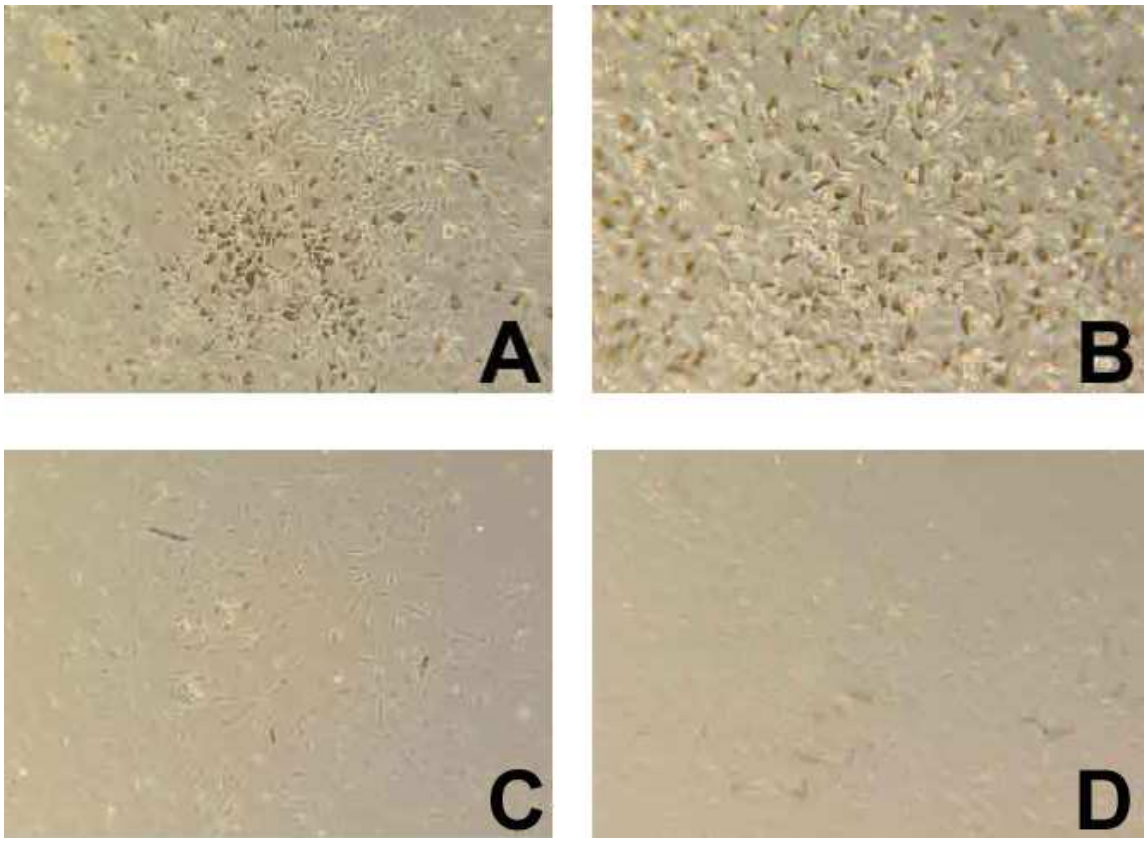

Figure 14: Comparison of mouse primary melanocytes cultured in different media. Mouse primary melanocytes cultured in 50/50 medium (A, B) and in Halaban medium (C, D) were compared and, 50/50 medium was verified as optimum for mouse melanocyte culture conditions. Significant differences in melanocytes morphologies were observed by day 6 in culture (A in 50/50 & C in Halaban). (A & B), all melanocytes in 50/50 medium are pigmented and grow on the keratinocytes feeder layer. (C & D), however, in Halaban medium there are few pigmented cells set amongst vast majority of non-pigmented melanocytes and residual differentiated keratinocytes. A & C photographs were taken at day 6 and B & D at day 9 in culture. All pictures were taken at 100x

Most primary keratinocytes in 50/50 medium totally disappeared by 2-3 weeks time leaving a relatively pure pigmented melanocytes population (Fig 15, A). By which time in Halaban medium the cells comprised numerous non-pigmentation cells (Fig 15, D). Furthermore, Halaban melanocytes had significantly changed morphology becoming more transformed and forming visible spontaneous colonies because of the gradual increase in the few melanocytes which had retained pigmentation (E), whereas cells in 50/50 medium grew in monolayer without morphological change (B) up to passage 6.

Under microscope at high magnification (200x), significant differences were revealed between cells cultured in these two mediums. Cells in 50/50 medium remained normal monolayer growth by retaining the contact-inhibition character (C) while some became pigmented in Halaban medium and most cells became more dendritic and lost their contact-inhibition character to pile up which resulted in impossible distinguish of any single cell (F) and thus would compromise any *in vitro* modelling of tumourigenesis.

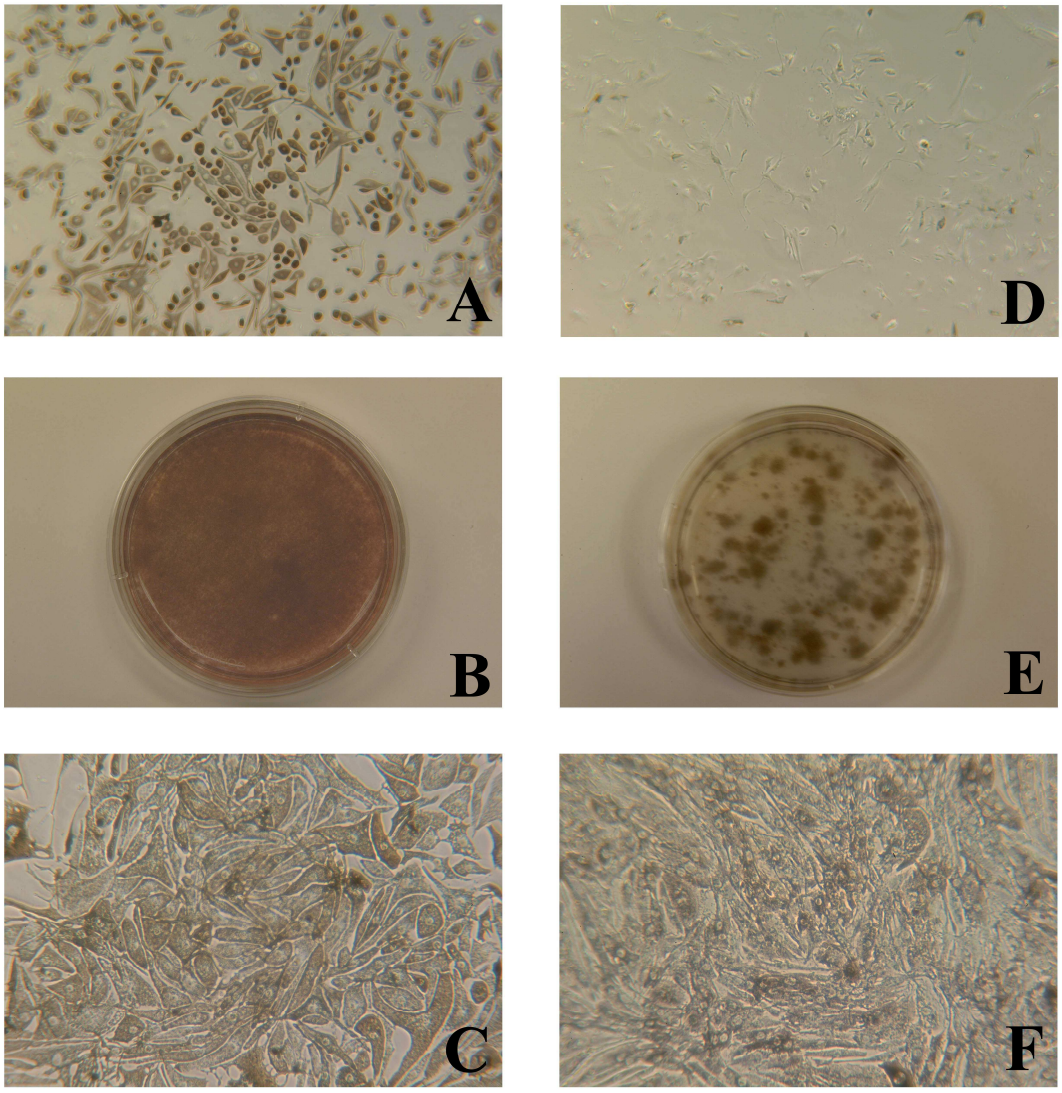

Figure 15: Different melanocyte morphologies displayed in different media. Melanocytes were cultured in 50/50 medium (left panel) and in Halaban medium (right panel) in primary culture (A, D) and sub-culture following long time continuous growth either in macro- (B, E) or micrographs (C, F). Primary cells in 50/50 (A) and in Halaban media (D) displayed different melanocyte morphologies (100x), approximately two weeks following the first culture with pure brown and various shaped (mainly round and oval) melanocytes in 50/50 medium (A) and with a few pigmented melanocytes amongst majority of non-pigmented spindle shape cells in Halaban medium (D). Spontaneous transformation-like melanocytes colonies formed in Halaban medium within 4 weeks of the first subculture (E) in contrast to cells in 50/50 medium remained a confluent, contact inhibited monolayer (B). (C) and (F) show the morphology of normal confluent melanocyte monolayer in 50/50 medium and transformed (some pigmented) melanocytes in Halaban medium respectively (200x).

3.3. Transfection

Following the successful cloning of both regulator and target vectors, biological activity and response to Ru486 treatment was confirmed by transfection prior to the transgenic line production. By comparison of several commercial transfection reagents, Fugene-6 was defined as the best transfection reagent for transfection of murine primary melanocytes. Regulator and/or target constructs were (co)-transfected into B16 melanoma cells initially due to the lack of report of primary mouse melanocyte transfection and later into primary melanocytes once delivery parameters had been defined. Comparison of the transfection efficiency between cultured primary melanocytes in 50/50 and Halaban media confirmed 50/50 as an optimum primary culture method for murine melanocytes in addition to the factor of growth and lack of morphological transformation during melanocyte culture.

3.3.1. Transfection of B16 cells

To confirm successful cloning, transfections were performed initially into B16 cells employing Fugene-6 transfection reagent and cmv.EGFP DNA as a positive control for transfection efficiency and co-transfection of pCrePR1 with cmv.stop.EGFP DNA as positive control for gene switch activity.

Following co-transfection of regulator and report target vectors into B16 cells and Ru486 treatment, EGFP expressing cells were detected by immunofluorescence microscopy 5 days after transfection (Fig 16, Table 2). Co-transfection of either EICre or TRP2Cre employing cmv.stop.EGFP as the Cre responsive target, demonstrated the successful cloning of biologically active constructs in terms of the functional activation of regulator protein by Ru486 and target gene switch specificity in B16 melanoma cell. It was noted that TRP2Cre transfected dishes produced more green cells than EICre although detectable EGFP expressing green cells were recorded in TRP2Cre transfection without Ru486 addition indicating whilst a stronger promoter, it possessed some gene switch leakage *in vitro*.

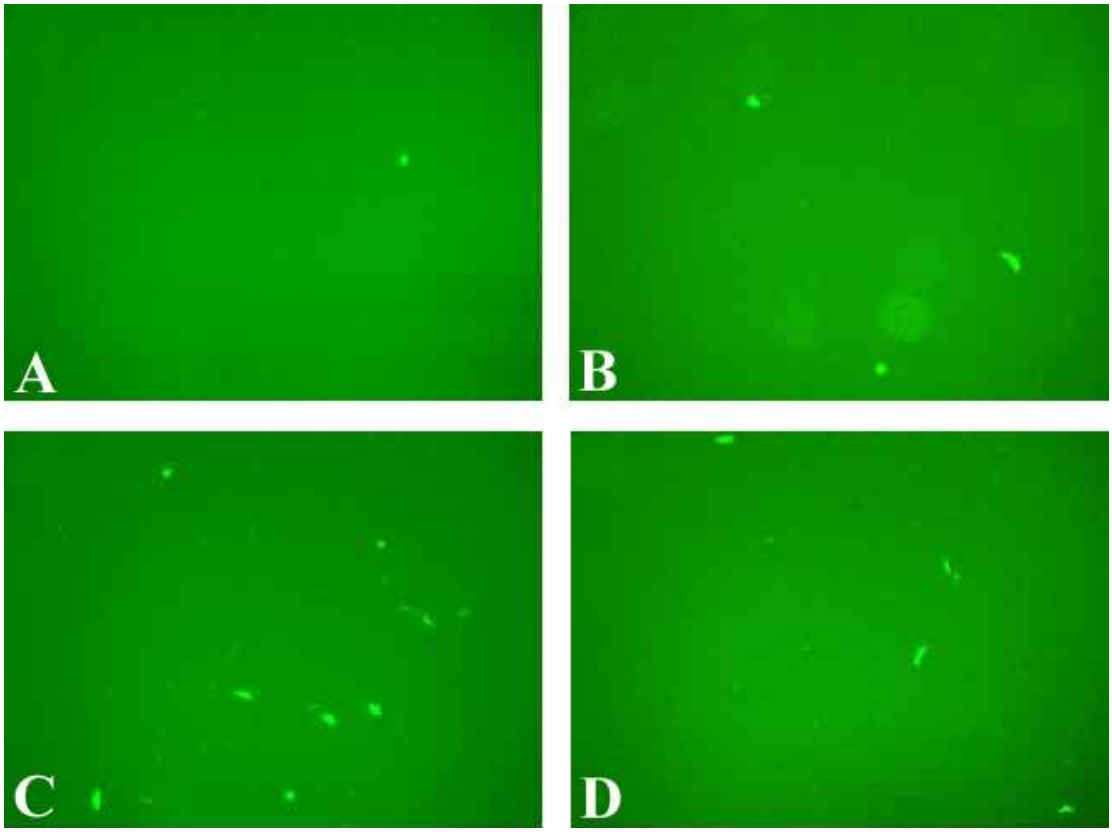

Figure 16: EGFP expressed in B16 following cotransfection. Detection of green fluorescent cells following cotransfection of regulator and report target vectors cmv.stop.EGFP into B16 melanoma cells demonstrated successful transgene construction and gene switch activity. B16 melanoma cells were cotransfected with regulator EICre (A) or TRP2Cre (B) and report target vector cmv.stop.EGFP DNA. Transfection of cmv.EGFP (C) and cotransfection of pCrePR1 together with cmv.stop.EGFP (D) were employed as a positive control of transfection efficiency and of gene switch activity respectively. Cells were photographed (40x) under immuno-fluorescence microscope 3 days (C) or 5 days (A, B, D) post transfection respectively. An approximately 1:3 ration of target gene switch was exploited between regulators EICre (A) and TRP2Cre (B). All pictures were taken at 50x. As the primary purpose of the experiment was to simply confirm gene switch function, the numbers of transfected cells were not counted while expression in the cells was relatively uniform, although was often stronger in the nucleus. Transmitted light photo was not taken for B16 cell transfections but was for primary melanocyte transfections (below).

3.3.2. Transfection of primary cultured melanocytes

As each transgenic founder was produced, to quickly confirm regulator transgene expression without excessive, expensive breeding of unnecessary bigenic cohorts, as required by the Animal licence, it became necessary to establish primary melanocyte culture conditions prior to defining transfection parameters.

Following successful transfection of B16 cells to identify functional gene switch components, co-transfection of regulator EICre (picture not show) or TRP2Cre and report target cmv.stop.EGFP was carried out in primary cultured melanocytes as outlined for B16 melanoma cells. This verified their transfectable capacity in 50/50 medium and confirmed functional gene switch exclusively in melanocyte. Detection of EGFP expressed green fluorescence cells in Fig 17 demonstrated the transfectable capacity (A) and functional gene switch in primary melanocytes employing our melanocyte-specific regulator TRP2Cre (C); although the reduced number of green cells indicated low transfection efficiency as determined by positive controls indicating the difficulty of primary melanocyte transfection (Table 2).

As with results obtained from transfection of B16 melanoma cells, the cmv.stop.EGFP target vector was totally silenced until the EICre regulator was activated following ligand Ru486 application. Furthermore, regulator EICre was again confirmed to be the less powerful activator of target gene than TRP2Cre in primary melanocytes as revealed in B16 melanoma cells, given the factor of less green fluorescence cells counted in EICre transfected dishes compared to TRP2Cre transfected dishes under the same transfection conditions. However, the leakage of TRP2Cre regulator was again detected in primary melanocytes as observed in B16 cells (Table 2).

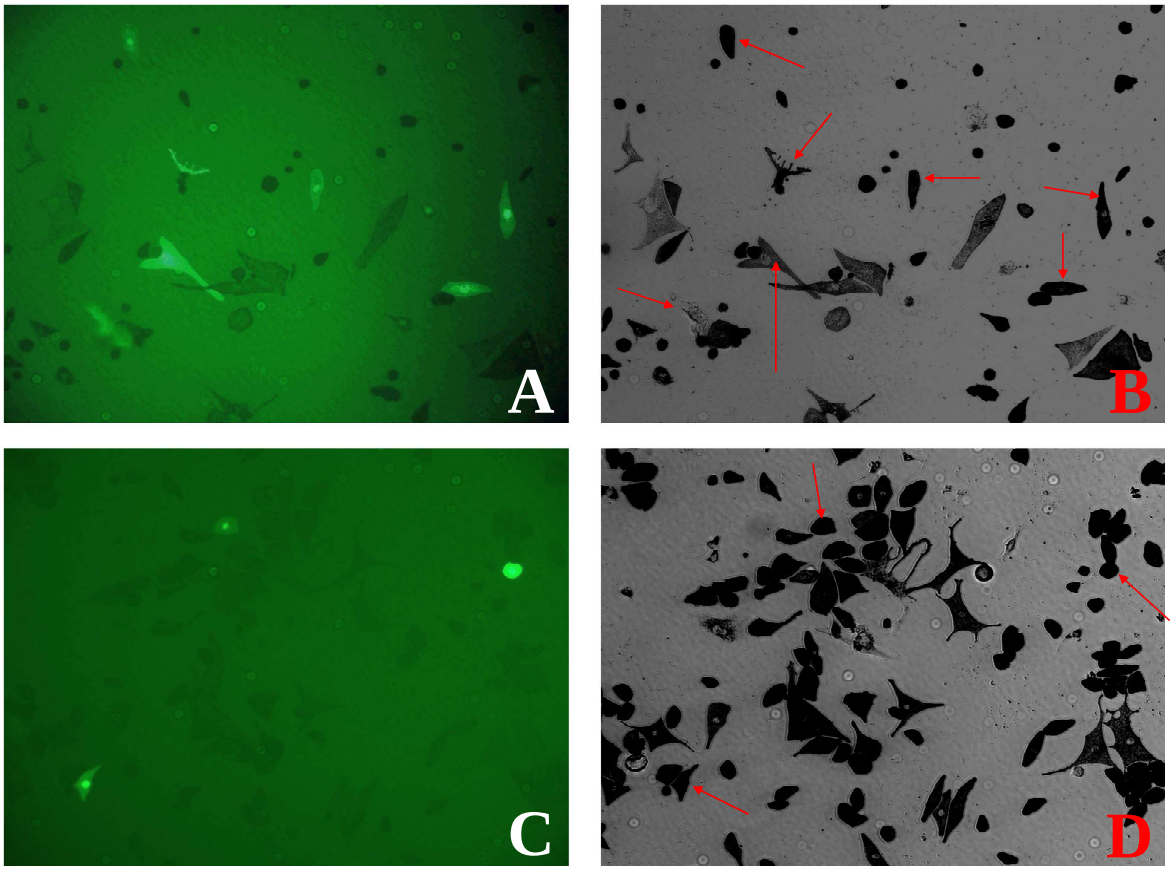

Figure 17: Target gene expressed in cotransfected primary melanocytes. To define the transfectable ability of cultured melanocytes and confirm melanocyte specificity, cells were cotransfected with regulator and report target 10 days post epidermal cells plating. (A) transfection positive control cmv.EGFP DNA and (C) TRP2Cre/cmv.stop.EGFP DNAs. 'B' and 'D' are light micrograph versions of 'A' and 'C' respectively to show the location and ideal morphology of transfected melanocytes and the arrows show the EGFP expressing melanocytes location. Photos were taken at 100x.

Table 2: Transfection efficiency comparison of two versions of regulator in B16 melanoma cells and primary culture melanocytes. GFP –positive (3.3.1 and 3.3.2) cells were counted under' fluorescence microscope and presented as the average number of positive cells per dish in repeat experiments. Control cells transfected with cmv.stop.EGFP report DNA alone possessed no green cells, which eliminated the possibility of a transfection background (target leakage) from this report gene. Cotransfection of TRP2/cmv.stop.EGFP DNAs in B16 or primary melanocytes gave higher numbers of positive cells both with and without Ru486 induction compared to regulator EICre/cmv.stop.EGFP DNAs. This revealed that although stronger TRP2 it possessed leakage and thus a greater potential for non regulatory phenotypes *in vivo.*

	B16 Cells		Primary melanocytes	
DNA Transfected	(-)Ru	(+)Ru	(-)Ru	(+)Ru
CMV-EGFP	1600	NA	500	NA
cmv.stop.EGFP	0	0	0	0
EICre/ cmv.stop.EGFP	0	480	0	70
TRP2Cre/cmv.stop.EGFP	300	620	120	310

3.3.3. Comparison of transfection efficiency in 50/50 and Halaban media

As mentioned above, murine melanocytes can be cultured in both 50/50 medium and Halaban medium and although Halaban possessed increased growth characteristics, 50/50 medium did not give spontaneous transformation whereas in contrast melanocytes cultured in Halaban medium mainly gave non-pigmented cells until later passages in culture thus raising concerns on their use to test Etyr or TRp2 regulated genes, and quickly spontaneously transformed negating their use in transformation experiments.

As transfectable capacity and transfection efficiency are critical factors for the identification of successful transgenes construction and functional gene switch analysis, primary and secondary melanocytes were thus cultured in both Halaban medium and 50/50 medium to test transfection efficiency with cmv.EGFP DNA. The results (Fig 18) revealed that melanocytes in 50/50 medium gave approximately 3 times higher transfection efficiency than cells in Halaban medium under the same transfection conditions. Moreover, an approximately 3 times higher transfection efficiency in 50/50 vs. Halaban medium was also found for secondary melanocytes (confluent primary melanocytes were trypsinized and seeded at 1:3 for the next day transfection), although the numbers of transfected cells in both media was reduced compared to primary cells. Interestingly, all transfected cells in Halaban medium were not pigmented and thus, the transfected cells are hardly visible under normal light because of the loss of their 3-D dimension as mentioned above (3.2.2). This observation suggested that melanocytes cultured in Halaban medium may not be transfectable once they became pigmented or that transfected Halaban cells lose ability to pigment.

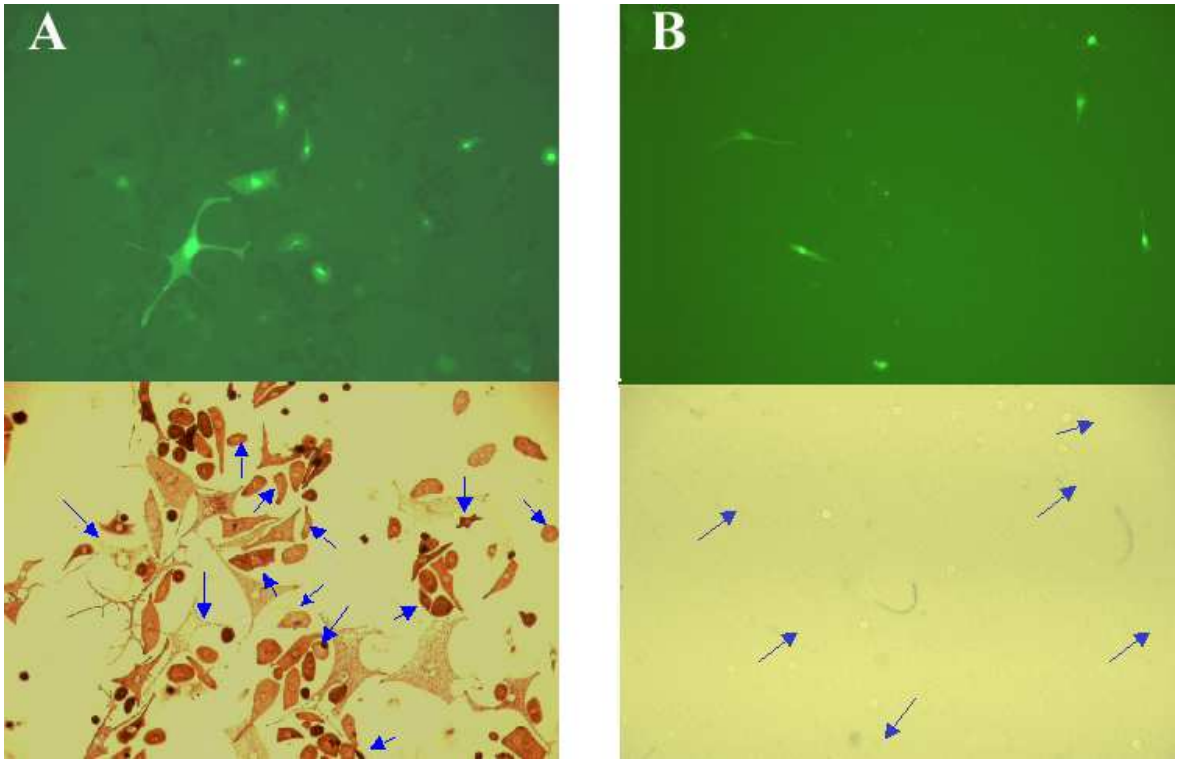

Figure 18: Photomicrographs of expressed target cells in different media. Photomicrographs (100x) of green cells (upper panel) and their localisation (lower panel) following transfection of cmv.EGFP into primary melanocytes cultured in (A) 50/50 medium and (B) Halaban medium. The table 3 below shows the average numbers of EGFP expressing green cells from duplicate or independent transfections (a).

Note: transfected cells are hardly visible in lower panel in Halaban medium under normal light version as mentioned.

Table 3: Transfection efficiency comparison in different media by counting of green (EGFP expressing) cells after transfection of cmv.EGFP. All GFP –positive cells were counted from transfection of approximately 10^6 primary cells/60-mm dish and 5 x 10^5 secondary melanocytes at 50x magnification. Numbers for primary transfection are the average of 2 dishes whilst numbers for secondary melanocyte transfections (a) are the average of 3 independent experiments.

	50/50	Halaban
Primary	1029	497
Secondary	97[a]	39[a]

3.4 Transgenic line production

3.4.1. Identification of the transgenic founders and germline transmitters

The transgenic EICre and cmv.stop.N-Ras^{lys61} DNAs were isolated, purified, quantified and 1-2ng/ml transgene DNA solution was microinjected into pronuclei harvested from B6/D2/F1 superovulated females as described in chapter 2 (material and methods). Successfully injected one-cell embryos were transplanted into pseudopregnant females, produced by mating ICR females with vasectomized males, and normal gestation allowed to produce pups for screening transgenic founders.

To identify potential transgenic founders, as no phenotype was expected, 5-6 week old mouse progenies were tail tipped and genomic DNA was isolated for PCR analysis. Using specific primers for each transgenic line (EICre forward: ATTGGTGCAGATTTTGTATG and reverse: CATCTTCAGGTTCTGCGG; N-Ras^{lys61} forward: ACACCACAGAAGTAAGGTTCCT and reverse: GCGGTACCTCTTGAACTATAGC, see table 1), a 436-bp EICre or 888-bp N-Ras^{lys61} fragment indicated positive transgenic mice respectively. Over a period of time, ten EICre and four N-Ras^{lys61} founders were produced. Seven EICre and two N-Ras^{lys61} lines were identified to be germline transmitters by breeding with C57BL6 and PCR analysis of F1 progenies (Fig 19 & Fig 20). All germline transmitters displayed the transgenes in a Mendelian fashion in their progenies and were employed to produce primary melanocytes for transgene expression analysis *in vitro*.

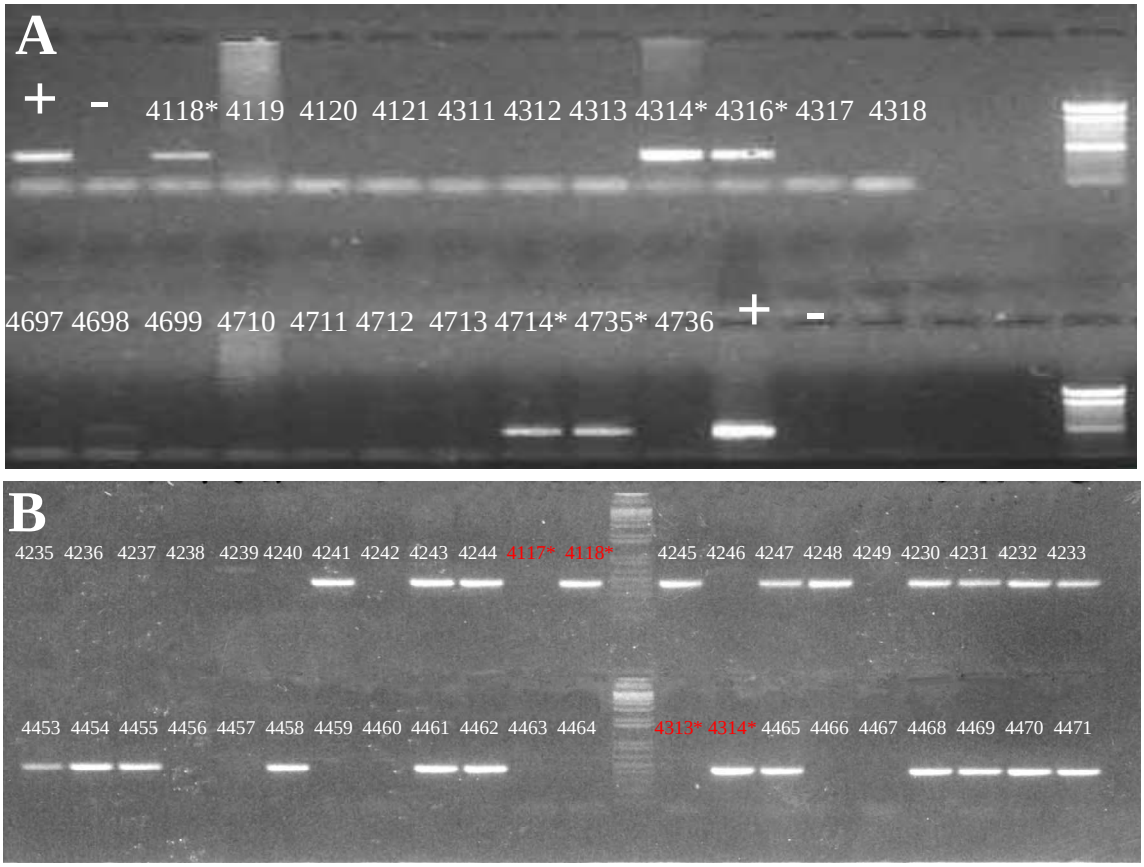

Figure 19: PCR product represents EICre transgenic founders 4314 etc. (A) A 436-bp PCR product represents EICre positive transgenic founders 4314 etc and (B) shows founders 4118 (top row) and 4314 (bottom row) are germline transmitters as their F1 progenies displayed the transgenes in an expected Mendelian fashion. (+), PCR from transgene DNA as positive control and (-), PCR from wild type C57BL6 DNA as negative control for 'A' while the parental negative and positive DNAs (red indicated) as controls for 'B'. DNA marker is Invitrogen 1kb plus DNA ladder (#10787-026).

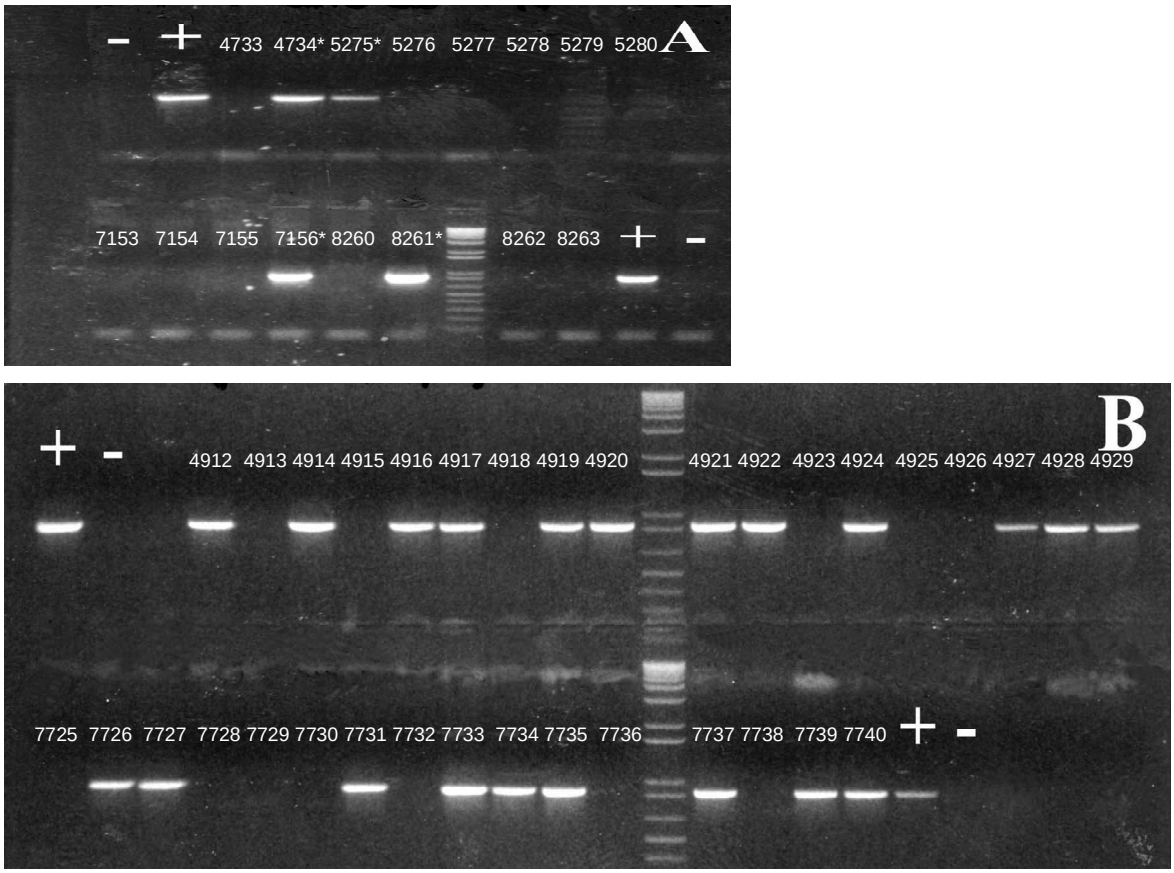

Figure 20: PCR of tail genomic DNA identified four cmv.stop.N-Ras^{lys61} founders. The 888-bp PCR product was identified in four cmv.stop.N-Ras^{lys61} founders 4734, 5275, 7156, and 8261 (A) and only two of them (4734 and 7156) proved to be germline transmitters (B: 4734 top row ; 7156, bottom row). (+), PCR from transgene DNA as positive control and (-), PCR from wild type C57BL6 DNA as negative control for 'A' while parental genomic DNA (4733, 4734 & 7156, 7157) as positive and negative controls for 'B'. DNA marker is Invitrogen 1kb plus DNA ladder (#10787-026).

3.4.2. Importation of K14CrePR1 and Δ5PTEN$^{flx/flx}$ mice

K14CrePR1, a line well characterised Ru486-based regulator expressed in keratinocytes, was imported from the USA under the Home Office regulations and was used as positive regulator control genotype to induce target transgene expression in keratinocytes. K14CrePR1 was successfully identified to switch N-Ras^{lys61} expression in primary bigenic K14CrePR1/cmv.stop.N-Ras^{lys61} keratinocytes and N-Ras^{lys61} expression in melanocytes was subsequently confirmed in EICre/cmv.stop.N-Ras^{lys61} bigenic mice *in vivo*. K14CrePR1 mice were also utilised in experiments to investigate the tumour microenvironment contribution to the oncogenic process given that melanomagenesis is not a process involved of only melanocyte mutation but a complex issue involved of multiple partners in the neighbourhood (e.g. keratinocytes) (465;466). Therefore, K14CrePR1 mice were employed to allow N-Ras^{lys61} expression and PTEN ablation in keratinocytes (246) to induce hyperplasia (in soil). Together with intrinsic N-Ras^{lys61} expression in melanocytes (seed), the induction of K14CrePR1 mice also give us permission to assess effects on promoting melanomagenesis.

PTEN loss is the second most common tumour suppressor gene deletion after p16 in melanoma (250;252). PTEN co-operated with p16 and H-Ras in melanoma both *in vivo* and *in vitro* experiments implicated that PTEN involved in mouse melanoma development (262). Therefore in collaboration with Hong Wu, UCLA in US, PTEN floxed mice (Δ5PTEN$^{flx/flx}$), expressing an exon 5 flanked by *lox*P sites to ablate functional PTEN TSG, were also imported from US under the home office regulations to cooperate with N-Ras^{lys61} expression in melanocyte/keratinocyte and to investigate their potential cooperation during melanomagenesis.

Following importation, rabies quarantine and re-derivation via embryo transfer, the mice were ear tagged and tail cut for genotyping via PCR using primers K14Cre.fwd

(TCATTTGGAAC GCCCACT), K14Cre.rev (GATCCGAATAACTACCTGTTTTG) and PTEN.fwd (ACTCAAGGCAGGGATGAGC), PTEN.rev (GTCATCTTCACTTAGCCAT TGG) as described in methods. Following identification of K14CrePR1 and floxed PTEN PCR positives, their progenies were produced in a C57BL6 background (Fig 21, 22) through seven back cross with wild type C57BL6 to ensure a genetically identical inbred C57 background. To produce floxed PTEN homozygotes ($\Delta 5PTEN^{flx/flx}$) for complete PTEN ablation, a brother-sister mating of F1 heterozygous (Fig 23) was set and $\Delta 5PTEN^{flx/flx}$ mice were obtained (Fig 24).

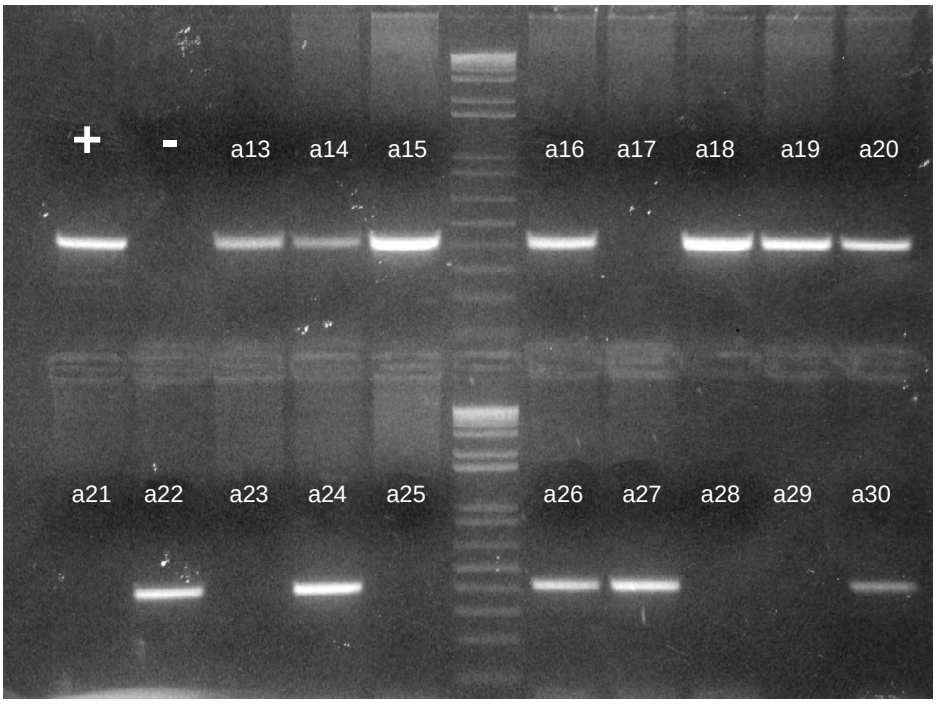

Figure 21: K14CrePR1 positive progenies were identified. K14CrePR1 positive progenies were identified from F1 (a13-a30) of K14CrePR1 imported mice in C57BL6 using primers K14Cre.fwd and K14Cre.rev. 410-bp PCR product represents K14CrePR1 transgenic positive mice. (+), PCR from genomic DNA of imported K14Cre mice as positive control and (-) PCR from C57BL6 DNA as negative control. DNA marker is Invitrogen 1kb plus DNA ladder (#10787-026).

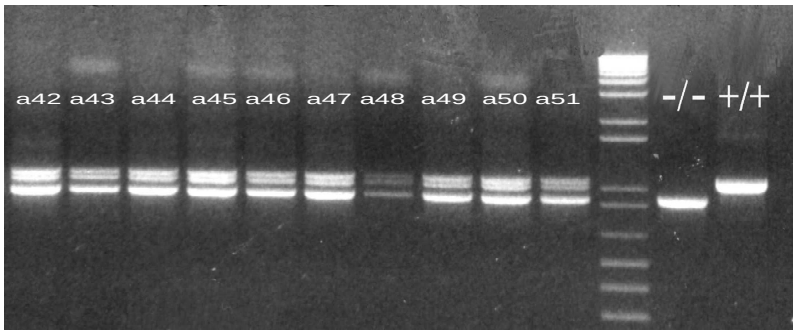

Figure 22: Heterozygous PTEN (+/-) obtained from F1 progenies. All are Heterozygous PTEN (+/-) obtained from F1 (a42-a51) progenies of imported floxed PTEN (Δ5PTEN$^{flx/flx}$) in C57BL6/ICR background. Top band represents floxed PTEN (+/+, Δ5PTEN$^{flx/flx}$) allele and lower band indicates wild type PTEN allele (-/-). Wild type control (-/-) and floxed PTEN control (+/+) are from C57BL6 and imported Δ5PTEN$^{flx/flx}$ mice respectively. DNA marker is Invitrogen 1kb plus DNA ladder (#10787-026).

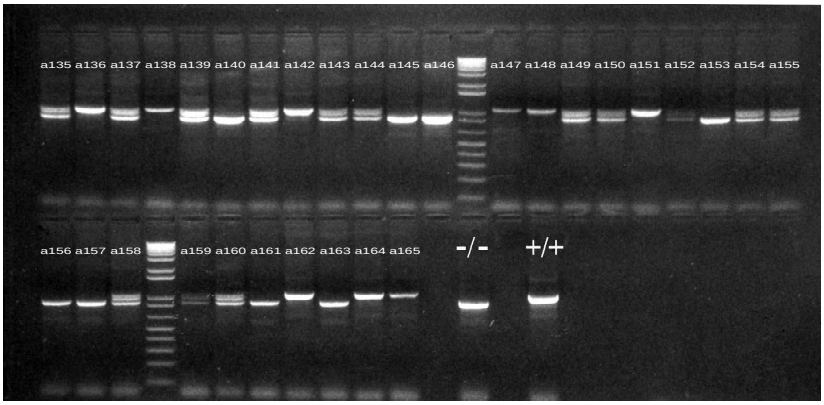

Figure 23: Expected Mendelian fashion (a135-a165) obtained from heterozygous breeding. Either wild type (1/4), heterozygous (2/4) or homozygous PTEN (Δ5PTEN$^{flx/flx}$) (1/4) were detected from progenies of F1 (heterozygous) sister-brother breeding (a42 x a46; a43 x a47; a44 x a50 and a45 x a51, see Figure 22) in the expected Mendelian fashion. Single small band (900-bp) presents wild type PTEN (-/-), single big band (1100-bp) presents Δ5PTEN$^{flx/flx}$ (+/+) and double band samples are for PTEN heterozygous. Parental genomic DNAs used as wild type (-/-) and floxed (+/+) controls. DNA marker is Invitrogen 1kb plus DNA ladder (#10787-026).

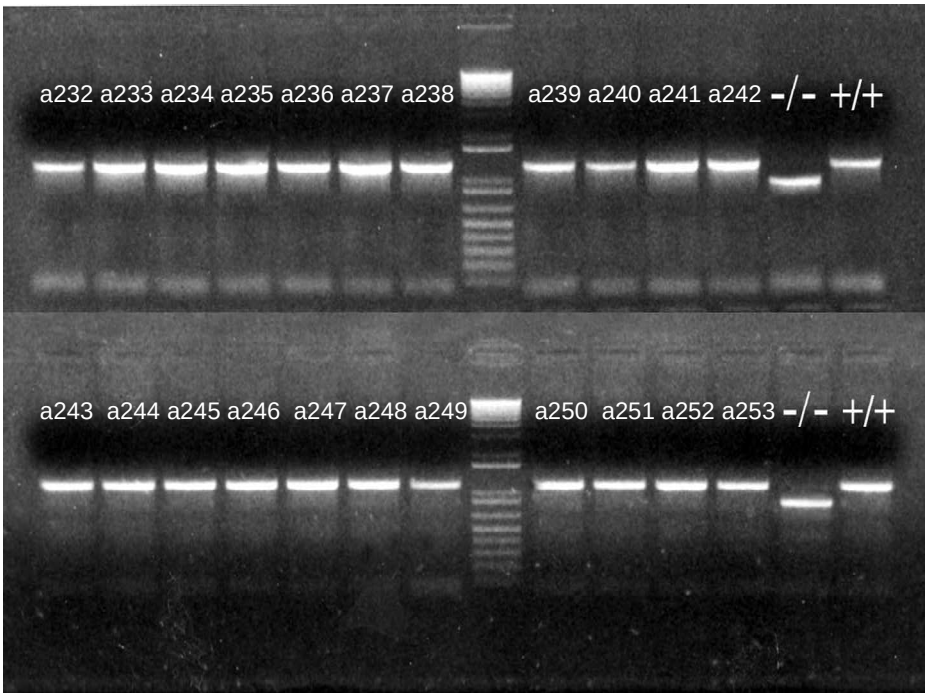

Figure 24: Pure Δ5PTEN$^{flx/flx}$ mice generated (a232-a253) from sister/brother homozygous breeding. Breeding of Δ5PTEN$^{flx/flx}$ mice (a136 x a142; a128 x a147and a148; a151 x a164 and a162 x a165 from Fig 23) produces pure Δ5PTEN$^{flx/flx}$ mice (all progenies are single 1100-bp band). -/- and +/+ are wild type and floxed PTEN control using parental genomic DNAs from a140 and a138 mouse respectively. DNA marker is Invitrogen 1kb plus DNA ladder (#10787-026).

3.4.3. Functional gene switch identification *in vivo*

Although Cre/*lox*P gene switch system has been well characterized, the imported K14CrePR1 and Δ5PTEN$^{flx/flx}$ were used to verify functional activity *in vivo*, to confirm the Ru486 Cre/*lox*P system and to obtain technical *in vivo* insights for the EICre melanoma model. Therefore, bigenic K14Cre/PTEN$^{flx/flx}$ were put on procedure for topical painting of Ru486 to activate K14CrePR1 to ablate floxed exon 5 of PTEN exclusively in the epidermis, resulting in keratinocyte hyperplasia and investigations on carcinogenesis (246)

Using primers P1 (located at exon 4, PTEN.fwd), P2 (a primer located within exon 5 for PTEN genotyping, PTEN.rev) and P3 (a primer located within exon 6 after the second *lox*P site) (Fig 25), production of a new 400-bp PCR product was indicative of the truncated Δ5 allele in either Ru486-treated heterozygous or homozygous skin, but not from untreated bigenic mice or treated/untreated wild type controls. This verified that the CrePR1 fusion recombinase protein was activated *in vivo* following Ru486 application and furthermore, the activated CrePR1 is responsible for ablation of 'floxed' fragment in keratinocytes because of the K14 promoter.

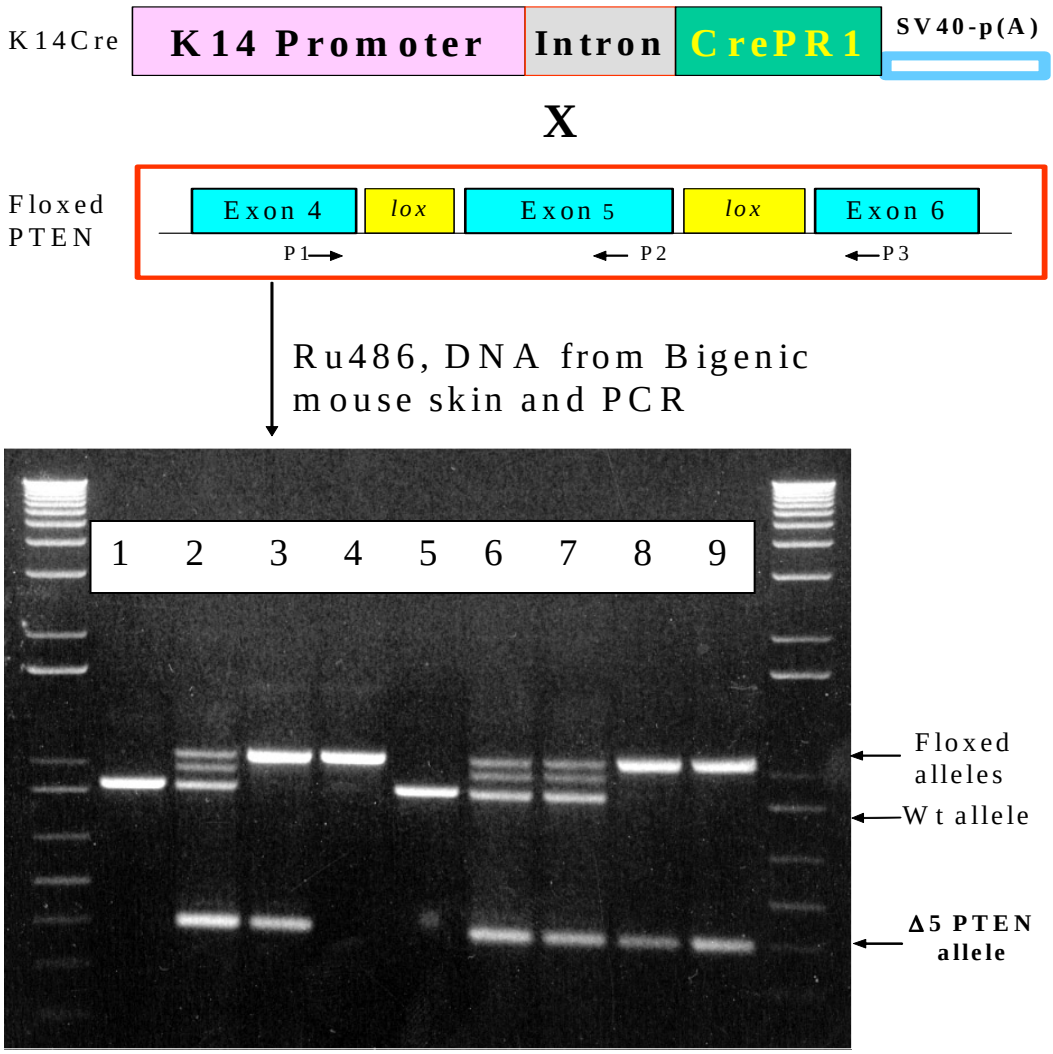

Figure 25: Scheme of gene-switch identification *in vivo*. Gene-switch specificity was identified *in vivo* employing K14CrePR1 and floxed PTEN ($\Delta5PTEN^{flx/flx}$) mice. Δ5 fragment obtained from either homozygous (+/+, lane 3,8,9) or heterozygous (+/-) PTEN/K14Cre (lane 2,6,7) bigenic mice skins via PCR of genomic DNA using primers P1, P2 and P3, but not from wild type (-/-) PTEN/K14Cre which also treated with Ru486 (lane 1) and untreated either $\Delta5PTEN^{flx/flx}$/K14Cre (lane 4) or wild type PTEN (lane 5) mice. 0.9-kb, 1.1/0.9-kb and 1.1-kb pattern of PTEN alleles represent wild type (-/-), heterozygous (+/-) and homozygous (+/+) PTEN respectively. The second top band (between homo and wild type) in lane 2, 6 and 7 (heterozygous) may be amplified from the wild type/floxed PTEN hybrid DNA (the fusion of 2 chromatids in chromosome) during the PCR annealing/extension steps, which also applies to Figs 22 and 23 above. DNA marker is Invitrogen 1kb plus DNA ladder (#10787-026).

3.5. Identification of the transgenic expressers of regulator EICre and target N-Ras^{lys61}

3.5.1. Identification of regulator EICre expressers

In order to identify transgene expressers following identification and confirmation of founder germline transmitters (above), primary melanocytes were isolated from the skin of F1 neonates and cultured in 50/50 medium. The following week, once sufficient number of melanocytes had grown, total RNA was isolated from trypsinized cells and expression of the EICre transgene analysed via RT-PCR. Exploiting primers that spanned the small intron cloned within the SV-40 poly(A) signal, detection of a smaller PCR product from RT samples than from tail DNA revealed that relatively a few of regulator EICre germline transmitters were expressers (Fig 26).

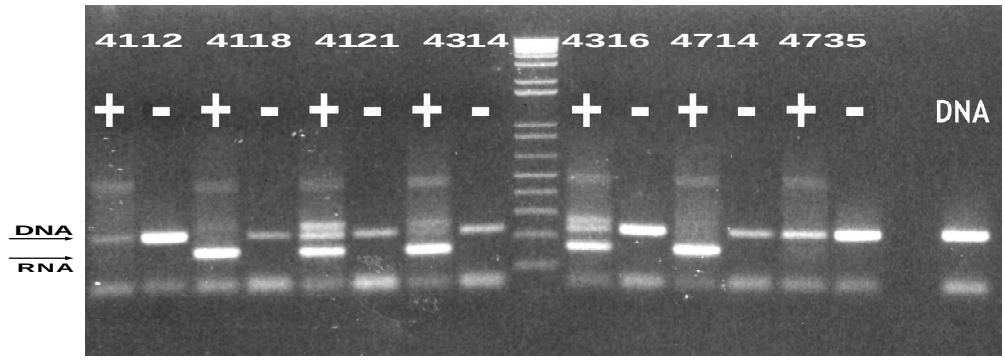

Figure 26: Analysis of regulator EICre expression in primary melanocytes. Regulator EICre expression was detected in primary melanocyte cDNA prepared from F1 neonates RNA of transmitters (4112–4735) using primers crossing the small intron within the SV40 p(A) tail. Lower band shows EICre expression in primary melanocytes and top band indicates DNA contamination from RNA samples. (+) with RT reaction, (-) without RT reaction. Lines 4118, 4121, 4314, 4316 and 4714 are EICre expressers, whereas lines 4112 and 4735 are not EICre expressers although they were germline transmitters. DNA marker is Invitrogen 1kb plus DNA ladder (#10787-026).

As expression of RNA does not necessarily mean successful biological activity, primary melanocytes of expresser lines 4118, 4121, 4314, 4316 and 4714 were subjected to transfection with the report target vector cmv.stop.EGFP to confirm successful gene switch function and their relative expression levels. Once the majority of primary keratinocytes died out and pure melanoblasts/melanocytes were present in dishes, cells were transfected and the following day incubated in 10^{-9}M Ru486 and 3 days later the different numbers of green cells assessed employing an immunofluorescence microscope.

Controls included lack of Ru486 treatment to determine gene switch leakage and Ru486 treated transfection of non-transgenic C57BL6 melanocytes both cohorts proving negative. By counting the number of green cells detectable in each line, the results revealed that lines 4118, 4314 and 4714 displayed reasonable strong and numerous EGFP expressing melanocytes, while other two lines 4121 and 4316 have relative weaker and less EGFP expressing cells in dishes. Furthermore, 4314 was the strongest expresser amongst the five investigated lines giving the most numerous (approximately 200 vs. 80-120 green cells in each transfected dish) and most intensively green cells following treatment of Ru486. Therefore, line 4314 was chosen for further analysis because the highest biological activity of Cre recombinase to result in highest level of target gene expression following Ru486 treatment in primary melanocytes *in vitro* (Fig 27).

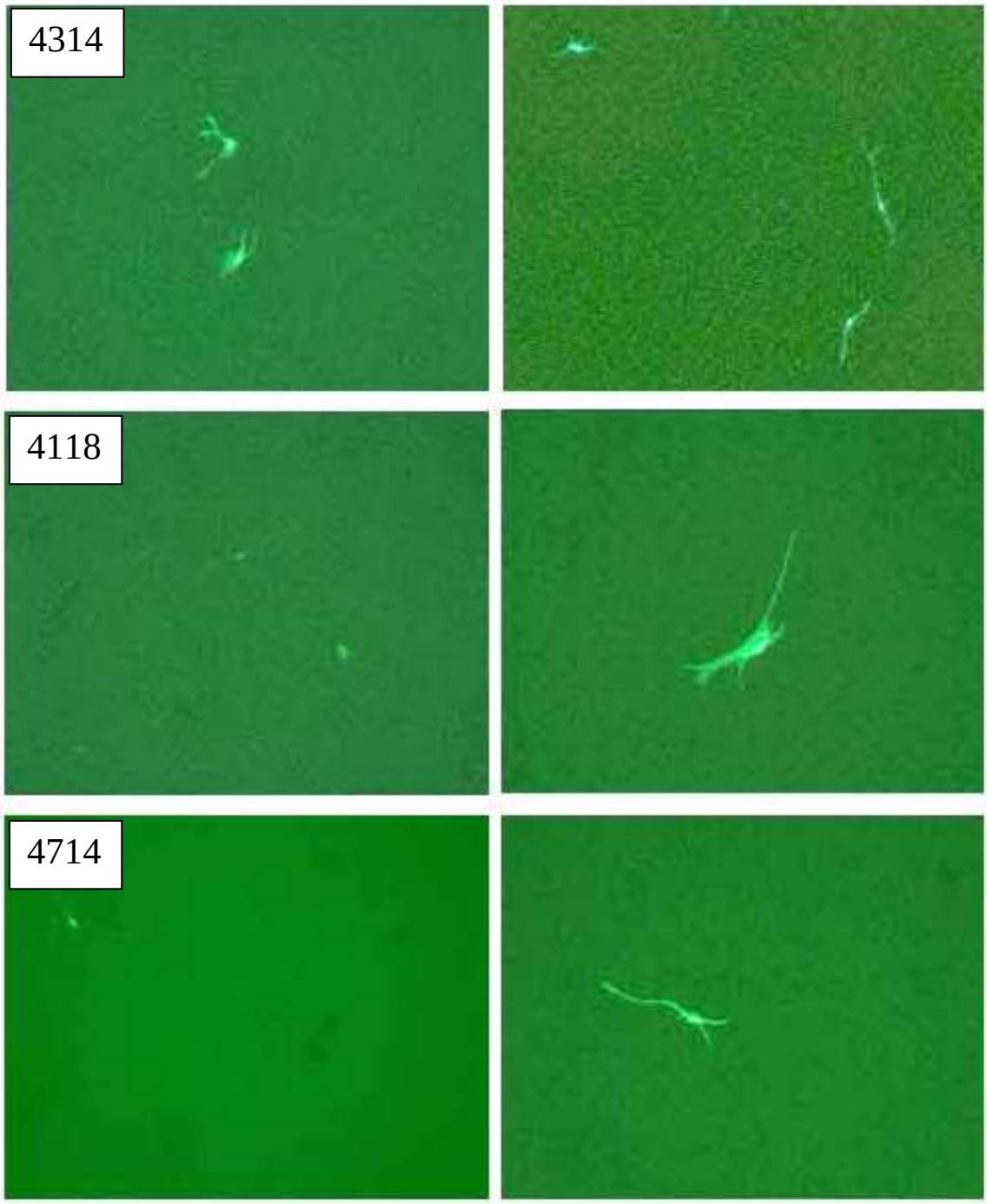

Figure 27: EGFP expression in report target transfected regulator melanocytes. EGFP expression in primary melanocytes from regulator expresser lines 4314, 4118 and 4714 were observed under fluorescent microscope following transfection of report target vector cmv.stop.EGFP and Ru486 treatment for 3 days. Untreated controls were negative and transfected melanocytes of lines 4121 and 4316 have only very weak and few green cells detected which were not shown here. Cells were cultured in 50/50 medium and transfection carried out using Fugene-6 transfection reagent. Pictures were taken at 100x

The number of EGFP expressing cells from each transfected dish was not many, which indicated the targeting protein level may have been low. However, the protein level may not exactly mean transcription level. Thus RT-PCR to semi-quantify targeting gene transcription level was carried out by isolating RNA from cmv.stop.EGFP transfected primary melanocytes of lines 4118, 4314 and 4714 which showed relatively stronger EGFP expression in the above analysis. A primer pair which spanned across generic intron within the target vector was employed to distinguish PCR products of RNA from contaminant DNA. This detected a smaller band from RT-PCR than from transfected target vector DNA in transgenic regulator melanocytes following Ru486 treatment, whereas no such band could be observed in without Ru486 treatment or Ru486 treated non-transgenic control melanocytes. This verified Cre activation in melanocytes of regulator expresser lines 4314, 4118 and 4714 following Ru486 treatment and the subsequent ablation of floxed 'Stop' sequences to result in the expression of target genes (Fig 28). Furthermore, all of the targeting gene expression levels were consistent with their transcription levels, with 4314 having both relative strongest protein activity and highest transcription level amongst the three lines analysed.

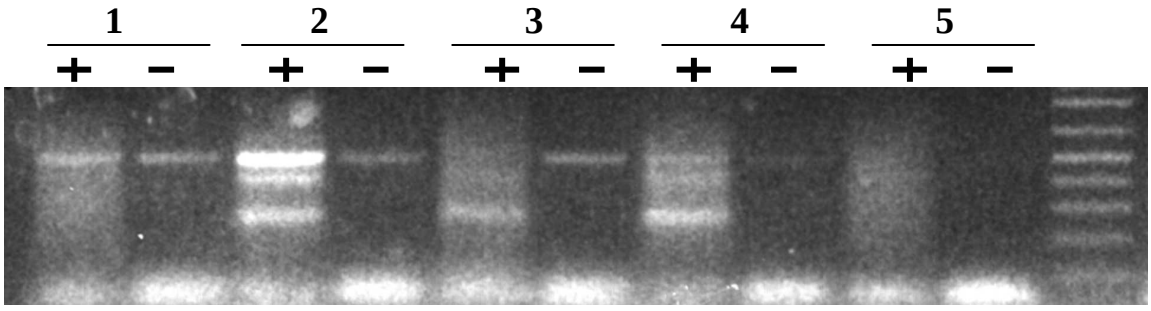

Figure 28: RT-PCR of report target transfected melanocytes of regulator expressers. RT-PCR products were detected from cmv.stop.EGFP transfected primary melanocytes of regulator EICre expresser lines 4314 (sample 2), 4118 (sample 3) and 4714 (sample 4). Higher band (490-bp) indicates DNA contamination of samples and lower band (290-bp) reveals expression of target gene EGFP. Sample 1 is without Ru486 treatment control and sample 5 is non-transgenic melanocytes control. (+) is with RT reaction and (-) is without RT reaction. DNA marker is Invitrogen 1kb plus DNA ladder (#10787-026).

3.5.2. Identification of target N-Ras^{lys61} expressers

As described for identification of germline transmitters, to quickly identify target N-Ras^{lys61} expressers, yet avoid the difficulty of primary melanocytes culture and variable transfection of numerous melanocyte lines, F1 keratinocytes cultures were established from breeding N-Ras founders with K14CrePR1 mice. This also had the advantage employing a known, well characterised gene switch regulator, strongly expressed in keratinocytes from a Keratin K14 promoter (467). Primary keratinocytes of K14Cre/N-Ras^{lys61} bigenic mice were cultured under proliferative low calcium conditions and treated with or without 10^{-9}M Ru486, followed by RNA isolation and RT-PCR reaction. Using primers forward one located in front of generic intron and reverse one within the N-Ras^{lys61} gene, detection of a smaller RT-PCR product of line 4734 primary keratinocytes than PCR product of contaminant DNA indicated correct splicing of the generic intron. These experiments also revealed that target gene expression in only 4734 (Fig 29a) not 7156 (data not shown) keratinocytes. Dishes were assessed in triplicate to ensure result in both transmitter lines.

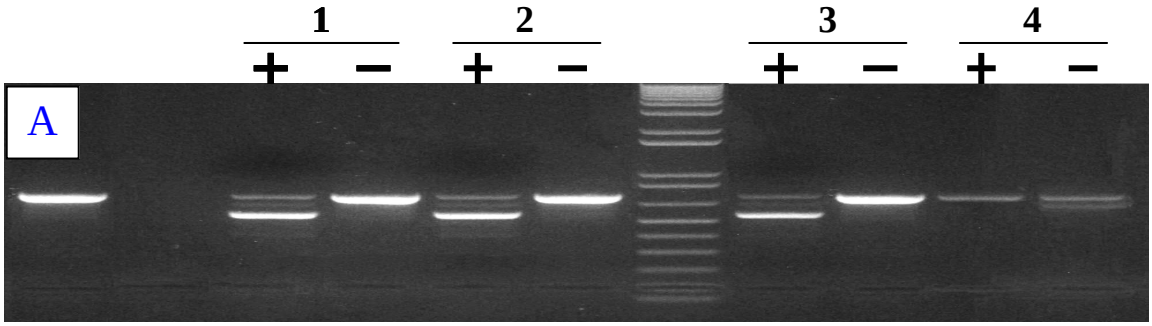

Figure 29a: Oncogenic target N-Ras^{lys61} expressed in K14Cre/N-Ras^{lys61} primary bigenic keratinocytes. N-Ras^{lys61} expression (line 4734) was detected from primary keratinocytes of K14Cre/N-Ras^{lys61} bigenic mice following Ru486 treatment for 3 days via RT-PCR using primers crossing over generic intron within target gene. Lower band shows N-Ras^{lys61} expression while top one indicates DNA contamination. Samples 1-3 are Ru486 treated bigenic keratinocytes with (+) or without (-) RT reaction from triplicate dishes, far left lane and sample 4 are transgene DNA and bigenic keratinocytes without Ru486 treatment control respectively. DNA marker is Invitrogen 1kb plus DNA ladder (#10787-026).

Because line 4734 was the only N-Ras^{lys61} target transgene expresser identified amongst few founders and thus its expression is uniquely important for this project, expression was further analysed employing a panel of primer pairs located at various positions (forward primers p76 sites within CMV promoter, p61 in front of generic intron and p66 locates at the 5' end of N-Ras gene, reverse primers p62 and p67 site at the C-terminal of N-Ras gene and SV40 poly(A) signal respectively) within the construct employing target monogenic N-Ras primary keratinocytes as control. Use of forward primers located either within the CMV promoter or the junction of 'Stop' cassette and intron, and reverse primers site at various positions within N-Ras^{lys61} respectively, gave different sizes of PCR product in Ru486 treated bigenic keratinocytes but not in monogenic cells (Fig 29b).

To confirm ablation of floxed sequences by the active CrePR1 fusion protein and successful splicing of generic intron, two forward primers one located in front of intron (P2) and one situated at the end of promoter (P1), together with a reverse primer (P3) within N-Ras^{lys61} gene were designed and employed for RT-PCR. Primers P2+P3 gave an only slightly smaller RT-PCR product than P1+P3 because of the location of forward primer and ablation of floxed 'Stop' cassette. A bigger band was detected from transgene DNA than from RNA in P2+P3 reaction due to the generic intron, whereas no PCR product was detectable from transgene DNA in reaction P1+P3 because the size (>3kb) of the expected product was too large to be detected under these PCR conditions (Fig 29c).

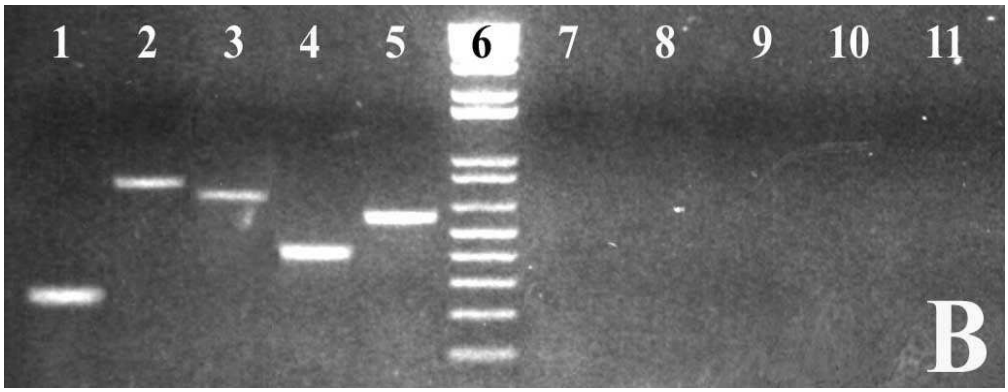

Figure 29b: Analysis of oncogenic target N-Ras^{lys61} expression. N-Ras^{lys61} expression detected from primary keratinocytes of K14Cre/N-Ras^{lys61} bigenic mice following Ru486 treatment for 3 days via RT-PCR employing additional series of primers. p61+p62; p66+p67; p76+p62; p66+p62 and p61+p67 represent lane 1 to 5 respectively, of which locate at various positions within target vector and the same order of primer pairs repeated for lane 7 to 11. Lane 1-5, K14Cre/N-Ras^{lys61} bigenic primary keratinocytes treated with Ru486 have N-Ras^{lys61} expression; lane 6, DNA marker (Invitrogen 1kb plus DNA ladder (#10787-026)); Lane 7-11, no N-Ras^{lys61} expression detectable in monogenic mouse cmv.stop.N-Ras^{lys61} control keratinocytes with Ru486 treatment.

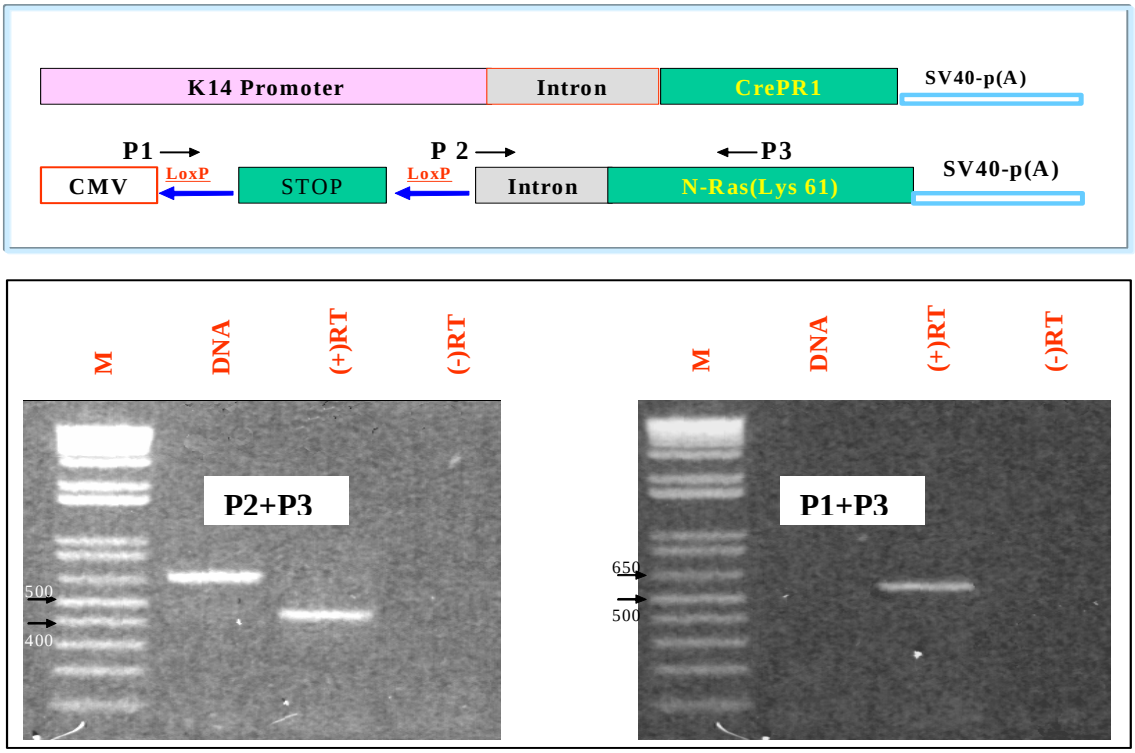

Figure 29c: Scheme of confirmation of N-Ras^{lys61} expresser. To confirm mouse 4734 as a germline expresser of the N-Ras^{lys61} transgene, Ru486 treated bigenic K14Cre/N-Ras^{lys61} primary keratinocytes were analysed via *in vitro* RT-PCR. Employing primer pair P2+P3, successful N-Ras^{lys61} expression in line 4734 was confirmed by detection of a ~450bp PCR product (DNA contamination produces a ~650bp band resulting from existence of intron). Employing primer pair P1+P3, successful expression of correctly spliced N-Ras^{lys61} transcript produced a ~550bp band owing to excision of the 'STOP' cassette in genomic DNA by Ru486 activated K14Cre while DNA contamination (product is more than 3kb in size) was not detectable by designing PCR programme for detection of less than 1kb product. DNA marker is Invitrogen 1kb plus DNA ladder (#10787-026)

3.6. Generation of compound transgenic genotypes EICre/N-Ras^{lys61} and EICre/N-Ras^{lys61}/Δ5PTEN$^{flx/flx}$, and identification of gene-switch specificity

Following the establishment of monogenic lines expressing both regulator EICre and target cmv.stop.N-Ras^{lys61}, confirmation of functional gene switch activity in melanocytes by transfection of target vector into regulator primary melanocytes and confirmation of target *in vivo* expression in K14Cre/cmv.stop.N-Ras^{lys61} bigenic keratinocytes (above), EICre/cmv.stop.N-Ras^{lys61} bigenic cohorts were bred and topically treated with Ru486 to determine whether N-Ras^{lys61} activation was an initiating event in this melanoma model.

Therefore, bigenic adult EICre/cmv.stop.N-Ras^{lys61} mice were put on procedure. In brief, plucking hair induces telogen phase follicles to re-enter into anagen and thus stimulates maximum melanocytes proliferation and expression of the tyrosinase promoter *in vivo* to produce cellular targets for topical Ru486 treatment whilst IP injection in addition ensured Ru486 delivery to the base of hair follicles. However, after 3-4 months of treatment these mice failed to produce melanoma unlike e.g. in the Chin's model where melanoma was induced by H-Ras expression on a CDKN2A deficient background (223), or even elicit any overt melanocyte hyperplastic phenotype as when H-Ras was expressed in melanocytes by Powell via a similar but constitutive, not gene switched, Tyr-based vector (216). Therefore, experiments quickly progressed to show that gene switch specificity *in vivo* was confirmed by detection of N-Ras target gene expression in treated mice skin and in the meantime, giving the frequency of PTEN mutations in human melanoma, conditional knockout of tumour suppressor gene PTEN (Δ5PTEN$^{flx/flx}$) instead of constitutive deficient of CDKN2A gene, was introduced to assess whether melanoma would be elicited by cooperation of PTEN function loss with N-Ras^{lys61} expression.

3.6.1. Line production and induction of N-Ras^{lys61} expression by treatment with Ru486

EICre/N-Ras^{lys61} bigenic line was first produced by crossing EICre with cmv.stop.N-Ras^{lys61} mice following typical breading procedures and PCR screening of progenies. To generate trigenic line EICre/N-Ras^{lys61}/Δ5PTEN$^{flx/flx}$, floxed PTEN (Δ5PTEN$^{flx/flx}$) was bred with EICre/N-Ras^{lys61} to obtain heterozygous Δ5PTEN in EICre/N-Ras^{lys61} bigenic mice (Δ5PTEN$^{flx/-}$/EICre/N-Ras^{lys61}) initially followed by brother-sister mating to produce floxed PTEN trigenic mice (Δ5PTEN$^{flx/flx}$/EICre/N-Ras^{lys61}) as described at 3.4.2 for Δ5PTEN$^{flx/flx}$ production. 6-8 week old transgenic mice with appropriate controls were then set for the experiments. Controls included ethanol treatment of compound transgenic mice and Ru486 treatment of mono genotype littermate siblings.

One aspect of this study is the necessity of tyrosinase expression in proliferative melanocytes for regulator expression and gene targeting. Murine melanocytes ceased proliferation and undergo apoptosis at catagen and thus, during telogen few epidermal melanocytes are apparent in adult epidermis. To initiate the hair cycle and obtain maximal target melanocytes for Ru486 treatment approximately 7-9 days later as determined in timed experiments (Fig 30), the mouse back hair was plucked at day zero of procedure and then approximately every 4 weeks as the hair grew back. Mice were topically painted with 100µl of 100µg/ml Ru486 (468) twice a week together with once a week IP injection of 0.4g Ru486/per kg mice weight to ensure efficient delivery of Ru486 to the hair follicle (469) (average weight 25g was considered).

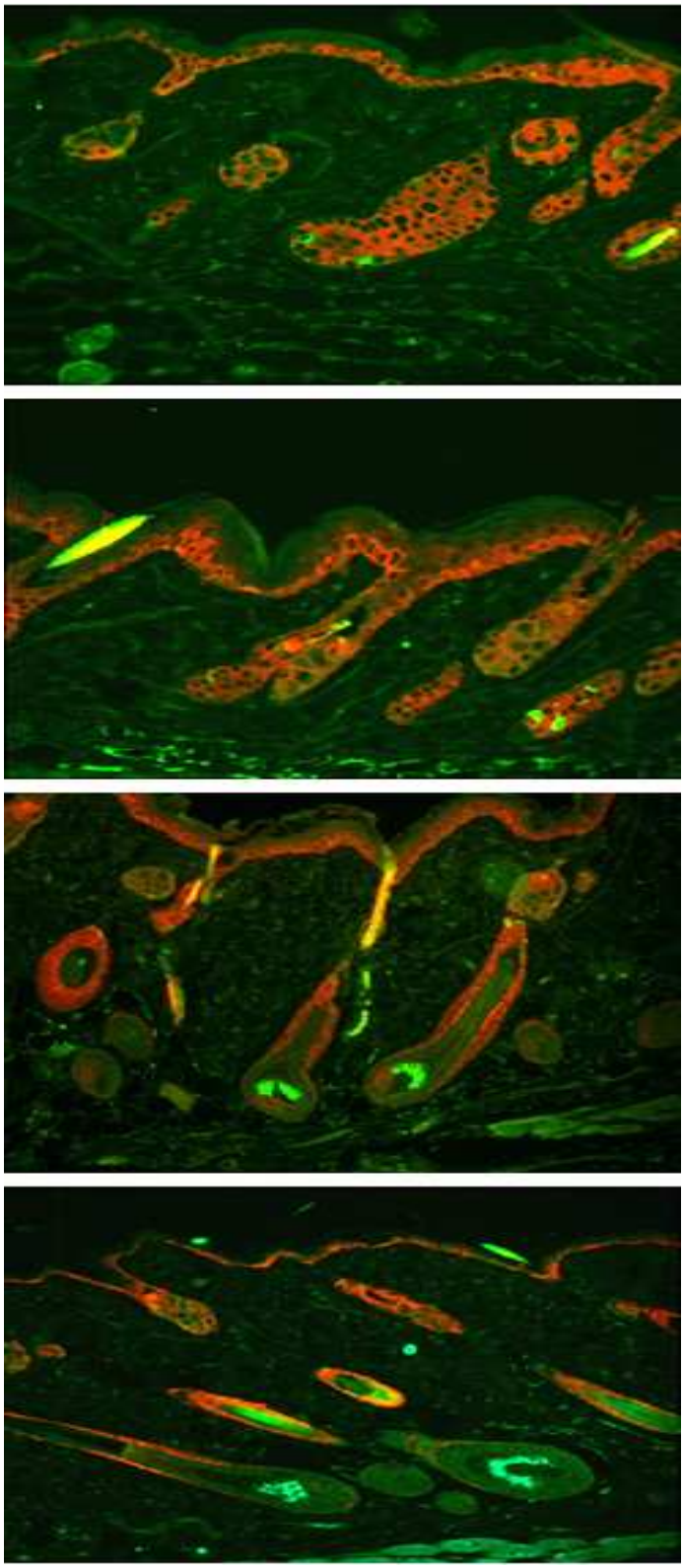

Figure 30: Melanocytes growth following hair plucking. TRP2-stained melanocytes (green) of skin biopsies show maximal melanocytes exist in hair follicle 7-9 days after plucking. From top to bottom pictures represent staining of biopsies from 1, 3, 7 and 9 days post-plucking respectively and K14 (red) used for counter staining. Pictures were taken at 100x.

3.6.2. Confirmation of N-Ras^{lys61} expression *in vivo*

Due to the failure of melanoma or any hyperplastic melanocyte production following mice on procedure for 3 months when the mice were expected to have produced phenotypes (216;223), N-Ras^{lys61} expressing was confirmed by *in vivo* detection via RT-PCR by isolating RNA from those Ru486 treated, plucked mice skins. Controls included vehicle treated bigenic mice skin and Ru486 treated wild type skin (Fig 31).

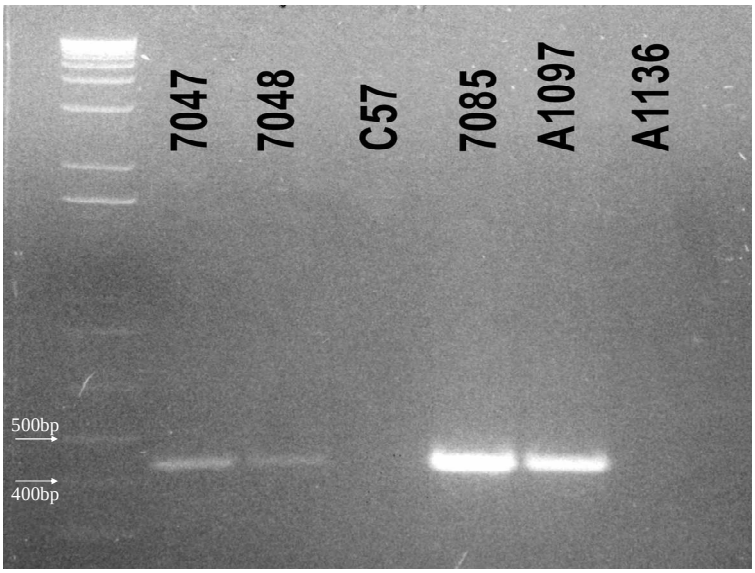

Figure 31: Confirmation of melanocyte specific gene-switch specificity *in vivo*. Target gene N-Ras^{lys61} expression was detected in Ru486 treated bigenic EICre/N-Ras^{lys61} mice skins but not in Ru486 applied wild type C57BL6 or vehicle treated bigenic mouse A1136 skins. As outlined above, primer pair P2+P3 used for Fig 29c were employed for RT-PCR here and a ~450bp fragment confirmed N-Ras^{lys61} expression *in vivo* in EICre/N-Ras^{lys61} bigenic mice. DNA marker is Invitrogen 1kb plus DNA ladder (#10787-026)

Following identification of N-Ras^{lys61} target gene expression and the identification of gene switch functional specificity *in vivo*, the mice were kept on procedure for longer to investigate whether inducible N-Ras ^{lys61} expression was sufficient to generate melanoma or any phenotypes with longer latency. Recently a similar but constitutive N-Ras(Q61K) expression model was shown to be able to generate melanoma although with a long latency of more than one year and following embryonic expression throughout development (215), whereas H-Ras expression gave simple melanocyte hyperplasia in the absence of UV or DMBA initiation (216;221).

A conditional knockout of tumour suppressor gene PTEN instead of common using CDKN2A gene, was introduced to promote eliciting of melanoma model by cooperation of PTEN function loss with N-Ras^{lys61} expression which cooperated quite successfully with H-Ras in a model of squamous cell carcinogenesis (246). However, again unexpectedly a lack of melanoma production resulted from EICre/N-Ras^{lys61}/Δ5PTEN$^{flx/flx}$ trigenic mouse, suggesting therefore a redundancy between these two insults in melanocytes *in vivo* and therefore, the investigation of whether PTEN function loss promoting N-Ras^{lys61} initiated tumourigenesis *in vitro* was performed employing colony formation assay in primary melanocytes (below).

Keratinocyte can secret numerous regulatory factors to control melanocyte development as well as to play potential roles in melanoma formation (470). K14Cre, a regulator controlling target gene expression in keratinocytes specifically, was introduced to induce epidermal hyperplasia by switching N-Ras^{lys61} expression in keratinocytes at the same time in melanocytes by EICre regulator. Disruption of melanocytes microenvironment (mainly keratinocytes) could release melanocytes from enslavement by keratinocytes, a seed/soil hypothesis (471) was therefore added to this model (see 3.9) to investigate PTEN functional loss promotion on N-Ras^{lys61} expression for melanoma production.

3.7. Colony formation in PTEN loss and N-Ras^{lys61} expressing melanocyte

As mentioned above, PTEN function loss did not appear to have a synergistic effect on inducible N-Ras^{lys61} initiation in the triple EICre/N-Ras^{lys61}/Δ5PTEN$^{flx/flx}$ transgenic mouse and there was no obvious difference observed from EICre/N-Ras^{lys61} mouse. Despite the successful expression of the gene switch *in vivo* and *in vitro*, serious concerns as to a lack of phenotype *in vivo* experiments and essential role of PTEN in carcinogenesis (245) prompted an *in vitro* analysis of whether N-Ras^{lys61} and PTEN biological function loss would co-operate to transform melanocytes, whereas TSG PTEN function-loss promoted tumourigenesis in cooperation with H-Ras in keratinocytes (246). Furthermore, whilst PTEN mutations, were often detected in melanoma cell lines but less often in short-term cell (STC) lines and solid melanomas (reviewed in (264)) implied that PTEN functions may play different roles between *in vitro* and *in vivo*. Therefore, to investigate whether PTEN function-loss promote N-Ras^{lys61} initiated tumourigenesis in melanocyte *in vitro*, colony formation assays were performed employing target transgenic melanocytes and the defined protocols of transfection. Here the relatively stronger (compare to EICre) TRP2Cre regulator was employed for transfection despite its previously discovered leakage (table 2, section 3.3.2) which would not interfere but actually enhance the analysis *in vitro*.

The results demonstrated that N-Ras^{lys61} expression or PTEN loss led to faster melanocyte proliferation and together PTEN promoted N-Ras^{lys61} expression to initiate transformed cell colony morphology in tagged immunofluorescent protein expressing (EGFP) as well as in G418 selection experiments. However, and consistent with the eventual redundancy concluded between these molecules *in vivo* (see below 3.8), *in vitro* although morphologically more transformed, N-Ras^{lys61}/Δ5PTEN$^{flx/flx}$ cell co-expressers were not immortalized because cells in 50/50 medium still senesced by passage 5 or 6 but remained viable for some more months in culture.

3.7.1. EGFP immunofluorescence tagging

The experiment to test the transforming ability of PTEN loss or/and N-Ras^{lys61} expressing in melanocytes was performed in 50/50 medium to avoid any spontaneous transformation (melanocytes in Halaban medium spontaneously transformed, see section 3.2.2). To quickly and easily confirm that transformation was induced by gene switch activities and produce colonies visible under immunofluorescence microscope, a cmv.stop.EGFP plasmid was co-transfected to tag melanocytes together with Trp2Cre at a ratio of 1:3 (to render all EGFP expressing cell are TRP2Cre transfected) into wild type, monogenic (Δ5PTEN$^{flx/flx}$ or N-Ras^{lys61}) and bigenic Δ5PTEN$^{flx/flx}$/N-Ras^{lys61} melanocytes. Following 4-5 weeks continuous culture in presence of 10^{-9}M Ru486, green colonies expressing EGFP were formed in all transfected different genotypic cells (Fig 32 and Fig 33). The morphology of colony cells, however, was significantly different between colonies formed from transfections of different genotypic cells.

In wild type control dishes, green cells without orientation were often observed as separate events (close individual transfected cells) rather than a colony proliferated from single transfected cells. Indeed, two likely colonies formed by single transfected cell amplification were observed among three C57BL6 dishes but cells retained a normal morphology. Moreover, there are only 3 and 4 cells comprised in each colony in contrast to the most of colonies formed in transgenic cells consisted of numerous cells (Fig 32, left panel).

Following biological function loss of TSG PTEN via co-transfection of TRP2Cre and cmv.stop.EGFP into Δ5PTEN$^{flx/flx}$ melanocytes, greater numbers of green colonies still without orientation were observed in transfected Δ5PTEN$^{flx/flx}$ melanocytes dishes than in transfected C57BL6 wild type control dishes. These colonies were also bigger than control colonies, as PTEN loss promoted cell proliferation. However, the melanocytes in PTEN null colonies remained contact inhibition characteristic (Fig 32, right panel).

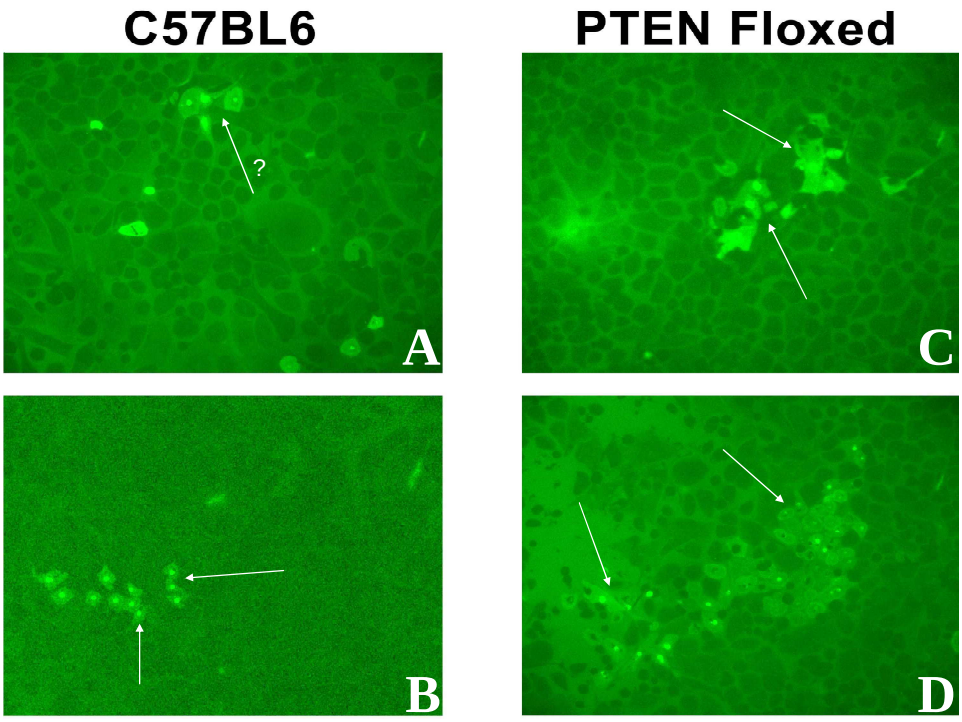

Figure 32: Colonies formed in wild type and Δ5PTEN$^{flx/flx}$ melanocytes. Green colonies without orientation formed in TRP2Cre/cmv.stop.EGFP cotransfected primary cultured melanocytes of wild type (left panel A, B) and of Δ5PTEN$^{flx/flx}$ (right panel C, D) following 4-5 weeks continuous culture in presence of Ru486. Photographs were taken at 200x. More and bigger green colonies obtained from Δ5PTEN$^{flx/flx}$ melanocytes (right panel) due to loss of PTEN function switched by active Cre recombinase under control of TRP2 promoter, whilst single transfected melanocyte-clusters rather than formed colony (2 pictures of left panel show a few such clusters or 'colonies') occasionally observed from transfected wild type C57BL6 melanocytes. Arrows show colonies without orientation or may be just green cell clusters.

In contrast to the colonies formed in wild type and Δ5PTEN$^{flx/flx}$ melanocytes, TRP2Cre transfected cmv.stop.N-Ras^{lys61} primary melanocytes formed more and various colonies due to the expression of oncogenic protein N-Ras^{lys61} following Ru486 treatment (Fig 33, A-C). N-Ras^{lys61} expressing colony cells presented as various shapes with most being spindle shaped consistent with a transformed nature. The green colony cells looked capable of a degree of migration/invasion either growing within another colony or grow on the top of another brown colony, which could be the result of non-EGFP transfection as TRP2Cre DNA was transfected at a higher 1:3 ration (EGFP : TRP2Cre applied) or possible result of EGFP expression turning off caused green immunofluorescent protein expression loss in some colony cells due to the toxicity of EGFP expression (A).

In bigenic Δ5PTEN$^{flx/flx}$/N-Ras^{lys61} melanocyte cells, loss of PTEN function in addition of N-Ras^{lys61} expression following TRP2Cre transfection and Ru486 treatment induced a lager number of colonies with obviously more cells in each colony. However the area of green colonies (D-F) seemed smaller than of those colonies formed in cmv.stop.N-Ras^{lys61} and Δ5PTEN$^{flx/flx}$ monogenic dishes suggesting that theses melanocytes piled up on each other. Cells in these colonies lost contact inhibition characteristic of normal cell to become multiple piled up layers and thus it was impossible to distinguish individual cells, and colonies were smaller and more compact despite more cells than some of those formed in monogenic dishes. This suggested an increased invasive ability especially in colony F by growing on top of the surrounding melanocytes. However, even these colony cells senesced eventually following 5-6 passage sub-culture suggesting that these cells were not immortalized. Moreover, this may have been the *in vitro* equivalent of the melanocyte cluster effect observed in pigmented papilloma aetiologies (Section 3.9).

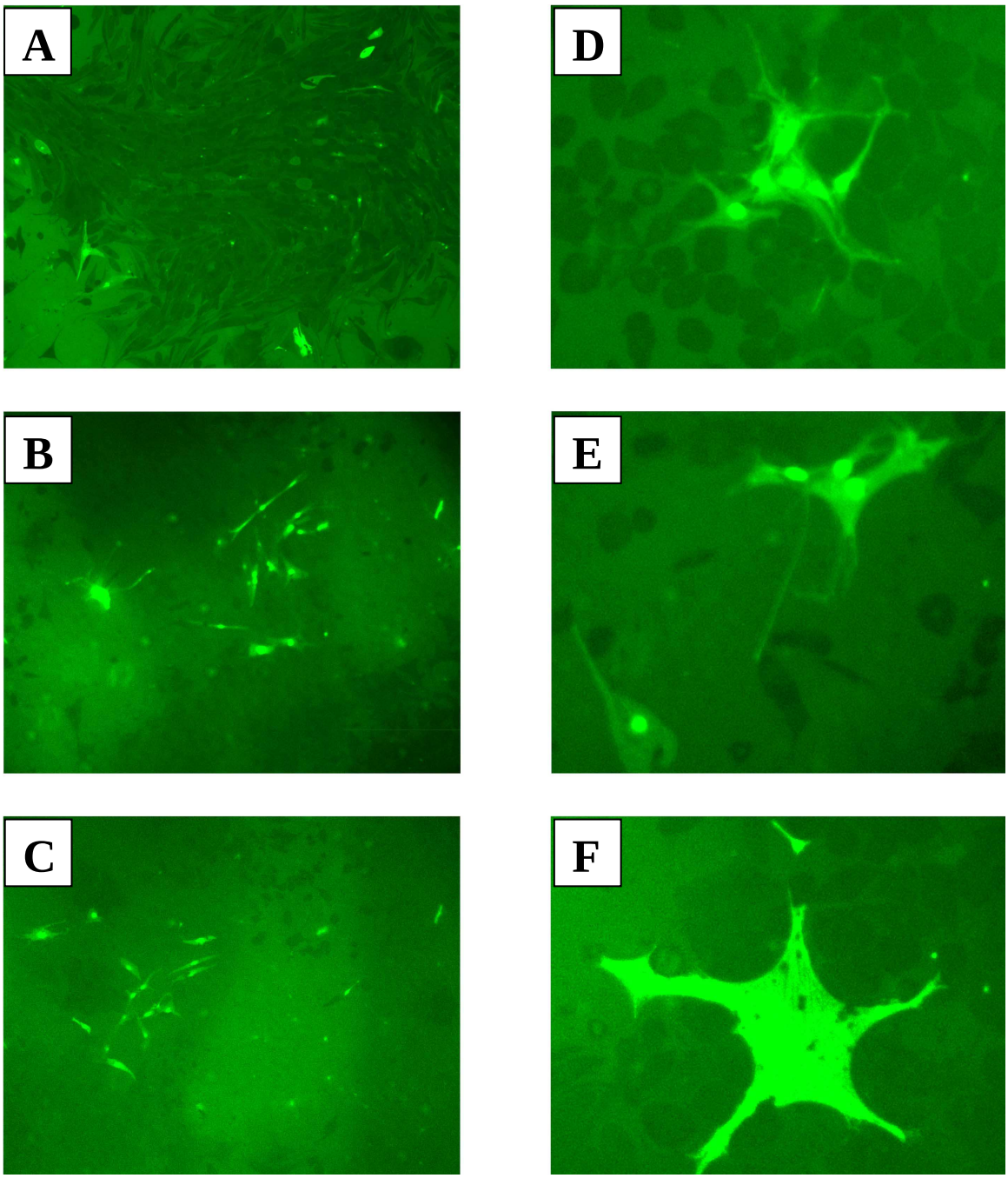

Figure 33: Colonies formed in N-Ras^{lys61} and Δ5PTEN$^{flx/flx}$/N-Ras^{lys61} melanocytes. Potential transformed colony formed in N-Ras^{lys61} (A-C, 100x) monogenic dishes and migratory/invasive ability promoted by PTEN function loss in Δ5PTEN$^{flx/flx}$/N-Ras^{lys61} (D-F, 200x) bigenic melanocytes following co-transfection of TRP2Cre and cmv.stop.EGFP (3:1). Photos were taken after 4-5 weeks continuous culture in presence of Ru486 post transfection.

3.7.2. G418 selection

To verify *in vitro* results obtained by immunofluorescence marking of transformed colonies as described above, CMV-neo (a plasmid allowing G418 selection in 50/50 medium applicable to result in only transgene expressing cell growth) was employed instead of cmv.stop.EGFP to transfect primary melanocytes and this provides a more stringent assessment of transformation potential and avoids potential problems from EGFP toxicity. Following co-transfection of TRP2Cre and CMV-neo (3:1 of DNA concentration to allow TRP2Cre transfect all CMV-neo transfected melanocytes), 200μg/ml of G418 (optimized in titration experiments to kill untransfected cells within 3 days but not too toxic to prevent colony selection) was added into transfected dishes to select CMV-neo transfected cells and 10^{-9}M Ru486 was presented to activate TRP2Cre to allow N-Ras^{lys61} expression and/or PTEN function loss.

Fig 34 shows different numbers of the colonies formed in each dish per transfected genotype following G418 selection. Possibly due to continuous G418 selection pressure and the slow growth of primary murine melanocytes without keratinocyte feeders, the time to obtain reasonable colony size took longer than expected. Tiny, visible colonies appeared at week 6-7 post transfection, with clear differences emerging between transfected colonies as show at 10-11 weeks selection of G418. In this figure, colonies appeared in all transfected dishes but with significant different number and size of colony in various genotypic cells. In C57BL6 melanocytes, very few cells survived G418 selection to occasionally form a very tiny spontaneous colony, normally visible only under the microscope, in contrast to big, black and obvious colonies formed in Δ5PTEN$^{flx/flx}$, N-Ras^{lys61} and Δ5PTEN$^{flx/flx}$/N-Ras^{lys61} melanocytes given function loss of PTEN or/and N-Ras^{lys61} expression. Additionally, N-Ras^{lys61} expressing dish formed more colonies than Δ5PTEN$^{flx/flx}$ dish. Furthermore, although various size of colonies formed in both Δ5PTEN$^{flx/flx}$ and N-Ras^{lys61} dishes, more significant size difference between colonies

presented in Δ5PTEN$^{flx/flx}$ dishes with some are extremely big while others are really tiny which are visible only under microscope, compared to colonies formed in Δ5PTEN$^{flx/flx}$/N-Ras^{lys61} that appeared almost similar sized. These results are consistent with the results obtained from the previous EGFP-based immunofluorescence transfection observations. Again, there are more colonies presented in Δ5PTEN$^{flx/flx}$/N-Ras^{lys61} than in Δ5PTEN$^{flx/flx}$ and N-Ras^{lys61}dishes.

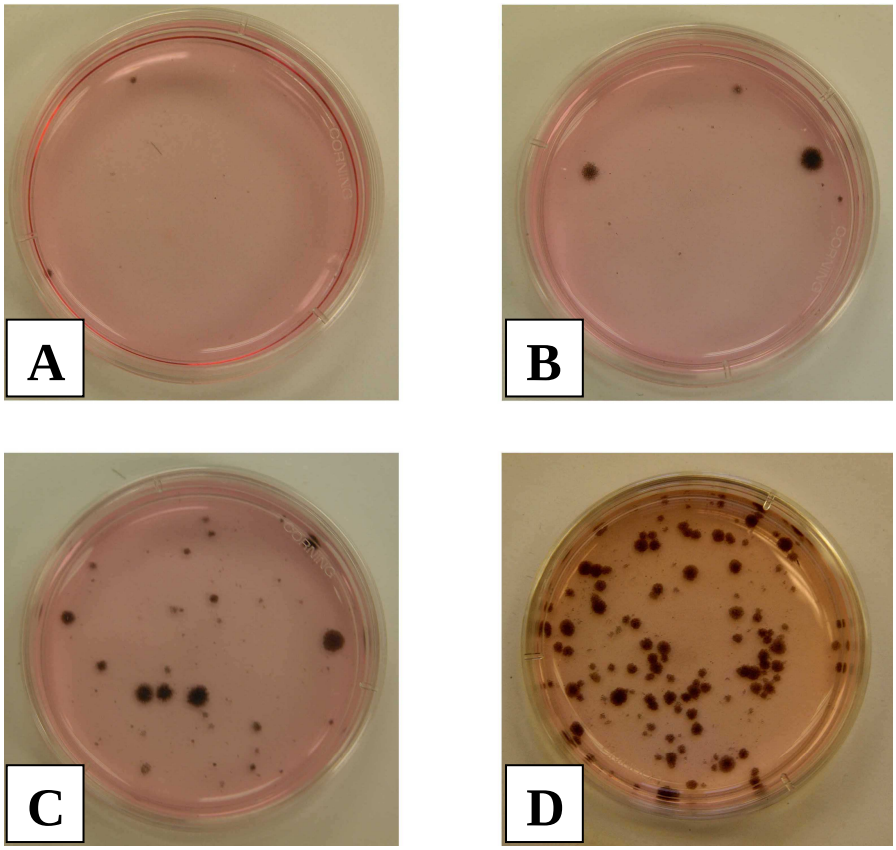

Figure 34: Colony formation in TRP2Cre/CMV.neo cotransfected primary melanocytes following G418 selection. Colonies formed in different genotypic primary melanocytes following cotransfection of regulator TRP2Cre together with selecting plasmid CMV-neo and G418 application. There are tiny and few difficult visible colonies in C57BL6 dishes (A), more and variable size colonies in monogenic melanocytes dishes Δ5PTEN$^{flx/flx}$ (B) and N-Ras^{lys61} (C) while Δ5PTEN$^{flx/flx}$/N-Ras^{lys61} (D) gave most colonies. The results are consistent with the previous observation of green colonies using EGFP protein as a marker.

By comparing (Fig 35) cell morphology between colonies formed in different genotypic melanocytes, identical results to the unselected experiments (3.7.1) were obtained. Again, selected C57BL6 cells grow very slowly eventually forming a few tiny colonies (A) with some are microscopic (B). Colonies formed in Δ5PTEN$^{flx/flx}$ melanocytes were much bigger than those in C57BL6 dishes because the function loss of PTEN promoted cell proliferation. Cells in both colonies retained their contact-inhibition characteristic and grew as monolayer even in the dense colonies (C). Cells in colonies formed in PTEN function loss presented a relatively normal morphology as described above suggesting that PTEN loss promoted cell proliferation but not transformation, unlike cells in N-Ras^{lys61} expressing colonies (3.7.1 and below)

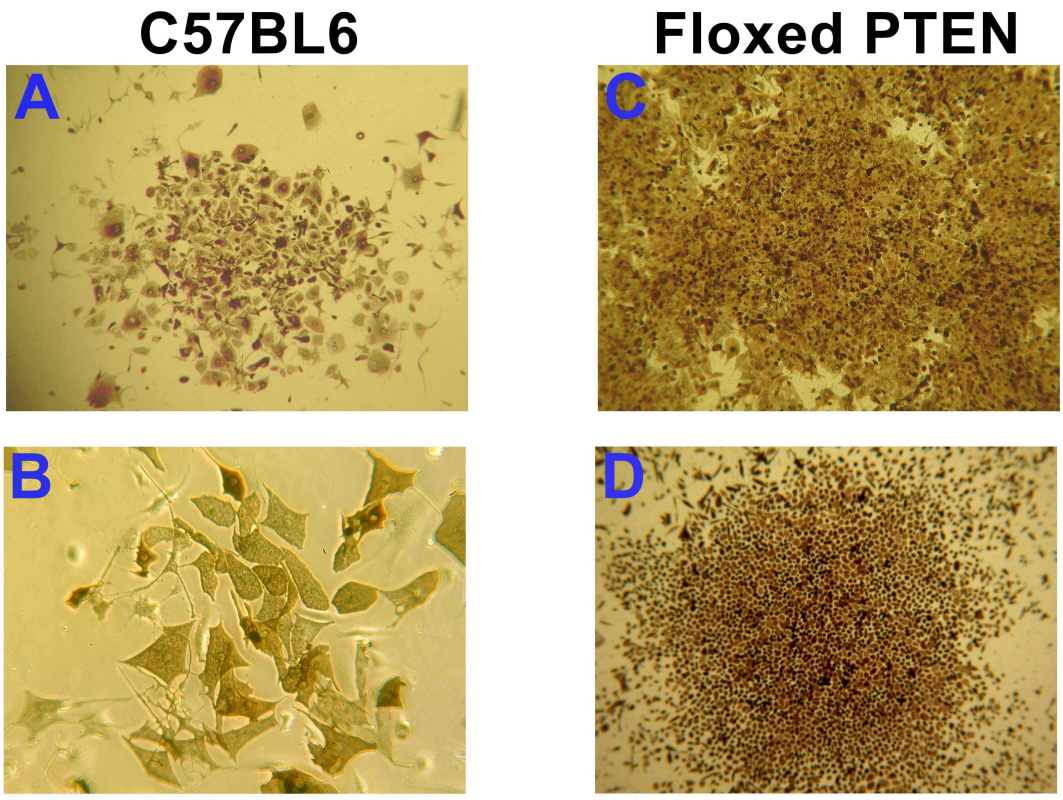

Figure 35: Colony cell morphologies in wild type and Δ5PTEN$^{flx/flx}$ melanocytes. Colonies formed in TRP2Cre transfected Δ5PTEN$^{flx/flx}$ primary melanocytes following 200µg/ml G418 for 10-11 weeks selection. PTEN function loss promotes cell proliferation to form very big colonies (C, D) compared to spontaneous colonies formed in wild type melanocytes (A, B). Photographs were taken at 100x except B (400x).

Consistent with the results obtained from 3.7.1 using green fluorescent protein as a marker, in contrast to the colonies formed in wild type, N-Ras^{lys61} expressing dishes form more colonies and furthermore, colony cells (Fig 36, A-B) presented different shapes from those cells in normal melanocytes dishes and in Δ5PTEN$^{flx/flx}$ dishes.

In addition to forming a greater number of colonies, than in monogenic and wild type cells (Fig 34), the morphology of bigenic melanocyte cells was significantly different from those monogenic and wild type colony cells (above 3.7.1). Addition of PTEN functional loss (Δ5PTEN$^{flx/flx}$) to N-Ras^{lys61} expressing promoted a further change of cell morphology in Δ5PTEN$^{flx/flx}$/N-Ras^{lys61} colonies (Fig 36). The most important factor among these differences is that cells in these colonies lost contact inhibition characteristics to gain multilayer growth ability of the characteristic of transformed cells, thus it is impossible to distinguish any single cell in the centre of these colonies. Furthermore, these colonies have more spindle shape cells with disappearing of those round and oval shaped cells which mainly presented in normal cultured melanocytes (Fig 13) and thus, cells in these bigenic colonies are different again from cells in those colonies formed in wild type and Δ5PTEN$^{flx/flx}$ or N-Ras^{lys61} monogenic melanocytes as presented in Fig 35.

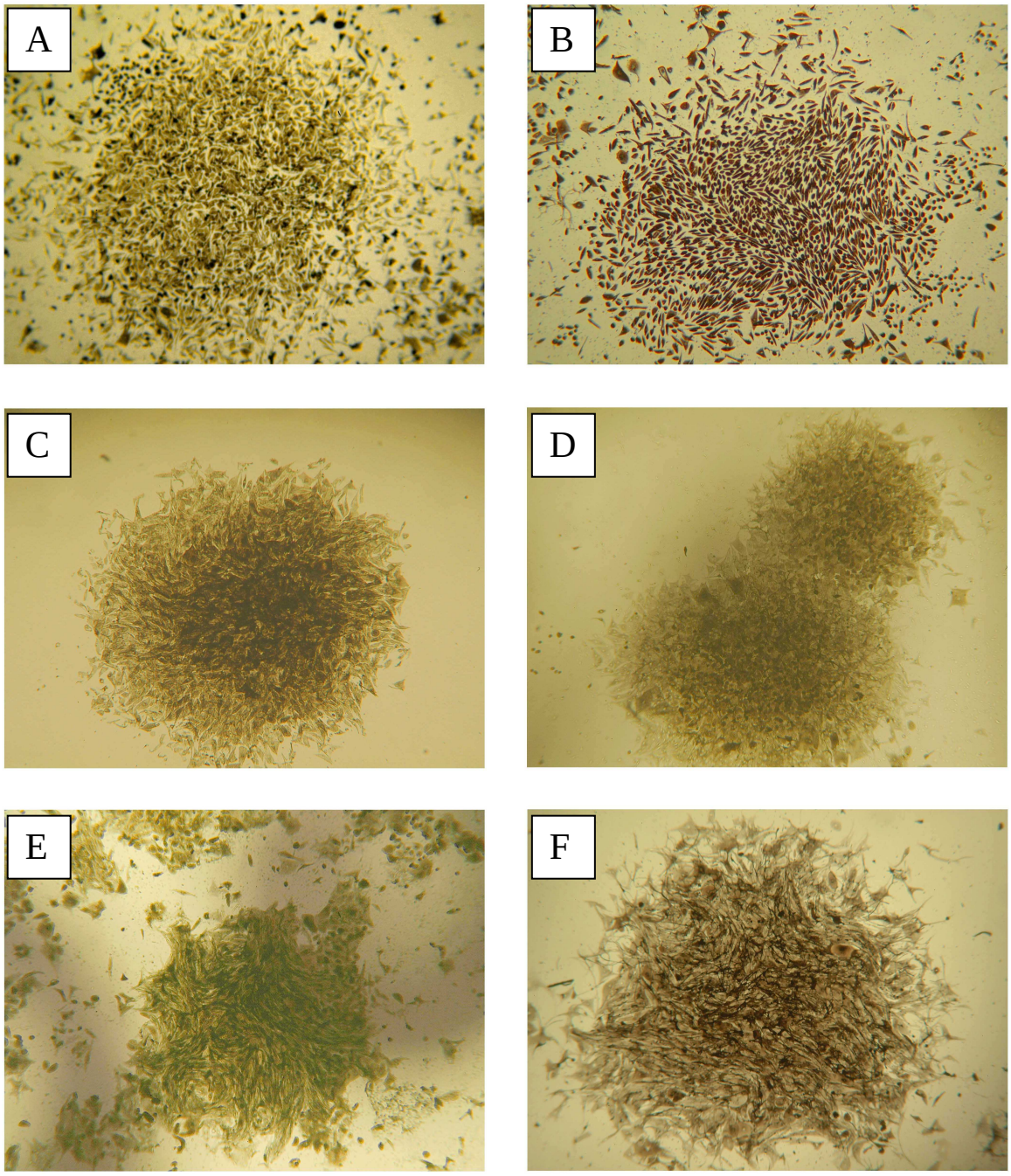

Figure 36: Morphology of colonies formed in N-Ras^{lys61} and Δ5PTEN$^{flx/flx}$/N-Ras^{lys61}. A number of different colonies formed in monogenic N-Ras^{lys61} (A, B) and bigenic Δ5PTEN$^{flx/flx}$/N-Ras^{lys61} (C-F) melanocytes following regulator TRP2Cre co-transfection with selective vector CMV-neo and continuous G418 selection. Cell morphologies in Δ5PTEN$^{flx/flx}$/N-Ras^{lys61} colonies are significantly different from those in colonies formed spontaneously (wild type, Fig 35 A, B) or monogenic N-Ras^{lys61} (and Δ5PTEN$^{flx/flx}$ in Fig 35 C, D) dishes due to promotion of PTEN function loss on N-Ras^{lys61} oncogenic protein. All photos were taken at 50x.

This colony formation analysis *in vitro* demonstrated that PTEN function loss promoted N-Ras initiated tumourigenesis to form colonies with a transformed nature. In addition, the finding that $\Delta 5PTEN^{flx/flx}$/N-Ras^{lys61} colony cells still senesced and were viable in dishes for months but were not immortalised, was consistent with the eventual conclusion to this study that an N-Ras/PTEN redundancy apparently exists *in vivo* (below).

Collectively, by inventing 50/50 medium where primary melanocytes grow without spontaneous transformation, unlike cells cultured in Halaban medium, and optimising transfectable capacity (see 3.2.2), an *in vitro* inducible gene switch model was established able to select colonies without contamination from keratinocytes or spontaneous transformation or spontaneous progressing to an immortalised phenotype. The results verified PTEN promotion of N-Ras initiated tumourigenesis *in vitro*, which is consistent with the previous reports in cell lines, and the fact that these cells were viable for months but senesced eventually, implied a redundancy between PTEN loss and N-Ras genes, which was also proven by the experiments *in vivo* where PTEN and N-Ras were both revealed to induce melanocyte apoptosis but lacked the power to ablate this protective pathway without additional genetics events for cross-talk.

3.8. Phenotypes obtained from EICre/N-Ras^{lys61} and EICre/N-Ras^{lys61} /Δ5PTEN$^{flx/flx}$

Initially no immediate phenotypes were obtained from EICre/N-Ras^{lys61} nor the mouse lines, EICre/N-Ras^{lys61}/Δ5PTEN$^{flx/flx}$ and EICre/Δ5PTEN$^{flx/flx}$, which were put on procedure later for the testing of PTEN loss promotion on N-Ras^{lys61} initiation, whereas H-Ras expression in a CDKN2A gene deficient background successfully produced melanoma (223). However, all mice were kept on procedure to test whether N-Ras^{lys61} expression and/or PTEN function loss would produce melanoma eventually or any other phenotypes.

Following more than one year on procedure, an eye phenotype, very similar to that presented in the recently published Ackermann model of constitutive N-Ras expression (215), was obtained in EICre/N-Ras^{lys61} bigenic mice. Yet the addition of PTEN functional loss in EICre/N-Ras^{lys61}/Δ5PTEN$^{flx/flx}$ trigenic mice failed to produce additional phenotypes, nor accelerate appearance of the N-Ras-associated eye phenotype, which indicated that in this case biological function loss of the PTEN gene lacked an ability to promote N-Ras^{lys61} initiation unlike H-Ras/PTEN synergism in keratinocytes (246). However cutaneous N-Ras expression apparently initially failed to result in a phenotype, but as outlined below, this was revealed later to be due to induction of a caspase-dependant apoptosis pathway which eliminated the melanocyte population resulting in white hair. Here functional PTEN loss still resulted in this apoptotic response in melanocyte and thus again, additional PTEN loss did not provide an alternative pathway to overcome this surveillance mechanism which therefore, negated melanoma formation in this model. Also unique to the EICre model was the presentation of Harderian gland adenoma, which was absent in alternate models, and may have been a consequence of different promoters and/or different Ras alleles as discussed below.

3.8.1. Phenotype 1— enlarged eyes and harderian gland adenoma

3.8.1.1 Enlarged eyes

Ru486-treated mice were checked twice a week for any phenotypes when the Ru486 (or vehicle control) treatment was applied. Although neither bigenic EICre/N-Ras^{lys61} nor trigenic mice EICre/N-Ras^{lys61}/Δ5PTEN$^{flx/flx}$ had developed melanoma, an unexpected phenotype of enlarged eye was displayed in both bigenic and trigenic mice following 12-15 months of systemic Ru486 treatment, which was absent in either Ru486 treated monogenic mice or vehicle (ethanol) treated bigenic and trigenic controls (Fig 37). This somewhat alleviated concern that the gene switch was non-functional *in vivo* because the controls remained normal although following treatment target expression was confirmed both in cultured cells and in skin biopsies (see 3.5.2. and 3.6.2.). Biopsies were obtained from phenotypic mice for further analysis although these phenotypes were unexpected particularly in Harderian glands ─but a site proved to express tyrosinase (472).

H&E stained micrographs of formalin fixed phenotypic eyes displayed a much larger size and a predominance of melanin (Fig 38 A-D), possibly indicative of melanocyte hyperplasia in the RPE rather than overt tumour at this stage, compared to control eye (Fig 38 E, F) when micrographs taken at the same magnification (50x). Furthermore, it had been expected that the trigenic EICre/N-Ras^{lys61}/Δ5PTEN$^{flx/flx}$ would elicit melanoma because given oncogenic N-Ras^{lys61} expression and PTEN tumour suppressor gene deletion, however this trigenic mouse line did not generate any additional phenotypes compared to bigenic mice.

This result coupled to the failure to develop melanoma in trigenic mice revealed that tumour suppressor gene PTEN deletion appears to be somewhat redundant in cooperation with oncogenic N-Ras^{lys61} expression in melanocytes *in vivo* and therefore, clearly PTEN loss functions differ from CDKN2A gene. Although when the role of whether PTEN loss

would cooperate with N-Ras^{lys61} was investigated further *in vitro* (see 3.7), the data demonstrated that PTEN and N-Ras would cooperate but melanocytes were still not immortalised. This would fit into a redundancy idea observed *in vivo* and the lack of a cutaneous melanocyte phenotype also prompted a test of whether microenvironment disruption via keratinocyte hyperplasia would affect melanocyte fate *in vivo* in a synergism that allowed N-Ras^{lys61} expressing melanocyte dysregulation to give a phenotype that resulted in melanoma (see 3.10 below).

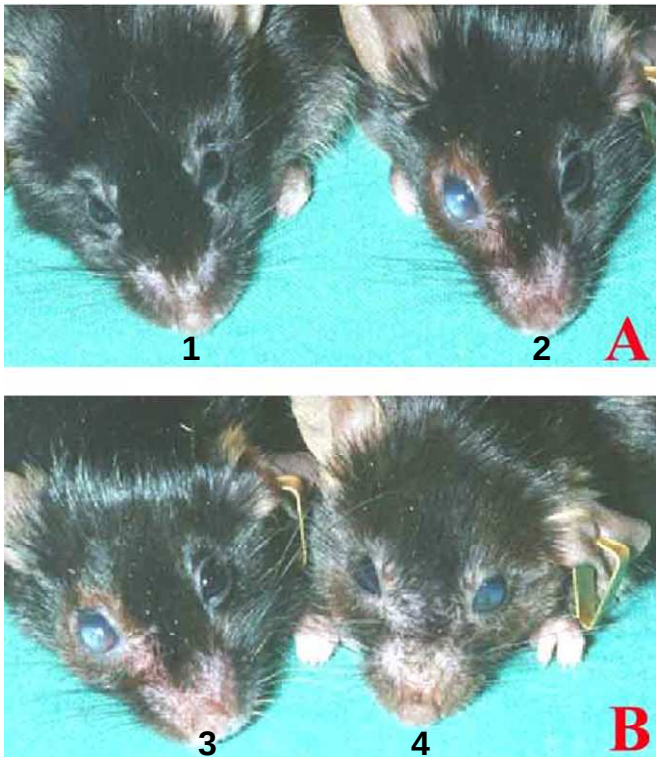

Figure 37: Presence of enlarged phenotypic eyes. Phenotypic eyes obtained in EICre/N-Ras^{lys61} and EICre/N-Ras^{lys61}/Δ5PTEN$^{flx/flx}$ mice following 12-15 months of systemic treatment of Ru486 (twice topical painting and once IP injection per week). Vehicle (ethanol painting and sesame seed oil injection) treated trigenic control mouse (mouse 1) remained normal while phenotypic eyes appeared in Ru486 treated bigenic and trigenic mice (left eyes of mice 2 and 3; right eye of mouse 4 which is mild compare to eyes of mice 2 and 3). The histology of formalin fixed phenotypic eyes was further assessed by pathologists in the Veterinary Pathology Department, Veterinary School, Glasgow University, who reported no evidence of melanoma, but the presence of corneal ulceration and mild hyperplasia in the RPE layer. However, the pathologists also reported harderian gland adenoma, an unexpected phenotype which turned out to be due to the expression characteristics of the EICre regulator transgene, which again relieved concerns over a lack of expression *in vivo* (468)(See below).

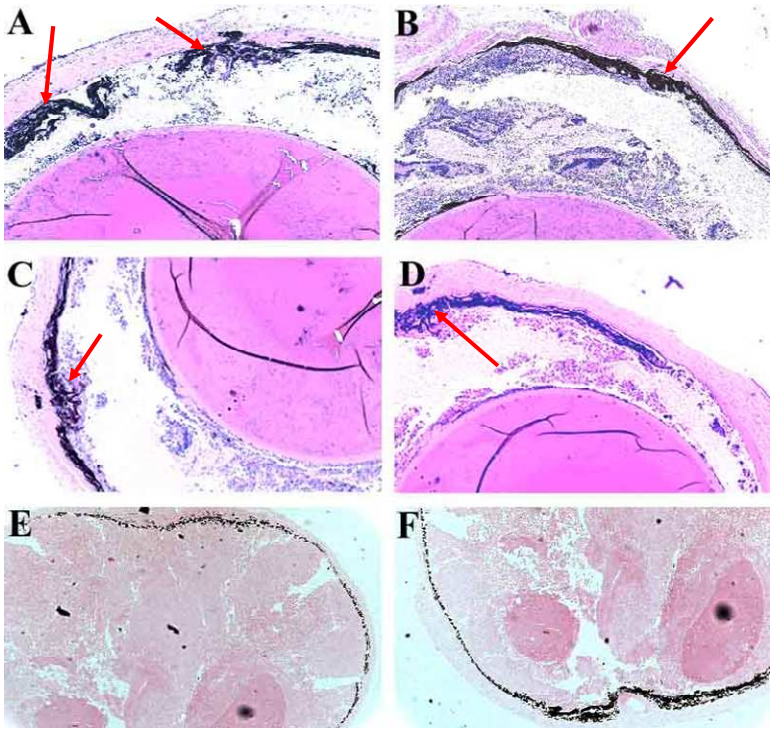

Figure 38: H & E staining of phenotypic EICre/N-Ras eyes (A-D) compared to normal controls (E, F) taken at the same magnification (50x). All phenotypic eyes displayed a larger size and a predominance of melanin (arrow) with a thicker RPE indicative of cellular hyperplasia. Abnormal folded neuroretinal and enlarged choroid were also observed in these phenotypic eyes (also see Fig 51 at section 4.4). The specimens were further checked by pathologists in Glasgow University who reported no evidence of melanoma, but the presence of corneal ulceration and mild hyperplasia in the RPE layer. The result simply exploited to confirm successful gene switch activity (N-Ras expression) following Ru486 treatment *in vivo* and we assume that N-Ras induced RPE hyperplasia which was absent in untreated or vehicle treated controls. This phenotype was not studied in further detail as it is not uveal melanoma but relieved concerns over whether the gene switch system was working *in vivo* and whether N-Ras was sufficiently expressed *in vivo* to give a phenotype.

3.8.1.2. Harderian gland adenoma

Employing similar tyrosinase transcriptional elements to express Cre and report alkaline phosphatase (AP) expression, Tonks *et al*, determined tissue specific Tyr-Cre transgene expression in embryonic cells and the fate maps revealed that the harderian gland had report gene activity (468). Due to the obvious eye bulge, when we harvested the enlarged eyes from those Ru486 treated EICre/N-Ras^{lys61} bigenic and EICre/N-Ras^{lys61}/Δ5PTEN$^{flx/flx}$ trigenic phenotypic mice, further dissection displayed another surprise unexpected phenotype ─enlarged harderian glands with a pathology diagnosed as adenoma by pathologists in Veterinary Pathology Department, Veterinary School, Glasgow University. The harderian glands obtained from the phenotypic mice were much bigger than the ones obtained from Ru486 treated wild type or vehicle treated transgenic mice, although the sizes of phenotypic harderian glands varied between individuals (Fig 39). H&E histological staining of both phenotypic and normal harderian glands also revealed that transverse sections of the phenotypic glands are much bigger than the normal, and possessed a significantly different histotype compared to normal under low magnification (Fig 40, 50x). Initially, under the low magnification, little histological difference was observed between normal and certain parts of phenotypic glands (Fig 40 B, 50x), but under the high magnification (100x for left panel and 200x for right panel) the differences between normal (Fig 41, A, B) and phenotypic glands (C-F) became obvious.

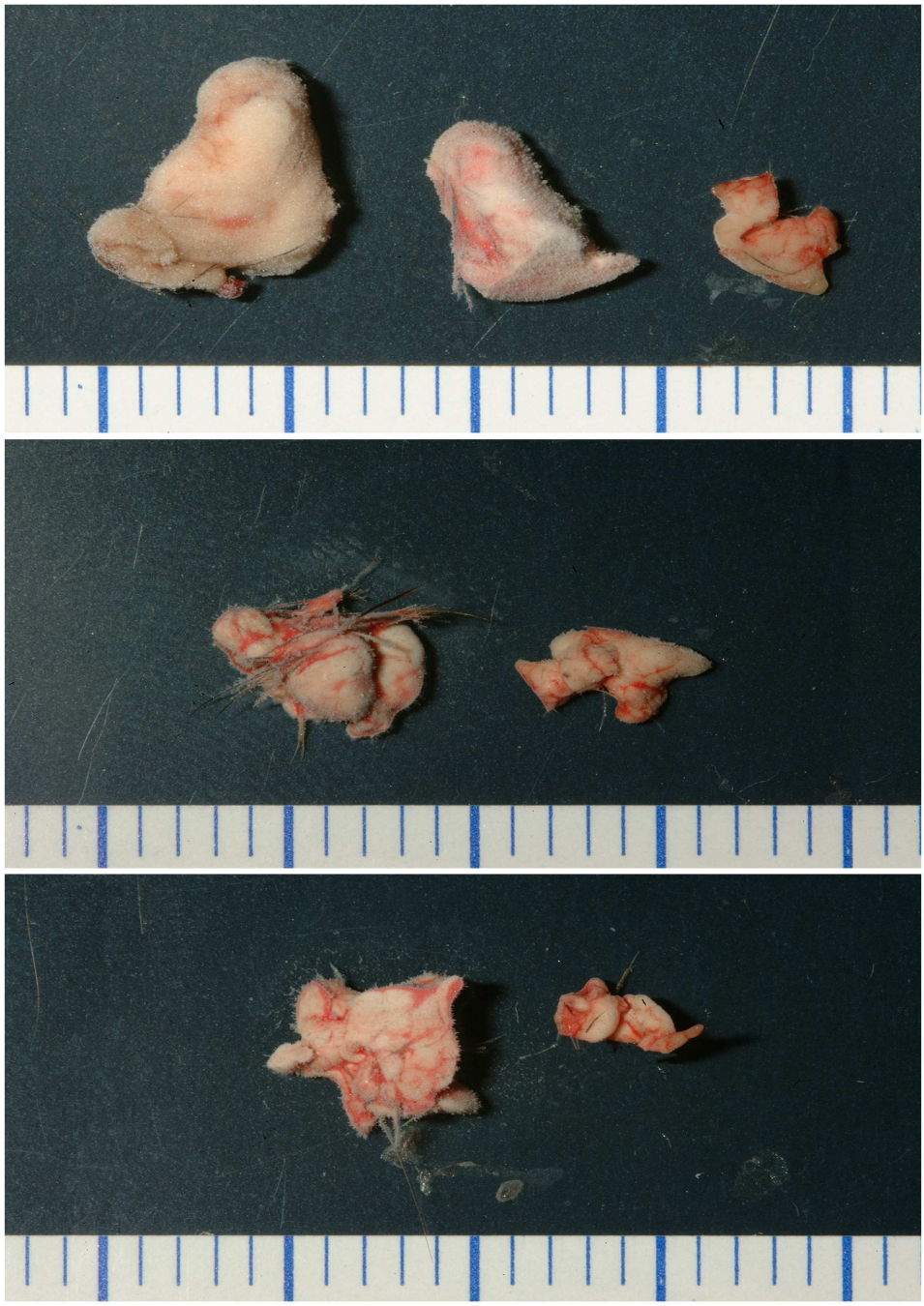

Figure 39: The size comparison of harderian glands between phenotypic mice and normal control mice. Harderian glands adenoma from Ru486 treated phenotypic bigenic EICre/N-Ras^{lys61} or EICre/N-Ras^{lys61}/PTEN$^{flx/flx}$ trigenic mice (left and middle in each panel) were of a much bigger size compared to wild type or vehicle treated bigenic mouse control (right in each panel).

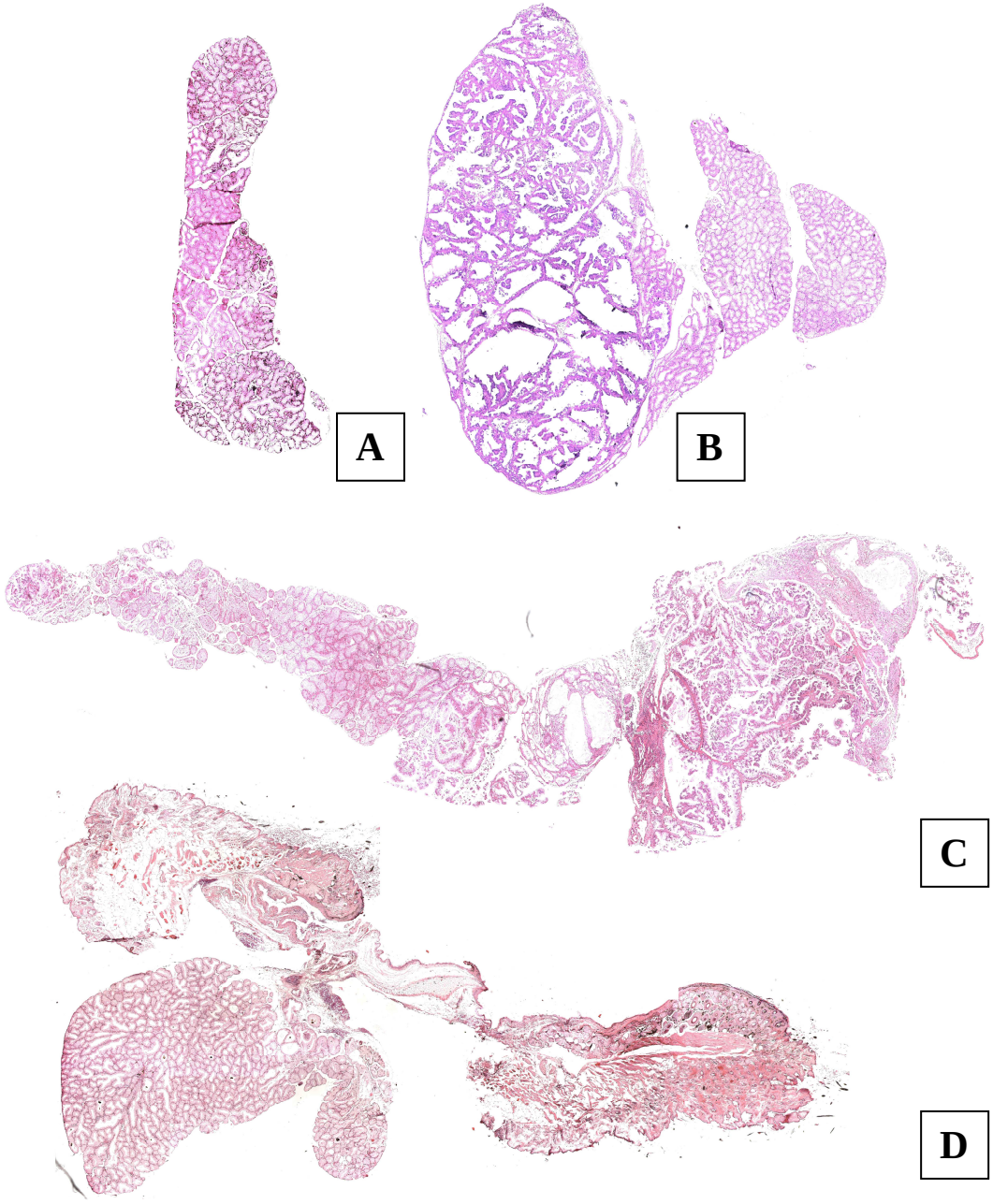

Figure 40: H&E staining of normal and phenotypic harderian glands. The transverse sections show the different sizes of harderian glands obtained from normal (A) and phenotypic (B-D) mice. The adenoma histology of phenotypic glands was also revealed in the larger phenotypic harderian glands under the low magnification (50x).

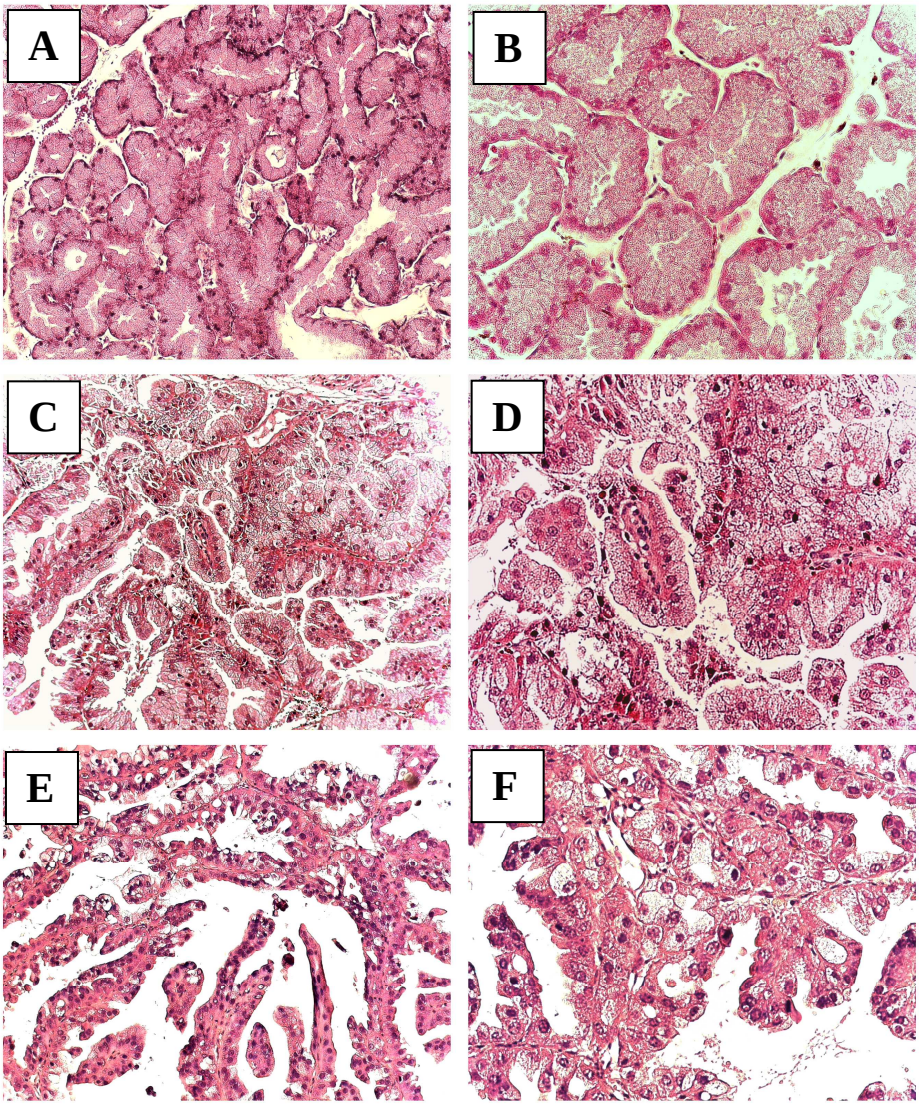

Figure 41: Higher magnification (100x for left panel A, C, E and 200x for right panel B, D, F) shows subtle differences between normal and phenotypic harderian glands. Compared to normal (A, B), significant structure difference was revealed in phenotypic glands (E, F). As shown on Fig 40 B, some parts of the phenotypic glands looked very similar to the normal gland under lower magnification (50x), however, an adenoma pathology was clearly indicated at higher magnification (C, 100x and D, 200x). This unexpected phenotype turned out to be due to the expression characteristics of the EICre regulator transgene as cited in the text that other groups reported harderian expression of this promoter (468). Thus these phenotypes were not studied in further detail but again simply exploited to confirm successful gene switch activity following Ru486 treatment *in vivo* and relieved concerns over a lack of expression *in vivo* as we assume that N-Ras induced harderian gland adenomas which were absent in untreated or vehicle treated controls.

3.8.2. Phenotype II-white hair and hair loss: An unexpected apoptotic phenotype

With time, collectively each logical stepwise analysis of the technical components of the model and troubleshooting both *in vitro* and *in vivo* began to clearly indicate that firstly transgene construction was correct; the transgenes eventually had biological activities *in vivo* and *in vitro*, N-Ras^{lys61} expression and PTEN loss transformed but did not immortalise primary melanocytes. Thus, the *in vivo* model was more closely examined and it became clear that what was originally assumed to be an artifact of plucking C57BL6 mice was in fact a real, but very subtle phenotype; i.e. the production of white hairs following treatment giving a more grey appearance to the treated site, and a premature (slight) greying to the overall coat colour in the long-term treated bigenic mice.

One aspect of activated Ras is that normal cells do not generally tolerate its expression well. Thus, deregulated or activated oncogenic Ras signalling can induce apoptosis *in vitro* through a caspase-independent pathway if the pro-apoptotic pathway overcomes anti-apoptotic mechanisms when the oncogenic Ras form is expressed and this effects the balance of cell fate determination (473;474). Following 12-15 months continuous systemic treatment, other than phenotypic eyes and harderian gland adenomas, it became clear that another phenotype of white hair and moderate hair loss was consistently observed in treated EICre/N-Ras^{lys61}, EICre/Δ5PTEN$^{flx/flx}$ and EICre/N-Ras^{lys61}/Δ5PTEN$^{flx/flx}$ mice separate to the general greying of the fur observed in older mice, such that younger individuals appeared older.

Given the well characterise apoptotic response to Ras activation *in vitro*, this result suggested that this subtle phenotype was due to the apoptosis of melanocytes induced in hair follicles by N-Ras^{lys61} expression in EICre/N-Ras^{lys61} mice. A very similar phenotype of white hair and hair loss was also observed following PTEN loss, and while TSG PTEN loss would suggest a reduction in apoptotic capacity via AKT up-regulation, this TSG plays

a multifunctional role in melanocyte and thus it appears that the loss of PTEN functions also resulted in melanocyte apoptosis in EICre/Δ5PTEN$^{flx/flx}$. Hence this apoptosis maybe a possible common pathway induced as a compensatory response to loss of Δ5PTEN$^{flx/flx}$ function as well to expression of mutant N-Ras^{lys61} in N-Ras^{lys61}/Δ5PTEN$^{flx/flx}$ mice, their lack of cooperation to overcome this response indicates that a redundancy may exist between TSG PTEN loss and N-Ras^{lys61} activation in melanocyte. If so this result would be an important finding, as it was known that Ras activation can induce an apoptotic response *in vitro* (473;474).

In such phenotypic mice, the dorsal hairs at treated sites re-grew as white un-pigmented shafts, as did the hair on back, sides or belly presumably due to Ru486 run off or IP injection, while age matched control mice remained normal. In addition these mice also began to exhibit hair loss starting during the 5th to 6th hair plucking cycle. On the back, hair loss is limited within the painting area although hair loss on sides and belly where are not the Ru486 treatment areas —however, Ru486 could be delivered to these areas by mice themselves scratching and by IP injection. The white hair was initially observed at only a few independent sites which sat among mostly black hairs and started to appear as early as at the 2nd hair plucking cycle (Fig 42) when the control cohorts remained normal. Indeed, control mice occasionally presented a few white hairs when at age of >6 months but they appeared randomly and the number of white hairs and the area they presented are markedly less than those presented in treated transgenic mice; as shown in Fig 42. To confirm this idea, skin biopsies were taken from white hair growth areas and compared with skin samples taken from hair growth normal mice. TRP2 staining, to identify melanocyte, revealed that there were more melanocyte-containing follicles in normal skin than in skins taken from Ru486-treated transgenic mice, a result consistent with appearance of white hair areas (Fig 43).

Figure 42: White hair or hair loss appeared in N-Ras^{lys61} expressing and/or PTEN functional loss transgenic mice. EICre/N-Ras^{lys61}, EICre/Δ5PTEN$^{flx/flx}$ and EICre/N-Ras^{lys61}/Δ5PTEN$^{flx/flx}$ mice gave white hair or lost hair (left mouse in both A and B) phenotypes following 7-8 month on procedure while the age-matched controls (right mouse in both A and B) hair growth remained quite normal.

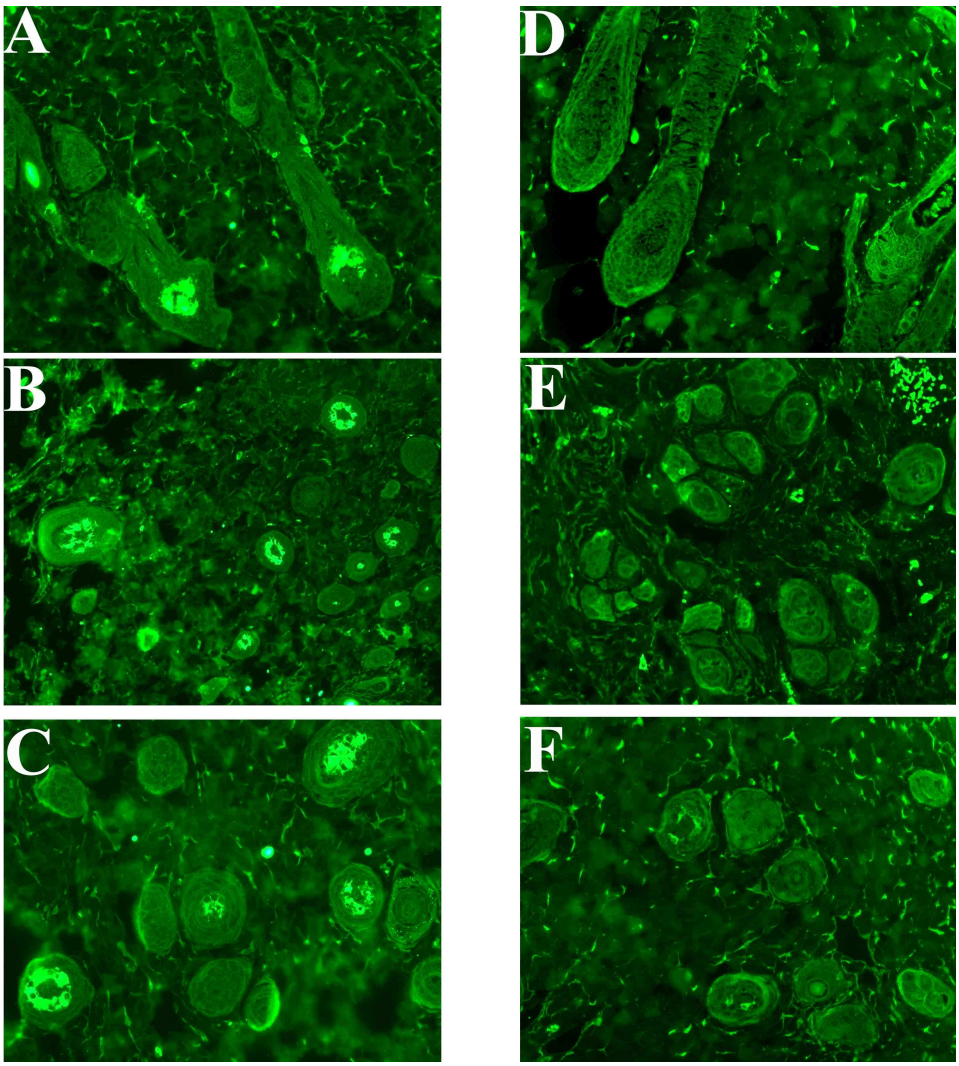

Figure 43: Different number of melanocytes and melanocyte-containing follicles between normal skins (A-C) and white hair/hair loss skins (D-F). Obvious melanocytes (green) reduction and melanocyte-containing follicles were observed in biopsies of skins taken from white hair/hair loss (D-F) mice while more melanocytes and a larger portion of melanocyte-containing follicles detected in control skins (A-C) employing immunostaining of melanocyte specific marker TRP2. Skin biopsies were taken at day 10 post-plucking when maximum melanocytes obtained as previously revealed. As seen in the figure, either vertical cut (A vs. D) or horizontal cut (B, C vs. E, F) sections possessed more melanocytes and more melanocyte-containing follicles in normal skins than in white hair/hair loss mouse skins. At least 5 separate fields from 5 separate transgenic biopsies taken 10 day post plucking and Ru486 or vehicle treatment presented these same features of reduced melanocytes as well reduced melanocyte-containing follicles in treated bigenic mice. See Fig 44 also.

3.9. Melanocytes loss in EICre/N-Ras^{lys61} and EICre/N-Ras^{lys61}/PTEN$^{flx/flx}$ mice via caspase-3 mediated premature apoptosis

Given that Ras expression can induced cell apoptosis *in vitro* (473;474), N-Ras^{lys61} expression in melanocyte *in vivo*, specifically at the low level initially induced by the gene switch, may cause apoptosis via a shift in the balance of pro-apoptotic and anti-apoptotic pathways in anagen and catagen, and thus negating melanoma formation. Therefore to investigate whether melanocyte apoptosis was induced by N-Ras^{lys61} expression and played a role in the failure of melanoma formation in EICre/N-Ras^{lys61} and whether a compensatory pathway of anti-PTEN loss resulted in the failure to promote N-Ras tumourigenesis in EICre/N-Ras^{lys61}/PTEN$^{flx/flx}$ mice, melanocyte growth in different genotypic mice were analysed *in vivo*. Anagen follicles were obtained by plucking back hair to initiate hair cycle followed by Ru486 treatment to induce N-Ras^{lys61} expression and inactivate PTEN function. The numbers of anagen follicles was assessed for melanocytes as in Fig. 44 via TRP2 expression and apoptosis analysed via immunostaining for active caspase-3 expression patterns in the different genotypes.

3.9.1. Reduced numbers of melanocytes

Following hair plucking and Ru486 topical treatment, skin biopsies were taken at different time points to monitor melanocyte growth by immunofluorescence analysis of TRP2 as defined before. Skin biopsy samples were embedded in paraffin and sections cut and stained for TRP2 (green) and the numbers of TRP2 positive (melanocyte) hair follicles counted. The results (Table 4 and Fig 44) revealed that at the time of plucking among all of genotypes, few melanocyte positive follicles were in the telogen phase. As always, the follicles harbouring growing melanocytes increased gradually to reach a peak at day 7-10 post plucking, which confirmed the results of experiments performed in Fig 26.

However, the trend of melanocyte disappearance in hair follicles following Ru486

treatment was different between genotypes. In normal wild type C57BL6 and N-Ras^{lys61} monogenic mice, the peak of the number of follicles which express Trp2 melanocyte extended to 14 days post-plucking by which time most, if not all, melanocytes had disappeared in EICre/N-Ras^{lys61}, EICre/Δ5PTEN$^{flx/flx}$ and EICre/N-Ras^{lys61}/Δ5PTEN$^{flx/flx}$ mice (pictures not shown because they are almost identical to that of EICre/N-Ras^{lys61}). There was no detectable melanocyte in any genotypes at the end time point (21 days post-plucking) of the experiment.

One interesting observation was that the peak time of melanocyte growth initiated by hair plucking appeared later in PTEN loss mice (EICre/Δ5PTEN$^{flx/flx}$) than in other genotypic mice (day 10 vs. day 7), although analysis was not carried at day 0 and day 3 due to the source shortage. Moreover, the percentage of melanocytes (1/3) stained follicles is less than others (1/2) when the maximum melanocytes obtained and the peak time is shorter (only at day 10) than others.

These observations are not in agreement with the previous results in which PTEN loss enhanced stem cell growth rate and proliferation *in vitro* (reviewed in (475)). However it appears in this context that possibly being the compensatory pathway of anti-PTEN loss in melanocyte *in vivo* in the same pathway as N-Ras based on their redundancy, the same apoptosis happens to protect the individual from developing deadly melanoma.

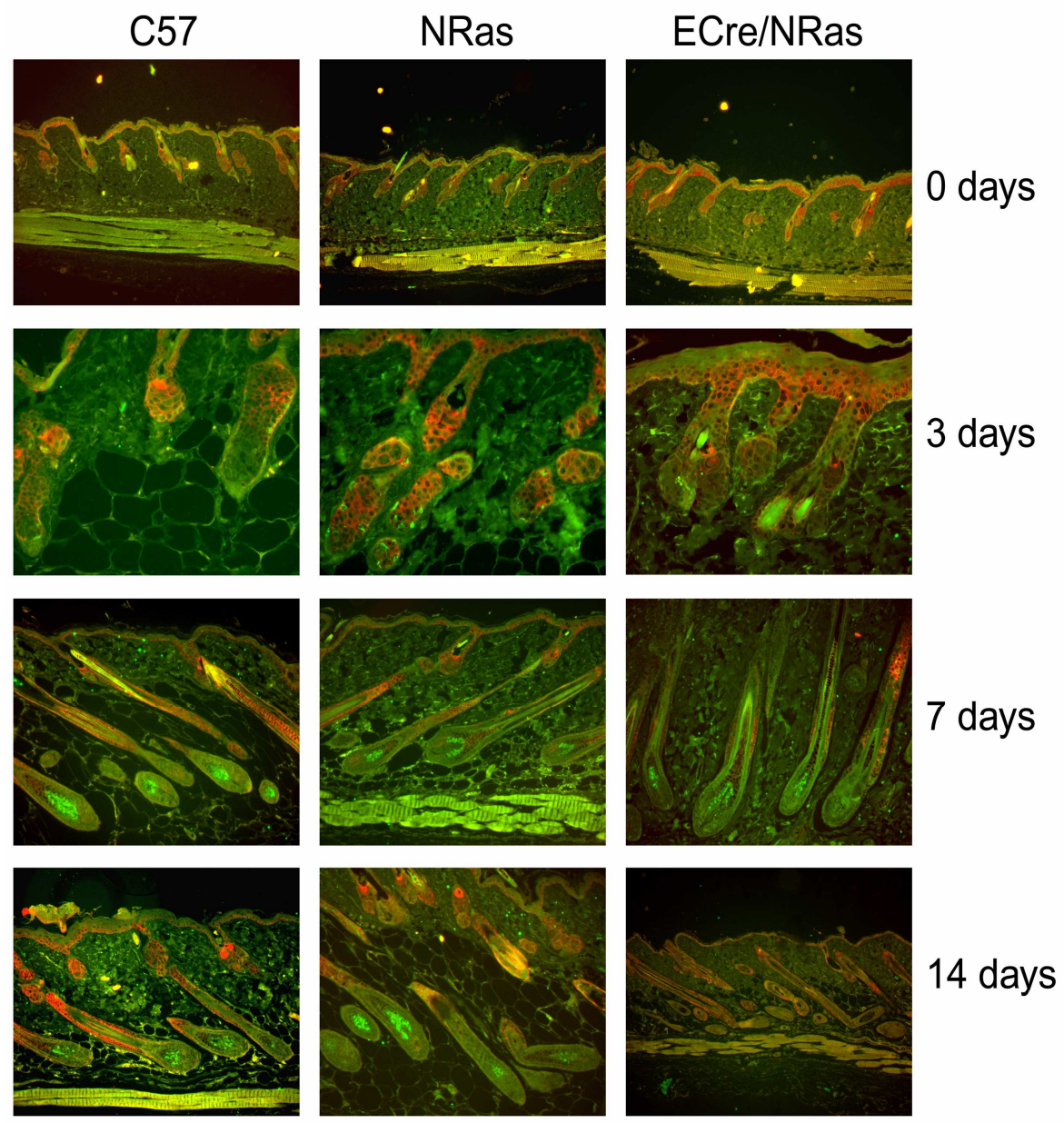

Figure 44: *In vivo* melanocyte growth in different mouse genotypes. Anagen was induced by plucking, followed by Ru486 treatment to activate target gene expression. Skin biopsies from plucked/Ru486 treated areas were taken at different time points and subjected to immunofluorescence analysis for melanocyte specific TRP2 expression (green). All 0 days photographs and the photograph of EICre/N-Ras^{lys61} at 14 days were taken at 50x to show as many follicles as possible, while others were taken at 100x to show reduced numbers of melanocytes in treated vs. normal skin. These were quantitated in Table 4. Figures of 21 days post-plucking are not shown because all are in catagen where no melanocyte is detected.

Table 4: Ratio of melanocyte-containing follicles/total follicles at different time points following hair plucking (days) and Ru486 treatment. As shown in IF micrograph (Fig 44) each section counted was oriented and cut to show the full length of each follicle, regardless of stage and not squint cut where the melanocyte-containing bulb regions may be lost. The data are the average numbers from 3 different mice where 3 separate fields of 3 separate sections were observed via immunofluorescence microscope at magnification of 50x (Fig 44).

	0	1	3	7	10	14	21
C57	7/43	5/53	3/45	29/59	40/72	33/72	0
N-Ras^{lys61}	0/42	0/53	12/33	10/43	35/52	22/54	0
EICre/ Δ5PTEN$^{flx/flx}$	na	2/43	na	3/44	17/61	4/62	0
EICre/ N-Ras^{lys61}	1/44	0/58	58/91	29/61	27/71	0/78	0
EICre/N-Ras^{lys61}/Δ5PTEN$^{flx/flx}$	0/35	6/58	24/54	32/78	1/64	0/65	0

3.9.2. Melanocytes under go a caspase-3 mediated apoptosis

Investigations revealed that in treated N-Ras^{lys61} and Δ5PTEN expressing mice there were fewer hair follicles bearing melanocytes than in age matched control mice. This suggested that expression of activated N-Ras^{lys61} and/or PTEN loss induced an apoptotic response in melanocyte consistent with the growth of white hair and earlier *in vitro* studies where activated Ras was shown to induce apoptosis (473;474). To address this question and determine whether melanocyte undergo apoptosis *in vivo* through a caspase-dependent pathway, immuno-staining for the cleaved, active form of caspase-3/9 was performed, using K14 expression as a counterstain to delineate keratinocytes from melanocytes (Fig 45). In control mice, 14 days post plucking, only a single caspase-3 positive melanocyte was observed (Fig 45 A), whereas in all Ru486 treated bi- or tri-transgenic genotypes analysed, caspase-3 expressing melanocytes were detected in numerous follicles (B: EICre/N-Ras^{lys61}; C, D: EICre/Δ5PTEN$^{flx/flx}$ and E, F: EICre/N-Ras^{lys61}/Δ5PTEN$^{flx/flx}$). Typically mice expressing N-Ras^{lys61} and/or Δ5PTEN exhibited more than 10 hair follicles with various numbers of caspase-3 expressing melanocytes throughout a section. However, it was noted that while N-Ras^{lys61} or Δ5PTEN expression gave more caspase-3 positive melanocytes than wild type controls, the number of caspase-3 expressing follicles was not additive in trigenic EICre/N-Ras^{lys61}/Δ5PTEN$^{flx/flx}$ mice. Hence, PTEN loss apparently induced a similar mechanism of caspase-3 mediated apoptosis to that of N-Ras, which suggests a redundancy in their oncogenic functions despite the result *in vitro* co-expression was synergistic although unable to achieve immortality (see above section 3.7 and Discussion).

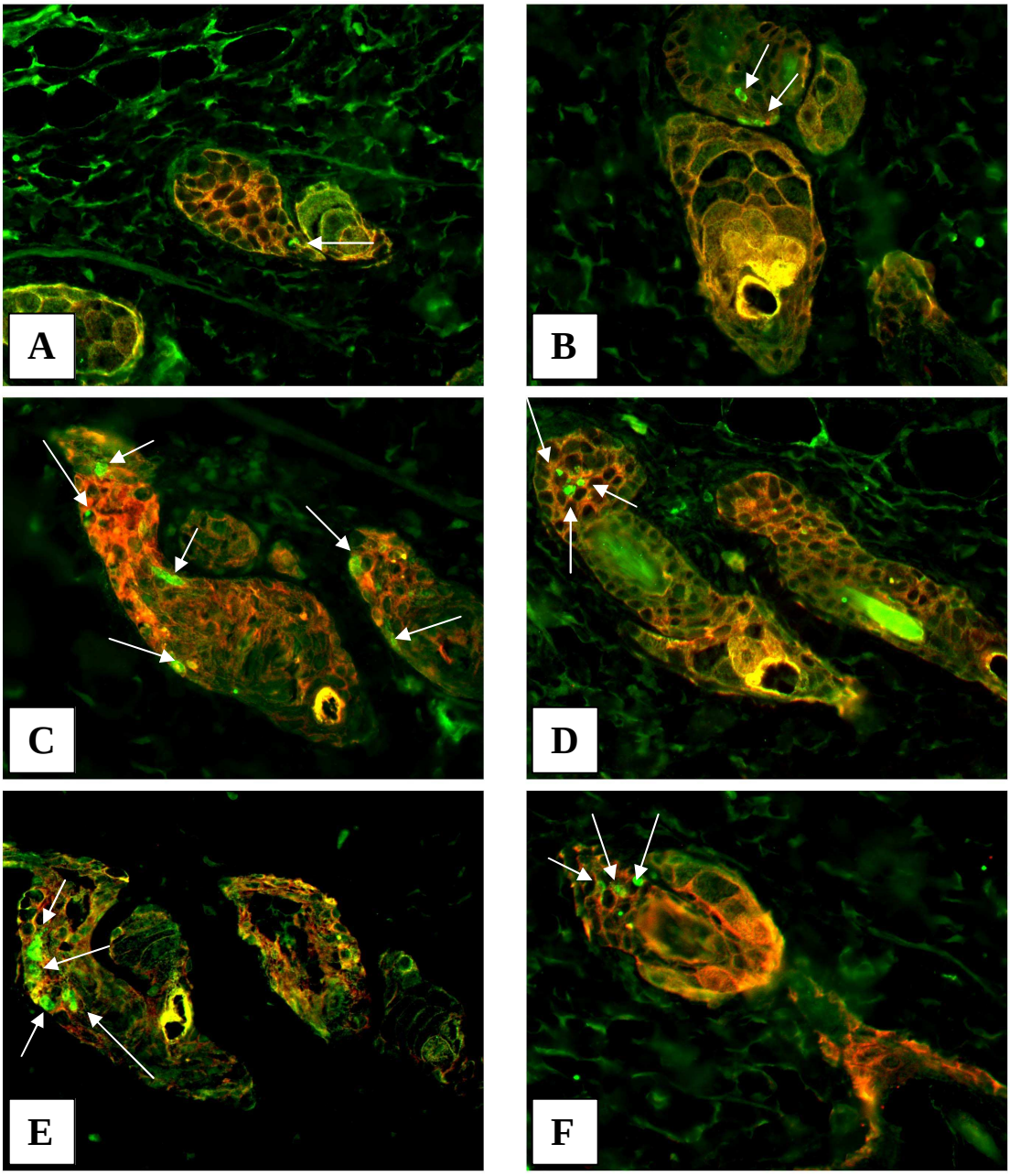

Figure 45: Analysis of Caspase-3 expression in hair follicles. Double-label staining for caspase-3 (green) and K14 (red) expression in skin biopsies to investigate potential melanocyte apoptosis at day 14 post plucking, shows increased caspase-3 expression in N-Ras^{lys61} and/or PTEN^{null} mouse skin vs. wild type skin at sites of melanocyte locations. Although not directly labelled for melanocyte markers, this location, cell shape and dendrites as well the lack of K14 expression suggest that these cells were not keratinocytes but melanocytes under going apoptosis. A: C57BL6 mice; B: EICre/N-Ras^{lys61}; C-D: EICre/Δ5PTEN$^{flx/flx}$; E-F: EICre/N-Ras^{lys61}/Δ5PTEN$^{flx/flx}$. All photographs were taken at 400x.

3.10. Effects of the microenvironment on inducible melanoma model generation: Melanocyte survival during papillomagenesis

Keratinocytes can secrete numerous regulatory factors to control melanocyte development as well as to play potential roles in melanoma formation (470). Thus, it is thought that keratinocytes exert significant control over the regulation of melanocyte physiology and failure of this regulation by keratinocytes may contribute to melanoma formation (465;476). Further, it is well known that the microenvironment can influence melanoma aetiology, as observed in several models e.g. transgenic HGF/SF overexpression where melanoma formation was accompanied by epidermal hyperplasia in neonates (40). Indeed, many transgenic mouse models of melanoma are accompanied by keratinocyte hyperplasia at early stages (216;217;221). Therefore, to assess whether N-Ras^{lys61} expression and PTEN functional loss would produce melanoma if the microenvironment was disrupted and to test this seed/soil hypothesis (471), a K14Cre regulator was introduced into the model to express these inducible mutations in keratinocytes. Previously this was employed to assess H-Ras cooperation with PTEN loss in carcinogenesis, which induced epidermal hyperplasia and formation of benign squamous cell papillomas (246). In this model, induction of epidermal hyperplasia by N-Ras^{lys61} and PTEN loss in keratinocytes did not produce melanoma or melanocyte hyperplasia. Instead in a fascinating result, expression of mutant N-Ras and functional loss of PTEN in both melanocytes and keratinocytes produced pigmented papillomas. Thus, it now appears that in the hyperplastic environment of papillomagenesis, melanocytes did not undergo this N-Ras- or PTEN^{null}-induced apoptosis or the normal programmed apoptosis of catagen, but rather these melanocytes acquired a survival potential.

The K14Cre transgenic regulator strain was introduced into EICre/N-Ras^{lys61}/Δ5PTEN$^{flx/flx}$ mice to generate a tetragenic line K14Cre/EICre/N-Ras^{lys61}/Δ5PTEN$^{flx/flx}$ in which both keratinocytes and melanocytes expressed N-Ras^{lys61} and functional PTEN loss following

Ru486 treatment. K14Cre/N-Ras^{lys61}/Δ5PTEN$^{flx/flx}$ mice produced similar hyperplasia results to H-Ras cooperation with Δ5PTEN (246), e.g. PTEN loss promoted N-Ras^{lys61} initiated tumourigenesis to induce hyperplastic skin and given the disruption to follicular keratinocytes alongside N-Ras^{lys61} activation and PTEN ablation in melanocytes, pigmented tumours were produced (Fig 46a). However despite their overt pigmented appearance, histological analysis (Fig 46b) confirmed that these lesions were pigmented papillomas, not melanomas or nevi. These tumours possessed typical squamous cell papilloma pathology, where in each case darkly staining melanocytes can be observed (Fig 46b, A-B) with occasional clusters (Fig 46b, B and D). The majority of melanocytes appeared to be restricted in the proliferative basal layers at higher magnification (Fig 46, C), a result consistent with the requirement for proliferative keratinocytes as feeders *in vitro* melanocyte culture and with immunofluorescence analysis of TRP2 expression in Fig 47.

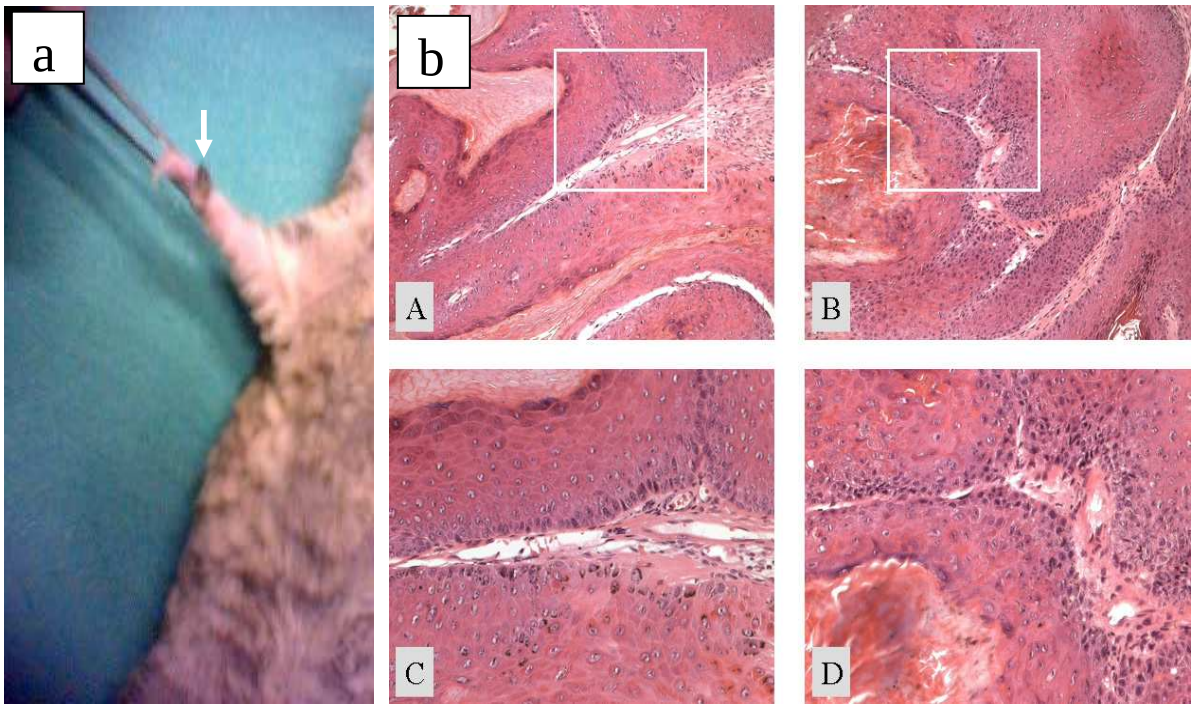

Figure 46: Macroscopic and histological appearance of pigmented papillomas. (a) Following Ru486 treatment, tetragenic K14Cre/EICre/N-Ras^{lys61}/Δ5PTEN$^{flx/flx}$ mice exhibit tiny pigmented tumours as on the media aspect of the carpus (arrow); (b) Histology of pigmented tumours from Ru486 treated K14Cre/EICre/N-Ras^{lys61}/PTEN$^{flx/flx}$ compound mice 9909 (A) and 9912 (B) possess a typical squamous cell papilloma pathology with the tumour in 9912 exhibiting a slightly more aggressive histotype. In each case, darkly staining melanocytes can be observed and at higher magnification of the boxed areas, (C) shows the majority of melanocytes appeared in the basal layer, whilst (D) shows the occasional cluster of darkly staining melanocytes. These histotypes are consistent with the results of immunofluorescence analysis of TRP2 expression to detect melanocytes in these papillomas (Fig 47).

As outlined above in melanocytes, N-Ras^{lys61} expression and PTEN functional loss lacked the strength to overcome cell's sentinel mechanism to initiate tumourigenesis. This failure to obtain a neoplastic phenotype may have derived from the inducible approach taken, where the skin developed normally into adulthood. Whereas in previous models developmental expression/deletion of transgene may prevent the retention of this kind of sentinel response in adults.

However, in this new approach on incorporation of follicular keratinocyte hyperplasia, this did not occur in these compound mice. Thus to investigate melanocyte survival in the aetiology of these pigmented papillomas further, the Kit/SCF signalling pathway was analysed. The Kit/SCF signalling system has been shown to be very important for normal melanocyte development and proved to be a survival factor that defined the melanocyte stem cell niche (53). Further, the migration of melanoblast from murine epidermis to the hair follicle in neonates is controlled by SCF expression in follicular keratinocytes (60), and in the development of melanoma Kit expression was undetectable or was significant reduced, allowing for overgrowth and invasion, or possibly a reversion to a stem cell phenotype (53;273;274;293;294). Thus Kit/SCF expression and co-localization of Kit with melanocytes were analysed in pigmented papillomas elicited in K14Cre/EICre/N-Ras^{lys61}/Δ5PTEN$^{flx/flx}$ to investigate a role in the survival of pigmented papilloma melanocytes.

3.10.1. Pigmented papilloma aetiology: Melanocyte localization

In immuno-double staining, pigmented papillomas (Fig. 46) were analysed (Fig 47) for TRP2 (green) and K14 (red), together with differentiation marker keratin 1 (K1, red), as its super-basal expression pattern helped delineate the basal from suprabasal layers for melanocyte location, and also indicated that the tumours were benign papillomas, as typically up to 100% of squamous cell carcinomas lose K1 expression on conversion to malignancy in many murine carcinogenesis studies (477;478), with the notable exception of novel K1 retention in TPA promoted c-Ras/PTEN^{null} carcinomas (246), where progression proceeded independently of Ras expression.

The patterns of TRP2 staining indicated that PTEN loss in addition to N-Ras^{lys61} expression confirmed the histological analysis that the tumours were not melanomas but pigmented papillomas, in which TRP2 expressing melanocytes survived the apoptosis of normal catagen and of N-Ras expression as well PTEN loss induced during papillomagenesis. Comparing the patterns of TRP2 expression (Fig 47) in pigmented papillomas and hyperplastic skins against normal skin with anagen stage follicles, the results demonstrated that melanocytes remained detectable and restricted to the hair follicle of normal and hyperplastic skins following hair plucking (A-C) until the papillomagenesis stage when the hair follicles degraded (D-F). In an untreated normal (A) and hyperplasia (B, C) skins of K14Cre/EICre/N-Ras^{lys61}/Δ5PTEN$^{flx/flx}$ mice, melanocytes were still confined to hair follicle in samples taken at the anagen (5-7 days after plucking), before the melanocytes disappeared (7-10 days in Ru486 treated EICre/N-Ras^{lys61}/Δ5PTEN$^{flx/flx}$ vs. 14-21 days post-plucking in normal, see table 4). In contrast, papillomas induced in K14Cre/EICre/N-Ras^{lys61}/Δ5PTEN$^{flx/flx}$ mice (D-F) show that melanocytes successfully escaped apoptosis induced by N-Ras^{lys61} expression and/or PTEN loss in melanoblasts/melanocytes, to survive and proliferate leading to a sub-set of pigmented papillomas during the papillomagenesis resulting from N-Ras^{lys61} expression and PTEN function loss in

keratinocytes.

Interestingly two most common patterns of melanocytes were detected in pigmented papillomas: the cluster formation (D) and the more common streaks of melanocyte confined to the K1 negative (E)/K14 positive (F) basal layer. Thus, these results revealed that melanoblasts/melanocytes survived within the proliferative K14 stained basal cells, which proved to be consistent with the later finding of basal keratinocyte expression of SCF creating a paracrine survival loop with Kit (below).

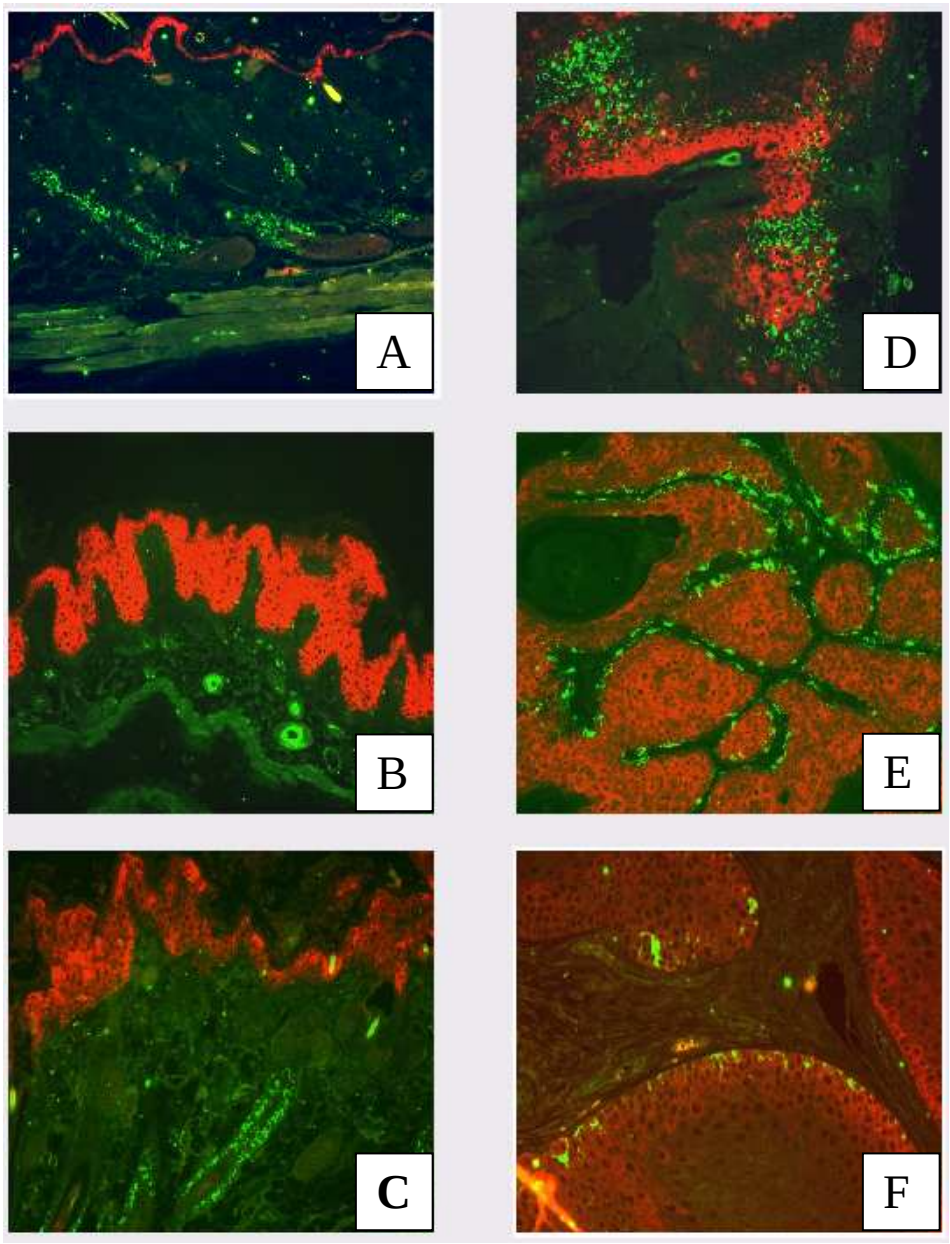

Figure 47: Melanocytes location in normal skin, hyperplastic skin and pigmented papillomas. Localization of melanocytes via TRP2 (green) immunofluorescence in vehicle treated skin (A) or Ru486 treatment elicited hyperplastic skin (B, C) and papillomas (D-F) in K14Cre/EICre/N-Ras^{lys61}/PTEN$^{flx/flx}$ mice. D-F are squamous cell papillomas because they express K1 (early differentiation maker which is lost on conversion to malignancy) nor do these benign tumours express K13 (a simple keratin employed as a marker of progression which appears sporadically in benign papillomas and uniform in carcinomas (data not shown) (477;478)). K1 (red) was used for counterstain in A-E confirming their benign papilloma status in D & E, while K14 (red) was used in F for basal layer location purpose. Photographs were taken at 100x magnification except 400x for F.

3.10.2. Pigmented papilloma aetiology: Immunofluorescence analysis indicates a paracrine melanocyte survival loop established by intrinsic Kit expression and extrinsic keratinocyte SCF secretion

Given melanocyte survival following the anagen stage and proliferation in pigmented papillomas, coupled to the important roles of the Kit/SCF for melanocyte physiology and melanoma development (53), Kit and SCF expression during papillomagenesis development was determined via immunofluorescence. Initially, Kit (green) expression was performed (Fig 48) in pigmented papillomas against normal newborn and H-Ras expressing newborn hyperplastic skin (246), employing keratin K14 as a counterstain to delineate the epidermis and appendages.

In normal newborn (24 hours) skin, Kit expression was mainly detected in the developing hair follicle with sporadic expression in a subpopulation of basal cells (A). In H-Ras hyperplastic newborn skin, Kit expression was detectable in most layers of the epidermis and hair follicles, with interfollicular basal cells retaining an expression level as strong as in the follicles (B). In all pigmented papillomas (C-F), Kit expression levels was elevated significantly even compared to the hyperplasia, and strongly expressed throughout the proliferative epidermal areas of the expanded basal layers, and less so in the differentiated stratified layers although still detectable, as confirmed at higher magnification (E 100x; F, 200x), where Kit expression in basal layer was higher than in other areas.

The results implied that if papillomagenesis occurred alongside the anagen stage of hair follicles, the proliferative melanocytes survived by expressing Kit (receptor) to receive survival signals (e.g. Kit ligand SCF) from disrupted microenvironmental keratinocytes and suggests therefore, that a Kit/SCF related cell survival/proliferation signalling pathway overcome pro-apoptotic pathway of catagen or that induced by N-Ras^{lys61} expression and/or PTEN loss in melanocytes, to result in melanocytes escaping from apoptosis. Surviving

melanocytes may further proliferate to produce more progeny due to this active Kit/SCF loop and this idea was investigated by assessing expression of the SCF (Kit ligand) keratinocytes and melanocytes.

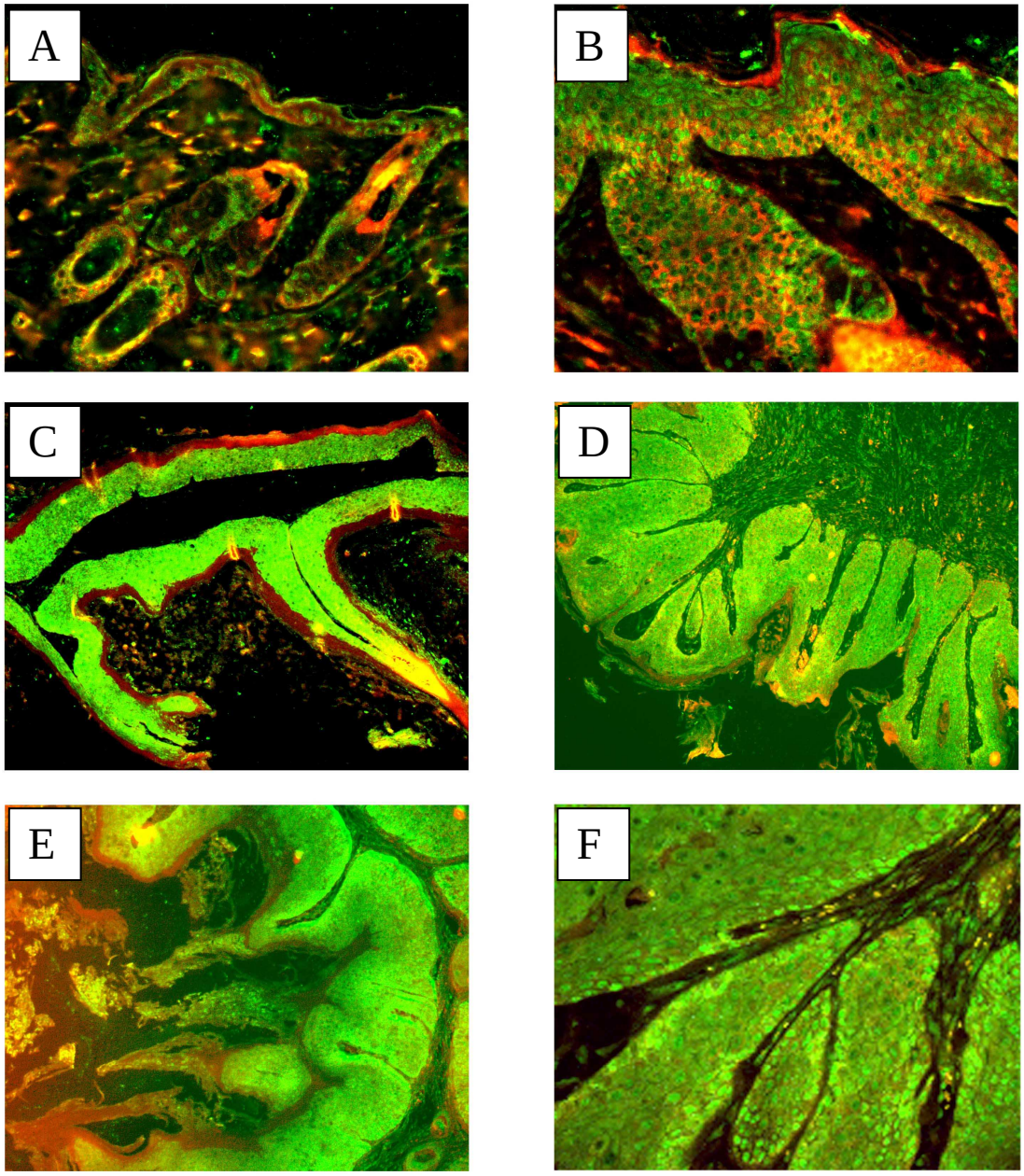

Figure 48: Kit expression in normal skin, hyperplastic skin and papillomas. Kit expression (green) levels elevated in pigmented papillomas elicited in K14Cre/EICre/N-Ras^{lys61}/Δ5PTEN$^{flx/flx}$ mice. A: normal new born skin (100x); B: transformed (H-Ras) hyperplastic new born skin (100x) and C-F: pigmented papillomas show significant elevation of Kit expression (C and D, 50x) and stronger Kit expression in basal layer (E, 100x; F, 200x) than other parts of epidermis. K14 (red) was used for counterstain.

3.10.3. SCF expression by basal cell keratinoyte acts as a survival loop

TRP2 staining suggests that melanocytes survived in pigmented papillomas where/if tumourigenesis occurred at the anagen phase of hair follicles when a population of target melanocytes was available, and the elevated Kit expression in most cells of pigmented papillomas suggested that melanocytes survival may have been through the Kit/SCF paracrine loop. To investigate whether this was due to SCF secretion and released from keratinocytes because of the disruption of melanocytes microenvironment, which binds to Kit receptors on expressing melanocytes to allow survival, SCF (green) expression was performed in normal adult and normal newborn skin, which is naturally briefly hyperplastic for the first few days, as well as pigmented papillomas employing immuno-staining with K14 counterstain (red) (Fig 49).

The SCF expression pattern was very similar to Kit expression patterns, being detected mainly in hair follicles of normal skin, and also sporadic expression was detectable in outer root sheath keratinocytes, but only very little interfollicular epidermis SCF expression was observed (A). Similarly in new born skin which possesses a normal, mild hyperplasia (B), SCF expression level was elevated and strongest in hair follicles, with a few interfollicular epidermal keratinocytes exhibiting a relative higher level of SCF expression which was in contrast to normal skin. In papillomas in a similar fashion to melanocytes localization described at 3.9.1 via TRP2 immunofluorescence, again, two categories of SCF expression were observed: clusters and streaks respectively were demonstrated in all papillomas. In a striking result, under the low magnification (C and D, 50x) and SCF expression in papillomas was mainly localized in basal layers under the higher magnification (E, 200x and F, 400x), which is in a direct repeat of localization of melanocytes via marker TRP2 and the expression of Kit.

These results are consistent with the idea that secreted SCF by disrupted keratinocytes

supplied ligand to the Kit receptor expressed in melanoblasts/melanocytes at the anagen stage of hair follicles, and thus during subsequent papillomagenesis this Kit/SCF survival loop overcome pro-apoptotic pathways induced by N-Ras^{lys61} expression and/or PTEN function loss in melanocytes to result in melanocytes survival and proliferation. To verify these results, co-localization of Kit and TRP2 in melanocytes in those pigmented papillomas was identified below.

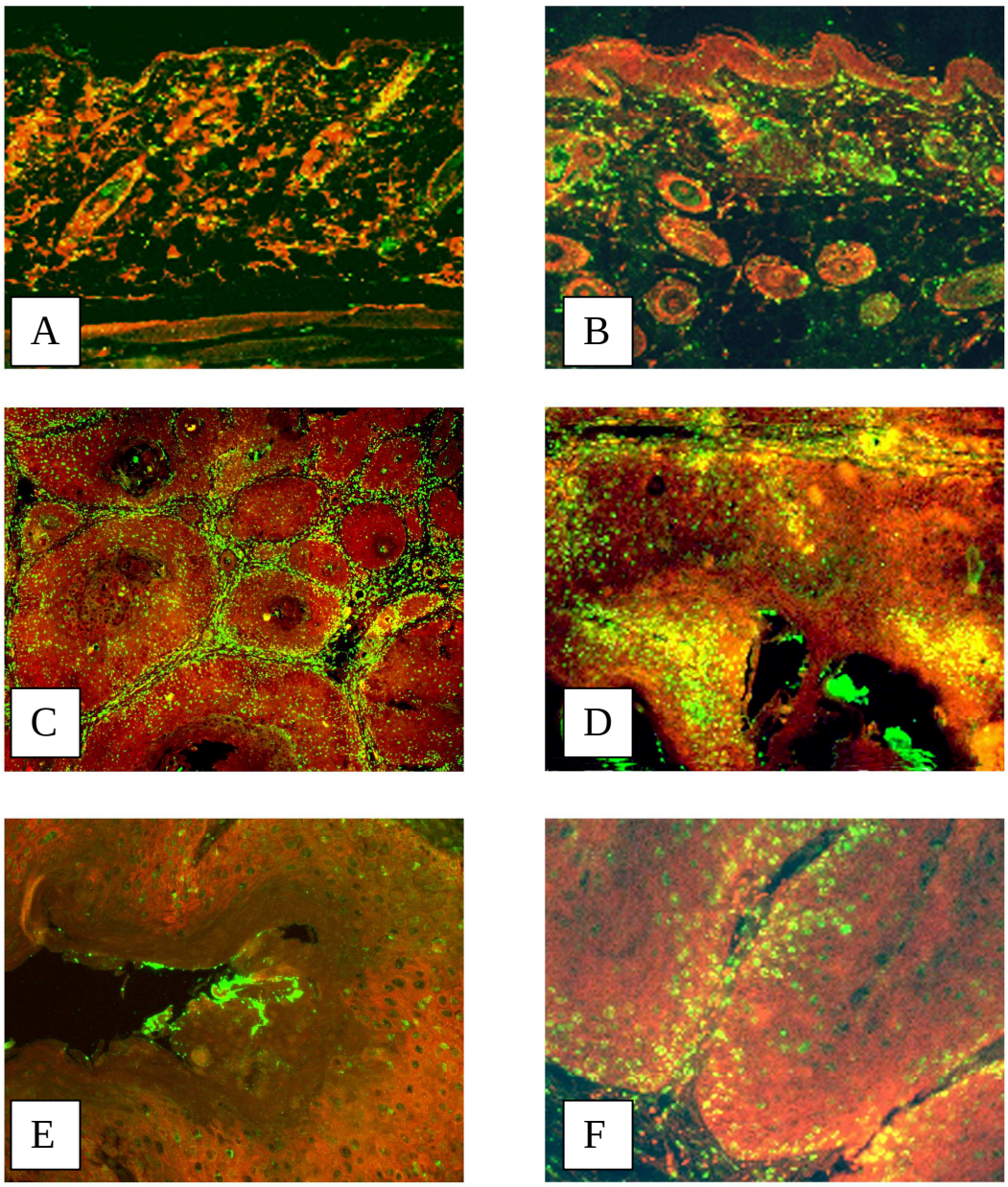

Figure 49: SCF expression in normal skin, hyperplastic skin and papillomas. SCF expression in normal adult and newborn skin and pigmented papillomas via double immunofluorescence staining of SCF (green) and K14 (red). SCF was detected in sporadic keratinocytes and in hair follicles of normal skin (A, 100x). In new born hyperplastic skin, focal SCF expression was detected in all layers, with the occasional streak in basal cells, whilst hair follicles retained the strongest expression (B, 100x). In contrast all papillomas investigated exhibited elevated strong expression (C-F) in two distinct categories. Under low magnification (50x), SCF expression was mostly observed in streaks (C) but occasional clusters of expression were observed (D). Higher magnification (E, 200x; F, 400x) demonstrates the localization of SCF in basal cell layer.

3.10.4. Localization of Kit expression in melanocytes

The results obtained from TRP2, Kit and SCF immuno-staining described above, suggested that melanoblasts/melanocytes survival in pigmented papillomas was a consequence event of keratinocytes disruption which secreted and released SCF signal to Kit expressing anagen stage melanocytes during papillomagenesis. To confirm if this was true and that Kit expression in melanocytes was able to receive this signal from the disrupted keratinocytes, the localization of Kit expression in melanocytes was performed via double staining of Kit (green) and TRP2 (red) employing normal 9 days post-plucking C57BL6 skin as a positive control.

The co-localisation of Kit and TRP2 is shown in Fig 50, which again demonstrates that the maximum melanocytes were presented at day 9 post-plucking, where both TRP2 and Kit were strongly detectable in plucked normal skin as melanocytes entered the cell cycle in anagen (A). Here Kit expression was detected in all Trp2 positive melanocytes. This proved to be the case also in melanoblasts/melanocytes which survived and proliferated in all papillomas investigated. Consistent with the results described above, where TRP2, Kit and SCF exhibited stronger expression in the papilloma basal layers, here once again co-localised Kit and TRP2 expression was mostly detectable in the basal cells of papillomas elicited by Ru486 treatment in K14Cre/EICre/N-Ras^{lys61}/Δ5PTEN$^{flx/flx}$ mice either under low (B, 50x; C, 100x) or higher magnification (400x, D-F).

This co-localisation of Kit and TRP2 expression in melanocytes confirmed the mechanism outlined above, that PTEN functional loss promoted N-Ras^{lys61} initiation in keratinocytes and pigmented papillomas may result via disrupted keratinocytes secretion of SCF which provided the signal to Kit expressing melanocytes that lead to SCF/Kit survival loop which overcame Ru486-induced melanocyte apoptosis.

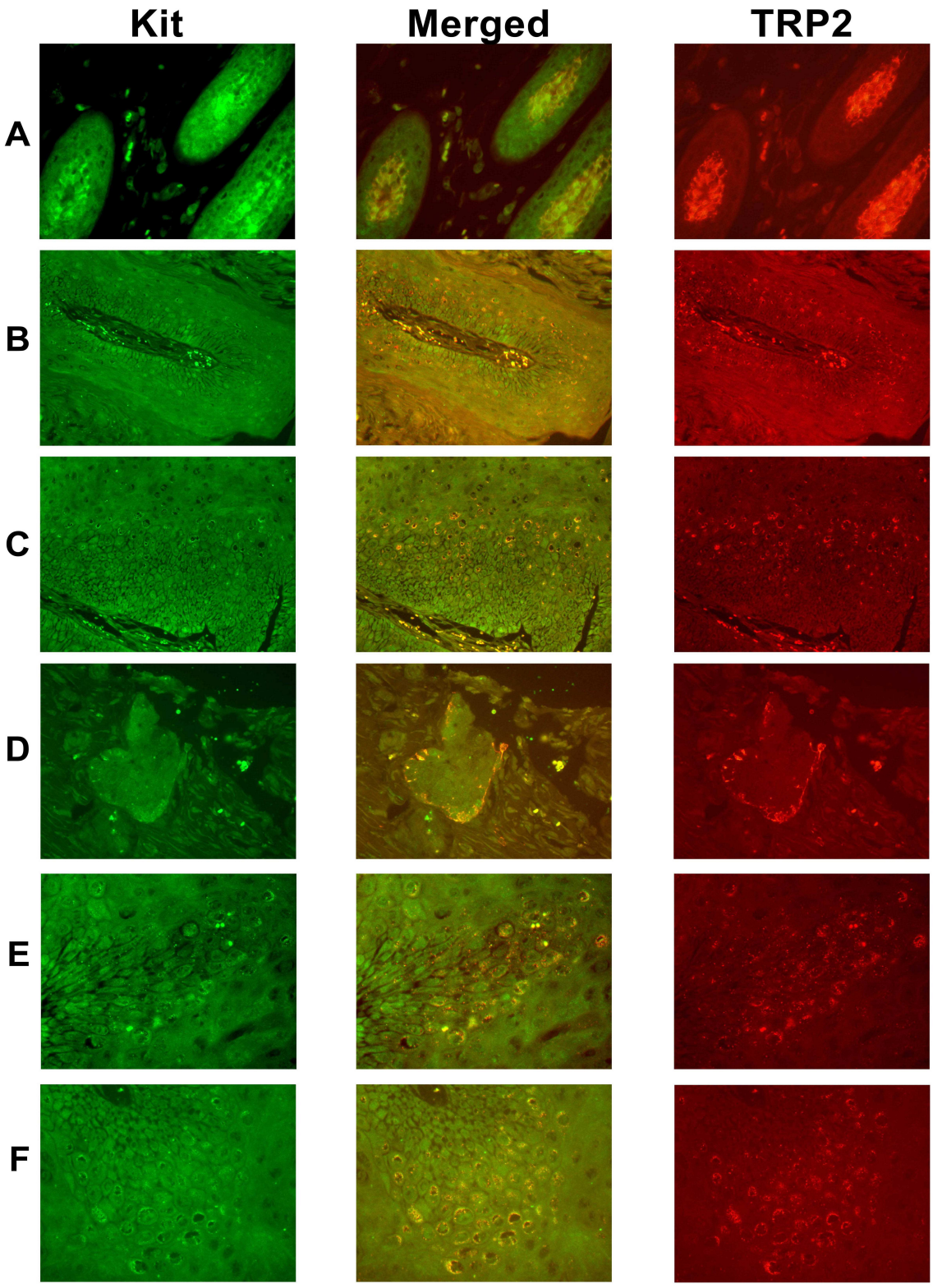

Figure 50: Kit and TRP2 co-expression in skin and pigmented papillomas. Kit expression was localized to melanocytes via double immunofluorescence staining of Kit (green) and TRP2 (red), a melanocyte specific marker. A, normal C57BL6 9-day post-plucking (100x); Papillomas B, 50x; C, 100x and D-F, 400x.

Chapter 4: Discussion

With the goal of development of an inducible gene-switch mouse melanoma model, both regulator (EICre) and target constructs (cmv.stop.N-Ras^{lys61}) were successfully constructed and functional gene switch specificity subsequently identified both *in vitro* and *in vivo*. With the time however, despite induction of anagen to obtain a target population of proliferative adult melanocytes and confirmation of N-Ras expression *in vivo*, bigenic lines failed to produce melanoma following systemic application of Ru486 and additional inducible loss of PTEN function via introduction of Δ5PTEN$^{flx/flx}$ in this model. The repeated lack of melanoma production in trigenic mice (EICre/Ras^{lys61}/Δ5PTEN$^{flx/flx}$) drove the experiments that established *in vitro* assays to investigate and confirm N-Ras and PTEN transformation potential, until the eventual phenotypes obtained in eyes and harderian glands, whilst not melanoma, indicated that the switch approach was working *in vivo*, a result consistent with the *in vitro* N-Ras/PTEN cooperation data. This prompted a closer and careful analysis of treated skin for any subtle cutaneous phenotype, which discovered that one potential reason for lack of melanoma was due to a caspase-3 mediated apoptotic response to N-Ras^{lys61} expression and/or compensation to PTEN function loss and therefore gene function redundancy *in vivo*.

Even so, in the interim experiments had progressed to asses the effects of seed/soil hypothesis on melanoma aetiology by incorporating follicular keratinocyte hyperplasia in the model to affect the microenvironment. Here the effect was to overcome this melanocyte apoptosis allowing their survival, but this resulted in a pigmented papilloma not melanoma. The aetiology of pigmented papillomas in this N-Ras/PTEN murine model suggests that such tumours arise when papilloma formation occurs alongside hair growth and incorporates anagen melanocytes. This ideas is supported by the facts that only a subpopulation of papillomas were pigmented and most papillomas containing melanocytes arose at approximately 4 weeks when the second phase of synchronised hair cycle occurs. This may also happen in humans where seborrheic keratoses also contain melanocytes,

although in humans the melanocytes may also arise from the interfollicular melanin unit. Nonetheless, our data suggest that the SCF secreted by transformed, proliferative basal layer keratinocytes provides a survival loop for Kit expressing melanocytes during papillomagenesis.

Although this model failed to produce melanoma, due to compensatory apoptotic mechanism, several other studies have provided valuable insight into melanoma aetiology in humans. Such models often require p16/p19 deficient mice (215;223;439) and exploit keratinocyte hyperplasia to develop melanoma in HGF expressing mice (40). Here in the latter models neonatal UV exposure directly led to melanoma in adults, thus mimicking human pathology (See section 4.6) whilst in adults UV exposure promoted Ras tumourigenesis (221), as did INK4a/ARF deficiency promotes (349). Recently, oncogenic N-Ras was shown to collaborate with deficiency in ARF, but interestingly not p53, to fully transform melanocytes (357). Indeed for murine models, the introduction of p16/p19 deficient mice and/or other melanocyte/melanoma development related factors in this inducible gene-switch model will provide an up-to-date superior mouse model to mimic multi-stage human melanoma development.

4.1. Construction and identification of transgenes

Through DNA recombination, a hetero DNA fragment forced into a mammalian cell can locate and recombine with the endogenous homologous sequences. Site-specific gene targeting systems have made it possible to genetically manipulate embryonic stem cells and the mouse germline. Recent advances using Cre-*lox*P and Flp-*FRT* systems give scientists the possibility to design and generate germline mutations following a single gene targeting event, as well as inactivation of genes in a conditional manner in the living mouse. In a Cre-*lox*P based conditional gene-switch system, Cre recombinase recognizes sequences of *lox*P to determine whether to excise DNA fragment between 2 directly orientated *lox*P sites or to invert the intervening DNA between 2 inverted *lox*P sites (Fig 4). Two inducible systems based on Cre recombinase have been independently developed by fusing a truncated progesterone ligand-binding domain (CrePR) which binds mefipristone (Ru486) but not progesterone (440;479;480); and a mutant estrogen receptor (CreER) which is activated by binding 4-hydroxy (OH)-tamoxifen, but not to natural beta-estrodial (481-485) thus minimising interference with normal hormone physiology whilst providing temporal Cre recombinase activity for conditional gene expression/inactivation *in vivo*.

To initiate a CrePR/*lox*P conditional gene-switch model, two components of a gene switch are required: the cell-specific regulator half incorporating CrePR and target transgene half containing *lox*P-gene-*lox*P or *lox*P-stop-*lox*P-gene, and followed by crossing of transgenic lines expressing these two halves. In this study, melanocyte specific EICre and TRP2Cre (a cited stronger and earlier expression promoter than EICre) regulator were successfully constructed. To further increase gene expression to achieve as strong expression as possible, a generic intron, which increases message RNA stability and efficient processing was included, thereby elevating gene expression in transgenic mice (452;453). This generic intron was isolated from K14CrePR1 and inserted into constructs between promoter (Etyr or TRP2) and CrePR gene. The insertion of an intron into the transgenic vector also

provides a convenient protocol to distinguish gene expression from DNA contamination following RT-PCR as deletion of the intron during transcription process to give a smaller band than contaminating DNA (Fig 26, 28).

The biological activities of cloned regulator vectors were subsequently identified through transfection of B16 melanoma cells (Fig 16) and of primary melanocytes (Fig 17). To enable the detection of target expression easier following regulator activation by Ru486 treatment, a useful report target (cmv.stop.EGFP) which contains EGFP to render target expressing cells visible under microscope was constructed as well as the oncogenic target vector cmv.stop.N-Ras^{lys61}. Employing a Cre responsive report target plasmid and the newly defined transfection protocols, active function of regulators was revealed following Ru486 treatment on the cultured cells (Fig 16 & 17) and accordingly, the successful target gene switch was identified *in vitro*. This report vector supplied a very simple and helpful protocol for identification of targeting gene expression and therefore for gene-switch specificity confirmation *in vitro* prior to *in vivo* analysis in CrePR/*lox*P system.

Although stronger expression levels were detected in TRP2Cre vs. EICre transfected B16 melanoma cells and primary melanocytes (table 2), an obvious leakage was detected in TRP2Cre transfection and therefore EICre, in which CrePR fusion protein was under the control of an enhanced tyrosinase promoter (0.22kb/2.2kb), was chosen to produce transgenic lines despite its weaker expression levels compared to TRP2Cre constructor. The target gene EGFP expressing following transfection and Ru486 treatment indicated that primary melanocytes as well as B16 cells are transfectable whilst the number of EGFP expressing cells (table 2 & Figs 16, 17) implied a low transfection efficiency.

Once the biological activities had been confirmed *in vitro*, the regulator expression in transgenic melanocytes was initially verified in the primary transgenic melanocytes by RT-

PCR (Fig 26) and its functional activity verification was followed by transfection of EGFP report target for microscopic analysis (Fig 27) and for RT-PCR detection (Fig 28).

Interestingly, the EGFP expressing cells were not as numerous as expected following transfection of report target vector cmv.stop.EGFP into regulator melanocytes and Ru486 treatment, but it was cell specific, as no keratinocytes were positive and did not leak, both by microscope viewing and by RT-PCR when compared to the EICre expression at the RNA level (Fig 26). This may have been a consequence if transfection variability of EGFP toxicity. However, binding sites for regulatory proteins and RNAs secondary structure upstream of the open reading frame of the untranslated regions (5' and 3') of mRNA, can determine gene expression level by influencing mRNA stability and translation efficiency (486) and thus, although insertion of a generic intron and the KOZAK sequences (487) that was cloned in front of start cordon ATG, the translation level of EICre transgene may not be as high as we needed or expected. Another possibility derived from comparing the morphology of EGFP expressing primary melanocytes in Fig 17 and Fig 27, where all EGFP positive cells in the latter were well differentiated melanocytes which had numerous dendrites. Brn-2 (its human homologue N-Oct3) is a class II POU domain factor and a melanoma-specific octamer binding protein, its mRNA expression is found both in melanoma cell lines and melanoblast but not in normal melanocyte. Its expression prevents activation of the tyrosinase promoter via displace factors required for tyrosinase expression (7). EICre regulator could be repressed by the Brn-2 expression in mouse melanoblasts but might not in those well differentiated melanocytes by loss of Brn-2 expression and therefore only those differentiated melanocytes but not melanoblasts expressed CrePR fusion protein to result in target gene (EGFP) activation.

To achieve high expression level of fusion protein CrePR in mouse melanoblast as well as in melanocytes, a longer promoter in which more 5' untranslated region (UTR) included

could be an alternative useful approach according to the successful Cre expression in mouse skin melanoblasts employing a 6.1-kb promoter (488), but this may not be critical since either short or long promoter was successfully employed in melanoma generation by H-Ras initiation in CDKN2A gene deficient mice (223;439) and also mouse hair cycle physiology has to be accounted for these inducible purposes. Indeed, TRP2, a cited stronger and in melanoblasts expressing promoter (288;454) which was also identified in this study (table 2), could be another alternative choice to replace this short version of tyrosinase enhancer/promoter to obtain stronger expression in melanoblasts as well as in melanocytes. However, the leakage of this promoter is another issue has to be carefully concerned and solved before application because the unexpected phenotype(s) may appear before inducer application to interfere the study of developmental stage related.

The same cloning strategy of report target vector cmv.stop.EGFP was employed for oncogenic cmv.stop.N-Ras^{lys61} construction and as only two lines proved to be germline transmitters, K14Cre/N-Ras^{lys61} primary keratinocytes were employed to rapidly confirm N-Ras^{lys61} expressers. This confirmed successful cloning and target expression following regulator activation obtained from the *in vivo* primary keratinocytes cultured *in vitro* (Fig 29 a-c) without the difficulties of primary melanocyte culture and transfection. It proved to be difficult to initial culture and later transfect mouse primary melanocytes, compared to their human counterparts or keratinocytes, but this was eventually achieved (below).

Collectively, both regulators and report target constructions were confirmed successfully *in vitro* employing transfection in B16 melanoma cells and later in primary melanocytes and the results indicated the gene-switch specificity *in vitro*. N-Ras expression in bigenic K14Cre/N-Ras primary keratinocytes following Ru486 treatment also indicated the gene-switch specificity *in vivo* in keratinocytes and inferred in melanocytes *in vivo*.

4.2. Optimisation of media for primary melanocyte culture and transfection

Murine melanocyte primary culture and transfection was not as easy as human melanocyte, although the other groups have achieved some success in culture of primary murine melanocyte exploiting ideally the requirement for feeder (457;458). Development of murine melanocyte primary culture, however, was a very useful and necessary protocol for identification of transgene construction prior to *in vivo* breeding and helped to cut the experimental running cost as well as to cut the animal usage to meet the ethic goals required by home office.

In human skin, each melanocyte is surrounded by 50-60 keratinocytes in the epidermal melanin unit and 95% of epidermal cells are keratinocytes, thus keratinocytes regulation of melanocyte proliferation and differentiation is as indispensable to the regulation by intrinsic genetic factors in melanocytes themselves. To date, α-MSH, b-FGF, SCF, HGF amongst many others, have all been suggested to be the important keratinocyte-derived factors which regulate the proliferation and/or differentiation of mammalian epidermal melanocytes through different signal pathways (reviewed by (470)). The same can be said for mouse melanocytes with the distinction that murine melanocytes are mainly follicular and proliferate during anagen, and thus *in vitro* grow from residual follicles, hence why SP1 cells, a transformed papilloma line derived from hair follicle stems cells via two stage chemical carcinogenesis proved a very useful feeder layer, both in our hands (not shown) and Yoon *et al* (457).

However, with the goal to produce a relatively pure population of tyrosinase expressing melanocytes, without the degree of spontaneous transformation that would hamper development of any transformation assay, primary melanocytes isolated from new born mice were cultured in a variety of different recipes either developed by ourselves, other

laboratories or commercial sources, we concluded that the recipes which supported initial keratinocyte growth as a feeder layer gave the best murine primary melanoblast/ melanocyte morphologies and highest transfection efficiency (Fig 12-15, 18 and table 3) but without spontaneous transformation. This observation was consistent with previous results employing feeders obtained by Bennett *et al* (459;460), but did not agree with another popular recipe developed by Halaban and co-workers, which did not employ keratinocytes as a feeder layer, but exploited horse serum and sodium orthovanadate (Na_3VO_4) as critical additives (449).

In the 50/50 culture medium of this system, the differentiation status of keratinocyte, controlled by extracellular calcium concentration (50) was exploited to maintain undifferentiated proliferative (e.g. basal layer) keratinocytes as a feed layer to secrete melanoblast/melanocyte growth-stimulation factors to promote melanoblast/melanocyte growth to obtain maximum number of pigmented cells. The effect of calcium in regulation of keratinocyte differentiation is well characterised *in vitro* and *in vivo*. Using particle probe methods (electron probe and proton probe X-ray microanalysis) and cytochemical methods (oxalate-pyroantimonate technique) respectively, the investigation of the distribution of elements and water in the different layers of the epidermis revealed a gradient of Ca^{2+}. In normal human and mouse skin, the concentration of Ca^{2+} increased steadily from the basal region to the stratum granulosum (489;490). Changes in intracellular calcium concentration, which result from both the intercellular Ca^{2+} accumulation in the mid granular layers and Ca^{2+} influx from the upper granular layers, helped regulate epidermal differentiation (491) e.g. via Scarf and its binding target proteins (492). *In vitro,* regulation of epidermal differentiation is also mediated by these Ca^{2+}-dependent processes. Mouse keratinocytes cultured in low Ca^{2+} medium (0.05mM) proliferate repeatedly, and begin to differentiate once the Ca^{2+} concentration exceeds 0.1mM (50;493;494). Thus if required terminal differentiation can be induced by

increasing the calcium concentration from 0.05mM to > 0.1mM and it is note worthy that in experiments to analyse melanocyte survival in pigmented papillomas (section 3.10), melanocytes mainly populated in the proliferative basal layers of papillomas. This result was consistent with *in vitro* observations where successful culture of melanocyte initially required low calcium culture conditions to maintain proliferative keratinocyte populations (NB: In alternate studies, secondary melanocytes grew poorly on SP1 papilloma cells cultured in high calcium media, which partially differentiated).

Keratinocytes in 50/50 medium grow well for the first few days and then gradually lost their proliferative ability and either spontaneously or were induced to terminally differentiate over 2-3 weeks of culture (Fig 13-15), while the pigmented melanoblasts/ melanocytes gradually appeared in presence of TPA (459) and other factors, including the matrix secreted by earlier proliferative keratinocytes. Thus once developed this 50/50 media incorporated all the factors of lower calcium concentration (0.05mM in our 50/50 medium vs. 1.802mM in Bennett and 0.278mM in Halaban recipes) as well as the lower concentrations of TPA (10ng/ml in 50/50 medium vs. 200ng/ml in Bennett and 50ng/ml in Halaban medium respectively) to maintain and promote melanocytes proliferation yet minimise spontaneous keratinocytes transformation (495). Whilst compared to other media, pigmented melanoblasts/melanocytes presented later in dishes of 50/50 medium, use of this optimised primary mouse melanocyte culture medium was able to produce sufficient number of cells possessing a normal morphology for identification of cell specific gene-switch activity *in vitro*, of transgene expression prior to *in vivo* breeding as well as of *in vitro* modelling of N-Ras and PTEN synergism.

The recipe developed by Halaban has been wildly used for murine primary culture, thus the comparison of melanocytes cultured in Halaban medium and in our house optimised 50/50 medium was performed to verify any (dis)advantages against each other. On culture

using exactly the same protocols, obvious differences were revealed between these two recipes. In Halaban medium, keratinocytes were not optimised to grow and then to support melanocytes/melanoblasts in contrast to our 50/50 medium in which keratinocytes were considered to be an important factor providing an initial feeder layer for residual primary (follicular) melanocyte growth and therefore a medium containing low Ca^{2+} was chosen.

Addition of TPA in the medium was essential for murine melanoblasts/melanocytes growth (459) and thus, TPA was included in both media. In Halaban medium, although Na_3VO_4 was included to inhibit tyrosine phosphatases to prolong the activity of endogenous tyrosine kinases (449), the vast majority of melanocytes are not pigmented which indicated the little tyrosinase activity in these cells and therefore they are not suitable for our purpose where regulator expression relies on the tyrosinase activity. Indeed, the proportion of pigmented cells in Halaban medium gradually increased following long term culture with a very slow speed and moreover, pigmented cells had spontaneously transformed very quickly as had pigmentation within 1 or 2 passages (Fig 15) and thus, again melanocytes grown in Halaban medium were not consistent with our goals to investigate Ras roles in transformation and its synergism with PTEN gene deletion *in vitro*.

Despite the advantages being demonstrated by 50/50 medium, melanoblasts/melanocytes actually grew well in both media despite an initial lack of pigmentation and eventual spontaneous transformation in Halaban medium. Cells in Halaban medium, however, may still have had enhanced transfection efficiency. Given that a transfectable capacity was an essential test using primary melanocytes to identify transgenic mouse expressers and mouse primary melanocytes were expected to be very difficult to transfect, transfection efficiency of cells cultured in 50/50 or Halaban medium was estimated. Here Fugene-6 had been verified to be the transfection reagent of choice via transfection into B16 cells. As

revealed in table 3, even the transfection efficiency was not high in 50/50 medium, the transfected cells in Halaban medium are only approximately 1/3 of cells cultured in 50/50 medium either in primary or sub-cultured secondary cells under exactly the same conditions.

Taken together, murine primary melanocytes grew better in 50/50 and Halaban media than others. However, cells cultured in house optimised 50/50 medium gave advantages of no spontaneous transformation which is an essential factor for our *in vitro* modelling analysis, and of cell pigmentation (tyrosinase expression) which is also the necessary factor for our regulator expressing. Furthermore, higher transfection efficiency was also revealed in 50/50 than in Halaban medium, which is very useful for identification of transgenic expressers as well as for *in vitro* modelling. Indeed this effort proved to be quite worthwhile, as it developed an *in vitro* transformation assay with a minimum degree of spontaneous melanocyte transformation, which allowed a successful direct test of the oncogenic potential of N-Ras and PTEN loss in this inducible system when concerns had arisen regarding an unexpected lack of a melanoma phenotype (below).

4.3. Modelling melanoma *in vitro*

Due to the failure of mouse melanoma production by inducible N-Ras^{lys61} expression accompanied by PTEN function deletion, employing our optimized murine primary melanocyte culture protocol, an *in vitro* model was established initially to confirm biological activity of these transgenes and later to investigate the role(s) of N-Ras^{lys61} expressing and PTEN loss and their potential synergism in melanocyte transformation.

It was initially theorised that a low level of N-Ras^{lys61} expression induced in adult mouse could have been the cause of melanoma production failure. As TRP2Cre has been identified to be a stronger regulator in the initial tests of transgene activity that resulted in higher target gene expression, despite its leakage (Fig 16, table 2), TRP2Cre, not EICre, was employed in the transfections for *in vitro* modelling. This showed that unlike *in vivo*, PTEN function loss could promote cell proliferation and was synergistic with mutant N-Ras^{lys61} expression resulting in a significant change of melanocyte morphology which shows more aggressive by losing contact-inhibition characteristics, but critically did not induce immortalisation, a result consistent with the redundancy in cooperation revealed *in vivo*. The difference revealed here between *in vitro* and *in vivo* agreed with the finding that mutation of PTEN is quite common in melanoma cell lines but relative less in STC lines and melanoma specimens (264) and thus, different roles of PTEN function loss in melanoma cell line and solid melanoma are not surprising.

It may be that PTEN-controlled cell renewal depends on modulation of G_0-G_1 transition and therefore, PTEN function loss would trigger G_0-G_1 arrested cell proliferation possibly without perturbing the fate of cell differentiation (475). PTEN function loss activates Akt which associates with p21Cip1/WAF1 to lead cytoplasmic localization of p21Cip1/WAF1 and consequently results in HER-2/neu-mediated resistance to apoptosis and promotion of cell growth in tumours (496). Following co-transfection of TRP2Cre into Δ5PTEN$^{flx/flx}$

transgenic melanocyte and subsequent Ru486-mediated deletion of PTEN exon 5, PTEN function loss in transfected melanoblasts/melanocytes (EGFP tagging or G418 resistant) resulted in faster proliferation than wild type cells (Fig 32, 34-35) to produce colonies, but the morphology of cells remained normal. This suggests that PTEN conferred a proliferative ability via lack of modulation of downstream molecules, which did not interfere with the cell characteristic of retaining monolayer growth and cell contact inhibition. This also implies that the combined effects of the loss of PTEN lipid and protein phosphatase activity may result in aberrant cell growth, but not overt transformation, hence the lack of tumourigenesis potential via PTEN deletion alone in the EICre model *in vivo* (apart from white hair/hair loss, below).

Active forms of Ras play a causal role in more than one quarter of human cancers and, unlike PTEN functional deletion, is a well characterised initiator of tumourigenesis (497). Ras proteins are tethered to the inner cell membrane, coupling growth factor receptors to regulate downstream signalling pathways through further a series molecules activation or function loss that control cell growth, proliferation, survival and transformation despite in some cases expression of Ras active form resulted in non-transformed diseases (Fig 2). Comparing Fig 32 with Fig 33 and Fig 35 with 36, morphological differences were apparent between N-Ras^{lys61} expressing and PTEN function loss melanoblasts/melanocytes following activation of CrePR1 recombinase by transfection and Ru486 treatment. Other than promoting cell proliferation as observed in PTEN functional loss cells, N-Ras^{lys61} expressing cells also exhibited a transformed morphology, although the cells remained monolayer growth and retained cell contact inhibition characteristics.

As PTEN acts downstream of Ras signalling to down-regulate Ras functions via the MAPK pathway (Fig 2, 3), together PTEN functional loss in addition to the N-Ras^{lys61} expression in melanocytes resulted in more severe morphological changes (D-F of Fig 33

and C-F of Fig 36) which presented spindle shape and lost cell contact inhibition characteristic to cause these melanocytes to pile up and therefore, unlike in N-Ras^{lys61} expressing alone cells, it became impossible to distinguish any single cell. Thus, unlike the results obtained *in vivo* where PTEN function loss did not change the N-Ras^{lys61} expressing mouse phenotypic profiles, except for a subtle increase in caspase-3 activity. Addition of PTEN function loss *in vitro* by transfection did co-operate with N-Ras^{lys61} expression to produce an increased transforming morphology but no immortalisation as these cells senesced at approximately passage 5-6. PTEN is able to promote N-Ras initiation possibly due to being *in vitro* but the transformed cells die out possibly due to the function redundancy between these two genes was also consistent with the results obtained from the *in vivo* model (below) in which a compensatory mechanism of PTEN functional loss resulted in caspase-3 mediated apoptosis as N-Ras expression induced, hence no PTEN promotion on N-Ras melanomagenesis *in vivo*. Thus, it would be an interesting study to investigate whether these *in vitro* PTEN loss and N-Ras expressing cells gain the characteristics to become immortalised if other genetic pathways deregulations and/or UV exposure are introduced.

4.4. Modelling *in vivo*

In mouse skin, few melanocytes are present in interfollicular epidermis by day four after birth and declined gradually until no interfollicular epidermal melanocytes are detectable by day eighteen, except the occasional cells in the ear, whereas the follicular melanocytes increased for about two weeks after the birth during the first synchronised anagen but then undergo a programmed apoptosis as the hair growth ceases on progression from anagen to catagen (56;57). Their melanocyte stem cells remain quiescent in telogen until the next anagen phase, unless triggered following environmental stimulation to force telogen hair follicles re-enter hair cycle by proliferation, differentiation and migration of stem cells located in the follicular bulge (53). Thus in this inducible gene switch system, very few target cells (stem cell/melanoblast/melanocyte) existed in an adult mouse skin and induction of anagen at the time of Ru486 treatment was essential for regulator activation and subsequently resulting N-Ras^{lys61} target gene expression and/or PTEN inactivation and unless treated, in any random anagen follicle, N-Ras^{lys61} would be inactive while PTEN gene functions active as normal.

Therefore, the mouse hair cycle was initiated by plucking back hair to obtain maximum melanoblasts/melanocytes expressing regulator EICre for activation by Ru486 treatment subsequently to activate oncogenic N-Ras^{lys61} gene expression in a maximum number of melanocytes following excision of silence cassette of 'Stop' in target gene cmv.stop.N-Ras^{lys61}. In initial experiments the maximum melanoblasts/melanocytes were achieved at day 7-9 post plucking (Fig 30) and declined gradually until finally became undetectable approximately at day 21 post-plucking (table 4). Thus, to obtain as many proliferative tyrosinase expressing melanocytes as possible for exposure to Ru486 treatment, back hairs were plucked to initiate anagen and the time course for maximum numbers of Trp2 expressing cells determined, and hair plucking was repeated every 4 weeks. Also in mouse, follicular melanocytes are well protected in the follicle from UV radiation and chemical

induction and therefore UV and/or chemical carcinogens induced mainly non-melanoma skin tumours (57;76). As no overt phenotypes had appeared, a second consideration was whether the penetration of Ru486 was sufficient to reach the papillary melanocytes. Thus, despite the indications from separate studies that this was so (246;467), to ensure Ru486 was delivered to its target cells efficiently, Ru486 was dissolved in sesame oil for IP injection once a week and in ethanol for topical painting twice a week at 0.4mg/kg (469) (average weight 25g of mouse was considered) and 10μg/100μl respectively.

This IP injection protocol resulted in the eventual appearance of enlarged eyes with mild hyperplasia in the RPE layer in EICre/N-Ras^{lys61} and EICre/N-Ras^{lys61}/Δ5PTEN$^{flx/flx}$ compound transgenics and thus indicated that the gene switch was working *in vivo*. These phenotypic eyes possessed retinal pigment epithelia hyperplasia and enlarged choroid rather than melanoma. This histotype was quite similar to that produced in a similar, non-inducible model of Tyr-based N-Ras^{lys61} transgenic mice (215) where the Ackermann model eye phenotype appeared in adult mice by 6-8 weeks old presumably due to constitutive oncogenic N-Ras^{lys61} expression throughout embryonic development as tyrosinase transcriptional elements based construct would be expressed in neural crest derived melanoblasts from day E10.5 (468).

Phenotypic eyes from both models have enlarged choroids and abnormal folded neuroretinal, although the folding of the RPE was worse in the Ackermann model than the EICre model (Fig 51) consistent with constitutive expression throughout development in Ackermann model, unlike induction of phenotypes in EICre/N-Ras^{lys61} where adults were allowed to develop normally. Apart from these phenomena as displayed in Ackermann model, phenotypic eyes from the EICre/N-Ras^{lys61} model also displayed a larger size and more predominant melanin in the retinal pigmented epithelium (Fig 38).

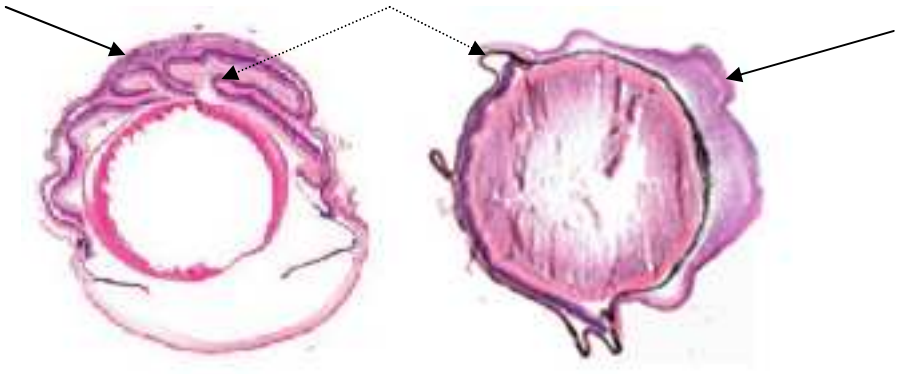

Figure 51: Comparison of phenotypic eyes. Abnormal folded neuroretinal (dash arrow) and enlarged choroid (black arrow) were observed in phenotypic eyes from both Ackermann (left) and our (right) models. Eye of Ackermann model was copied from Ackermann, Cancer Research 65(10):4005, 2005 for comparison purpose.

One major difference between the two models was the harderian gland adenoma in EICre/N-Ras^{lys61} and EICre/N-Ras^{lys61}/Δ5PTEN$^{flx/flx}$ mice. These harderian gland adenomas displayed a much larger size (up to 4 times) as well as an adenoma histology from those harderian glands obtained from normal C57 mice which also have been treated with Ru486 or from bigenic mice which has been treated with vehicle, thus eliminating any integration effects or background responses to Ru486 (Fig 39-41). Despite lack of melanoma production in this model, unlike that eventually produced in the constitutive Ackermann model, this model showed a separate harderian gland phenotype. This unexpected phenotype of harderian gland adenoma resulted from prolonged systemic treatment with Ru486 as this only appeared in treated mice because following the oncogenic expression and/or TSG inactivation. However, a subsequent literature search discovered a paper on the expression characteristics of the enhanced tyrosinase promoter, using a lacZ report transgene (468). This study reported novel lacZ staining in cells of the harderian gland consistent with eventual adenoma formation in mice expressing N-Ras (and/or PTEN) over long periods of time.

Most likely this difference also centred on the different promoters employed, and in cell

lineage studies Tonks *et al*, showed that there was unexpected report activity in harderian gland employing this tyrosinase enhancer/promoter combination and from which they concluded as a population of neural crest derived cells possibly melanocytes in this gland. As this report could not find a population of TRP2 staining cells in the harderian glands, and given the adenoma phenotype but not melanocytic-type tumour, we conclude that the difference between enhancers/promoters in these two models (0.22kb/2.2kb in our model vs. 3.6kb/6.1kb in Ackermann) might contribute to such extra phenomena, as well as to the production of melanoma in Ackermann model (discussed below). On considering the differences between enhancers/promoters used in Chin (3.6kb/6.5kb of enhancer/promoter) (217;223) and Huijbers (0.8kb/2.5kb of enhancer/promoter) models (439), these two models show clear different locations of melanoma development and a difference in tumour pigmentation, although the same H-Ras (V12G) oncogene was used in both models. As discussed by Huijbers *et al*, Cre-mediated recombination was mainly observed in follicular melanocytes and consequently therefore, appearance of melanomas on hairy skin was to be expected in their model (shorter version). In contrast, melanomas produced in Chin's model (long version) showed a preference on skin areas with sparse or no hairs, such as the pinna of the ear, the tail, or the anus where dermal melanocytes are primarily present in an adult mice and the Cre recombinase expression were detected and thus, melanomas produced were mainly amelanotic.

However, such difference between the Chin and Huijbers models could also be the results of the different gene switch systems used. CDKN2A was a conditional knock out and H-Ras(V12G) gene was followed by P1A gene which used the same mRNA transcript of Ras to encode a tumour specific antigen in Huijbers model, whereas CDKN2A gene was permanently knocked out and H-Ras(V12G) was expressed by an independent construct in the Chin model. Thus, we conclude that such a size difference of promoters used in these independent models contributed to the phenotypic difference obtained from each model but

was not the sole contributor.

Despite the appearance of an eye phenotype, the continued lack of cutaneous phenotypes and unexpected in addition of PTEN biological function loss in the light of the findings from these alternative models, prompted a careful re-analysis of treated EICre/N-Ras^{lys61}, EICre/Δ5PTEN$^{flx/flx}$ and EICre/N-Ras^{lys61}/Δ5PTEN$^{flx/flx}$ skins. As an oncogenic gene, persistence of active N-Ras expression in normal melanocytes may not be well tolerated, and active Ras expression can result in developmental defects (Costello syndrome, Noonan syndrome) but not tumours (154;155). Oncogenic Ras expression also activates cellular defence mechanisms (e.g. apoptosis and senescence) which need to be overcome, typically by a cross-talk of co-operating oncogenic alteration(s) for full malignant transformation. Thus, in cells harbouring active Ras gene, the question whether Ras triggers cellular anti-proliferation defence mechanisms or interferes with a cell capability of preventing the completion of such responses, could be a major determinant of the cell fate and the eventual phenotype (474). Active Ras has either positive or negative effects on the regulation of apoptosis to determine cell fate depending on the balance of the apoptotic and anti-apoptotic signalling pathways which vary in different cell types (473). Ras stimulates apoptotic signal Raf-1 (C-Raf) in lymphocytes or fibroblasts and brown adipocytes in absence of survival factors, whereas other signalling pathways downstream of Ras stimulate PIP3/Akt, survival signals for epithelial and myeloid cells.

In treated EICre/N-Ras^{lys61} skin, careful analysis of oncogenic N-Ras expression in mouse epidermis found a consistency of white hair/hair loss (Fig 42) suggesting that melanocyte apoptosis in hair follicles (Fig 43) was responsible for the lack of overt melanoma. In this model, levels of N-Ras^{lys61} (Fig 31) and expression being induced in the normal adult stage may be not efficient enough to cause dysregulation of cell proliferation, differentiation and transformation, but efficient enough to induce pro-apoptotic molecules and overcome those anti-apoptotic molecules induced by activated N-Ras^{lys61} which results in the observed

melanocyte apoptosis. Indeed the rapidity of the induced apoptosis suggests that specific mechanisms exist that act as sentinels to prevent the onset of melanoma and are hyper-sensitive to changes in molecules that induce these early stages.

It may be that only very high Ras expression in melanocytes (e.g. in Ackermann model) or through embryonic development (40;215-217) can induce an anti-apoptotic mechanism in melanocytes to overcome this defence system and thus dysregulate cell development to result in production of melanomas. Whereas in other models (e.g. this report), Ras expression may activate cell defence mechanism to result in the observed apoptosis if murine skin was allowed to develop normally. To assess whether this was so, an apoptotic analysis was performed finding that in all N-Ras^{lys61} expressing mouse skin, caspase-3 was expressed in greater number of melanocytes and in more hair follicles compared to normal, although melanocytes do normally express caspase-3 as expected and shown by one follicle under going apoptosis at the catagen phase (Fig 45). This differs from previous observations in cell lines transformed by H- or K-Ras (474;498), which probably reflects being an *in vivo* model vs. *in vitro* and different Ras alleles analysed, but clearly N-Ras expressing melanocyte undergo apoptosis in a caspase-3 dependant manner *in vivo*.

Depending upon the study, even no or sometimes quite low N-Ras mutation incidence was detected in common acquired nevi, but higher rates in congenital nevi (9;11;12;220) and as up to 95% of INK4a mutated familial melanoma cases have N-Ras codon 61 mutation in human (212-214). These data indicate that activated N-Ras^{lys61} expression alone was not sufficient to produce full melanoma, but maybe involved at pre-malignant stages (222). Indeed, induced N-Ras expression in central nerve cells only produced neurofibroma-like tumours but not any tumour suggested a requirement for signal(s) other than the activated N-Ras pathway to induce tumours (499). However, N-Ras clearly plays a role in melanomagenesis as shown by the short latency (two months) of melanoma induction in

H-Ras/p16^{INK4a} model (223). In this current study, the idea that a conditional knock out mouse of PTEN gene, the second most abnormal TSG gene after CDKN2A in melanomas (250;252) and loss of heterozygosity (LOH) quite often observed in primary and metastatic melanomas (264), could substitute for such CDKN2A mutation. However, PTEN involvement did not change the course of melanoma aetiology, as trigenic EICre/N-Ras^{lys61}/Δ5PTEN$^{flx/flx}$ mice repeatedly failed to produce melanoma following more than one year of Ru486 application.

Incorporation of PTEN functional loss in this N-Ras^{lys61} model did not produce the promotion of tumourigenesis as observed in H-Ras model of carcinogenesis (246) and CDKN2A did in other melanoma models, suggesting a redundancy between PTEN and N-Ras genes in melanocytes *in vivo*. This idea was supported by the finding that PTEN function loss in melanocyte produced white hair was consistent with one of the PTEN primary functions of which is to regulate cell development by negatively control cell proliferation through apoptosis (243;245;259;500). Therefore, there may also be an important component of compensatory surveillance system sensitive to PTEN loss which exists in melanocyte *in vivo* and that prevents cell dysregulation in absence of PTEN function and results in melanocyte programmed death to negate melanoma production. This lack of promotion of PTEN on N-Ras tumourigenesis may be due to PTEN functions to negatively regulate the N-Ras MAPK signalling pathway and thus its loss is redundant to resultant melanocytes expressing activated Ras and elevated MAPK (Fig 3, 45) (152;271). In addition as outlined above, *in vitro* PTEN loss only accelerated/enhanced Ras transformation but not immortalisation, rather than cooperation with another potent Ras-independent pathway which could co-operate with constitutively activated Ras-GTP pathway to induce full malignancy.

To assess whether PTEN function loss also induced melanocyte apoptosis *in vivo* and

whether any additive functions in addition to those detected in N-Ras^{lys61} expression, caspase-3 and -9 expression detections were performed in both EICre/Δ5PTEN$^{flx/flx}$ and EICre/N-Ras^{lys61}/Δ5PTEN$^{flx/flx}$ mice employing immunofluorescence staining and the results (Fig 45) revealed that as in N-Ras expressing mice, PTEN function loss resulted in melanocyte apoptosis *in vivo* again through caspase-3 dependant pathway but not caspase-9. Furthermore, as the same apoptosis mechanism involving caspase-3 and the number of caspase-3 expressing follicles are not additive in EICre/N-Ras^{lys61}/Δ5PTEN$^{flx/flx}$ mice, it again suggested that these two gene functions are redundant in melanocytes *in vivo*. Therefore, PTEN promotion capability to N-Ras^{lys61} initiated melanomagenesis was prevented and resulted in no production of melanoma in EICre/N-Ras^{lys61}/Δ5PTEN$^{flx/flx}$ mice. Such a gene redundancy *in vivo* is possibly due to PTEN and Ras functions on the same signal pathway to regulate cell death/proliferation/differentiation, but not providing alternative additional genetic signalling pathway to cross-talk with Ras signalling pathway which may be essential for Ras induced tumour formation. Moreover, this may indicate how vital these genes are to the development of melanoma as such sentinel systems have evolved to defend against these mutations and other pathways are required to circumvent these mechanisms. The importance of these genes despite the failure of melanoma production was also consistent with the results obtained from the *in vitro* model (above) in which, PTEN is able to promote N-Ras initiation possibly due to being *in vitro* but the transformed cells promoted by PTEN loss are not immortalized due to the function redundancy between these two genes.

Searching the literature, all successful Ras driven mouse melanoma models either were created in a CDKN2A (p16/p19) background (215-217;223;439) or melanoma cells bear hetero/homozygous deletion of CDKN2A locus if the models were produced by H-Ras expression in a normal background followed by UV radiation or chemical treatment (221;349). Therefore, loss of function of CDKN2A gene seems an essential event for

melanoma development in Ras mouse models to date. Other gene(s) (e.g. CDKN2A) cooperation is necessary for tumour development (152) although Ras activation is essential for melanoma maintenance (223). Inducible N- and H-Ras expression alone is not sufficient to induce melanoma in all developed mouse models and only constitutive expressing N-Ras^{lys61} produced melanoma with longer latency (>12 vs. 6 month) and much lower penetrance (25% vs. >94%) compared to those melanomas induced in CDKN2A deficient background from the same experiment (215). This may have been due to higher expression from its larger promoter to cause CDKN2A ablation although CDKN2A gene mutations in these late onset constitutive N-Ras^{lys61} expressing melanomas were not analysed and therefore, whether the CDKN2A gene expressed normal or function inactivated eventually in those melanomas is unknown. Indeed, as only 4 melanomas were induced by N-Ras^{lys61} expression control cohort, maintaining the characteristics of familial cutaneous melanoma with germline INK4a mutation, as the authors acknowledged that these melanomas may have had spontaneous CDKN2A mutation and thus, it is not N-Ras^{lys61} alone but cooperation again with CDKN2A ablation which is the causal mechanism underlying these 4 melanomas.

Hence in those H-Ras expressing generated melanoma following UV or chemical application (216;221), the other gene(s) that undergo ablation/mutation may be the necessary hallmark to complete melanoma formation. Thus it is not surprising that there was no melanoma generated by N-Ras^{lys61} expression alone in our inducible gene switch model because the induced N-Ras^{lys61} expression in adult mice is not sufficient to cause hyperplasia from cell dysregulation as other models did during embryogenesis, without the consequent molecules aberration to co-operate and subsequently to overcome cell defence systems such as the induced apoptosis in adult follicular melanocytes.

Although continual expression of fully activated Ras is unexpected to be well tolerated, to

form tumour eventually many other molecular steps are needed other than activation of Ras pathway components for progression (152) and thus, CDKN2A ablation provides such a Ras-independent pathway to co-operate with Ras signalling pathway to result in melanoma formation in mouse models, but PTEN deletion in adult may not. Comparing our model with all relative close (H-Ras gene-switch and N-Ras constitutive expressing) successful mouse melanoma models (215;223;439), the main, possibly critical, points are that in all other three models Ras expressed in a CDKN2A deficient background which allows gene cooperation through different genetic pathways other than PTEN functional deletion which may only affect Ras signalling pathway by enhancing/promoting Ras function, but insufficient to provide the alternative additional molecular steps to form overt melanoma. Therefore, even in EICre/N-Ras^{lys61}/Δ5PTEN$^{flx/flx}$ mice, targeted cells received essentially one hit in our model in adult rather than multiple hits (p16/p19 and Ras) in CDKN2A deficient models, including unknown events elicited during embryonic expression of these mutations in several of the models.

In EICre/N-Ras^{lys61}/Δ5PTEN$^{flx/flx}$ model despite PTEN loss, the N-Ras expression induced an anti-apoptotic mechanism and apparently this response is too low to overcome the induced cell defence apoptotic pathway. As discussed in 4.1, the enhancer/promoter as well as the 5' and 3' untranslated region may also influence the Ras expression level to consequently result in different phenotype (486). But it should not be the critical factor since the relative short enhancer/promoter (very similar to this model) employed in Huijbers model generated mouse melanoma successfully using H-Ras(V12G) (439) despite the differences of phenotypic macrology and histology from another H-Ras (V12G) model by using a longer version of enhancer/promoter (223).

Collectively, to date the mice have been successfully established and technical difficulties overcome such as awkward mouse hair cycle physiology (e.g. there are only 6-8 days for

tumourigenesis to begin) that provides the foundations of an inducible system. Inducible models where temporal effects are added into adult mice may be a better mimic of human carcinogenesis in somatic cells and thus gave different results to e.g. the closest model of Ackermann. This approach certainly lets us add more events in to test ideas including extrinsic keratinocytes and/or more gene mutations. This may be a critical technical component for studying of melanoma development from nevi to RGP and RGP to VGP.

This *in vivo* inducible model shows that the mouse could utilise the normal defence systems to overcome anti-apoptotic mechanism triggered by N-Ras expression and PTEN function loss through the activation of pro-apoptotic system. Thus, the mouse will develop normal if any of these genes ablation is not accompanied by the subsequent molecular event(s) to cross-talk to Ras initiated pathway, whereas Ras initiated anti-apoptotic pathway more likely to overcome its pro-apoptotic system to result in cell dysregulation if Ras expression and/or other TSGs loss events happened through embryonic process in other models. Comparing this model with other relative close models, we concluded that Ras mutation may not be an independent event in somatic melanoma but one of steps involved with many other molecules (specifically not on the Ras signalling pathway) despite the high mutation rate of N-Ras had been revealed in human melanoma. To form tumour successfully, consequent gene ablation which can supply a different signalling pathway to co-operate with any oncogenic gene expression and/or loss of TSG is necessary to overcome mouse self-defence systems. Therefore, the formation of melanoma is highly expected if CDKN2A deficient mouse background was introduced into this model and such introduction is the primary goal of future work.

4.5. Investigation of the role of the microenvironment on EICre/N-Ras^{lys61} /Δ5PTEN$^{flx/flx}$ phenotypes

White hair or hair loss produced by N-Ras^{lys61} expression in melanocytes indicated that a premature melanocyte apoptosis occurred in anagen hair follicles which may have been responsible in part for the lack of melanoma, despite additional PTEN loss which also appeared to induce a pro-apoptosis via caspase-3 to stimulate cell defence system (Fig 45).

In addition to these complex intrinsic genetic factors within melanocyte, regulation by the microenvironmental cells/tissues, especially keratinocytes, also play a very important role in the physiology underlying melanoblast/melanocyte survival, migration, proliferation and differentiation and in the development of melanoma, via a complex interaction of cues secreted by and releases from keratinocytes, the seed/soil hypothesis (reviewed in (470)).

Increase of melanin-a in malignant melanoma cell lines augmented by the presence of a keratinocyte papilloma cell line SP-1, derived from the hair follicle stem cells in two stage chemical carcinogenesis, suggested that keratinocytes secret melanogens toward melanocytes and as outlined above SP1 action as a successful feeder layer occurred when cultures in low calcium media (457;458) and in a proliferative basal cell phase. In adult mice, pigmented spots in hairless mice were induced long after UVB exposure indicating that epidermal melanocyte proliferation and differentiation were regulated by keratinocytes rather than by melanocytes, which was verified by irradiated keratinocytes stimulating the proliferation and differentiation of non-irradiated melanocytes more greatly than keratinocytes from non-irradiated mice and whereas, irradiated adult keratinocytes have very similar affection on non- and irradiated adult melanocytes proliferation and differentiation (501;502).

In melanoma models, melanomas are often accompanied by keratinocyte hyperplasia. In

the Ackermann system, constitutive N-Ras expression in melanocytes produced mice with epidermal hyperplasia, hyperkeratosis in adults (215). In model of Noonan, a good close mimic of human melanomagenesis as it elicits epidermal melanoma with the potential to investigate junctional pathology unlike the other models e.g. Chin (223), UV exposure on neonates gives melanomas in adults, this model also has neonatal keratinocyte hyperplasia from HGF expression in keratinocytes (40). Skin hyperplasia was also revealed by H-Ras constitutive expressing in H-Ras mediated mouse melanoma models (216). Both *in vitro* and *in vivo* models implied a role of abnormal keratinocyte during melanoma development.

Therefore to test whether disruption of the follicular microenvironment of melanocyte would change the *in vivo* responses and initiate melanoma production, N-Ras^{lys61} expression and PTEN deletion in keratinocyte was incorporated into this model. This was achieved employing a K14Cre regulator transgenic line bred into trigenic EICre/N-Ras^{lys61}/Δ5PTEN$^{flx/flx}$ mice. Here, in a similar fashion to cooperation between PTEN loss and H-Ras (246), disruption of follicular morphology was envisaged via induction of keratinocyte hyperplasia as K14 promoter is expressed in the hair follicles, including keratinoyte stem cells. This proved to be the case but instead of producing melanoma phenotype following K14Cre/EICre/N-Ras^{lys61}/PTEN$^{flx/flx}$ treatment with Ru486, N-Ras^{lys61} expression cooperated with PTEN functional loss in keratinocytes give squamous cell papillomas which possessed a population of melanocytes creating pigmented papillomas.

These results firstly indicated that in keratinocytes N-Ras^{lys61} expression acted as an initiator with which PTEN loss acted as a promoter given that N-Ras or PTEN loss alone in controls did not produce tumours. This was similar to the findings employing H-Ras mice (246). Secondly, by active regulator and consequent dysregulation downstream of Ras signalling pathway (including PTEN function loss) in keratinocytes may have contributed to the decision of melanocytes fate in addition to regulation of the melanocyte own genetic

factors as clearly here anagen melanocytes now survived and did not undergo apoptosis.

As discussed above, level and the initial time of N-Ras^{lys61} expression may contribute to papilloma genesis because expression in keratinocytes using the K14 promoter may be stronger than EICre in melanocytes, including stem cells (467;503) and therefore, more cells expressing strong K14Cre than melanocytes expressing relative weak EICre to result in keratinocyte hyperplasia and papillomas, or it may be that keratinocytes do not respond to N-Ras via induction of apoptosis, as this would compromise their important barrier functions.

The pigmentation of induced papillomas could be derived from interfollicular relocation of melanocytes which migrated out of the hair follicle following N-Ras^{lys61} expression in melanocytes (215) and in its microenvironmental keratinocytes. Given the lack of interfollicular melanocytes in adult murine skin the pigmentation of induced papillomas could be derived from survival of melanocytes from an anagen hair follicle following N-Ras^{lys61} expression in melanocytes (215). In this microenvironment of keratinocyte hyperplasia, melanocytes were able to continue to proliferate during papilloma development (see Fig 46b, 47) or simply continue to exist as hair follicle residues during papilloma development due to there is no interfollicular melanocytes exist (please see Fig 46b, 47). To confirm that these were indeed melanocytes and not melanin produced in melanocytes and melanosomes transferred into neighbouring keratinocytes, TRP2 antibody immunostaining demonstrated the survival of melanocytes during pigmented papilloma development, similar to those hyperproliferative examples of Powell or Ackermann Ras alone controls (215;216). Moreover, employing a combination of suprabasal keratin 1 (K1) and basal keratin 14 (K14) expression against TRP2 staining, it became clear that these melanocytes occupied mainly the proliferative keratinocyte basal layers of papillomas (503). Thus N-Ras^{lys61} expressing and/or PTEN function loss in keratinocyte allowed

melanocyte to survive from the apoptosis and therefore proliferated and accumulated to result in pigmentation in papillomas during the papillomagenesis.

These kinds of pigmented papillomas, may relevant to seborrheic keratoses in human, are of intense worry to patients whether the possibility of melanoma is high prior to histological analysis. Thus, the mechanism of melanocyte survival was investigated further to answer the questions of why melanocytes in hair follicle programmes exhibited premature apoptosis when N-Ras^{lys61} was expressed in melanocytes but anagen melanocytes survived when keratinocyte hyperplasia and then papillomagenesis occurred in parallel. The disruption of the microenvironment in addition to N-Ras^{lys61}/PTEN mutation in melanocytes and resultant melanocytes survival rather than apoptosis, suggested that a survival loop was initiated that by-passed the apoptotic response allowing melanocytes survival and proliferation. That this did not produce overt melanomas suggested that this was provided by keratinocytes disruption to the normal regulation of melanocyte survival factors.

As cited above, microenvironmental regulation of melanocytes specifically by keratinocytes is indispensable to their physiology in addition to the regulation of melanocytes by their own intrinsic factors. One important growth regulatory loop in melanocyte development is mediated by Kit and its ligand SCF (Kit/SCF), which plays an essential role during embryogenesis for melanocyte survival, migration, proliferation and differentiation and may well define the melanocyte stem cell niche, hence the importance of correct Kit/SCF regulation in the development of melanomas (414). Indeed, malignant melanomas and cell lines established from melanoma samples and transformed murine melanocytes do not express detectable Kit, in contrast to readily detectable Kit protein observed in normal human and murine (review in (504)) melanocytes, which suggested Kit loss or a marked reduction either promoted or was a consequence of transformation in

melanocytes (293;294). Moreover, this may have profound effects on metastasis, the most clinically relevant stage in terms of patient survival as while RGP melanocytes retained Kit expression, and thus a relative degree of control by keratinocytes, VGP melanomas lost Kit expression and thus escaped this control (505).

Data shown in Fig 48 and 49 revealed that Kit and its ligand SCF were expressed in a complementary fashion in either normal or hyperplastic skin and papillomas. Kit was expressed mainly in the proliferative layers of epidermal and hair follicle in normal and hyperplastic skin where the strongest expression remained in hair follicles (Fig 48, A and B) and expression levels of Kit were significantly elevated in all papillomas investigated (Fig 48, C-F). That this Kit expression was involved in melanocyte survival in these pigmented papillomas, was suggested by the very strong Kit expression observed throughout the proliferative epidermal papilloma layers where most of the surviving melanocytes were located (Fig 46b, Fig 48) and later confirmed by co-localisation experiments (below, Fig 50), which further verified Kit involvement in pigmented melanocytes survival. Significant increases in SCF expression levels in pigmented papillomas (Fig 49) also indicated that disrupted keratinocytes in the immediate melanocyte microenvironment secreted high levels of SCF and thus could complete a paracrine growth signalling loop for the Kit receptor expression in melanocytes and thus provide a Kit/SCF melanocyte survival loop during tumourigenesis.

To confirm that increased Kit and SCF expression levels were involved in melanocytes survival and not just that this expression was the result of keratinocytes dysregulation in papillomagenesis, double staining of Kit and TRP2 (Figs 50) was performed. The co-localisation of Kit expression with TRP2 in melanocytes in pigmented papillomas confirmed that as disrupted keratinocytes released SCF it provided the ligand to Kit receptor in melanocytes which therefore managed to escape apoptosis driven by the cell

defence system and to result melanocyte survival. This predominantly basal location of melanocytes was in direct agreement with the use of hair follicles derived SP1 papilloma cells as a good feeder for primary melanocytes culture (457) and also the growth of proliferative melanocytes in low calcium conditions alongside SCF–secreting primary keratinocytes, as mentioned in 4.2. However as revealed in Fig 47 and Fig 48, melanocytes and Kit expressing occasionally detected as cluster pattern although these cells also surrounded by some proliferative keratinocytes (Fig 48) and therefore, whether there is an autocrine functional survival loop taking in part in those survived melanocytes is unknown and would be interesting to investigate further.

Melanoma cells and the microenvironment have an intimate relationship and regulate each other in both positive and negative aspects that prevent or assist the process of tumour growth and invasion. On one hand melanoma cell released cues, for instance Nodal, as a potent embryonic morphogen, can induce ectopic formation of the embryonic axis. Its presence in human metastatic tumours but not in normal skin suggested that Nodal may be involved in melanoma pathogenesis. Using zebrafish developmental system as a biosensor for tumour-derived signals study, Topczewska et al revealed that aggressive melanoma cells secrete Nodal and consequently inhibition of Nodal signalling reduces melanoma cell invasiveness, colony formation and tumourigenicity (8). On the other hand, embryonic microenvironmental regulation could re-programme metastatic melanoma cell to lose its tumourigenicity and to assume a neural crest cell-like phenotype(506). The results obtained in this study are consistent with previous studies which indicated that the interaction of melanocytes and the microenvironment is critical to the determination of melanocytes fate. Inducible N-Ras^{lys61} expression and/or PTEN function loss in melanocyte alone failed to produce any melanocytic phenotype in mice until pigmented papilloma induction by N-Ras^{lys61} and PTEN loss in keratinocyte allowed melanocyte to avoid apoptosis and is a classic example of the results of cooperation of melanocyte and its microenvironment.

4.6. Requirement for melanoma transgenic models and the relevance of the models to human disease

Employing transgenic technology, the first transgenic melanoma model was developed in 1991 using the SV40 transforming gene driven by a tyrosinase promoter (441;442). The mice were categorized according to susceptibility of tumour development, with gene copy number delineating the groups. UV exposure promoted the more susceptible lines to develop cutaneous tumours, but aggressive ocular tumours limited investigation of cutaneous tumour development giving a short life span. Thus to study cutaneous tumours they were transplanted to less susceptible mice where they progressed to metastasis. While being the first model to develop melanoma using transgenic technology, proving a targeted model in principle, the SV40 early transform gene is not a melanoma related gene and as lethal ocular melanomas developed prior to cutaneous melanoma this was not a good melanoma mouse model to mimic human melanoma development.

To develop a mouse model closer to human melanoma aetiology, an activated Ras gene (albeit the H-allele) was expressed again under control of a mini-tyrosinase promoter. These H-Ras transgenic mice however developed only dermal melanocytic hyperplasia, a mutated agouti coat and pigmented skin (216) and were again prone to ocular melanoma (507). Nonetheless, following DMBA/TPA or UV treatment, the H-Ras expressing transgenic mice develop nevi as well as cutaneous melanoma, of which more than 40% are metastatic and these results demonstrated a good model for multistage melanoma development (221;222). Melanomas developed in mouse dermis directly and only albino phenotype mice developed cutaneous melanomas, this model was therefore not the fulfilment of melanoma development as a multistage disease in human.

In 1994 CDKN2A, as a candidate tumour suppressor gene, was pinpointed to chromosome 9p21 because of deletions in melanoma cell lines and later identified as a candidate for the

chromosome 9p melanoma susceptibility locus (93;311;313). Initially production of INK4a/ARF knockout mice did not exhibit melanoma susceptibility (316), but $p16^{INK4a}$ specific gene targeting can facilitate melanomagenesis, particularly after exposure to DMBA. The cutaneous melanoma developed in H-Ras expressing transgenic mice following DMBA treatment was also accompanied by either complete or partial loss of the p16 (221). By expressing active oncogenic H-Ras gene in melanocytes in INK4a deficient background mouse, the first melanoma transgenic mouse model without the need of chemical/UV promotion was generated and this model provides the first *in vivo* experimental evidence for a causal relationship between INK4a deficiency and the pathogenesis of melanoma (217). This H-Ras/p16 model was further developed by using the Tet-gene switch system and provided the genetic evidence that H-Ras is important in both the genesis and maintenance of solid tumours (223). The cutaneous melanomas generated from both models are again originated in dermis directly as the other models (221;278) did with no apparent epidermal involvement, which does not mimic human melanoma development. Further H-Ras, an allele of Ras gene, has a much less often mutation rate than its counterpart N-allele in human melanoma although the Tet-gene switch model provided a very good system to be able to control the melanoma development by application/removal of gene-switch inducer.

It is widely recognized that UV is at least partly responsible for the development of melanoma (22;508;509). Using H-Ras expressing transgenic mouse, UV promotion on melanoma development was revealed (222) and in groundbreaking classical work, a later model employing HGF/SF transgenic expression Noonan et al demonstrated that a single neonatal dose of UV was sufficient to induce staged melanocytic lesions (40) and p16/p19 deficiency promoted this UV induced melanomagenesis (349) although chronic UV failed to accelerate melanoma development (510). Furthermore, this model overcame the problem of the previous models that tumours are dermal origin and lack the epidermal

component that characterizes conventional human melanoma (40). By possessing a junctional as well as a dermal component and lesions exhibiting upward migration of single and nested atypical melanocytes into the epidermis, reminiscent of the authors called 'pagetoid' spread that characterizes human RGP melanoma, this model directly mimic the human melanoma multistage aetiology. This model still does not fulfil an ability to mimic the development of RGP to VGP in human, which is the most important clinical event for patient survival (511). Furthermore, HGF expression alone spontaneously produces melanoma alongside many other malignancies, and the embryonic HGF expression is not often seen in melanoma although HGF, ligand of receptor tyrosine kinase c-MET, is a multifunctional regulator of cellular growth, motility and invasiveness including in cutaneous melanoma development (512-514). The involvement of the most abnormal TSG gene (CDKN2A) of melanoma in this model resulted in lethality (349) indicating that constitutive HGF overexpression may cause potential developmental problem beside the effects on melanocytes.

All the previous transgenic mouse melanoma models were developed by expressing H-allele but not the highly mutated N-allele of Ras oncogene in human melanoma specimen, only recently was a mouse model with melanotic and metastatic melanoma produced that recapitulated genetic lesions frequently found in human melanoma. This was achieved by crossing activated N-Ras(Q61K), a hot spot N-Ras mutation in human melanomas, to a CDKN2A deficient mouse (215;225). But again, the N-Ras expressed embryonic not inducible and therefore, the control of N-Ras expression is impossible which limits the full investigation of N-Ras roles during melanoma development, whereas a recent study revealed that Ras functional outcome including downstream genes regulation is expression level-dependent (515).

An 'ideal' animal model would accurately recapitulate human disease particularly the

molecular genetics and the histopathological architecture of human cutaneous melanoma. As a multistage disease of melanoma, the conditional gene switch approach which leaves animal free until inducer treatment to activate regulator and subsequently to switch the target on, may be an 'ideal' transgenic model for melanoma investigation because it allows melanoma related genetic and environmental factors involved at the time as designed to investigate their stage related effect. Up to date, there are only two gene-switch melanoma mouse models available (223;439) which are not yet fulfilment all the criteria for modelling human melanoma development. In both models, melanomas originated in dermis and invade the surrounding tissues locally whereas the epidermal remained intact possibly due to relying on the less common H-Ras activation rather than N-Ras or B-Raf. Also in the more recent model (439), target gene can not be switched off because the regulator Cre was inactivated following the target gene on.

Chin's model seems to be a perfect model if the more specific melanoma related gene such as N-Ras, B-Raf and the other not N-Ras pathway related genes MC1R, MITF etc investigated. Very surprisingly, however, there is no further investigation published up to date using this system. Furthermore, there is not any B-Raf, the most mutated gene in human melanoma, mouse model generated yet by any means neither overexpression alone nor co-operation with TSG genetic deficiency mouse apart from a zebrafish model created by Patton in 2005. In this fish model, active B-Raf (V600E) led to dramatic patches of ectopic melanocytes (authors termed fish nevi ─f-nevi) and induced formation of melanocyte lesions that rapidly developed into invasive melanomas in p53-deficient fish (413) which different from the most of mouse models generated in a CDKN2A deficient background as discussed above. The reason of why there is not a B-Raf mouse model yet given the high incidence V600E mutation reported in human melanoma specimens in 2002 remains unclear, but it is interesting to speculate that activated B-Raf expression in mouse melanocytes induced apoptosis as N-Ras in this model to negate melanoma formation. If

this is true how can we modify the mouse transgenic expression profile to overcome such a surveillance mechanism and to generate an ‘ideal’ mouse model to mimic human melanoma development aetiology? This could be a big challenge to scientists who are studying the melanoma molecular aetiology employing mouse transgenic models.

One feature created by experiments designed to assess the effects of destabilising interactions between melanocytes and keratinocytes in this model was the development of pigmented tumours during N-Ras/PTEN-mediated papillomagenesis. These murine tumours may shed light on the aetiology of pigmented benign lesions in human skin termed seborrheic keratoses (SK), a benign skin tumour neither nevi nor melanoma. SKs are a keratinocyte-derived, benign acanthotic skin tumour that never progresses to an invasive phenotype, which exhibit several histological sub-types (5). Seborrheic keratoses progress from an initial hyper-pigmented maculae to the characteristic plaque (516) and eventually exhibit a wart-like papilloma appearance, although no HPV involvement has been recorded (517). Histologically, prominent melanocytes and their dendritic processes are usually quite obvious and scattered individually throughout the section, and dendritic melanocytes presented in the basal and suprabasal layers (516;518;519) in melanoacanthoma, one of variant of seborrheic keratoses. These lesions can have dendritic melanocytes in the basal layers (Fig 46b and 47 E), as appeared in human oral melanoacanthoma (6). Thus it may be that the expression of N-Ras and Δ5PTEN in melanocytes and keratinocytes creating the SCF/Kit survival loop during papillomagenesis (Fig 46a) provides a microenvironment that similar to aetiology of such seborrheic keratoses in humans.

Whether this aetiology depends on the genes mutated or simply establishment of a survival loop for proliferative melanocytes (e.g. SCF /Kit or HGF/Met (520)) is unclear and there are few studies exploring the relationship of gene mutation, expression and SK development. Among the genes studied in SKs, some show a similar expression profile to that of normal skin, such as p120 catenin (521), proliferating cell nuclear antigen (PCNA)

(522), proto-oncogenes c-fos and c-jun,(523), p63 (524), E-cadherin and p-STAT3 (525); while the others show a different expression pattern compared to the normal skin. p16 expressed in all keratinocytes from SK lesions but only in granular cells of normal keratinocytes in culture (526). p53 and Bcl-2 expression is higher in SK than in normal skin but significant lower than in SCC in keratinocytes (527) although p53 binding protein-1 remained unchanged in SK (528) while Bcl-2 may be increased as an anti-apoptotic mechanism (529). Strong expression of the cyclin-dependent kinase inhibitor p27(KIP1) in SK revealed that p27(KIP1), which is regulated by PTEN via cyclin E, may be a major mechanism controlling keratinocyte proliferation (530). Similarly a role for FGF3 mutation has been confirmed by a series studies both in transgenic model (531) and in human SK samples (532-535) but without intra-individual hot spot (533) revealed. The mechanism for the high rate of somatic FGFR3 mutations in SK remains elusive although UV may play a potential role, especially in the R248C mutations (535). FGF3b bears transforming ability by transfection of NIH-3T3 cells with a mutated form S249C (536) but FGF3 mutations obviously do not account for all papillary urothelial cancers and acanthotic skin tumours implied that further genes must be involved in tumourigenesis (537;538). Downstream pathways of FGFR3 such as the PI-3K/PTEN/Akt or the Ras/Raf/MAPK pathway are therefore suggested to be promising candidates (537). Linking this idea to the data presented here together with the previous studies that revealed a role of Ras expression in SK development (539;540), which imply that deregulated Ras expression in keratinocytes may contribute to SK development, either independently or in co-operation with FGF pathway, although further studies will be necessary to confirm this hypothesis.

A more recent interesting study that links to PTEN functions, revealed that PIK3CA (p110 α subunit of PIK3) mutation in seborrheic keratoses bears no relevant risk of progression to malignancy (541). This finding and the N-Ras/PTEN results reported here in the melanoma model and lack of progression in the pigmented papilloma development, show that other genetic alterations must occur to progress to a more malignant phenotype. Our

results are also consistent with previous studies that specific mutations may activate protective cellular mechanisms which act as a barrier for tumour progression (542). For instance employing the doxycycline-inducible transgenic mice that permit K-Ras activation to be titrated, authors found that physiological levels of Ras stimulate cellular proliferation and mammary epithelial hyperplasia and but surprisingly, high levels of Ras activation induced a CDKN2A-dependent cellular senescence (515). A three-stage model for Ras-induced tumourigenesis was thus suggested that consists of an initial Ras mutation, overexpression of the activated Ras allele and evasion of p53-CDKN2A-dependent senescence checkpoints (515). Hence failed melanoma production in our model is supportive for this 3-stage theory because the last step of Ras-independent senescence checkpoint is not interrupted in our model. These studies support the conclusion that introduction of p16/p19 deficient mice in this system may be essential for production the early stages of a useful model to investigate multistage melanoma complete with junctional pathology in the epidermis, to then investigate progression from RGP to VGP, as there is no model available yet able to model this most significant change in relatively benign to highly malignant/metastatic melanoma.

Another lesser phenotype developed in this murine model was the loss of hair at treated sites, although it may be possible that inducible expression of N-Ras in the follicle, gave rise to an immune response. One such disease in humans is Alopecia Areata (AA), an autoimmune disease where white blood cells attack the hair follicles. This mainly depends on an individual's genetic makeup in combination with other factors that trigger AA (543;544). Apart from a familial occurrence of AA (545) where the pattern of familiality suggests that the genetic basis is multifactorial (546), the aetiopathogenesis of AA is poorly understood (543;544). Although AA is thought to be a tissue-specific autoimmune disease directed against the hair follicle, an association with other autoimmune diseases has been reported (547-549). To date, only the involvement of the major histocompatibility

complex (MHC) has been confirmed by means of independent replication (550-552) and it has been postulated that various genes related to immune response are associated with AA.

Although the only confirmation is the involvement of the MHC in AA aetiology, there are a few other immuno-related genes have also been suggested the relationships with AA development. The non-synonymous C1858T substitution in the PTPN22 gene, a gene encodes lymphoid protein tyrosine phosphatase and is associated with susceptibility to autoimmune disorders, may have an influence on the severity of AA and further evidence provided for autoimmunity as an aetiological factor in this disorder (553). Freyschimidt-Paul's study revealed an essential requirement for interferon-gamma-mediated Th1 activation in the induction of AA (554). Loss-of-function mutations in the filaggrin gene may be considered as promising candidates in AA because when AA occurs in conjunction with filaggrin gene-associated atopic disorder, the clinical presentation of AA may be more severe (555). Substance P (SP) plays a critical role in the cutaneous neuroimmune network and influences immune cell functions through the neurokinin-1 receptor (NK-1R) may also serve as important regulators in the molecular signalling network modulating inflammatory response in autoimmune hair loss (556). Ran, a Ras related nuclear protein, may play a role in shrimp immunity against virus infection (557) and N-Ras or K-Ras inhibition increases the number and enhances the function of Foxp3 regulatory T cells (558). A recent more interesting study revealed that activities of Rho/Ras family GTPases were reduced by lovastatin while myelin repair is induced in experimental autoimmune encephalomyelitis (EAE) (559). These recent studies as well as our finding of Ras-induced hair loss imply that oncogenic Ras not only causes carcinogenesis and developmental diseases (154;155) but may also be related to development of some immune diseases like AA, although this hypothesis is at its initial stage and many further studies need to be done to verify it.

The hair loss found in this murine study may bear some similarities to AA in humans, but

it is not a model designed to study this disease, nor does it resemble androgenetic alopecia (AGA) —a disease is characterized by a defined pattern of hair loss from the scalp (560), neither congenital atrichia (AUC) —a form of isolated alopecia with an autosomal recessive mode of inheritance and the patients are born with normal hair but this is shed almost completely during the first weeks or months of life and never re-grows (546). It may simply be a feature of the inducible N-Ras expression in melanocytes, induces an immune response that on occasion can attack the specific target structure where the apoptotic melanocytes reside —i.e. anagen hair follicles, and the hair cycle re-entry was subsequently arrested. Another similar feature of AA in humans to this murine model is that the hair may re-grow white and very fine (543;544). In N-Ras mice, fine hairs can grow back although these areas are still mainly ‘bare’, whilst the hair generally grows back white in other areas (Fig 42) which may be the results of melanocytes apoptosis induced by Ras expression as discussed at section 4.4. As in the hairless areas of human AA (543), in N-Ras mice there was no actual loss of hair follicles (i.e. the "root") in these fine white hairs (Fig 43). Therefore, this unexpected hair loss produced in this study may offer a surprise model for the study of AA in human.

4.7. Summary and future work

4.7.1. Summary

All current available Ras transgenic models either employ constitutive expression of oncogenic or/and null TSGs, often on a CDKN2A background, through embryonic stages which only happens in melanoma prone families in humans and often utilise the H-Ras allele which is seldom mutated in human melanomas. The exact gene-switch models to accurately mimic this human disease therefore still need to be developed. In addition, although PTEN biological function loss lacks promotion of N-Ras initiated tumourigenesis and inducible N-Ras expression in adult mouse triggered normal body defence system to overcome its anti-apoptotic mechanism to result melanocyte apoptosis, the identification of such protective mechanisms may provide further insights to identify new targets that encourage these sentinel pathways in novel therapeutic approaches to prevent human melanomagenesis. This initial early model provides the foundations and technical insights for the successful development of further inducible gene-switch approaches by introducing additional melanoma relevant molecules into the system.

The eye phenotypes developed in this model were a consequence of technical needs to ensure that the gene switch was working *in vivo* and unlike other models are not expected to occur in straight forward topical administration. Such additional phenotypes are not good for a cutaneous melanoma model because they reduce viability and would compromise multistage compound mice attempting to asses several mutations in a stage specific manner. Indeed, this was a real problem for the early models developed in Mintz (441;442) and Merlino (510) labs resulting in early death or disease in alternate tissue(s). Even in the recent Ackermann model, phenotypic eyes were also produced by constitutive N-Ras expression although no uveal melanoma developed (215). The phenotypic eyes displayed in our inducible model is very similar to those displayed in Ackermann model and resulted in the termination of these experiments given our operating licence, however,

we concluded that the eye problem in our model was a result of systemic Ru486 IP injection rather than topical administration and thus would be eliminated by withdrawal of IP injection. Furthermore, only 2 out of 5 expressers were viable for analysis in the Ackermann model indicating that constitutive N-Ras expressing resulted in developmental problems, which is avoidable in our inducible system because N-Ras would only be expressed in adults, once the anti-Ras apoptosis mechanism could be overcome.

The caspase-3 detection in those N-Ras expression and/or PTEN loss skins show that there is a defence system in normal mouse body to protect melanocyte from oncogenic Ras protein expression, which is consistent with the concept of that oncogenic protein is not really well tolerated by normal body, whereas constitutive N-Ras expressing resulted in melanoma formation in adult and/or developmental defects (215). This finding could be important for causal role study of oncogenic protein expression in cancer development because the level and time of oncogene expression in specific contexts may be important for the determination of eventual outcome. For instance, discovery of caspase-3 dependant apoptosis *in vivo* melanocyte differs from MEK caspase-independent pathway *in vitro* induced by Ras, possibly indicates factors of MEKs vs. melanocytes; the different alleles employed or possibly that Ras simply plays different roles between *in vivo* and *in vitro,* as revealed for PTEN gene functions in this study.

PTEN did promote N-Ras tumourigenesis *in vitro* as discussed above, being another difference of *in vitro* from *in vivo* experimentation and the results are consistent with the finding of that PTEN ablation more often being detected in cell lines than in solid tumours and STC. The reason that PTEN loss lacked synergism with N-Ras initiation is possibly due to functional redundancy being on the same signalling pathway it provides the same neoplastic hit at this stage unlike CDNK2A deletion which provides different genetic ablation of p16/p19 and cross-talk to numerous synergistic Ras pathways e.g. p53, Rb, cell

cycle regulators such as cyclin D1. This is supported by colony melanocytes promoted by PTEN function loss *in vitro* were not immortalised which is consistent with melanoma induction failure in a double genes (N-Ras/PTEN) ablation line *in vivo*. It appears most likely that at this stage, the combination of PTEN loss and N-Ras activation could not overcome a sentinel mechanism of caspease-3 mediated apoptosis. Thus, if this was compromised in other conditions, the observations of N-Ras cooperation with PTEN may prove to be positive, as in papillomagenesis. However the pigmented papillomas obtained from the current microenvironment disruption, appear to depend on establishment of a paracrine Kit/SCF survival loop and N-Ras expression alongside PTEN loss gives hyperplastic melanocytes. Even so this may be relevant to the human condition, because the data suggest that this kind of pigmented papilloma may develop when papillomagenesis and anagen melanocytes exist in parallel. Thus in humans, pigmented papillomas may arise when tumourigenesis occurs in parallel to hair follicle growth and follicular melanocyte survival is maintained by Kit and SCF expression allowing this survival loop.

4.7.2. Future work

All other Ras melanoma models employed a CDKN2A deficient background as well the necessity of TSG deficiency for tumourigenesis from other studies discussed above and therefore, introduction of the p16/19 floxed mice into this model is the primary task of future work to mimic human disease. PTEN redundancy to N-Ras in this model does not rule out its cooperation at the later stage of melanoma development and thus, the role of PTEN and its synergism are also of interest in the future CDKN2A deficient models, specifically to investigate the different roles at different stages of melanomagenesis.

The increased size of promoter containing additional elements to enhance regulator expression and melanocyte specificity is another point to define in future work, since the same allele of H-Ras expressed from different sized promoters displayed different expression patterns in mouse skin and subsequently melanomas at different locations and with different histology. From this model, another interesting study to undertake is whether increased N-Ras expression under longer versions of the Tyr promoter would also activate this mouse defence mechanism to either overcome it or remain susceptible to it as revealed in this model. If so, this result may produce the further evidence for the study by Sarkisian and colleagues in which they found that near physiological levels of Ras (K-allele) led to hyperproliferation of epithelial cells whilst high levels of Ras expression led to cell senescence but not in CDKN2A deficient mice (515), by using the longer version promoter in regulator Cre it may result in higher N-Ras expression as discussed at section 4.1 to increase Ras expression level *in vivo.* If not will this still proceed through a caspase-3 dependant manner or different manner if apoptosis is induced, i.e. is caspase-3 mediated apoptosis a default programme to prevent the initiation of melanoma?

p53 gene is the most mutated TSG in human cancers, however, mutational analyses by many groups have reported a complete absence or very low incidence of point mutation or

allelic loss of p53 in surgical specimens of primary and metastatic melanomas, while others have estimated the incidence of p53 mutation to be 15–25% of primary and metastatic samples (561-563). Current data collected in Sanger centre in UK also revealed a reasonable high mutation rate in malignant melanoma (564). Therefore, the role of p53 in melanoma remained still controversial. Indeed, p53 heterozygous and null mice harbouring H-Ras did develop cutaneous melanomas which are very similar with those developed in p19 mull mice (565), whereas p16 remained intact. The results indicated that p19-p53 functions as a melanoma suppression axis *in vivo*. In zebrafish expressing the most common B-Raf mutant (V600E) under the control of the melanocyte promoter (see below), led to dramatic patches of ectopic melanocytes in wild type p53 but B-Raf induced melanocyte lesions rapidly developed into invasive melanoma in a p53 deficient background (413). These models implied the functional roles of p53 gene in melanoma development and therefore, the introduction of p53 mouse into this model could be interesting too and the difference (if any) compared to p16 and p19 mice.

Kit/SCF loops may play different roles at different stages or in different contexts. Kit/SCF provided a survival function in those pigmented papilloma melanocytes and is essential to melanoblast migration and survival during embryogenesis. Kit function is lost or greatly reduced in later stage melanoma(505), which significantly appears to be the facts underlying the melanocyte stem cell niche (53) and thus could lead to the rise of a melanoma stem cell, or at least cells that no longer are regulated by keratinocyte SCF signalling. Thus, conditional deletion of Kit locus would be really interesting to introduce in this model for the study of gene function patterns at difference stages of melanoma development.

Melanocytes survival from apoptosis by disruption of its microenvironment but no further progression from dysregulated by N-Ras^{lys61} expressing and PTEN aberrant to produce

melanoma is interesting. As cells release cues to microenvironment and numerous growth factor signalling loops are overexpressed to promote tumour progression, it is likely that many other intrinsic (seed) and extrinsic (soil) factors (e.g. Nodal, Notch signalling) are involved in this survival model and currently under intensive study. By secreting Nodal factor, a potent embryonic morphogen in melanoma cells but not in normal human skin, melanoma cells modulated its immediate microenvironment to induce ectopic formation of the embryonic axis when transplant melanoma cells into blastula-stage embryo (8), and its expression can be induced by Notch signalling (446;566;567). The Notch signalling pathway is simple but other signalling pathways cross-talk with Notch signalling appears to be extraordinarily complex (567). Involvement of Notch in cancers was first highlighted in human T-cell leukaemia in which the aberrant Notch signalling promotes tumourigenesis (568). Notch1 directly stimulates expression of the cell-cycle regulator Waf1 in primary mouse keratinocytes (569), which negatively links Notch1 and Wnt signalling (570) and was downregulated by p53 homology p51/p63 (571). Notch signalling pathway was also identified to promote primary melanoma progression through regulation of PIP3-Akt pathway activities and expression of N-Cadherin (572). Notch signalling, acting through Hes1, plays a crucial role in the survival of immature melanoblast and melanocyte stem cell by preventing initiation of apoptosis (573). However, there is mounting evidence that Notch signalling is not exclusively oncogenic. It can instead function as a tumour suppressor (574;575). Whether Nodal, Notch signalling and other cell survival factors would induce overt melanoma in this inducible model by cross-talk to the Ras pathway would be also very interesting to investigate.

While a redundancy was apparently created *in vivo*, the results *in vitro* verified that Δ5PTEN cooperated with N-Ras initiated tumourigenesis, which was consistent with the previous reports in cell lines. However, despite the fact that these cells were viable for months they eventually senesced, implying that these insults were similar but insufficient

to achieve immortalisation, consistent with the redundancy observed *in vivo* between PTEN loss and N-Ras genes. Thus by introducing UVR-B irradiation, a well know environment risk factor cause DNA damage in melanocyte (66), Δ5PTEN/N-Ras transformed cells may gain an immortalised potential for further studies. For instance, UVR also induces melanocyte apoptosis and alpha-MSH has the anti-apoptotic activity (66), while α-MSH's immunosuppressive effects in humans through MC1R on monocyte and B lymphocyte (31) involves beta-defensin 103 (CBD103), a protein family previously implicated in innate immunity, that binds with high affinity to the MC1R, and has a simple and strong effect on pigment type-switching in transgenic mice (397). Thus these MC1R pathway related factors, would also be of significant interest to be introduced in this model and generate a very good melanogenesis model, separate to that of the Ras/PTEN pathway, to explore the potential cross-talk of different pathways involved in melanoma development.

The development of appropriate models may require several other genetic aberrations which function on a different signalling pathway to cross-talk with Ras, possibly to overcome protective responses and develop cutaneous melanoma. The other genes which function on the Ras signalling pathway e.g. B-Raf, PTEN and those genes (e.g. Kit/SCF, Nodal, Notch, b-FGF, HGF etc) involved in melanocyte/melanoma development, including survival, migration and differentiation would also be of interest to investigate their roles and to develop successful highly flexible inducible models, specifically to delineate the possible different roles underlying the developmental stages of melanoma and identify new therapeutic targets.

Reference List

(1) Walker GJ, Hayward NK. Pathways to melanoma development: Lessons from the mouse. Journal of Investigative Dermatology 2002; 119(4):783-792.

(2) Ngan ES, Ma ZQ, Chua SS, DeMayo FJ, Tsai SY. Inducible expression of FGF-3 in mouse mammary gland. Proc Natl Acad Sci U S A 2002; 99(17):11187-11192.

(3) Parker SL, Tong T, Bolden S, Wingo PA. Cancer statistics, 1997. CA Cancer J Clin 1997; 47(1):5-27.

(4) Wallace H.Clark J. Pigmented solar keratoses-Melanokeratinocytomas. human cutaneous melanoma. 1979: 45-46.

(5) Grace F.Kao. Benign Tumours of the Epidermis. In: Evan R.Farmer, Antoinette F.Hood, editors. Pathology of the Skin. Appleton & Lange, 1990: 533-549.

(6) Michael J.Imber, Martin C.Mihm J. Benign Melanocytic Tumours. In: Evan R.Farmer, Antoinette F.Hood, editors. Pathology of the Skin. Appleton & Lange, 1990: 663-683.

(7) Eisen T, Easty DJ, Bennett DC, Goding CR. The POU domain transcription factor Brn-2: elevated expression in malignant melanoma and regulation of melanocyte-specific gene expression. Oncogene 1995; 11(10):2157-2164.

(8) Topczewska JM, Postovit LM, Margaryan NV, Sam A, Hess AR, Wheaton WW et al. Embryonic and tumorigenic pathways converge via Nodal signaling: role in melanoma aggressiveness. Nature Medicine 2006; 12(8):925-932.

(9) Carr J, Mackie RM. Point mutations in the N-ras oncogene in malignant melanoma and congenital naevi. Br J Dermatol 1994; 131(1):72-77.

(10) Ichii-Nakato N, Takata M, Takayanagi S, Takashima S, Lin J, Murata H et al. High frequency of BRAFV600E mutation in acquired nevi and small congenital nevi, but low frequency of mutation in medium-sized congenital nevi. J Invest Dermatol 2006; 126(9):2111-2118.

(11) Poynter JN, Elder JT, Fullen DR, Nair RP, Soengas MS, Johnson TM et al. BRAF and NRAS mutations in melanoma and melanocytic nevi. Melanoma Res 2006; 16(4):267-273.

(12) Indsto JO, Kumar S, Wang L, Crotty KA, Arbuckle SM, Mann GJ. Low prevalence of RAS-RAF-activating mutations in Spitz melanocytic nevi compared with other melanocytic lesions. J Cutan Pathol 2007; 34(6):448-455.

(13) Edlundh-Rose E, Egyhazi S, Omholt K, Mansson-Brahme E, Platz A, Hansson J et al. NRAS and BRAF mutations in melanoma tumours in relation to clinical characteristics: a study based on mutation screening by pyrosequencing. Melanoma Res 2006; 16(6):471-478.

(14) Healy E, Belgaid CE, Takata M, Vahlquist A, Rehman I, Rigby H et al. Allelotypes of primary cutaneous melanoma and benign melanocytic nevi.

Cancer Res 1996; 56(3):589-593.

(15) Clark WH. From the Melanocyte to Melanoma to Tumor Biology. 1994.

(16) Clark WH, Jr., Ainsworth AM, Bernardino EA, Yang CH, Mihm CM, Jr., Reed RJ. The developmental biology of primary human malignant melanomas. Semin Oncol 1975; 2(2):83-103.

(17) Clark WH, Jr., Tucker MA. Problems with lesions related to the development of malignant melanoma: common nevi, dysplastic nevi, malignant melanoma in situ, and radial growth phase malignant melanoma. Hum Pathol 1998; 29(1):8-14.

(18) Ackerman AB. Disagreements about classification of malignant melanomas. Am J Dermatopathol 1982; 4(5):447-452.

(19) Ackerman AB, Mihara I. Dysplasia, dysplastic melanocytes, dysplastic nevi, the dysplastic nevus syndrome, and the relation between dysplastic nevi and malignant melanomas. Hum Pathol 1985; 16(1):87-91.

(20) Ackerman AB. Melanoma in situ and matters that transcend it. Hum Pathol 1998; 29(1):4-5.

(21) Mackie RM, Bray CA, Hole DJ, Morris A, Nicolson M, Evans A et al. Incidence of and survival from malignant melanoma in Scotland: an epidemiological study. Lancet 2002; 360(9333):587-591.

(22) Jemal A, Devesa SS, Hartge P, Tucker MA. Recent trends in cutaneous melanoma incidence among whites in the United States. J Natl Cancer Inst 2001; 93(9):678-683.

(23) Jhappan C, Noonan FP, Merlino G. Ultraviolet radiation and cutaneous malignant melanoma. Oncogene 2003; 22(20):3099-3112.

(24) WHO. How comman is skin cancer. WHO 2008; http://www.who.int/uv/faq/skincancer/en/index1.html.

(25) AAD. Melanoma Fact Sheet. American Academy of Dermatology Web 2008; http://www.aad.org/public/News/DermInfo/MelanomaFAQ.htm.

(26) Poole Catherine M, DuPont Guerry IV. Melanoma-Prevention, Detection and Treatment. New Haven & London: Yale University Press, 1998.

(27) Mackie RM, Hole D, Hunter JA, Rankin R, Evans A, McLaren K et al. Cutaneous malignant melanoma in Scotland: incidence, survival, and mortality, 1979-94. The Scottish Melanoma Group. BMJ 1997; 315(7116):1117-1121.

(28) Melia J. Changing incidence and mortality from cutaneous malignant melanoma. BMJ 1997; 315(7116):1106-1107.

(29) Roberts DL, Anstey AV, Barlow RJ, Cox NH, Newton Bishop JA, Corrie PG et al. U.K. guidelines for the management of cutaneous melanoma. Br J Dermatol 2002; 146(1):7-17.

(30) Abdel-Malek ZA, Knittel J, Kadekaro AL, Swope VB, Starner R. The Melanocortin 1 Receptor and the UV Response of Human Melanocytes-A Shift

in Paradigm. Photochem Photobiol 2008.

(31) Cooper A, Robinson SJ, Pickard C, Jackson CL, Friedmann PS, Healy E. Alpha-melanocyte-stimulating hormone suppresses antigen-induced lymphocyte proliferation in humans independently of melanocortin 1 receptor gene status. J Immunol 2005; 175(7):4806-4813.

(32) Smith AG, Luk N, Newton RA, Roberts DW, Sturm RA, Muscat GE. Melanocortin-1 receptor signalling markedly induces the expression of the NR4A nuclear receptor subgroup in melanocytic cells. J Biol Chem 2008.

(33) Valverde P, Healy E, Jackson I, Rees JL, Thody AJ. Variants of the melanocyte-stimulating hormone receptor gene are associated with red hair and fair skin in humans. Nat Genet 1995; 11(3):328-330.

(34) Valverde P, Healy E, Sikkink S, Haldane F, Thody AJ, Carothers A et al. The Asp84Glu variant of the melanocortin 1 receptor (MC1R) is associated with melanoma. Hum Mol Genet 1996; 5(10):1663-1666.

(35) Beddingfield FC. The melanoma epidemic: Res ipsa loquitur. Oncologist 2003; 8(5):459-465.

(36) Holman CD, Armstrong BK, Heenan PJ, Blackwell JB, Cumming FJ, English DR et al. The causes of malignant melanoma: results from the West Australian Lions Melanoma Research Project. Recent Results Cancer Res 1986; 102:18-37.

(37) Perlis C, Herlyn M. Recent advances in melanoma biology. Oncologist 2004; 9(2):182-187.

(38) Weinstock MA, Colditz GA, Willett WC, Stampfer MJ, Bronstein BR, Mihm MC et al. Nonfamilial Cutaneous Melanoma Incidence in Women Associated with Sun Exposure Before 20 Years of Age. Pediatrics 1989; 84(2):199-204.

(39) Hacker E, Irwin N, Muller HK, Powell MB, Kay G, Hayward N et al. Neonatal ultraviolet radiation exposure is critical for malignant melanoma induction in pigmented Tpras transgenic mice. J Invest Dermatol 2005; 125(5):1074-1077.

(40) Noonan FP, Recio JA, Takayama H, Duray P, Anver MR, Rush WL et al. Neonatal sunburn and melanoma in mice - Severe sunburn in newborn, but not adult, mice is linked with melanoma in later life. Nature 2001; 413(6853):271-272.

(41) Marks R. Campaigning for melanoma prevention: a model for a health education program. J Eur Acad Dermatol Venereol 2004; 18(1):44-47.

(42) Karlsson PM, Fredrikson M. Cutaneous malignant melanoma in children and adolescents in Sweden, 1993-2002: the increasing trend is broken. Int J Cancer 2007; 121(2):323-328.

(43) Staples MP, Elwood M, Burton RC, Williams JL, Marks R, Giles GG. Non-melanoma skin cancer in Australia: the 2002 national survey and trends since 1985. Med J Aust 2006; 184(1):6-10.

(44) Coory M, Baade P, Aitken J, Smithers M, McLeod GR, Ring I. Trends for in situ and invasive melanoma in Queensland, Australia, 1982-2002. Cancer

Causes Control 2006; 17(1):21-27.

(45) Nola I, Kruslin B, Muller D, Oremovic L, Belicza M. The rise in melanoma incidence in Croatia. Acta Dermatovenerol Croat 2002; 10(1):3-7.

(46) Wang SQ, Halpern AC. Management of cutaneous melanoma: a public health and individual patient care perspective. Adv Dermatol 2007; 23:81-98.

(47) Kelly JW, Henderson MA, Thursfield VJ, Slavin J, Ainslie J, Giles GG. The management of primary cutaneous melanoma in Victoria in 1996 and 2000. Med J Aust 2007; 187(9):511-514.

(48) Fuchs E, Green H. Changes in keratin gene expression during terminal differentiation of the keratinocyte. Cell 1980; 19(4):1033-1042.

(49) Moll R, Moll I, Wiest W. Changes in the pattern of cytokeratin polypeptides in epidermis and hair follicles during skin development in human fetuses. Differentiation 1982; 23(2):170-178.

(50) Hennings H, Michael D, Cheng C, Steinert P, Holbrook K, Yuspa SH. Calcium regulation of growth and differentiation of mouse epidermal cells in culture. Cell 1980; 19(1):245-254.

(51) Westerhof W. The discovery of the human melanocyte. Pigment Cell Res 2006; 19(3):183-193.

(52) Hadley ME, Quevedo WC, Jr. Vertebrate epidermal melanin unit. Nature 1966; 209(30):1334-1335.

(53) Nishimura EK, Jordan SA, Oshima H, Yoshida H, Osawa M, Moriyama M et al. Dominant role of the niche in melanocyte stem-cell fate determination. Nature 2002; 416(6883):854-860.

(54) Jimbow K, Salopek TG, Dixon WT, Searles GE, Yamada K. The epidermal melanin unit in the pathophysiology of malignant melanoma. Am J Dermatopathol 1991; 13(2):179-188.

(55) Nordlund JJ. The melanocyte and the epidermal melanin unit: an expanded concept. Dermatol Clin 2007; 25(3):271-81, vii.

(56) Hirobe T. Control of Melanocyte Proliferation and Differentiation in the Mouse Epidermis. Pigment Cell Research 1992; 5(1):1-11.

(57) Hirobe T. Structure and Function of Melanocytes - Microscopic Morphology and Cell Biology of Mouse Melanocytes in the Epidermis and Hair Follicle. Histology and Histopathology 1995; 10(1):223-237.

(58) Stenn KS, Paus R. Controls of hair follicle cycling. Physiol Rev 2001; 81(1):449-494.

(59) Tobin DJ, Paus R. Graying: gerontobiology of the hair follicle pigmentary unit. Exp Gerontol 2001; 36(1):29-54.

(60) Kunisada T, Yoshida H, Yamazaki H, Miyamoto A, Hemmi H, Nishimura E et al. Transgene expression of steel factor in the basal layer of epidermis promotes survival, proliferation, differentiation and migration of melanocyte precursors.

Development 1998; 125(15):2915-2923.

(61) Peters EM, Tobin DJ, Botchkareva N, Maurer M, Paus R. Migration of melanoblasts into the developing murine hair follicle is accompanied by transient c-Kit expression. J Histochem Cytochem 2002; 50(6):751-766.

(62) Slominski A, Paus R. Melanogenesis is coupled to murine anagen: toward new concepts for the role of melanocytes and the regulation of melanogenesis in hair growth. J Invest Dermatol 1993; 101(1 Suppl):90S-97S.

(63) Tobin DJ, Hagen E, Botchkarev VA, Paus R. Do hair bulb melanocytes undergo apoptosis during hair follicle regression (catagen)? J Invest Dermatol 1998; 111(6):941-947.

(64) Commo S, Bernard BA. Melanocyte subpopulation turnover during the human hair cycle: an immunohistochemical study. Pigment Cell Res 2000; 13(4):253-259.

(65) Mancuso M, Leonardi S, Tanori M, Pasquali E, Pierdomenico M, Rebessi S et al. Hair cycle-dependent basal cell carcinoma tumorigenesis in Ptc1neo67/+ mice exposed to radiation. Cancer Res 2006; 66(13):6606-6614.

(66) Bohm M, Wolff I, Scholzen TE, Robinson SJ, Healy E, Luger TA et al. alpha-Melanocyte-stimulating hormone protects from ultraviolet radiation-induced apoptosis and DNA damage. J Biol Chem 2005; 280(7):5795-5802.

(67) Healy E, Flannagan N, Ray A, Todd C, Jackson IJ, Matthews JN et al. Melanocortin-1-receptor gene and sun sensitivity in individuals without red hair. Lancet 2000; 355(9209):1072-1073.

(68) Diffey BL, Healy E, Thody AJ, Rees JL. Melanin, melanocytes, and melanoma. Lancet 1995; 346(8991-8992):1713.

(69) Healy E, Reynolds NJ, Smith MD, Campbell C, Farr PM, Rees JL. Dissociation of erythema and p53 protein expression in human skin following UVB irradiation, and induction of p53 protein and mRNA following application of skin irritants. J Invest Dermatol 1994; 103(4):493-499.

(70) Kunisada T, Yamazaki H, Hirobe T, Kamei S, Omoteno M, Tagaya H et al. Keratinocyte expression of transgenic hepatocyte growth factor affects melanocyte development, leading to dermal melanocytosis. Mech Dev 2000; 94(1-2):67-78.

(71) Sulaimon SS, Kitchell BE. The biology of melanocytes. Vet Dermatol 2003; 14(2):57-65.

(72) Wehrle-Haller B. The role of Kit-ligand in melanocyte development and epidermal homeostasis. Pigment Cell Res 2003; 16(3):287-296.

(73) Cohen Y, Rosenbaum E, Begum S, Goldenberg D, Esche C, Lavie O et al. Exon 15 BRAF mutations are uncommon in melanomas arising in nonsun-exposed sites. Clin Cancer Res 2004; 10(10):3444-3447.

(74) Hearing VJ. Biochemical control of melanogenesis and melanosomal organization. J Investig Dermatol Symp Proc 1999; 4(1):24-28.

(75) Nakamura M, Tobin DJ, Richards-Smith B, Sundberg JP, Paus R. Mutant laboratory mice with abnormalities in pigmentation: annotated tables. J Dermatol Sci 2002; 28(1):1-33.

(76) Gallagher CH, Canfield PJ, Greenoak GE, Reeve VE. Characterization and histogenesis of tumors in the hairless mouse produced by low-dosage incremental ultraviolet radiation. J Invest Dermatol 1984; 83(3):169-174.

(77) Besaratinia A, Kim SI, Pfeifer GP. Rapid repair of UVA-induced oxidized purines and persistence of UVB-induced dipyrimidine lesions determine the mutagenicity of sunlight in mouse cells. FASEB J 2008.

(78) Muller HK, Malley RC, McGee HM, Scott DK, Wozniak T, Woods GM. Effect of UV radiation on the neonatal skin immune system- implications for melanoma. Photochem Photobiol 2008; 84(1):47-54.

(79) Thomas J, Liu T, Cotter MA, Florell SR, Robinette K, Hanks AN et al. Melanocyte expression of survivin promotes development and metastasis of UV-induced melanoma in HGF-transgenic mice. Cancer Res 2007; 67(11):5172-5178.

(80) De Fabo EC. Initial studies on an in vivo action spectrum for melanoma induction. Prog Biophys Mol Biol 2006; 92(1):97-104.

(81) de Gruijl FR, van Kranen HJ, van Schanke A. UV exposure, genetic targets in melanocytic tumors and transgenic mouse models. Photochem Photobiol 2005; 81(1):52-64.

(82) De Fabo EC, Noonan FP, Fears T, Merlino G. Ultraviolet B but not ultraviolet A radiation initiates melanoma. Cancer Res 2004; 64(18):6372-6376.

(83) Williams M, Ouhtit A. Towards a Better Understanding of the Molecular Mechanisms Involved in Sunlight-Induced Melanoma. J Biomed Biotechnol 2005; 2005(1):57-61.

(84) Lens MB, Dawes M. Global perspectives of contemporary epidemiological trends of cutaneous malignant melanoma. British Journal of Dermatology 2004; 150(2):179-185.

(85) Hallberg O, Johansson O. Malignant melanoma of the skin - not a sunshine story! Medical Science Monitor 2004; 10(7):CR336-CR340.

(86) McCarthy WH. The Australian experience in sun protection and screening for melanoma. J Surg Oncol 2004; 86(4):236-245.

(87) Daniotti M, Oggionni M, Ranzani T, Vallacchi V, Carnpi V, Di Stasi D et al. BRAF alterations are associated with complex mutational profiles in malignant melanoma. Oncogene 2004; 23(35):5968-5977.

(88) Tucker MA, Goldstein AM. Melanoma etiology: where are we? Oncogene 2003; 22(20):3042-3052.

(89) Aitken J, Welch J, Duffy D, Milligan A, Green A, Martin N et al. CDKN2A variants in a population-based sample of queensland families with melanoma. Journal of the National Cancer Institute 1999; 91(5):446-452.

(90) Soufir N, Avril MF, Chompret A, Demenais F, Bombled J, Spatz A et al. Prevalence of p16 and CDK4 germline mutations in 48 melanoma- prone families in France. Human Molecular Genetics 1998; 7(2):209-216.

(91) Zuo L, Weger J, Yang QB, Goldstein AM, Tucker MA, Walker GJ et al. Germline mutations in the p16(INK4a) binding domain of CDK4 in familial melanoma. Nature Genetics 1996; 12(1):97-99.

(92) Hussussian CJ, Struewing JP, Goldstein AM, Higgins PAT, Ally DS, Sheahan MD et al. Germline P16 Mutations in Familial Melanoma. Nature Genetics 1994; 8(1):15-21.

(93) Kamb A, Shattuckeidens D, Eeles R, Liu Q, Gruis NA, Ding W et al. Analysis of the P16 Gene (Cdkn2) As A Candidate for the Chromosome 9P Melanoma Susceptibility Locus. Nature Genetics 1994; 8(1):22-26.

(94) Crombie IK. Racial differences in melanoma incidence. Br J Cancer 1979; 40(2):185-193.

(95) Jamal S, Schneider RJ. UV-induction of keratinocyte endothelin-1 downregulates E-cadherin in melanocytes and melanoma cells. J Clin Invest 2002; 110(4):443-452.

(96) Vajdic CM, Kricker A, Giblin M, McKenzie J, Aitken J, Giles GG et al. Sun exposure predicts risk of ocular melanoma in Australia. Int J Cancer 2002; 101(2):175-182.

(97) Youl P, Aitken J, Hayward N, Hogg D, Liu L, Lassam N et al. Melanoma in adolescents: a case-control study of risk factors in Queensland, Australia. Int J Cancer 2002; 98(1):92-98.

(98) Whiteman D, Valery P, McWhirter W, Green A. Incidence of cutaneous childhood melanoma in Queensland, Australia. Int J Cancer 1995; 63(6):765-768.

(99) McWhirter WR, Dobson C. Childhood melanoma in Australia. World J Surg 1995; 19(3):334-336.

(100) de Vries E, Coebergh JW. Cutaneous malignant melanoma in Europe. Eur J Cancer 2004; 40(16):2355-2366.

(101) Hocker T, Tsao H. Ultraviolet radiation and melanoma: a systematic review and analysis of reported sequence variants. Hum Mutat 2007; 28(6):578-588.

(102) Setlow RB. Spectral regions contributing to melanoma: a personal view. J Investig Dermatol Symp Proc 1999; 4(1):46-49.

(103) Crombie IK. Variation of melanoma incidence with latitude in North America and Europe. Br J Cancer 1979; 40(5):774-781.

(104) McGovern VJ. Melanoblastoma. Med J Aust 1952; 1(5):139-142.

(105) Ragnarsson-Olding BK. Primary malignant melanoma of the vulva - An aggressive tumor for modeling the genesis of non-UV light-associated melanomas. Acta Oncologica 2004; 43(5):421-435.

(106) Afaq F, Adhami VM, Mukhtar H. Photochemoprevention of ultraviolet B signaling and photocarcinogenesis. Mutat Res 2005; 571(1-2):153-173.

(107) Matsumura Y, Ananthaswamy HN. Molecular mechanisms of photocarcinogenesis. Front Biosci 2002; 7:d765-d783.

(108) Sarkar-Agrawal P, Vergilis I, Sharpless NE, DePinho RA, Runger TM. Impaired processing of DNA photoproducts and ultraviolet hypermutability with loss of p16INK4a or p19ARF. J Natl Cancer Inst 2004; 96(23):1790-1793.

(109) Warters RL, Adamson PJ, Pond CD, Leachman SA. Melanoma cells express elevated levels of phosphorylated histone H2AX foci. J Invest Dermatol 2005; 124(4):807-817.

(110) Kopf AW, Hellman LJ, Rogers GS, Gross DF, Rigel DS, Friedman RJ et al. Familial Malignant-Melanoma. Jama-Journal of the American Medical Association 1986; 256(14):1915-1919.

(111) Barnhill RL, Roush GC, Titus-Ernstoff L, Ernstoff MS, Duray PH, Kirkwood JM. Comparison of nonfamilial and familial melanoma. Dermatology 1992; 184(1):2-7.

(112) Ford D, Bliss JM, Swerdlow AJ, Armstrong BK, Franceschi S, Green A et al. Risk of cutaneous melanoma associated with a family history of the disease. The International Melanoma Analysis Group (IMAGE). Int J Cancer 1995; 62(4):377-381.

(113) Cho E, Rosner BA, Feskanich D, Colditz GA. Risk factors and individual probabilities of melanoma for whites. J Clin Oncol 2005; 23(12):2669-2675.

(114) Ruiz LA, Kuznitzky R, Cuestas E, Mainardi C, Albertini R, Borello A et al. Risk factors for cutaneous melanoma: case-control study in Cordoba, Argentina. Medicina (B Aires) 2004; 64(6):504-508.

(115) Kerber RA, O'Brien E. A cohort study of cancer risk in relation to family histories of cancer in the Utah population database. Cancer 2005; 103(9):1906-1915.

(116) Begg CB, Hummer A, Mujumdar U, Armstrong BK, Kricker A, Marrett LD et al. Familial aggregation of melanoma risks in a large population-based sample of melanoma cases. Cancer Causes Control 2004; 15(9):957-965.

(117) Holly EA, Aston DA, Cress RD, Ahn DK, Kristiansen JJ. Cutaneous melanoma in women. II. Phenotypic characteristics and other host-related factors. Am J Epidemiol 1995; 141(10):934-942.

(118) Bauer J, Garbe C. Acquired melanocytic nevi as risk factor for melanoma development. A comprehensive review of epidemiological data. Pigment Cell Res 2003; 16(3):297-306.

(119) Swerdlow AJ, English J, Mackie RM, O'Doherty CJ, Hunter JA, Clark J et al. Benign melanocytic naevi as a risk factor for malignant melanoma. Br Med J (Clin Res Ed) 1986; 292(6535):1555-1559.

(120) Green A, Maclennan R, Siskind V. Common acquired naevi and the risk of malignant melanoma. Int J Cancer 1985; 35(3):297-300.

(121) Grob JJ, Gouvernet J, Aymar D, Mostaque A, Romano MH, Collet AM et al. Count of benign melanocytic nevi as a major indicator of risk for nonfamilial nodular and superficial spreading melanoma. Cancer 1990; 66(2):387-395.

(122) Landi MT, Baccarelli A, Tarone RE, Pesatori A, Tucker MA, Hedayati M et al. DNA repair, dysplastic nevi, and sunlight sensitivity in the development of cutaneous malignant melanoma. J Natl Cancer Inst 2002; 94(2):94-101.

(123) Halpern AC, Guerry D, Elder DE, Clark WH, Jr., Synnestvedt M, Norman S et al. Dysplastic nevi as risk markers of sporadic (nonfamilial) melanoma. A case-control study. Arch Dermatol 1991; 127(7):995-999.

(124) Holly EA, Kelly JW, Shpall SN, Chiu SH. Number of melanocytic nevi as a major risk factor for malignant melanoma. J Am Acad Dermatol 1987; 17(3):459-468.

(125) Garbe C, Buttner P, Weiss J, Soyer HP, Stocker U, Kruger S et al. Risk factors for developing cutaneous melanoma and criteria for identifying persons at risk: multicenter case-control study of the Central Malignant Melanoma Registry of the German Dermatological Society. J Invest Dermatol 1994; 102(5):695-699.

(126) Bataille V, Bishop JA, Sasieni P, Swerdlow AJ, Pinney E, Griffiths K et al. Risk of cutaneous melanoma in relation to the numbers, types and sites of naevi: a case-control study. Br J Cancer 1996; 73(12):1605-1611.

(127) Watt AJ, Kotsis SV, Chung KC. Risk of melanoma arising in large congenital melanocytic nevi: a systematic review. Plast Reconstr Surg 2004; 113(7):1968-1974.

(128) Chaudru V, Chompret A, Bressac-de Paillerets B, Spatz A, Avril MF, Demenais F. Influence of genes, nevi, and sun sensitivity on melanoma risk in a family sample unselected by family history and in melanoma-prone families. J Natl Cancer Inst 2004; 96(10):785-795.

(129) Bauer J, Buttner P, Wiecker TS, Luther H, Garbe C. Risk factors of incident melanocytic nevi: a longitudinal study in a cohort of 1,232 young German children. Int J Cancer 2005; 115(1):121-126.

(130) Titus-Ernstoff L, Perry AE, Spencer SK, Gibson JJ, Cole BF, Ernstoff MS. Pigmentary characteristics and moles in relation to melanoma risk. Int J Cancer 2005; 116(1):144-149.

(131) Borbola K, Banfalvi T, Fejos Z, Liszkay G, Papp A, Horvath B et al. Etiologic factors of malignant melanoma in young adults. Orv Hetil 2005; 146(28):1481-1487.

(132) Hammer H, Toth-Molnar E, Olah J, Dobozy A. Connection between uveal melanoma and dysplastic naevus syndrome. Magy Onkol 2005; 49(1):15-18.

(133) Rokuhara S, Saida T, Oguchi M, Matsumoto K, Murase S, Oguchi S. Number of acquired melanocytic nevi in patients with melanoma and control subjects in Japan: Nevus count is a significant risk factor for nonacral melanoma but not for acral melanoma. J Am Acad Dermatol 2004; 50(5):695-700.

(134) Nijsten T, Leys C, Verbruggen K, Verlinden V, Drieghe J, Stas M et al. Case-control study to identify melanoma risk factors in the Belgian population: the

significance of clinical examination. J Eur Acad Dermatol Venereol 2005; 19(3):332-339.

(135) Richtig E, Langmann G, Mullner K, Smolle J. Ocular melanoma: epidemiology, clinical presentation and relationship with dysplastic nevi. Ophthalmologica 2004; 218(2):111-114.

(136) Nordlund JJ, Lerner AB. On the causes of melanomas. Am J Pathol 1977; 89(2):443-448.

(137) Bliss JM, Ford D, Swerdlow AJ, Armstrong BK, Cristofolini M, Elwood JM et al. Risk of cutaneous melanoma associated with pigmentation characteristics and freckling: systematic overview of 10 case-control studies. The International Melanoma Analysis Group (IMAGE). Int J Cancer 1995; 62(4):367-376.

(138) Strouse JJ, Fears TR, Tucker MA, Wayne AS. Pediatric melanoma: risk factor and survival analysis of the surveillance, epidemiology and end results database. J Clin Oncol 2005; 23(21):4735-4741.

(139) Walker GJ, Palmer JM, Walters MK, Hayward NK. A genetic model of melanoma tumorigenesis based on allelic losses. Genes Chromosomes Cancer 1995; 12(2):134-141.

(140) Dracopoli NC, Fountain JW. CDKN2 mutations in melanoma. Cancer Surv 1996; 26:115-132.

(141) Healy E, Rehman I, Angus B, Rees JL. Loss of heterozygosity in sporadic primary cutaneous melanoma. Genes Chromosomes Cancer 1995; 12(2):152-156.

(142) Millikin D, Meese E, Vogelstein B, Witkowski C, Trent J. Loss of heterozygosity for loci on the long arm of chromosome 6 in human malignant melanoma. Cancer Res 1991; 51(20):5449-5453.

(143) Herbst RA, Weiss J, Ehnis A, Cavenee WK, Arden KC. Loss of heterozygosity for 10q22-10qter in malignant melanoma progression. Cancer Res 1994; 54(12):3111-3114.

(144) Brown KM, Macgregor S, Montgomery GW, Craig DW, Zhao ZZ, Iyadurai K et al. Common sequence variants on 20q11.22 confer melanoma susceptibility. Nat Genet 2008; 40(7):838-840.

(145) Goldstein AM, Dracopoli NC, Ho EC, Fraser MC, Kearns KS, Bale SJ et al. Further evidence for a locus for cutaneous malignant melanoma-dysplastic nevus (CMM/DN) on chromosome 1p, and evidence for genetic heterogeneity. Am J Hum Genet 1993; 52(3):537-550.

(146) Rao UN, Jones MW, Finkelstein SD. Genotypic analysis of primary and metastatic cutaneous melanoma. Cancer Genet Cytogenet 2003; 140(1):37-44.

(147) Reifenberger J, Wolter M, Bostrom J, Buschges R, Schulte KW, Megahed M et al. Allelic losses on chromosome arm 10q and mutation of the PTEN (MMAC1) tumour suppressor gene in primary and metastatic malignant melanomas. Virchows Arch 2000; 436(5):487-493.

(148) Harvey JJ. An unidentified virus which causes the rapid production of tumours

in mice. Nature 1964; 204:1104-1105.

(149) Kirsten WH, Mayer LA. Malignant lymphomas of extrathymic origin induced in rats by murine erythroblastosis virus. J Natl Cancer Inst 1969; 43(3):735-746.

(150) Marshall CJ, Hall A, Weiss RA. A transforming gene present in human sarcoma cell lines. Nature 1982; 299(5879):171-173.

(151) Lenzen C, Cool RH, Prinz H, Kuhlmann J, Wittinghofer A. Kinetic analysis by fluorescence of the interaction between Ras and the catalytic domain of the guanine nucleotide exchange factor Cdc25Mm. Biochemistry 1998; 37(20):7420-7430.

(152) Downward J. SIGNAL TRANSDUCTION: Prelude to an Anniversary for the RAS Oncogene. Science 2006; 314(5798):433-434.

(153) Kadrmas JL, Smith MA, Clark KA, Pronovost SM, Muster N, Yates JR, III et al. The integrin effector PINCH regulates JNK activity and epithelial migration in concert with Ras suppressor 1. J Cell Biol 2004; 167(6):1019-1024.

(154) Aoki Y, Niihori T, Kawame H, Kurosawa K, Ohashi H, Tanaka Y et al. Germline mutations in HRAS proto-oncogene cause Costello syndrome. Nat Genet 2005; 37(10):1038-1040.

(155) Schubbert S, Zenker M, Rowe SL, Boll S, Klein C, Bollag G et al. Germline KRAS mutations cause Noonan syndrome. Nat Genet 2006; 38(3):331-336.

(156) Hall A, Marshall CJ, Spurr NK, Weiss RA. Identification of transforming gene in two human sarcoma cell lines as a new member of the ras gene family located on chromosome 1. Nature 1983; 303(5916):396-400.

(157) Shimizu K, Goldfarb M, Suard Y, Perucho M, Li Y, Kamata T et al. Three human transforming genes are related to the viral ras oncogenes. Proc Natl Acad Sci U S A 1983; 80(8):2112-2116.

(158) Murray MJ, Cunningham JM, Parada LF, Dautry F, Lebowitz P, Weinberg RA. The HL-60 transforming sequence: a ras oncogene coexisting with altered myc genes in hematopoietic tumors. Cell 1983; 33(3):749-757.

(159) de Martinville B, Cunningham JM, Murray MJ, Francke U. The N-ras oncogene assigned to the short arm of human chromosome 1. Nucleic Acids Res 1983; 11(15):5267-5275.

(160) Brown R, Marshall CJ, Pennie SG, Hall A. Mechanism of activation of an N-ras gene in the human fibrosarcoma cell line HT1080. EMBO J 1984; 3(6):1321-1326.

(161) Willumsen BM, Papageorge AG, Hubbert N, Bekesi E, Kung HF, Lowy DR. Transforming p21 ras protein: flexibility in the major variable region linking the catalytic and membrane-anchoring domains. EMBO J 1985; 4(11):2893-2896.

(162) Shih TY, Weeks MO, Gruss P, Dhar R, Oroszlan S, Scolnick EM. Identification of a precursor in the biosynthesis of the p21 transforming protein of harvey murine sarcoma virus. J Virol 1982; 42(1):253-261.

(163) Goldfarb M, Shimizu K, Perucho M, Wigler M. Isolation and preliminary characterization of a human transforming gene from T24 bladder carcinoma cells. Nature 1982; 296(5856):404-409.

(164) Capon DJ, Chen EY, Levinson AD, Seeburg PH, Goeddel DV. Complete nucleotide sequences of the T24 human bladder carcinoma oncogene and its normal homologue. Nature 1983; 302(5903):33-37.

(165) Lowy DR, Willumsen BM. Function and regulation of ras. Annu Rev Biochem 1993; 62:851-891.

(166) Adjei AA. Blocking oncogenic Ras signaling for cancer therapy. J Natl Cancer Inst 2001; 93(14):1062-1074.

(167) Bos JL. ras oncogenes in human cancer: a review. Cancer Res 1989; 49(17):4682-4689.

(168) Hanahan D, Weinberg RA. The hallmarks of cancer. Cell 2000; 100(1):57-70.

(169) Field JK, Spandidos DA. The role of ras and myc oncogenes in human solid tumours and their relevance in diagnosis and prognosis (review). Anticancer Res 1990; 10(1):1-22.

(170) Vageli D, Kiaris H, Delakas D, Anezinis P, Cranidis A, Spandidos DA. Transcriptional activation of H-ras, K-ras and N-ras proto-oncogenes in human bladder tumors. Cancer Lett 1996; 107(2):241-247.

(171) Shivakumar L, Minna J, Sakamaki T, Pestell R, White MA. The RASSF1A tumor suppressor blocks cell cycle progression and inhibits cyclin D1 accumulation. Mol Cell Biol 2002; 22(12):4309-4318.

(172) Cichowski K, Jacks T. NF1 tumor suppressor gene function: narrowing the GAP. Cell 2001; 104(4):593-604.

(173) Serrano M, Lin AW, McCurrach ME, Beach D, Lowe SW. Oncogenic ras provokes premature cell senescence associated with accumulation of p53 and p16INK4a. Cell 1997; 88(5):593-602.

(174) Mu DQ, Peng YS, Xu QJ. Values of mutations of K-ras oncogene at codon 12 in detection of pancreatic cancer: 15-year experience. World J Gastroenterol 2004; 10(4):471-475.

(175) Bos JL, Fearon ER, Hamilton SR, Verlaan-de Vries M, van Boom JH, van der Eb AJ et al. Prevalence of ras gene mutations in human colorectal cancers. Nature 1987; 327(6120):293-297.

(176) Cerny WL, Mangold KA, Scarpelli DG. K-ras mutation is an early event in pancreatic duct carcinogenesis in the Syrian golden hamster. Cancer Res 1992; 52(16):4507-4513.

(177) Taparowsky E, Suard Y, Fasano O, Shimizu K, Goldfarb M, Wigler M. Activation of the T24 bladder carcinoma transforming gene is linked to a single amino acid change. Nature 1982; 300(5894):762-765.

(178) Sukumar S, Notario V, Martin-Zanca D, Barbacid M. Induction of mammary carcinomas in rats by nitroso-methylurea involves malignant activation of H-

ras-1 locus by single point mutations. Nature 1983; 306(5944):658-661.

(179) Manne V, Bekesi E, Kung HF. Ha-ras proteins exhibit GTPase activity: point mutations that activate Ha-ras gene products result in decreased GTPase activity. Proc Natl Acad Sci U S A 1985; 82(2):376-380.

(180) Theillet C, Lidereau R, Escot C, Hutzell P, Brunet M, Gest J et al. Loss of a c-H-ras-1 allele and aggressive human primary breast carcinomas. Cancer Res 1986; 46(9):4776-4781.

(181) Cichutek K, Duesberg PH. Harvey ras genes transform without mutant codons, apparently activated by truncation of a 5' exon (exon -1). Proc Natl Acad Sci U S A 1986; 83(8):2340-2344.

(182) Balmain A, Pragnell IB. Mouse skin carcinomas induced in vivo by chemical carcinogens have a transforming Harvey-ras oncogene. Nature 1983; 303(5912):72-74.

(183) Bizub D, Wood AW, Skalka AM. Mutagenesis of the Ha-ras oncogene in mouse skin tumors induced by polycyclic aromatic hydrocarbons. Proc Natl Acad Sci U S A 1986; 83(16):6048-6052.

(184) Parsons BL, Beland FA, Von Tungeln LS, Delongchamp RR, Fu PP, Heflich RH. Levels of 4-aminobiphenyl-induced somatic H-ras mutation in mouse liver DNA correlate with potential for liver tumor development. Mol Carcinog 2005; 42(4):193-201.

(185) Quintanilla M, Brown K, Ramsden M, Balmain A. Carcinogen-specific mutation and amplification of Ha-ras during mouse skin carcinogenesis. Nature 1986; 322(6074):78-80.

(186) Pierceall WE, Goldberg LH, Tainsky MA, Mukhopadhyay T, Ananthaswamy HN. Ras gene mutation and amplification in human nonmelanoma skin cancers. Mol Carcinog 1991; 4(3):196-202.

(187) van der Schroeff JG, Evers LM, Boot AJ, Bos JL. Ras oncogene mutations in basal cell carcinomas and squamous cell carcinomas of human skin. J Invest Dermatol 1990; 94(4):423-425.

(188) Campbell C, Quinn AG, Rees JL. Codon 12 Harvey-ras mutations are rare events in non-melanoma human skin cancer. Br J Dermatol 1993; 128(2):111-114.

(189) Rady P, Kinsella AR, Fox M, Arany I, Kertai P. N-ras mutation in chemically induced rat brain tumour. Acta Biochim Biophys Hung 1989; 24(4):313-316.

(190) Suzuki Y, Orita M, Shiraishi M, Hayashi K, Sekiya T. Detection of ras gene mutations in human lung cancers by single-strand conformation polymorphism analysis of polymerase chain reaction products. Oncogene 1990; 5(7):1037-1043.

(191) Stratton MR, Fisher C, Gusterson BA, Cooper CS. Detection of point mutations in N-ras and K-ras genes of human embryonal rhabdomyosarcomas using oligonucleotide probes and the polymerase chain reaction. Cancer Res 1989; 49(22):6324-6327.

(192) Padua RA, Barrass NC, Currie GA. Activation of N-ras in a human melanoma cell line. Mol Cell Biol 1985; 5(3):582-585.

(193) Lemoine NR, Mayall ES, Wyllie FS, Farr CJ, Hughes D, Padua RA et al. Activated ras oncogenes in human thyroid cancers. Cancer Res 1988; 48(16):4459-4463.

(194) Nishida J, Kobayashi Y, Hirai H, Takaku F. A point mutation at codon 13 of the N-ras oncogene in a human stomach cancer. Biochem Biophys Res Commun 1987; 146(1):247-252.

(195) Hirai H, Kobayashi Y, Mano H, Hagiwara K, Maru Y, Omine M et al. A point mutation at codon 13 of the N-ras oncogene in myelodysplastic syndrome. Nature 1987; 327(6121):430-432.

(196) van Elsas A, Zerp SF, van der FS, Kruse KM, Aarnoudse C, Hayward NK et al. Relevance of ultraviolet-induced N-ras oncogene point mutations in development of primary human cutaneous melanoma. Am J Pathol 1996; 149(3):883-893.

(197) Sivertsson A, Platz A, Hansson J, Lundeberg J. Pyrosequencing as an alternative to single-strand conformation polymorphism analysis for detection of N-ras mutations in human melanoma metastases. Clin Chem 2002; 48(12):2164-2170.

(198) Polsky D, Cordon-Cardo C. Oncogenes in melanoma. Oncogene 2003; 22(20):3087-3091.

(199) Jiveskog S, Ragnarsson-Olding B, Platz A, Ringborg U. N-ras mutations are common in melanomas from sun-exposed skin of humans but rare in mucosal membranes or unexposed skin. J Invest Dermatol 1998; 111(5):757-761.

(200) Davies H, Bignell GR, Cox C, Stephens P, Edkins S, Clegg S et al. Mutations of the BRAF gene in human cancer. Nature 2002; 417(6892):949-954.

(201) Eskandarpour M, Hashemi J, Kanter L, Ringborg U, Platz A, Hansson J. Frequency of UV-inducible NRAS mutations in melanomas of patients with germline CDKN2A mutations. J Natl Cancer Inst 2003; 95(11):790-798.

(202) Omholt K, Karsberg S, Platz A, Kanter L, Ringborg U, Hansson J. Screening of N-ras codon 61 mutations in paired primary and metastatic cutaneous melanomas: mutations occur early and persist throughout tumor progression. Clin Cancer Res 2002; 8(11):3468-3474.

(203) Satyamoorthy K, Li G, Gerrero MR, Brose MS, Volpe P, Weber BL et al. Constitutive mitogen-activated protein kinase activation in melanoma is mediated by both BRAF mutations and autocrine growth factor stimulation. Cancer Res 2003; 63(4):756-759.

(204) Smalley KS. A pivotal role for ERK in the oncogenic behaviour of malignant melanoma? Int J Cancer 2003; 104(5):527-532.

(205) Raybaud F, Noguchi T, Marics I, Adelaide J, Planche J, Batoz M et al. Detection of a low frequency of activated ras genes in human melanomas using a tumorigenicity assay. Cancer Res 1988; 48(4):950-953.

(206) Albino AP, Nanus DM, Mentle IR, Cordon-Cardo C, McNutt NS, Bressler J et al. Analysis of ras oncogenes in malignant melanoma and precursor lesions: correlation of point mutations with differentiation phenotype. Oncogene 1989; 4(11):1363-1374.

(207) Ball NJ, Yohn JJ, Morelli JG, Norris DA, Golitz LE, Hoeffler JP. Ras mutations in human melanoma: a marker of malignant progression. J Invest Dermatol 1994; 102(3):285-290.

(208) Stark M, Hayward N. Genome-wide loss of heterozygosity and copy number analysis in melanoma using high-density single-nucleotide polymorphism arrays. Cancer Res 2007; 67(6):2632-2642.

(209) Demunter A, Ahmadian MR, Libbrecht L, Stas M, Baens M, Scheffzek K et al. A novel N-ras mutation in malignant melanoma is associated with excellent prognosis. Cancer Res 2001; 61(12):4916-4922.

(210) Jafari M, Papp T, Kirchner S, Diener U, Henschler D, Burg G et al. Analysis of ras mutations in human melanocytic lesions: activation of the ras gene seems to be associated with the nodular type of human malignant melanoma. J Cancer Res Clin Oncol 1995; 121(1):23-30.

(211) Platz A, Ringborg U, Grafstrom E, Hoog A, Lagerlof B. Immunohistochemical analysis of the N-ras p21 and the p53 proteins in naevi, primary tumours and metastases of human cutaneous malignant melanoma: increased immunopositivity in hereditary melanoma. Melanoma Res 1995; 5(2):101-106.

(212) Omholt K, Platz A, Kanter L, Ringborg U, Hansson J. NRAS and BRAF mutations arise early during melanoma pathogenesis and are preserved throughout tumor progression. Clin Cancer Res 2003; 9(17):6483-6488.

(213) Shinozaki M, Fujimoto A, Morton DL, Hoon DS. Incidence of BRAF oncogene mutation and clinical relevance for primary cutaneous melanomas. Clin Cancer Res 2004; 10(5):1753-1757.

(214) Reifenberger J, Knobbe CB, Sterzinger AA, Blaschke B, Schulte KW, Ruzicka T et al. Frequent alterations of Ras signaling pathway genes in sporadic malignant melanomas. Int J Cancer 2004; 109(3):377-384.

(215) Ackermann J, Frutschi M, Kaloulis K, Mckee T, Trumpp A, Beermann F. Metastasizing melanoma formation caused by expression of activated N-Ras(Q61K) on an INK4a-deficient background. Cancer Res 2005; 65(10):4005-4011.

(216) Powell MB, Hyman P, Bell OD, Balmain A, Brown K, Alberts D et al. Hyperpigmentation and melanocytic hyperplasia in transgenic mice expressing the human T24 Ha-ras gene regulated by a mouse tyrosinase promoter. Mol Carcinog 1995; 12(2):82-90.

(217) Chin L, Pomerantz J, Polsky D, Jacobson M, Cohen C, Cordon-Cardo C et al. Cooperative effects of INK4a and ras in melanoma susceptibility in vivo. Genes Dev 1997; 11(21):2822-2834.

(218) Bardeesy N, Bastian BC, Hezel A, Pinkel D, DePinho RA, Chin L. Dual inactivation of RB and p53 pathways in RAS-induced melanomas. Mol Cell Biol 2001; 21(6):2144-2153.

(219) Chudnovsky Y, Adams AE, Robbins PB, Lin Q, Khavari PA. Use of human tissue to assess the oncogenic activity of melanoma-associated mutations. Nat Genet 2005; 37(7):745-749.

(220) Bauer J, Curtin JA, Pinkel D, Bastian BC. Congenital melanocytic nevi frequently harbor NRAS mutations but no BRAF mutations. J Invest Dermatol 2007; 127(1):179-182.

(221) Gause PR, Lluria-Prevatt M, Keith WN, Balmain A, Linardopolous S, Warneke J et al. Chromosomal and genetic alterations of 7,12-dimethylbenz[a]anthracene-induced melanoma from TP-ras transgenic mice. Mol Carcinog 1997; 20(1):78-87.

(222) Broome PM, Gause PR, Hyman P, Gregus J, Lluria-Prevatt M, Nagle R et al. Induction of melanoma in TPras transgenic mice. Carcinogenesis 1999; 20(9):1747-1753.

(223) Chin L, Tam A, Pomerantz J, Wong M, Holash J, Bardeesy N et al. Essential role for oncogenic Ras in tumour maintenance. Nature 1999; 400(6743):468-472.

(224) Kannan K, Sharpless NE, Xu J, O'Hagan RC, Bosenberg M, Chin L. Components of the Rb pathway are critical targets of UV mutagenesis in a murine melanoma model. Proc Natl Acad Sci U S A 2003; 100(3):1221-1225.

(225) Ackermann J, Beermann F. The fibroblast growth factor-2 is not essential for melanoma formation in a transgenic mouse model. Pigment Cell Res 2005; 18(4):315-319.

(226) Stokoe D. PTEN. Curr Biol 2001; 11(13):R502.

(227) Steck PA, Pershouse MA, Jasser SA, Yung WK, Lin H, Ligon AH et al. Identification of a candidate tumour suppressor gene, MMAC1, at chromosome 10q23.3 that is mutated in multiple advanced cancers. Nat Genet 1997; 15(4):356-362.

(228) Li J, Yen C, Liaw D, Podsypanina K, Bose S, Wang SI et al. PTEN, a putative protein tyrosine phosphatase gene mutated in human brain, breast, and prostate cancer. Science 1997; 275(5308):1943-1947.

(229) Li DM, Sun H. TEP1, encoded by a candidate tumor suppressor locus, is a novel protein tyrosine phosphatase regulated by transforming growth factor beta. Cancer Res 1997; 57(11):2124-2129.

(230) Lee YC. The role of PTEN in allergic inflammation. Arch Immunol Ther Exp (Warsz) 2004; 52(4):250-254.

(231) Waite KA, Eng C. Protean PTEN: form and function. Am J Hum Genet 2002; 70(4):829-844.

(232) Lee JO, Yang H, Georgescu MM, Di Cristofano A, Maehama T, Shi Y et al. Crystal structure of the PTEN tumor suppressor: implications for its phosphoinositide phosphatase activity and membrane association. Cell 1999; 99(3):323-334.

(233) Maehama T, Dixon JE. The tumor suppressor, PTEN/MMAC1,

dephosphorylates the lipid second messenger, phosphatidylinositol 3,4,5-trisphosphate. J Biol Chem 1998; 273(22):13375-13378.

(234) Myers MP, Stolarov JP, Eng C, Li J, Wang SI, Wigler MH et al. P-TEN, the tumor suppressor from human chromosome 10q23, is a dual-specificity phosphatase. Proc Natl Acad Sci U S A 1997; 94(17):9052-9057.

(235) Furnari FB, Huang HJ, Cavenee WK. The phosphoinositol phosphatase activity of PTEN mediates a serum-sensitive G1 growth arrest in glioma cells. Cancer Res 1998; 58(22):5002-5008.

(236) Myers MP, Pass I, Batty IH, Van der KJ, Stolarov JP, Hemmings BA et al. The lipid phosphatase activity of PTEN is critical for its tumor supressor function. Proc Natl Acad Sci U S A 1998; 95(23):13513-13518.

(237) Chang HW, Aoki M, Fruman D, Auger KR, Bellacosa A, Tsichlis PN et al. Transformation of chicken cells by the gene encoding the catalytic subunit of PI 3-kinase. Science 1997; 276(5320):1848-1850.

(238) Bellacosa A, Testa JR, Staal SP, Tsichlis PN. A retroviral oncogene, akt, encoding a serine-threonine kinase containing an SH2-like region. Science 1991; 254(5029):274-277.

(239) Mahimainathan L, Choudhury GG. Inactivation of platelet-derived growth factor receptor by the tumor suppressor PTEN provides a novel mechanism of action of the phosphatase. J Biol Chem 2004; 279(15):15258-15268.

(240) Chen WC, Lin MS, Bai X. Induction of apoptosis in colorectal cancer cells by peroxisome proliferators-activated receptor gamma activation up-regulating PTEN and inhibiting PI3K activity. Chin Med J (Engl) 2005; 118(17):1477-1481.

(241) Cantley LC, Neel BG. New insights into tumor suppression: PTEN suppresses tumor formation by restraining the phosphoinositide 3-kinase/AKT pathway. Proc Natl Acad Sci U S A 1999; 96(8):4240-4245.

(242) Sun H, Lesche R, Li DM, Liliental J, Zhang H, Gao J et al. PTEN modulates cell cycle progression and cell survival by regulating phosphatidylinositol 3,4,5,-trisphosphate and Akt/protein kinase B signaling pathway. Proc Natl Acad Sci U S A 1999; 96(11):6199-6204.

(243) Yamada KM, Araki M. Tumor suppressor PTEN: modulator of cell signaling, growth, migration and apoptosis. J Cell Sci 2001; 114(Pt 13):2375-2382.

(244) Freeman DJ, Li AG, Wei G, Li HH, Kertesz N, Lesche R et al. PTEN tumor suppressor regulates p53 protein levels and activity through phosphatase-dependent and -independent mechanisms. Cancer Cell 2003; 3(2):117-130.

(245) Chung JH, Eng C. Nuclear-cytoplasmic partitioning of phosphatase and tensin homologue deleted on chromosome 10 (PTEN) differentially regulates the cell cycle and apoptosis. Cancer Res 2005; 65(18):8096-8100.

(246) Yao D, Alexander CL, Quinn JA, Porter MJ, Wu H, Greenhalgh DA. PTEN loss promotes rasHa-mediated papillomatogenesis via dual up-regulation of AKT activity and cell cycle deregulation but malignant conversion proceeds via PTEN-associated pathways. Cancer Res 2006; 66(3):1302-1312.

(247) Marsh DJ, Coulon V, Lunetta KL, Rocca-Serra P, Dahia PL, Zheng Z et al. Mutation spectrum and genotype-phenotype analyses in Cowden disease and Bannayan-Zonana syndrome, two hamartoma syndromes with germline PTEN mutation. Hum Mol Genet 1998; 7(3):507-515.

(248) Guldberg P, thor SP, Birck A, Ahrenkiel V, Kirkin AF, Zeuthen J. Disruption of the MMAC1/PTEN gene by deletion or mutation is a frequent event in malignant melanoma. Cancer Res 1997; 57(17):3660-3663.

(249) Poetsch M, Dittberner T, Woenckhaus C. PTEN/MMAC1 in malignant melanoma and its importance for tumor progression. Cancer Genet Cytogenet 2001; 125(1):21-26.

(250) Whiteman DC, Zhou XP, Cummings MC, Pavey S, Hayward NK, Eng C. Nuclear PTEN expression and clinicopathologic features in a population-based series of primary cutaneous melanoma. Int J Cancer 2002; 99(1):63-67.

(251) Deichmann M, Thome M, Benner A, Egner U, Hartschuh W, Naher H. PTEN/MMAC1 expression in melanoma resection specimens. Br J Cancer 2002; 87(12):1431-1436.

(252) Pollock PM, Walker GJ, Glendening JM, Que NT, Bloch NC, Fountain JW et al. PTEN inactivation is rare in melanoma tumours but occurs frequently in melanoma cell lines. Melanoma Res 2002; 12(6):565-575.

(253) Zhou XP, Gimm O, Hampel H, Niemann T, Walker MJ, Eng C. Epigenetic PTEN silencing in malignant melanomas without PTEN mutation. Am J Pathol 2000; 157(4):1123-1128.

(254) Tsao H, Goel V, Wu H, Yang G, Haluska FG. Genetic interaction between NRAS and BRAF mutations and PTEN/MMAC1 inactivation in melanoma. J Invest Dermatol 2004; 122(2):337-341.

(255) Tsao H, Mihm MC, Jr., Sheehan C. PTEN expression in normal skin, acquired melanocytic nevi, and cutaneous melanoma. J Am Acad Dermatol 2003; 49(5):865-872.

(256) Robertson GP, Furnari FB, Miele ME, Glendening MJ, Welch DR, Fountain JW et al. In vitro loss of heterozygosity targets the PTEN/MMAC1 gene in melanoma. Proc Natl Acad Sci U S A 1998; 95(16):9418-9423.

(257) Birck A, Ahrenkiel V, Zeuthen J, Hou-Jensen K, Guldberg P. Mutation and allelic loss of the PTEN/MMAC1 gene in primary and metastatic melanoma biopsies. J Invest Dermatol 2000; 114(2):277-280.

(258) Tsao H, Zhang X, Benoit E, Haluska FG. Identification of PTEN/MMAC1 alterations in uncultured melanomas and melanoma cell lines. Oncogene 1998; 16(26):3397-3402.

(259) Mikhail M, Velazquez E, Shapiro R, Berman R, Pavlick A, Sorhaindo L et al. PTEN expression in melanoma: relationship with patient survival, Bcl-2 expression, and proliferation. Clin Cancer Res 2005; 11(14):5153-5157.

(260) Hwang PH, Yi HK, Kim DS, Nam SY, Kim JS, Lee DY. Suppression of tumorigenicity and metastasis in B16F10 cells by PTEN/MMAC1/TEP1 gene. Cancer Lett 2001; 172(1):83-91.

(261) Lo RS, Witte ON. Transforming growth factor-beta activation promotes genetic context-dependent invasion of immortalized melanocytes. Cancer Res 2008; 68(11):4248-4257.

(262) You MJ, Castrillon DH, Bastian BC, O'Hagan RC, Bosenberg MW, Parsons R et al. Genetic analysis of Pten and Ink4a/Arf interactions in the suppression of tumorigenesis in mice. Proc Natl Acad Sci U S A 2002; 99(3):1455-1460.

(263) Tae Inoue-Narita, Koichi Hamada, Takehiko Sasaki, Sachiko Hatakeyama, Sachiko Fujita, Kohichi Kawahara et al. Pten Deficiency in Melanocytes Results in Resistance to Hair Graying and Susceptibility to Carcinogen-Induced Melanomagenesis. Cancer Res 2008; 68(14):5760-5768.

(264) Rodolfo M, Daniotti M, Vallacchi V. Genetic progression of metastatic melanoma. Cancer Lett 2004; 214(2):133-147.

(265) Celebi JT, Shendrik I, Silvers DN, Peacocke M. Identification of PTEN mutations in metastatic melanoma specimens. J Med Genet 2000; 37(9):653-657.

(266) Cruz F, III, Rubin BP, Wilson D, Town A, Schroeder A, Haley A et al. Absence of BRAF and NRAS mutations in uveal melanoma. Cancer Res 2003; 63(18):5761-5766.

(267) Weber A, Hengge UR, Urbanik D, Markwart A, Mirmohammadsaegh A, Reichel MB et al. Absence of mutations of the BRAF gene and constitutive activation of extracellular-regulated kinase in malignant melanomas of the uvea. Lab Invest 2003; 83(12):1771-1776.

(268) Cohen Y, Goldenberg-Cohen N, Parrella P, Chowers I, Merbs SL, Pe'er J et al. Lack of BRAF mutation in primary uveal melanoma. Invest Ophthalmol Vis Sci 2003; 44(7):2876-2878.

(269) Rimoldi D, Salvi S, Lienard D, Lejeune FJ, Speiser D, Zografos L et al. Lack of BRAF mutations in uveal melanoma. Cancer Res 2003; 63(18):5712-5715.

(270) Naus NC, Zuidervaart W, Rayman N, Slater R, van Drunen E, Ksander B et al. Mutation analysis of the PTEN gene in uveal melanoma cell lines. Int J Cancer 2000; 87(1):151-153.

(271) Wu H, Goel V, Haluska FG. PTEN signaling pathways in melanoma. Oncogene 2003; 22(20):3113-3122.

(272) Xia S, Lu Y, Wang J, He C, Hong S, Serhan CN et al. Melanoma growth is reduced in fat-1 transgenic mice: impact of omega-6/omega-3 essential fatty acids. Proc Natl Acad Sci U S A 2006; 103(33):12499-12504.

(273) Huang S, Jean D, Luca M, Tainsky MA, Bar-Eli M. Loss of AP-2 results in downregulation of c-KIT and enhancement of melanoma tumorigenicity and metastasis. EMBO J 1998; 17(15):4358-4369.

(274) Tellez C, Bar-Eli M. Role and regulation of the thrombin receptor (PAR-1) in human melanoma. Oncogene 2003; 22(20):3130-3137.

(275) Besmer P, Murphy JE, George PC, Qiu FH, Bergold PJ, Lederman L et al. A new acute transforming feline retrovirus and relationship of its oncogene v-kit

with the protein kinase gene family. Nature 1986; 320(6061):415-421.

(276) Yarden Y, Kuang WJ, Yang-Feng T, Coussens L, Munemitsu S, Dull TJ et al. Human proto-oncogene c-kit: a new cell surface receptor tyrosine kinase for an unidentified ligand. EMBO J 1987; 6(11):3341-3351.

(277) Chabot B, Stephenson DA, Chapman VM, Besmer P, Bernstein A. The proto-oncogene c-kit encoding a transmembrane tyrosine kinase receptor maps to the mouse W locus. Nature 1988; 335(6185):88-89.

(278) Geissler EN, Ryan MA, Housman DE. The dominant-white spotting (W) locus of the mouse encodes the c-kit proto-oncogene. Cell 1988; 55(1):185-192.

(279) Copeland NG, Gilbert DJ, Cho BC, Donovan PJ, Jenkins NA, Cosman D et al. Mast cell growth factor maps near the steel locus on mouse chromosome 10 and is deleted in a number of steel alleles. Cell 1990; 63(1):175-183.

(280) Williams DE, Eisenman J, Baird A, Rauch C, Van Ness K, March CJ et al. Identification of a ligand for the c-kit proto-oncogene. Cell 1990; 63(1):167-174.

(281) Crosier PS, Ricciardi ST, Hall LR, Vitas MR, Clark SC, Crosier KE. Expression of isoforms of the human receptor tyrosine kinase c-kit in leukemic cell lines and acute myeloid leukemia. Blood 1993; 82(4):1151-1158.

(282) Reith AD, Ellis C, Lyman SD, Anderson DM, Williams DE, Bernstein A et al. Signal transduction by normal isoforms and W mutant variants of the Kit receptor tyrosine kinase. EMBO J 1991; 10(9):2451-2459.

(283) Hayashi S, Kunisada T, Ogawa M, Yamaguchi K, Nishikawa S. Exon skipping by mutation of an authentic splice site of c-kit gene in W/W mouse. Nucleic Acids Res 1991; 19(6):1267-1271.

(284) Wehrle-Haller B, Weston JA. Soluble and cell-bound forms of steel factor activity play distinct roles in melanocyte precursor dispersal and survival on the lateral neural crest migration pathway. Development 1995; 121(3):731-742.

(285) Lecoin L, Lahav R, Martin FH, Teillet MA, Le Douarin NM. Steel and c-kit in the development of avian melanocytes: a study of normally pigmented birds and of the hyperpigmented mutant silky fowl. Dev Dyn 1995; 203(1):106-118.

(286) Grichnik JM, Burch JA, Burchette J, Shea CR. The SCF/KIT pathway plays a critical role in the control of normal human melanocyte homeostasis. J Invest Dermatol 1998; 111(2):233-238.

(287) Keshet E, Lyman SD, Williams DE, Anderson DM, Jenkins NA, Copeland NG et al. Embryonic RNA expression patterns of the c-kit receptor and its cognate ligand suggest multiple functional roles in mouse development. EMBO J 1991; 10(9):2425-2435.

(288) Steel KP, Davidson DR, Jackson IJ. TRP-2/DT, a new early melanoblast marker, shows that steel growth factor (c-kit ligand) is a survival factor. Development 1992; 115(4):1111-1119.

(289) Scott G, Ewing J, Ryan D, Abboud C. Stem cell factor regulates human melanocyte-matrix interactions. Pigment Cell Res 1994; 7(1):44-51.

(290) Cable J, Jackson IJ, Steel KP. Mutations at the W locus affect survival of neural crest-derived melanocytes in the mouse. Mech Dev 1995; 50(2-3):139-150.

(291) Mackenzie MA, Jordan SA, Budd PS, Jackson IJ. Activation of the receptor tyrosine kinase Kit is required for the proliferation of melanoblasts in the mouse embryo. Dev Biol 1997; 192(1):99-107.

(292) Yoshida H, Hayashi S, Shultz LD, Yamamura K, Nishikawa S, Nishikawa S et al. Neural and skin cell-specific expression pattern conferred by steel factor regulatory sequence in transgenic mice. Dev Dyn 1996; 207(2):222-232.

(293) Lassam N, Bickford S. Loss of c-kit expression in cultured melanoma cells. Oncogene 1992; 7(1):51-56.

(294) Ohashi A, Funasaka Y, Ueda M, Ichihashi M. c-KIT receptor expression in cutaneous malignant melanoma and benign melanotic naevi. Melanoma Res 1996; 6(1):25-30.

(295) Mouriaux F, Kherrouche Z, Maurage CA, Demailly FX, Labalette P, Saule S. Expression of the c-kit receptor in choroidal melanomas. Melanoma Res 2003; 13(2):161-166.

(296) Grabber J, Welker P, Dippel E, Czarnetzki BM. Stem cell factor, a novel cutaneous growth factor for mast cells and melanocytes. Arch Dermatol Res 1994; 287(1):78-84.

(297) Luca MR, Bar-Eli M. Molecular changes in human melanoma metastasis. Histol Histopathol 1998; 13(4):1225-1231.

(298) Zakut R, Perlis R, Eliyahu S, Yarden Y, Givol D, Lyman SD et al. KIT ligand (mast cell growth factor) inhibits the growth of KIT-expressing melanoma cells. Oncogene 1993; 8(8):2221-2229.

(299) Welker P, Schadendorf D, Artuc M, Grabber J, Henz BM. Expression of SCF splice variants in human melanocytes and melanoma cell lines: potential prognostic implications. Br J Cancer 2000; 82(8):1453-1458.

(300) Willmore-Payne C, Holden JA, Tripp S, Layfield LJ. Human malignant melanoma: detection of BRAF- and c-kit-activating mutations by high-resolution amplicon melting analysis. Human Pathology 2005; 36(5):486-493.

(301) Curtin JA, Busam K, Pinkel D, Bastian BC. Somatic activation of KIT in distinct subtypes of melanoma. J Clin Oncol 2006; 24(26):4340-4346.

(302) Ricotti E, Fagioli F, Garelli E, Linari C, Crescenzio N, Horenstein AL et al. c-kit is expressed in soft tissue sarcoma of neuroectodermic origin and its ligand prevents apoptosis of neoplastic cells. Blood 1998; 91(7):2397-2405.

(303) Huang S, Luca M, Gutman M, McConkey DJ, Langley KE, Lyman SD et al. Enforced c-KIT expression renders highly metastatic human melanoma cells susceptible to stem cell factor-induced apoptosis and inhibits their tumorigenic and metastatic potential. Oncogene 1996; 13(11):2339-2347.

(304) Ito M, Kawa Y, Ono H, Okura M, Baba T, Kubota Y et al. Removal of stem cell factor or addition of monoclonal anti-c-KIT antibody induces apoptosis in murine melanocyte precursors. J Invest Dermatol 1999; 112(5):796-801.

(305) McGill GG, Horstmann M, Widlund HR, Du J, Motyckova G, Nishimura EK et al. Bcl2 regulation by the melanocyte master regulator Mitf modulates lineage survival and melanoma cell viability. Cell 2002; 109(6):707-718.

(306) Kimura S, Kawakami T, Kawa Y, Soma Y, Kushimoto T, Nakamura M et al. Bcl-2 reduced and fas activated by the inhibition of stem cell factor/KIT signaling in murine melanocyte precursors. J Invest Dermatol 2005; 124(1):229-234.

(307) Jordan SA, Speed RM, Bernex F, Jackson IJ. Deficiency of Trp53 rescues the male fertility defects of Kit(W-v) mice but has no effect on the survival of melanocytes and mast cells. Dev Biol 1999; 215(1):78-90.

(308) Poulaki V, Mitsiades CS, Mitsiades N. The role of Fas and FasL as mediators of anticancer chemotherapy. Drug Resist Updat 2001; 4(4):233-242.

(309) Sharov AA, Li GZ, Palkina TN, Sharova TY, Gilchrest BA, Botchkarev VA. Fas and c-kit are involved in the control of hair follicle melanocyte apoptosis and migration in chemotherapy-induced hair loss. J Invest Dermatol 2003; 120(1):27-35.

(310) Hyer ML, Samuel T, Reed JC. The FLIP-side of Fas signaling. Clin Cancer Res 2006; 12(20 Pt 1):5929-5931.

(311) Kamb A, Gruis NA, Weaver-Feldhaus J, Liu Q, Harshman K, Tavtigian SV et al. A cell cycle regulator potentially involved in genesis of many tumor types. Science 1994; 264(5157):436-440.

(312) Okamoto A, Demetrick DJ, Spillare EA, Hagiwara K, Hussain SP, Bennett WP et al. Mutations and altered expression of p16INK4 in human cancer. Proc Natl Acad Sci U S A 1994; 91(23):11045-11049.

(313) Nobori T, Miura K, Wu DJ, Lois A, Takabayashi K, Carson DA. Deletions of the cyclin-dependent kinase-4 inhibitor gene in multiple human cancers. Nature 1994; 368(6473):753-756.

(314) Mao L, Merlo A, Bedi G, Shapiro GI, Edwards CD, Rollins BJ et al. A novel p16INK4A transcript. Cancer Res 1995; 55(14):2995-2997.

(315) Stone S, Jiang P, Dayananth P, Tavtigian SV, Katcher H, Parry D et al. Complex structure and regulation of the P16 (MTS1) locus. Cancer Res 1995; 55(14):2988-2994.

(316) Serrano M, Lee H, Chin L, Cordon-Cardo C, Beach D, DePinho RA. Role of the INK4a locus in tumor suppression and cell mortality. Cell 1996; 85(1):27-37.

(317) Quelle DE, Zindy F, Ashmun RA, Sherr CJ. Alternative reading frames of the INK4a tumor suppressor gene encode two unrelated proteins capable of inducing cell cycle arrest. Cell 1995; 83(6):993-1000.

(318) Sharpless E, Chin L. The INK4a/ARF locus and melanoma. Oncogene 2003; 22(20):3092-3098.

(319) Nairn RS, Kazianis S, McEntire BB, Della CL, Walter RB, Morizot DC. A CDKN2-like polymorphism in Xiphophorus LG V is associated with UV-B-

induced melanoma formation in platyfish-swordtail hybrids. Proc Natl Acad Sci U S A 1996; 93(23):13042-13047.

(320) Ruas M, Peters G. The p16INK4a/CDKN2A tumor suppressor and its relatives. Biochim Biophys Acta 1998; 1378(2):F115-F177.

(321) Zhang S, Ramsay ES, Mock BA. Cdkn2a, the cyclin-dependent kinase inhibitor encoding p16INK4a and p19ARF, is a candidate for the plasmacytoma susceptibility locus, Pctr1. Proc Natl Acad Sci U S A 1998; 95(5):2429-2434.

(322) Kamijo T, Zindy F, Roussel MF, Quelle DE, Downing JR, Ashmun RA et al. Tumor suppression at the mouse INK4a locus mediated by the alternative reading frame product p19ARF. Cell 1997; 91(5):649-659.

(323) Quelle DE, Cheng M, Ashmun RA, Sherr CJ. Cancer-associated mutations at the INK4a locus cancel cell cycle arrest by p16INK4a but not by the alternative reading frame protein p19ARF. Proc Natl Acad Sci U S A 1997; 94(2):669-673.

(324) Weber JD, Taylor LJ, Roussel MF, Sherr CJ, Bar-Sagi D. Nucleolar Arf sequesters Mdm2 and activates p53. Nat Cell Biol 1999; 1(1):20-26.

(325) Korgaonkar C, Zhao L, Modestou M, Quelle DE. ARF function does not require p53 stabilization or Mdm2 relocalization. Mol Cell Biol 2002; 22(1):196-206.

(326) Weber JD, Jeffers JR, Rehg JE, Randle DH, Lozano G, Roussel MF et al. p53-independent functions of the p19(ARF) tumor suppressor. Genes Dev 2000; 14(18):2358-2365.

(327) Kim WY, Sharpless NE. The regulation of INK4/ARF in cancer and aging. Cell 2006; 127(2):265-275.

(328) Funk JO, Schiller PI, Barrett MT, Wong DJ, Kind P, Sander CA. p16INK4a expression is frequently decreased and associated with 9p21 loss of heterozygosity in sporadic melanoma. J Cutan Pathol 1998; 25(6):291-296.

(329) Gonzalgo ML, Bender CM, You EH, Glendening JM, Flores JF, Walker GJ et al. Low frequency of p16/CDKN2A methylation in sporadic melanoma: comparative approaches for methylation analysis of primary tumors. Cancer Res 1997; 57(23):5336-5347.

(330) Healy E, Sikkink S, Rees JL. Infrequent mutation of p16INK4 in sporadic melanoma. J Invest Dermatol 1996; 107(3):318-321.

(331) Tang L, Li G, Tron VA, Trotter MJ, Ho VC. Expression of cell cycle regulators in human cutaneous malignant melanoma. Melanoma Res 1999; 9(2):148-154.

(332) Molven A, Grimstvedt MB, Steine SJ, Harland M, Avril MF, Hayward NK et al. A large Norwegian family with inherited malignant melanoma, multiple atypical nevi, and CDK4 mutation. Genes Chromosomes Cancer 2005; 44(1):10-18.

(333) Hayward NK. Genetics of melanoma predisposition. Oncogene 2003; 22(20):3053-3062.

(334) Whiteman DC, Milligan A, Welch J, Green AC, Hayward NK. Germline

CDKN2A mutations in childhood melanoma. J Natl Cancer Inst 1997; 89(19):1460.

(335) Tsao H, Zhang X, Kwitkiwski K, Finkelstein DM, Sober AJ, Haluska FG. Low prevalence of germline CDKN2A and CDK4 mutations in patients with early-onset melanoma. Arch Dermatol 2000; 136(9):1118-1122.

(336) Hayward N. New developments in melanoma genetics. Curr Oncol Rep 2000; 2(4):300-306.

(337) Puig S, Malvehy J, Badenas C, Ruiz A, Jimenez D, Cuellar F et al. Role of the CDKN2A locus in patients with multiple primary melanomas. J Clin Oncol 2005; 23(13):3043-3051.

(338) Lang J, Boxer M, Mackie RM. CDKN2A mutations in Scottish families with cutaneous melanoma: results from 32 newly identified families. Br J Dermatol 2005; 153(6):1121-1125.

(339) Goldstein AM, Chan M, Harland M, Gillanders EM, Hayward NK, Avril MF et al. High-risk melanoma susceptibility genes and pancreatic cancer, neural system tumors, and uveal melanoma across GenoMEL. Cancer Res 2006; 66(20):9818-9828.

(340) Bishop DT, Demenais F, Goldstein AM, Bergman W, Bishop JN, Bressac-de Paillerets B et al. Geographical variation in the penetrance of CDKN2A mutations for melanoma. J Natl Cancer Inst 2002; 94(12):894-903.

(341) Begg CB, Orlow I, Hummer AJ, Armstrong BK, Kricker A, Marrett LD et al. Lifetime risk of melanoma in CDKN2A mutation carriers in a population-based sample. J Natl Cancer Inst 2005; 97(20):1507-1515.

(342) Marini A, Mirmohammadsadegh A, Nambiar S, Gustrau A, Ruzicka T, Hengge UR. Epigenetic inactivation of tumor suppressor genes in serum of patients with cutaneous melanoma. J Invest Dermatol 2006; 126(2):422-431.

(343) Yang J, Luan J, Yu Y, Li C, DePinho RA, Chin L et al. Induction of melanoma in murine macrophage inflammatory protein 2 transgenic mice heterozygous for inhibitor of kinase/alternate reading frame. Cancer Res 2001; 61(22):8150-8157.

(344) Sharpless NE, Bardeesy N, Lee KH, Carrasco D, Castrillon DH, Aguirre AJ et al. Loss of p16Ink4a with retention of p19Arf predisposes mice to tumorigenesis. Nature 2001; 413(6851):86-91.

(345) Krimpenfort P, Quon KC, Mooi WJ, Loonstra A, Berns A. Loss of p16Ink4a confers susceptibility to metastatic melanoma in mice. Nature 2001; 413(6851):83-86.

(346) Sotillo R, Garcia JF, Ortega S, Martin J, Dubus P, Barbacid M et al. Invasive melanoma in Cdk4-targeted mice. Proc Natl Acad Sci U S A 2001; 98(23):13312-13317.

(347) Rane SG, Cosenza SC, Mettus RV, Reddy EP. Germ line transmission of the Cdk4(R24C) mutation facilitates tumorigenesis and escape from cellular senescence. Mol Cell Biol 2002; 22(2):644-656.

(348) Hacker E, Muller HK, Irwin N, Gabrielli B, Lincoln D, Pavey S et al. Spontaneous and UV radiation-induced multiple metastatic melanomas in Cdk4R24C/R24C/TPras mice. Cancer Res 2006; 66(6):2946-2952.

(349) Recio JA, Noonan FP, Takayama H, Anver MR, Duray P, Rush WL et al. Ink4a/arf deficiency promotes ultraviolet radiation-induced melanomagenesis. Cancer Res 2002; 62(22):6724-6730.

(350) Tang Y, Kim M, Carrasco D, Kung AL, Chin L, Weissleder R. In vivo assessment of RAS-dependent maintenance of tumor angiogenesis by real-time magnetic resonance imaging. Cancer Res 2005; 65(18):8324-8330.

(351) Benjamin CL, Ullrich SE, Kripke ML, Ananthaswamy HN. p53 tumor suppressor gene: a critical molecular target for UV induction and prevention of skin cancer. Photochem Photobiol 2008; 84(1):55-62.

(352) Gwosdz C, Scheckenbach K, Lieven O, Reifenberger J, Knopf A, Bier H et al. Comprehensive analysis of the p53 status in mucosal and cutaneous melanomas. Int J Cancer 2006; 118(3):577-582.

(353) Florenes VA, Oyjord T, Holm R, Skrede M, Borresen AL, Nesland JM et al. TP53 allele loss, mutations and expression in malignant melanoma. Br J Cancer 1994; 69(2):253-259.

(354) Albino AP, Vidal MJ, McNutt NS, Shea CR, Prieto VG, Nanus DM et al. Mutation and expression of the p53 gene in human malignant melanoma. Melanoma Res 1994; 4(1):35-45.

(355) Dahl C, Guldberg P. The genome and epigenome of malignant melanoma. APMIS 2007; 115(10):1161-1176.

(356) Zhang H. p53 plays a central role in UVA and UVB induced cell damage and apoptosis in melanoma cells. Cancer Lett 2006; 244(2):229-238.

(357) Ha L, Ichikawa T, Anver M, Dickins R, Lowe S, Sharpless NE et al. ARF functions as a melanoma tumor suppressor by inducing p53-independent senescence. Proc Natl Acad Sci U S A 2007; 104(26):10968-10973.

(358) Kamijo T, Weber JD, Zambetti G, Zindy F, Roussel MF, Sherr CJ. Functional and physical interactions of the ARF tumor suppressor with p53 and Mdm2. Proc Natl Acad Sci U S A 1998; 95(14):8292-8297.

(359) Yang G, Rajadurai A, Tsao H. Recurrent patterns of dual RB and p53 pathway inactivation in melanoma. J Invest Dermatol 2005; 125(6):1242-1251.

(360) Brose MS, Volpe P, Feldman M, Kumar M, Rishi I, Gerrero R et al. BRAF and RAS mutations in human lung cancer and melanoma. Cancer Res 2002; 62(23):6997-7000.

(361) Wellbrock C, Karasarides M, Marais R. The RAF proteins take centre stage. Nat Rev Mol Cell Biol 2004; 5(11):875-885.

(362) Gorden A, Osman I, Gai W, He D, Huang W, Davidson A et al. Analysis of BRAF and N-RAS mutations in metastatic melanoma tissues. Cancer Res 2003; 63(14):3955-3957.

(363) Libra M, Malaponte G, Navolanic PM, Gangemi P, Bevelacqua V, Proietti L et al. Analysis of BRAF Mutation in Primary and Metastatic Melanoma. Cell Cycle 2005; 4(10).

(364) Uribe P, Wistuba II, Gonzalez S. BRAF mutation: a frequent event in benign, atypical, and malignant melanocytic lesions of the skin. Am J Dermatopathol 2003; 25(5):365-370.

(365) Kumar R, Angelini S, Snellman E, Hemminki K. BRAF mutations are common somatic events in melanocytic nevi. J Invest Dermatol 2004; 122(2):342-348.

(366) Kumar R, Angelini S, Czene K, Sauroja I, Hahka-Kemppinen M, Pyrhonen S et al. BRAF mutations in metastatic melanoma: a possible association with clinical outcome. Clin Cancer Res 2003; 9(9):3362-3368.

(367) Lang J, Mackie RM. Prevalence of exon 15 BRAF mutations in primary melanoma of the superficial spreading, nodular, acral, and lentigo maligna subtypes. J Invest Dermatol 2005; 125(3):575-579.

(368) Lang J, Boxer M, MacKie R. Absence of exon 15 BRAF germline mutations in familial melanoma. Hum Mutat 2003; 21(3):327-330.

(369) Laud K, Kannengiesser C, Avril MF, Chompret A, Stoppa-Lyonnet D, Desjardins L et al. BRAF as a melanoma susceptibility candidate gene? Cancer Res 2003; 63(12):3061-3065.

(370) Meyer P, Klaes R, Schmitt C, Boettger MB, Garbe C. Exclusion of BRAFV599E as a melanoma susceptibility mutation. Int J Cancer 2003; 106(1):78-80.

(371) Edmunds SC, Cree IA, Di Nicolantonio F, Hungerford JL, Hurren JS, Kelsell DP. Absence of BRAF gene mutations in uveal melanomas in contrast to cutaneous melanomas. Br J Cancer 2003; 88(9):1403-1405.

(372) Pollock PM, Harper UL, Hansen KS, Yudt LM, Stark M, Robbins CM et al. High frequency of BRAF mutations in nevi. Nat Genet 2003; 33(1):19-20.

(373) Dong J, Phelps RG, Qiao R, Yao S, Benard O, Ronai Z et al. BRAF oncogenic mutations correlate with progression rather than initiation of human melanoma. Cancer Res 2003; 63(14):3883-3885.

(374) Sasaki Y, Niu C, Makino R, Kudo C, Sun C, Watanabe H et al. BRAF point mutations in primary melanoma show different prevalences by subtype. J Invest Dermatol 2004; 123(1):177-183.

(375) Michaloglou C, Vredeveld LC, Mooi WJ, Peeper DS. BRAF(E600) in benign and malignant human tumours. Oncogene 2008; 27(7):877-895.

(376) Price ER, Horstmann MA, Wells AG, Weilbaecher KN, Takemoto CM, Landis MW et al. alpha-Melanocyte-stimulating hormone signaling regulates expression of microphthalmia, a gene deficient in Waardenburg syndrome. J Biol Chem 1998; 273(49):33042-33047.

(377) Bertolotto C, Abbe P, Hemesath TJ, Bille K, Fisher DE, Ortonne JP et al. Microphthalmia gene product as a signal transducer in cAMP-induced differentiation of melanocytes. J Cell Biol 1998; 142(3):827-835.

(378) Goding CR. Mitf from neural crest to melanoma: signal transduction and transcription in the melanocyte lineage. Genes Dev 2000; 14(14):1712-1728.

(379) Gaggioli C, Busca R, Abbe P, Ortonne JP, Ballotti R. Microphthalmia-associated transcription factor (MITF) is required but is not sufficient to induce the expression of melanogenic genes. Pigment Cell Res 2003; 16(4):374-382.

(380) Bertolotto C, Busca R, Abbe P, Bille K, Aberdam E, Ortonne JP et al. Different cis-acting elements are involved in the regulation of TRP1 and TRP2 promoter activities by cyclic AMP: pivotal role of M boxes (GTCATGTGCT) and of microphthalmia. Mol Cell Biol 1998; 18(2):694-702.

(381) Levy C, Khaled M, Fisher DE. MITF: master regulator of melanocyte development and melanoma oncogene. Trends in Molecular Medicine 2006; 12(9):406-414.

(382) Chiaverini C, Beuret L, Flori E, Busca R, Abbe P, Bille K et al. Microphthalmia associated transcription factor (MITF regulates rab27A gene expression and controls melanosomes transport. J Biol Chem 2008.

(383) Bemis LT, Chen R, Amato CM, Classen EH, Robinson SE, Coffey DG et al. MicroRNA-137 targets microphthalmia-associated transcription factor in melanoma cell lines. Cancer Res 2008; 68(5):1362-1368.

(384) Hornyak TJ, Hayes DJ, Chiu LY, Ziff EB. Transcription factors in melanocyte development: distinct roles for Pax-3 and Mitf. Mech Dev 2001; 101(1-2):47-59.

(385) Hoek KS, Eichhoff OM, Schlegel NC, Dobbeling U, Kobert N, Schaerer L et al. In vivo switching of human melanoma cells between proliferative and invasive states. Cancer Res 2008; 68(3):650-656.

(386) King R, Weilbaecher KN, McGill G, Cooley E, Mihm M, Fisher DE. Microphthalmia transcription factor. A sensitive and specific melanocyte marker for MelanomaDiagnosis. Am J Pathol 1999; 155(3):731-738.

(387) Garraway LA, Widlund HR, Rubin MA, Getz G, Berger AJ, Ramaswamy S et al. Integrative genomic analyses identify MITF as a lineage survival oncogene amplified in malignant melanoma. Nature 2005; 436(7047):117-122.

(388) Miller AJ, Du J, Rowan S, Hershey CL, Widlund HR, Fisher DE. Transcriptional regulation of the melanoma prognostic marker melastatin (TRPM1) by MITF in melanocytes and melanoma. Cancer Res 2004; 64(2):509-516.

(389) Steingrimsson E, Copeland NG, Jenkins NA. Melanocytes and the microphthalmia transcription factor network. Annu Rev Genet 2004; 38:365-411.

(390) Rees JL. Genetics of hair and skin color. Annu Rev Genet 2003; 37:67-90.

(391) Cone RD, Lu D, Koppula S, Vage DI, Klungland H, Boston B et al. The melanocortin receptors: agonists, antagonists, and the hormonal control of pigmentation. Recent Prog Horm Res 1996; 51:287-317.

(392) Mountjoy KG, Robbins LS, Mortrud MT, Cone RD. The cloning of a family of genes that encode the melanocortin receptors. Science 1992; 257(5074):1248-1251.

(393) Gantz I, Yamada T, Tashiro T, Konda Y, Shimoto Y, Miwa H et al. Mapping of the gene encoding the melanocortin-1 (alpha-melanocyte stimulating hormone) receptor (MC1R) to human chromosome 16q24.3 by Fluorescence in situ hybridization. Genomics 1994; 19(2):394-395.

(394) Chhajlani V, Muceniece R, Wikberg JE. Molecular cloning of a novel human melanocortin receptor. Biochem Biophys Res Commun 1996; 218(2):638.

(395) Healy E, Jordan SA, Budd PS, Suffolk R, Rees JL, Jackson IJ. Functional variation of MC1R alleles from red-haired individuals. Hum Mol Genet 2001; 10(21):2397-2402.

(396) Kerns JA, Cargill EJ, Clark LA, Candille SI, Berryere TG, Olivier M et al. Linkage and segregation analysis of black and brindle coat color in domestic dogs. Genetics 2007; 176(3):1679-1689.

(397) Candille SI, Kaelin CB, Cattanach BM, Yu B, Thompson DA, Nix MA et al. A -defensin mutation causes black coat color in domestic dogs. Science 2007; 318(5855):1418-1423.

(398) Smith R, Healy E, Siddiqui S, Flanagan N, Steijlen PM, Rosdahl I et al. Melanocortin 1 receptor variants in an Irish population. J Invest Dermatol 1998; 111(1):119-122.

(399) Box NF, Wyeth JR, O'Gorman LE, Martin NG, Sturm RA. Characterization of melanocyte stimulating hormone receptor variant alleles in twins with red hair. Hum Mol Genet 1997; 6(11):1891-1897.

(400) Stratigos AJ, Dimisianos G, Nikolaou V, Poulou M, Sypsa V, Stefanaki I et al. Melanocortin receptor-1 gene polymorphisms and the risk of cutaneous melanoma in a low-risk southern European population. J Invest Dermatol 2006; 126(8):1842-1849.

(401) Palmer JS, Duffy DL, Box NF, Aitken JF, O'Gorman LE, Green AC et al. Melanocortin-1 receptor polymorphisms and risk of melanoma: is the association explained solely by pigmentation phenotype?. Am J Hum Genet 2000; 66(1):176-186.

(402) Box NF, Duffy DL, Chen W, Stark M, Martin NG, Sturm RA et al. MC1R genotype modifies risk of melanoma in families segregating CDKN2A mutations. Am J Hum Genet 2001; 69(4):765-773.

(403) van der Velden PA, Sandkuijl LA, Bergman W, Pavel S, van Mourik L, Frants RR et al. Melanocortin-1 receptor variant R151C modifies melanoma risk in Dutch families with melanoma. Am J Hum Genet 2001; 69(4):774-779.

(404) Goldstein AM, Landi MT, Tsang S, Fraser MC, Munroe DJ, Tucker MA. Association of MC1R variants and risk of melanoma in melanoma-prone families with CDKN2A mutations. Cancer Epidemiol Biomarkers Prev 2005; 14(9):2208-2212.

(405) Chaudru V, Laud K, Avril MF, Miniere A, Chompret A, Bressac-de Paillerets B et al. Melanocortin-1 receptor (MC1R) gene variants and dysplastic nevi modify penetrance of CDKN2A mutations in French melanoma-prone pedigrees. Cancer Epidemiol Biomarkers Prev 2005; 14(10):2384-2390.

(406) Fargnoli MC, Altobelli E, Keller G, Chimenti S, Hofler H, Peris K. Contribution of melanocortin-1 receptor gene variants to sporadic cutaneous melanoma risk in a population in central Italy: a case-control study. Melanoma Res 2006; 16(2):175-182.

(407) Debniak T, Scott R, Masojc B, Serrano-Fernandez P, Huzarski T, Byrski T et al. MC1R common variants, CDKN2A and their association with melanoma and breast cancer risk. Int J Cancer 2006; 119(11):2597-2602.

(408) Landi MT, Kanetsky PA, Tsang S, Gold B, Munroe D, Rebbeck T et al. MC1R, ASIP, and DNA repair in sporadic and familial melanoma in a Mediterranean population. J Natl Cancer Inst 2005; 97(13):998-1007.

(409) Vajdic C, Kricker A, Duffy DL, Aitken JF, Stark M, ter Huurne JA et al. Ocular melanoma is not associated with CDKN2A or MC1R variants--a population-based study. Melanoma Res 2003; 13(4):409-413.

(410) Goldstein AM, Chaudru V, Ghiorzo P, Badenas C, Malvehy J, Pastorino L et al. Cutaneous phenotype and MC1R variants as modifying factors for the development of melanoma in CDKN2A G101W mutation carriers from 4 countries. Int J Cancer 2007; 121(4):825-831.

(411) Benjamin CL, Ananthaswamy HN. p53 and the pathogenesis of skin cancer. Toxicol Appl Pharmacol 2007; 224(3):241-248.

(412) Giglia-Mari G, Sarasin A. TP53 mutations in human skin cancers. Hum Mutat 2003; 21(3):217-228.

(413) Patton EE, Widlund HR, Kutok JL, Kopani KR, Amatruda JF, Murphey RD et al. BRAF mutations are sufficient to promote nevi formation and cooperate with p53 in the genesis of melanoma. Curr Biol 2005; 15(3):249-254.

(414) Bar-Eli M. Molecular mechanisms of melanoma metastasis. J Cell Physiol 1997; 173(2):275-278.

(415) Lin TP. Microinjection of mouse eggs. Science 1966; 151(3708):333-337.

(416) Brinster RL, Chen HY, Messing A, van Dyke T, Levine AJ, Palmiter RD. Transgenic mice harboring SV40 T-antigen genes develop characteristic brain tumors. Cell 1984; 37(2):367-379.

(417) Gordon JW, Ruddle FH. Integration and stable germ line transmission of genes injected into mouse pronuclei. Science 1981; 214(4526):1244-1246.

(418) Capecchi MR. Altering the genome by homologous recombination. Science 1989; 244(4910):1288-1292.

(419) Jaenisch R. Transgenic animals. Science 1988; 240(4858):1468-1474.

(420) Kappel CA, Bieberich CJ, Jay G. Evolving concepts in molecular pathology.

FASEB J 1994; 8(9):583-592.

(421) Clark WH, Jr., From L, Bernardino EA, Mihm MC. The histogenesis and biologic behavior of primary human malignant melanomas of the skin. Cancer Res 1969; 29(3):705-727.

(422) Clark WH, Jr., Reimer RR, Greene M, Ainsworth AM, Mastrangelo MJ. Origin of familial malignant melanomas from heritable melanocytic lesions. 'The B-K mole syndrome'. Arch Dermatol 1978; 114(5):732-738.

(423) Stark WM, Boocock MR, Sherratt DJ. Catalysis by site-specific recombinases. Trends Genet 1992; 8(12):432-439.

(424) Dymecki SM. Site-specific recombination in cells and mice. Gene Targeting, A Practical Approach. Oxford University Press, 2002: 37-99.

(425) Golic KG, Lindquist S. The FLP recombinase of yeast catalyzes site-specific recombination in the Drosophila genome. Cell 1989; 59(3):499-509.

(426) Dang DT, Perrimon N. Use of a yeast site-specific recombinase to generate embryonic mosaics in Drosophila. Dev Genet 1992; 13(5):367-375.

(427) O'Gorman S, Fox DT, Wahl GM. Recombinase-mediated gene activation and site-specific integration in mammalian cells. Science 1991; 251(4999):1351-1355.

(428) Sauer B, Henderson N. Site-specific DNA recombination in mammalian cells by the Cre recombinase of bacteriophage P1. Proc Natl Acad Sci U S A 1988; 85(14):5166-5170.

(429) Lakso M, Sauer B, Mosinger B, Jr., Lee EJ, Manning RW, Yu SH et al. Targeted oncogene activation by site-specific recombination in transgenic mice. Proc Natl Acad Sci U S A 1992; 89(14):6232-6236.

(430) Dymecki SM. Flp recombinase promotes site-specific DNA recombination in embryonic stem cells and transgenic mice. Proc Natl Acad Sci U S A 1996; 93(12):6191-6196.

(431) Hoess RH, Ziese M, Sternberg N. P1 site-specific recombination: nucleotide sequence of the recombining sites. Proc Natl Acad Sci U S A 1982; 79(11):3398-3402.

(432) McLeod M, Craft S, Broach JR. Identification of the crossover site during FLP-mediated recombination in the Saccharomyces cerevisiae plasmid 2 microns circle. Mol Cell Biol 1986; 6(10):3357-3367.

(433) Sternberg N, Hamilton D. Bacteriophage P1 site-specific recombination. I. Recombination between loxP sites. J Mol Biol 1981; 150(4):467-486.

(434) Groth AC, Olivares EC, Thyagarajan B, Calos MP. A phage integrase directs efficient site-specific integration in human cells. Proc Natl Acad Sci U S A 2000; 97(11):5995-6000.

(435) Sadowski PD. The Flp recombinase of the 2-microns plasmid of Saccharomyces cerevisiae. Prog Nucleic Acid Res Mol Biol 1995; 51:53-91.

(436) Hoess R, Wierzbicki A, Abremski K. Formation of small circular DNA molecules via an in vitro site-specific recombination system. Gene 1985; 40(2-3):325-329.

(437) Amin A, Roca H, Luetke K, Sadowski PD. Synapsis, strand scission, and strand exchange induced by the FLP recombinase: analysis with half-FRT sites. Mol Cell Biol 1991; 11(9):4497-4508.

(438) Hoess RH, Wierzbicki A, Abremski K. The role of the loxP spacer region in P1 site-specific recombination. Nucleic Acids Res 1986; 14(5):2287-2300.

(439) Huijbers IJ, Krimpenfort P, Chomez P, van der Valk MA, Song JY, Inderberg-Suso EM et al. An inducible mouse model of melanoma expressing a defined tumor antigen. Cancer Res 2006; 66(6):3278-3286.

(440) Kellendonk C, Tronche F, Monaghan AP, Angrand PO, Stewart F, Schutz G. Regulation of Cre recombinase activity by the synthetic steroid RU 486. Nucleic Acids Res 1996; 24(8):1404-1411.

(441) Klein-Szanto A, Bradl M, Porter S, Mintz B. Melanosis and associated tumors in transgenic mice. Proc Natl Acad Sci U S A 1991; 88(1):169-173.

(442) Bradl M, Klein-Szanto A, Porter S, Mintz B. Malignant melanoma in transgenic mice. Proc Natl Acad Sci U S A 1991; 88(1):164-168.

(443) de Vries E, Nijsten TE, Visser O, Bastiaannet E, van Hattem S, Janssen-Heijnen ML et al. Superior survival of females among 10,538 Dutch melanoma patients is independent of Breslow thickness, histologic type and tumor site. Ann Oncol 2008; 19(3):583-589.

(444) Thorn M, Ponten F, Bergstrom R, Sparen P, Adami HO. Clinical and histopathologic predictors of survival in patients with malignant melanoma: a population-based study in Sweden. J Natl Cancer Inst 1994; 86(10):761-769.

(445) Downing A, Newton-Bishop JA, Forman D. Recent trends in cutaneous malignant melanoma in the Yorkshire region of England; incidence, mortality and survival in relation to stage of disease, 1993-2003. Br J Cancer 2006; 95(1):91-95.

(446) Lee JT, Herlyn M. Embryogenesis meets tumorigenesis. Nature Medicine 2006; 12(8):882-884.

(447) Cassarino DS, Cabral ES, Kartha RV, Swetter SM. Primary dermal melanoma: distinct immunohistochemical findings and clinical outcome compared with nodular and metastatic melanoma. Arch Dermatol 2008; 144(1):49-56.

(448) Yuspa SH, Harris CC. Altered differentiation of mouse epidermal cells treated with retinyl acetate in vitro. Exp Cell Res 1974; 86(1):95-105.

(449) Halaban R. Culture of Melanocytes from Normal, Benign, and Malignant Lesions. In: R.Ian Freshney and Roswitha Pfragner, editor. Culture of Human Tumour Cells. Wiley-Liss Inc, 2003.

(450) Ganss R, Montoliu L, Monaghan AP, Schutz G. A cell-specific enhancer far upstream of the mouse tyrosinase gene confers high level and copy number-related expression in transgenic mice. EMBO J 1994; 13(13):3083-3093.

(451) Overbeek PA, Aguilar-Cordova E, Hanten G, Schaffner DL, Patel P, Lebovitz RM et al. Coinjection strategy for visual identification of transgenic mice. Transgenic Res 1991; 1(1):31-37.

(452) Choi T, Huang M, Gorman C, Jaenisch R. A generic intron increases gene expression in transgenic mice. Mol Cell Biol 1991; 11(6):3070-3074.

(453) Huang MT, Gorman CM. Intervening sequences increase efficiency of RNA 3' processing and accumulation of cytoplasmic RNA. Nucleic Acids Res 1990; 18(4):937-947.

(454) Zhao S, Overbeek PA. Tyrosinase-related protein 2 promoter targets transgene expression to ocular and neural crest-derived tissues. Dev Biol 1999; 216(1):154-163.

(455) Wang Y, O'Malley BW, Jr., Tsai SY, O'Malley BW. A regulatory system for use in gene transfer. Proc Natl Acad Sci U S A 1994; 91(17):8180-8184.

(456) Brigig Hogan et al. Manipulating the Mouse Embryo. 2nd ed. Cold Spring Harbor Laboratory Press, 1994.

(457) Yoon TJ, Hearing VJ. Co-culture of mouse epidermal cells for studies of pigmentation. Pigment Cell Res 2003; 16(2):159-163.

(458) Lei TC, Virador VM, Vieira WD, Hearing VJ. A melanocyte-keratinocyte coculture model to assess regulators of pigmentation in vitro. Anal Biochem 2002; 305(2):260-268.

(459) Bennett DC, Cooper PJ, Dexter TJ, Devlin LM, Heasman J, Nester B. Cloned Mouse Melanocyte Lines Carrying the Germline Mutations Albino and Brown - Complementation in Culture. Development 1989; 105(2):379-385.

(460) Spanakis E, Lamina P, Bennett DC. Effects of the Developmental Color Mutations Silver and Recessive Spotting on Proliferation of Diploid and Immortal Mouse Melanocytes in Culture. Development 1992; 114(3):675-680.

(461) Torma H, Vahlquist A. Retinol uptake and metabolism to 3,4-didehydroretinol in human keratinocytes at various stages of differentiation. Skin Pharmacol 1991; 4(3):154-157.

(462) Tsang SH, Kan LS. 300 MHz proton NMR study of the differentiation of diploid human epidermal keratinocytes. Cell Biophys 1990; 16(3):127-138.

(463) Strickland JE, Greenhalgh DA, Koceva-Chyla A, Hennings H, Restrepo C, Balaschak M et al. Development of murine epidermal cell lines which contain an activated rasHa oncogene and form papillomas in skin grafts on athymic nude mouse hosts. Cancer Res 1988; 48(1):165-169.

(464) Romero-Graillet C, Aberdam E, Clement M, Ortonne JP, Ballotti R. Nitric oxide produced by ultraviolet-irradiated keratinocytes stimulates melanogenesis. J Clin Invest 1997; 99(4):635-642.

(465) Hsu MY, Meier F, Herlyn M. Melanoma development and progression: a conspiracy between tumor and host. Differentiation 2002; 70(9-10):522-536.

(466) Meier F, Caroli U, Satyamoorthy K, Schittek B, Bauer J, Berking C et al.

Fibroblast growth factor-2 but not Mel-CAM and/or beta3 integrin promotes progression of melanocytes to melanoma. Exp Dermatol 2003; 12(3):296-306.

(467) Berton TR, Wang XJ, Zhou Z, Kellendonk C, Schutz G, Tsai S et al. Characterization of an inducible, epidermal-specific knockout system: differential expression of lacZ in different Cre reporter mouse strains. Genesis 2000; 26(2):160-161.

(468) Tonks ID, Nurcombe V, Paterson C, Zournazi A, Prather C, Mould AW et al. Tyrosinase-Cre mice for tissue-specific gene ablation in neural crest and neuroepithelial-derived tissues. Genesis 2003; 37(3):131-138.

(469) Abruzzese RV, Godin D, Burcin M, Mehta V, French M, Li Y et al. Ligand-dependent regulation of plasmid-based transgene expression in vivo. Hum Gene Ther 1999; 10(9):1499-1507.

(470) Hirobe T. Role of keratinocyte-derived factors involved in regulating the proliferation and differentiation of mammalian epidermal melanocytes. Pigment Cell Research 2005; 18(1):2-12.

(471) Bugalho P, Chorao M, Fontoura P. Miliary brain metastases from primary gastric small cell carcinoma: illustrating the seed and soil hypothesis. J Neurooncol 2005; 73(1):53-56.

(472) Kociok N, Joussen AM. Varied expression of functionally important genes of RPE and choroid in the macula and in the periphery of normal human eyes. Graefes Arch Clin Exp Ophthalmol 2007; 245(1):101-113.

(473) Navarro P, Valverde AM, Benito M, Lorenzo M. Activated Ha-ras Induces Apoptosis by Association with Phosphorylated Bcl-2 in a Mitogen-activated Protein Kinase-independent Manner. J Biol Chem 1999; 274(27):18857-18863.

(474) Chi SJ, Kitanaka C, Noguchi K, Mochizuki T, Nagashima Y, Shirouzu M et al. Oncogenic Ras triggers cell suicide through the activation of a caspase-independent cell death program in human cancer cells. Oncogene 1999; 18(13):2281-2290.

(475) Stiles B, Groszer M, Wang S, Jiao J, Wu H. PTENless means more. Dev Biol 2004; 273(2):175-184.

(476) Haass NK, Smalley KS, Herlyn M. The role of altered cell-cell communication in melanoma progression. J Mol Histol 2004; 35(3):309-318.

(477) Greenhalgh DA, Wang XJ, Eckhardt JN, Roop DR. 12-O-tetradecanoylphorbol-13-acetate promotion of transgenic mice expressing epidermal-targeted v-fos induces rasHA-activated papillomas and carcinomas without p53 mutation: association of v-fos expression with promotion and tumor autonomy. Cell Growth Differ 1995; 6(5):579-586.

(478) Wang XJ, Greenhalgh DA, Lu XR, Bickenbach JR, Roop DR. TGF alpha and v-fos cooperation in transgenic mouse epidermis induces aberrant keratinocyte differentiation and stable, autonomous papillomas. Oncogene 1995; 10(2):279-289.

(479) Kellendonk C, Tronche F, Casanova E, Anlag K, Opherk C, Schutz G. Inducible site-specific recombination in the brain. J Mol Biol 1999; 285(1):175-

182.

(480) Vegeto E, Allan GF, Schrader WT, Tsai MJ, McDonnell DP, O'Malley BW. The mechanism of RU486 antagonism is dependent on the conformation of the carboxy-terminal tail of the human progesterone receptor. Cell 1992; 69(4):703-713.

(481) Danielian PS, White R, Hoare SA, Fawell SE, Parker MG. Identification of residues in the estrogen receptor that confer differential sensitivity to estrogen and hydroxytamoxifen. Mol Endocrinol 1993; 7(2):232-240.

(482) Feil R, Brocard J, Mascrez B, LeMeur M, Metzger D, Chambon P. Ligand-activated site-specific recombination in mice. Proc Natl Acad Sci U S A 1996; 93(20):10887-10890.

(483) Littlewood TD, Hancock DC, Danielian PS, Parker MG, Evan GI. A modified oestrogen receptor ligand-binding domain as an improved switch for the regulation of heterologous proteins. Nucleic Acids Res 1995; 23(10):1686-1690.

(484) Metzger D, Clifford J, Chiba H, Chambon P. Conditional site-specific recombination in mammalian cells using a ligand-dependent chimeric Cre recombinase. Proc Natl Acad Sci U S A 1995; 92(15):6991-6995.

(485) Schwenk F, Kuhn R, Angrand PO, Rajewsky K, Stewart AF. Temporally and spatially regulated somatic mutagenesis in mice. Nucleic Acids Res 1998; 26(6):1427-1432.

(486) Hughes TA. Regulation of gene expression by alternative untranslated regions. Trends Genet 2006; 22(3):119-122.

(487) Kozak M. Point mutations define a sequence flanking the AUG initiator codon that modulates translation by eukaryotic ribosomes. Cell 1986; 44(2):283-292.

(488) Delmas V, Martinozzi S, Bourgeois Y, Holzenberger M, Larue L. Cre-mediated recombination in the skin melanocyte lineage. Genesis 2003; 36(2):73-80.

(489) Menon GK, Grayson S, Elias PM. Ionic calcium reservoirs in mammalian epidermis: ultrastructural localization by ion-capture cytochemistry. J Invest Dermatol 1985; 84(6):508-512.

(490) Forslind B, Lindberg M, Malmqvist KG, Pallon J, Roomans GM, Werner-Linde Y. Human skin physiology studied by particle probe microanalysis. Scanning Microsc 1995; 9(4):1011-1025.

(491) Elias PM, Ahn SK, Denda M, Brown BE, Crumrine D, Kimutai LK et al. Modulations in epidermal calcium regulate the expression of differentiation-specific markers. J Invest Dermatol 2002; 119(5):1128-1136.

(492) Hwang J, Kalinin A, Hwang M, Anderson DE, Kim MJ, Stojadinovic O et al. Role of Scarf and its binding target proteins in epidermal calcium homeostasis. J Biol Chem 2007; 282(25):18645-18653.

(493) Zhang C, Li X, Lian X, Wang Y, Zeng Y, Yang K et al. Immunolocalization of protein C inhibitor in differentiation of human epidermal keratinocytes. Acta Histochem 2007; 109(6):461-467.

(494) Yuspa SH, Kilkenny AE, Steinert PM, Roop DR. Expression of murine epidermal differentiation markers is tightly regulated by restricted extracellular calcium concentrations in vitro. J Cell Biol 1989; 109(3):1207-1217.

(495) Greenhalgh DA, Welty DJ, Strickland JE, Yuspa SH. Spontaneous Ha-ras gene activation in cultured primary murine keratinocytes: consequences of Ha-ras gene activation in malignant conversion and malignant progression. Mol Carcinog 1989; 2(4):199-207.

(496) Zhou BP, Liao Y, Xia W, Spohn B, Lee MH, Hung MC. Cytoplasmic localization of p21Cip1/WAF1 by Akt-induced phosphorylation in HER-2/neu-overexpressing cells. Nat Cell Biol 2001; 3(3):245-252.

(497) To MD, Perez-Losada J, Mao JH, Balmain A. Crosstalk between Pten and Ras signaling pathways in tumor development. Cell Cycle 2005; 4(9):1185-1188.

(498) di Jeso B, Ulianich L, Racioppi L, D'Armiento F, Feliciello A, Pacifico F et al. Serum withdrawal induces apoptotic cell death in Ki-ras transformed but not in normal differentiated thyroid cells. Biochem Biophys Res Commun 1995; 214(3):819-824.

(499) Saito H, Yoshida T, Yamazaki H, Suzuki N. Conditional N-rasG12V expression promotes manifestations of neurofibromatosis in a mouse model. Oncogene 2007.

(500) Stambolic V, Suzuki A, de la Pompa JL, Brothers GM, Mirtsos C, Sasaki T et al. Negative regulation of PKB/Akt-dependent cell survival by the tumor suppressor PTEN. Cell 1998; 95(1):29-39.

(501) Hirobe T, Furuya R, Akiu S, Ifuku O, Fukuda M. Keratinocytes control the proliferation and differentiation of cultured epidermal melanocytes from ultraviolet radiation B-induced pigmented spots in the dorsal skin of hairless mice. Pigment Cell Res 2002; 15(5):391-399.

(502) Furuya R, Akiu S, Ideta R, Naganuma M, Fukuda M, Hirobe T. Changes in the proliferative activity of epidermal melanocytes in serum-free primary culture during the development of ultraviolet radiation B-induced pigmented spots in hairless mice. Pigment Cell Res 2002; 15(5):348-356.

(503) Moll R, Franke WW, Schiller DL, Geiger B, Krepler R. The Catalog of Human Cytokeratins - Patterns of Expression in Normal Epithelia, Tumors and Cultured-Cells. Cell 1982; 31(1):11-24.

(504) Miettinen M, Lasota J. KIT (CD117): a review on expression in normal and neoplastic tissues, and mutations and their clinicopathologic correlation. Appl Immunohistochem Mol Morphol 2005; 13(3):205-220.

(505) Leslie MC, Bar-Eli M. Regulation of gene expression in melanoma: new approaches for treatment. J Cell Biochem 2005; 94(1):25-38.

(506) Kulesa PM, Kasemeier-Kulesa JC, Teddy JM, Margaryan NV, Seftor EA, Seftor REB et al. Reprogramming metastatic melanoma cells to assume a neural crest cell-like phenotype in an embryonic microenvironment. Proceedings of the National Academy of Sciences of the United States of America 2006; 103(10):3752-3757.

(507) Kramer TR, Powell MB, Wilson MM, Salvatore J, Grossniklaus HE. Pigmented uveal tumours in a transgenic mouse model. Br J Ophthalmol 1998; 82(8):953-960.

(508) Armstrong BK, Kricker A, English DR. Sun exposure and skin cancer. Australas J Dermatol 1997; 38 Suppl 1:S1-S6.

(509) Marks R. Epidemiology of melanoma. Clin Exp Dermatol 2000; 25(6):459-463.

(510) Noonan FP, Otsuka T, Bang S, Anver MR, Merlino G. Accelerated ultraviolet radiation-induced carcinogenesis in hepatocyte growth factor/scatter factor transgenic mice. Cancer Res 2000; 60(14):3738-3743.

(511) Byers HR, Bhawan J. Pathologic parameters in the diagnosis and prognosis of primary cutaneous melanoma. Hematol Oncol Clin North Am 1998; 12(4):717-735.

(512) Natali PG, Nicotra MR, Di Renzo MF, Prat M, Bigotti A, Cavaliere R et al. Expression of the c-Met/HGF receptor in human melanocytic neoplasms: demonstration of the relationship to malignant melanoma tumour progression. Br J Cancer 1993; 68(4):746-750.

(513) Jeffers M, Rong S, Woude GF. Hepatocyte growth factor/scatter factor-Met signaling in tumorigenicity and invasion/metastasis. J Mol Med 1996; 74(9):505-513.

(514) Chin L, Merlino G, DePinho RA. Malignant melanoma: modern black plague and genetic black box. Genes Dev 1998; 12(22):3467-3481.

(515) Sarkisian CJ, Keister BA, Stairs DB, Boxer RB, Moody SE, Chodosh LA. Dose-dependent oncogene-induced senescence in vivo and its evasion during mammary tumorigenesis. Nat Cell Biol 2007; 9(5):493-505.

(516) Pariser RJ. Benign neoplasms of the skin. Med Clin North Am 1998; 82(6):1285-12vi.

(517) Kullander J, Handisurya A, Forslund O, Geusau A, Kirnbauer R, Dillner J. Cutaneous human papillomavirus 88: remarkable differences in viral load. Int J Cancer 2008; 122(2):477-480.

(518) Carlos-Bregni R, Contreras E, Netto AC, Mosqueda-Taylor A, Vargas PA, Jorge J et al. Oral melanoacanthoma and oral melanotic macule: a report of 8 cases, review of the literature, and immunohistochemical analysis. Med Oral Patol Oral Cir Bucal 2007; 12(5):E374-E379.

(519) Contreras E, Carlos R. Oral melanoacanthosis (melanoachantoma): report of a case and review of the literature. Med Oral Patol Oral Cir Bucal 2005; 10(1):11-12.

(520) Otsuka T, Takayama H, Sharp R, Celli G, LaRochelle WJ, Bottaro DP et al. c-Met autocrine activation induces development of malignant melanoma and acquisition of the metastatic phenotype. Cancer Res 1998; 58(22):5157-5167.

(521) Ishizaki Y, Omori Y, Momiyama M, Nishikawa Y, Tokairin T, Manabe M et al.

Reduced expression and aberrant localization of p120catenin in human squamous cell carcinoma of the skin. J Dermatol Sci 2004; 34(2):99-108.

(522) Iyengar B. Expression of proliferating cell nuclear antigen (PCNA): proliferative phase functions and malignant transformation of melanocytes. Melanoma Res 1994; 4(5):293-295.

(523) Basset-Seguin N, Escot C, Moles JP, Blanchard JM, Kerai C, Guilhou JJ. C-fos and c-jun proto-oncogene expression is decreased in psoriasis: an in situ quantitative analysis. J Invest Dermatol 1991; 97(4):672-678.

(524) Wrone DA, Yoo S, Chipps LK, Moy RL. The expression of p63 in actinic keratoses, seborrheic keratosis, and cutaneous squamous cell carcinomas. Dermatol Surg 2004; 30(10):1299-1302.

(525) Suiqing C, Min Z, Lirong C. Overexpression of phosphorylated-STAT3 correlated with the invasion and metastasis of cutaneous squamous cell carcinoma. J Dermatol 2005; 32(5):354-360.

(526) Nakamura S, Nishioka K. Enhanced expression of p16 in seborrhoeic keratosis; a lesion of accumulated senescent epidermal cells in G1 arrest. Br J Dermatol 2003; 149(3):560-565.

(527) Hussein MR, Al Badaiwy ZH, Guirguis MN. Analysis of p53 and bcl-2 protein expression in the non-tumorigenic, pretumorigenic, and tumorigenic keratinocytic hyperproliferative lesions. J Cutan Pathol 2004; 31(10):643-651.

(528) Naruke Y, Nakashima M, Suzuki K, Matsuu-Matsuyama M, Shichijo K, Kondo H et al. Alteration of p53-binding protein 1 expression during skin carcinogenesis: association with genomic instability. Cancer Sci 2008; 99(5):946-951.

(529) Ko CJ, Shintaku P, Binder SW. Comparison of benign keratoses using p53, bcl-1, and bcl-2. J Cutan Pathol 2005; 32(5):356-359.

(530) Bruecks AK, Kalia S, Trotter MJ. Overexpression of p27KIP1 in seborrheic keratosis. J Cutan Med Surg 2007; 11(5):174-178.

(531) Logie A, Dunois-Larde C, Rosty C, Levrel O, Blanche M, Ribeiro A et al. Activating mutations of the tyrosine kinase receptor FGFR3 are associated with benign skin tumors in mice and humans. Hum Mol Genet 2005; 14(9):1153-1160.

(532) Hafner C, Hartmann A, van Oers JM, Stoehr R, Zwarthoff EC, Hofstaedter F et al. FGFR3 mutations in seborrheic keratoses are already present in flat lesions and associated with age and localization. Mod Pathol 2007; 20(8):895-903.

(533) Hafner C, Hartmann A, Real FX, Hofstaedter F, Landthaler M, Vogt T. Spectrum of FGFR3 mutations in multiple intraindividual seborrheic keratoses. J Invest Dermatol 2007; 127(8):1883-1885.

(534) Hafner C, Vogt T, Hartmann A. FGFR3 mutations in benign skin tumors. Cell Cycle 2006; 5(23):2723-2728.

(535) Hafner C, van Oers JM, Hartmann A, Landthaler M, Stoehr R, Blaszyk H et al. High frequency of FGFR3 mutations in adenoid seborrheic keratoses. J Invest Dermatol 2006; 126(11):2404-2407.

(536) Bernard-Pierrot I, Brams A, Dunois-Larde C, Caillault A, Diez de Medina SG, Cappellen D et al. Oncogenic properties of the mutated forms of fibroblast growth factor receptor 3b. Carcinogenesis 2006; 27(4):740-747.

(537) Hernandez S, Toll A, Baselga E, Ribe A, Azua-Romeo J, Pujol RM et al. Fibroblast growth factor receptor 3 mutations in epidermal nevi and associated low grade bladder tumors. J Invest Dermatol 2007; 127(7):1664-1666.

(538) Hafner C, Hartmann A, Vogt T. FGFR3 mutations in epidermal nevi and seborrheic keratoses: lessons from urothelium and skin. J Invest Dermatol 2007; 127(7):1572-1573.

(539) Kikuchi A, Amagai M, Nishikawa T. Association of ras p21 with differentiation of epidermal keratinocytes in proliferating skin diseases. J Dermatol Sci 1992; 4(2):83-86.

(540) Zioga C, Malamou-Mitsis VD, Kamina S, Agnantis NJ. Immunohistochemical detection of ras P21 oncoprotein in human skin lesions. Anticancer Res 1995; 15(3):1015-1022.

(541) Hafner C, Lopez-Knowles E, Luis NM, Toll A, Baselga E, Fernandez-Casado A et al. Oncogenic PIK3CA mutations occur in epidermal nevi and seborrheic keratoses with a characteristic mutation pattern. Proc Natl Acad Sci U S A 2007; 104(33):13450-13454.

(542) Collado M, Serrano M. The senescent side of tumor suppression. Cell Cycle 2005; 4(12):1722-1724.

(543) American Osteopathic College of Dermatology. Dermatologica Disease Database -Alopecia Areata. American Osteopathic College of Dermatology . 2008. Ref Type: Electronic Citation

(544) AAD. Alopecia Areata. American Academy of Dermatology Web . 2008. Ref Type: Electronic Citation

(545) Blaumeiser B, van dG, I, Fimmers R, Hanneken S, Ritzmann S, Seymons K et al. Familial aggregation of alopecia areata. J Am Acad Dermatol 2006; 54(4):627-632.

(546) Betz RC, Indelman M, Pforr J, Schreiner F, Bauer R, Bergman R et al. Identification of mutations in the human hairless gene in two new families with congenital atrichia. Arch Dermatol Res 2007; 299(3):157-161.

(547) Goh C, Finkel M, Christos PJ, Sinha AA. Profile of 513 patients with alopecia areata: associations of disease subtypes with atopy, autoimmune disease and positive family history. J Eur Acad Dermatol Venereol 2006; 20(9):1055-1060.

(548) Shellow WV, Edwards JE, Koo JY. Profile of alopecia areata: a questionnaire analysis of patient and family. Int J Dermatol 1992; 31(3):186-189.

(549) Cunliffe WJ, Hall R, Stevenson CJ, Weightman D. Alopecia areata, thyroid disease and autoimmunity. Br J Dermatol 1969; 81(12):877-881.

(550) McDonagh AJ, Tazi-Ahnini R. Epidemiology and genetics of alopecia areata. Clin Exp Dermatol 2002; 27(5):405-409.

(551) Entz P, Blaumeiser B, Betz RC, Lambert J, Seymons K, Eigelshoven S et al. Investigation of the HLA-DRB1 locus in alopecia areata. Eur J Dermatol 2006; 16(4):363-367.

(552) Betz RC, Konig K, Flaquer A, Redler S, Eigelshoven S, Kortum AK et al. The R620W polymorphism in PTPN22 confers general susceptibility for the development of alopecia areata. Br J Dermatol 2008; 158(2):389-391.

(553) Kemp EH, McDonagh AJ, Wengraf DA, Messenger AG, Gawkrodger DJ, Cork MJ et al. The non-synonymous C1858T substitution in the PTPN22 gene is associated with susceptibility to the severe forms of alopecia areata. Hum Immunol 2006; 67(7):535-539.

(554) Freyschmidt-Paul P, McElwee KJ, Hoffmann R, Sundberg JP, Vitacolonna M, Kissling S et al. Interferon-gamma-deficient mice are resistant to the development of alopecia areata. Br J Dermatol 2006; 155(3):515-521.

(555) Betz RC, Pforr J, Flaquer A, Redler S, Hanneken S, Eigelshoven S et al. Loss-of-function mutations in the filaggrin gene and alopecia areata: strong risk factor for a severe course of disease in patients comorbid for atopic disease. J Invest Dermatol 2007; 127(11):2539-2543.

(556) Siebenhaar F, Sharov AA, Peters EM, Sharova TY, Syska W, Mardaryev AN et al. Substance P as an immunomodulatory neuropeptide in a mouse model for autoimmune hair loss (alopecia areata). J Invest Dermatol 2007; 127(6):1489-1497.

(557) Han F, Zhang X. Characterization of a ras-related nuclear protein (Ran protein) up-regulated in shrimp antiviral immunity. Fish Shellfish Immunol 2007; 23(5):937-944.

(558) Mor A, Keren G, Kloog Y, George J. N-Ras or K-Ras inhibition increases the number and enhances the function of Foxp3 regulatory T cells. Eur J Immunol 2008; 38(6):1493-1502.

(559) Paintlia AS, Paintlia MK, Singh AK, Singh I. Inhibition of rho family functions by lovastatin promotes myelin repair in ameliorating experimental autoimmune encephalomyelitis. Mol Pharmacol 2008; 73(5):1381-1393.

(560) Hillmer AM, Hanneken S, Ritzmann S, Becker T, Freudenberg J, Brockschmidt FF et al. Genetic variation in the human androgen receptor gene is the major determinant of common early-onset androgenetic alopecia. Am J Hum Genet 2005; 77(1):140-148.

(561) Akslen LA, Monstad SE, Larsen B, Straume O, Ogreid D. Frequent mutations of the p53 gene in cutaneous melanoma of the nodular type. Int J Cancer 1998; 79(1):91-95.

(562) Sparrow LE, Soong R, Dawkins HJ, Iacopetta BJ, Heenan PJ. p53 gene mutation and expression in naevi and melanomas. Melanoma Res 1995; 5(2):93-100.

(563) Zerp SF, van Elsas A, Peltenburg LT, Schrier PI. p53 mutations in human cutaneous melanoma correlate with sun exposure but are not always involved in melanomagenesis. Br J Cancer 1999; 79(5-6):921-926.

(564) Wellcome trust sanger institute. Distribution of somatic mutations in TP53. http://www sanger ac uk/perl/genetics/CGP/ 2007.

(565) Yang FC, Merlino G, Chin L. Genetic dissection of melanoma pathways in the mouse. Semin Cancer Biol 2001; 11(3):261-268.

(566) Bray SJ. Notch signalling: a simple pathway becomes complex. Nat Rev Mol Cell Biol 2006; 7(9):678-689.

(567) Miele L, Golde T, Osborne B. Notch signaling in cancer. Curr Mol Med 2006; 6(8):905-918.

(568) Reynolds TC, Smith SD, Sklar J. Analysis of DNA surrounding the breakpoints of chromosomal translocations involving the beta T cell receptor gene in human lymphoblastic neoplasms. Cell 1987; 50(1):107-117.

(569) Rangarajan A, Talora C, Okuyama R, Nicolas M, Mammucari C, Oh H et al. Notch signaling is a direct determinant of keratinocyte growth arrest and entry into differentiation. EMBO J 2001; 20(13):3427-3436.

(570) Devgan V, Mammucari C, Millar SE, Brisken C, Dotto GP. p21WAF1/Cip1 is a negative transcriptional regulator of Wnt4 expression downstream of Notch1 activation. Genes Dev 2005; 19(12):1485-1495.

(571) Okuyama R, Ogawa E, Nagoshi H, Yabuki M, Kurihara A, Terui T et al. p53 homologue, p51/p63, maintains the immaturity of keratinocyte stem cells by inhibiting Notch1 activity. Oncogene 2007.

(572) Liu ZJ, Xiao M, Balint K, Smalley KS, Brafford P, Qiu R et al. Notch1 signaling promotes primary melanoma progression by activating mitogen-activated protein kinase/phosphatidylinositol 3-kinase-Akt pathways and up-regulating N-cadherin expression. Cancer Res 2006; 66(8):4182-4190.

(573) Moriyama M, Osawa M, Mak SS, Ohtsuka T, Yamamoto N, Han H et al. Notch signaling via Hes1 transcription factor maintains survival of melanoblasts and melanocyte stem cells. J Cell Biol 2006; 173(3):333-339.

(574) Radtke F, Raj K. The role of Notch in tumorigenesis: oncogene or tumour suppressor? Nat Rev Cancer 2003; 3(10):756-767.

(575) Nicolas M, Wolfer A, Raj K, Kummer JA, Mill P, van Noort M et al. Notch1 functions as a tumor suppressor in mouse skin. Nat Genet 2003; 33(3):416-421.